Numéro d'ordre: 2013-31 Année: 2013

Thèse de Doctorat

présentée pour obtenir le titre de

DOCTEUR

de l'**ÉCOLE CENTRALE DE LYON**
dans le cadre de l'**École Doctorale MEGA**

(Mécanique, Énergétique, Génie civil, Acoustique)

Spécialité : Mécanique

par

Kai Zhang

Mechantronic Design under Uncertainties

Présentée et soutenue publiquement le 22/10/2013 à l'École Centrale de Lyon, devant le jury d'examen:

N.K. M'Sirdi, Professeur, LSIS	Rapporteur
N. Bouhaddi, Professeur, FEMTO-ST	Rapporteur
M. Massenzio, Professeur, LBMC	Examinateur
M. Collet, Directeur de recherche, ECL	Examinateur
F. Demourant, Chercheur, CERT-ONERA	Examinateur
M.N. Ichchou, Professeur, ECL	Directeur de thèse
G. Scorletti, Professeur, ECL	Co-directeur de thèse
F. Mieyeville, Maître de conférences, ECL	Co-encadrant de thèse

Laboratoire de Tribologie et Dynamique des Systèmes, UMR-CNRS 5513
36 Avenue Guy de Collongue, 69134 Ecully Cedex, France
Laboratoire Ampère, UMR-CNRS 5005
36 Avenue Guy de Collongue, 69134 Ecully Cedex, France

ÉCOLE CENTRALE LYON **Direction de la recherche**

Liste des personnes Habilitées à Diriger des Recherches en poste à l'Ecole Centrale de Lyon

Nom-Prénom	*Corps grade*	Laboratoire ou à défaut département ECL	Etablissement
BEROUAL Abderrahmane	*professeur*	AMPERE	ECL
BURET François	*professeur*	AMPERE	ECL
JAFFREZIC-RENAULT Nicole	*directeur de recherche*	AMPERE	CNRS/ECL
KRÄHENBÜHL Laurent	*directeur de recherche*	AMPERE	CNRS/ECL
NICOLAS Alain	*professeur*	AMPERE	ECL
NICOLAS Laurent	*directeur de recherche*	AMPERE	CNRS/ECL
SCORLETTI Gérard	*professeur*	AMPERE	ECL
SIMONET Pascal	*directeur de recherche*	AMPERE	CNRS/ECL
VOLLAIRE Christian	*professeur*	AMPERE	ECL
		Nbre Ampère 9	
HELLOUIN Yves	*maître de conférences*	DER EEA	ECL
		Nbre DER EEA 1	
GUIRALDENQ Pierre	*professeur émérite*	DER STMS	ECL
VINCENT Léo	*professeur*	DER STMS	ECL
		Nbre DER STMS 2	
LOHEAC Jean-Pierre	*maître de conférences*	ICJ	ECL
MAITRE Jean-François	*professeur émérite*	ICJ	ECL
MARION Martine	*professeur*	ICJ	ECL
MIRONESCU Elisabeth	*professeur*	ICJ	ECL
MOUSSAOUI Mohand	*professeur*	ICJ	ECL
MUSY François	*maître de conférences*	ICJ	ECL
ZINE Abdel-Malek	*maître de conférences*	ICJ	ECL
		Nbre ICJ 7	
CALLARD Anne-Ségolène	*professeur*	INL	ECL
CLOAREC Jean-Pierre	*maître de conférences*	INL	ECL
GAFFIOT Frédéric	*professeur*	INL	ECL
GAGNAIRE Alain	*maître de conférences*	INL	ECL
GARRIGUES Michel	*directeur de recherche*	INL	CNRS/ECL
GENDRY Michel	*directeur de recherche*	INL	CNRS/ECL
GRENET Geneviève	*directeur de recherche*	INL	CNRS/ECL
HOLLINGER Guy	*directeur de recherche*	INL	CNRS/ECL
KRAWCZYK Stanislas	*directeur de recherche*	INL	CNRS/ECL
LETARTRE Xavier	*chargé de recherche*	INL	CNRS/ECL
O'CONNOR Ian	*professeur*	INL	ECL
PHANER-GOUTORBE Magali	*professeur*	INL	ECL
ROBACH Yves	*professeur*	INL	ECL
SAINT-GIRONS Guillaume	*chargé de recherche*	INL	CNRS/ECL
SEASSAL Christian	*directeur de recherche*	INL	CNRS/ECL

SOUTEYRAND Eliane	directeur de recherche	INL	CNRS/ECL
TARDY Jacques	directeur de recherche	INL	CNRS/ECL
VIKTOROVITCH Pierre	directeur de recherche	INL	CNRS/ECL

Nbre INL 18

CHEN Liming	professeur	LIRIS	ECL
DAVID Bertrand	professeur	ICTT	ECL

Nbre LIRIS 2

BAILLY Christophe	professeur	LMFA	ECL
BERTOGLIO Jean-Pierre	directeur de recherche	LMFA	CNRS/ECL
BLANC-BENON Philippe	directeur de recherche	LMFA	CNRS/ECL
BOGEY Christophe	chargé de recherche	LMFA	CNRS/ECL
CAMBON Claude	directeur de recherche	LMFA	CNRS/ECL
CARRIERE Philippe	directeur de recherche	LMFA	CNRS/ECL
CHAMPOUSSIN J-Claude	professeur émérite	LMFA	ECL
COMTE-BELLOT geneviève	professeur émérite	LMFA	ECL
FERRAND Pascal	directeur de recherche	LMFA	CNRS/ECL
GALLAND Marie-Annick	professeur	LMFA	ECL
GODEFERD Fabien	directeur de recherche	LMFA	CNRS/ECL
GOROKHOVSKI Mikhail	professeur	LMFA	ECL
HENRY Daniel	directeur de recherche	LMFA	CNRS/ECL
JEANDEL Denis	professeur	LMFA	ECL
JUVE Daniel	professeur	LMFA	ECL
LE RIBAULT Catherine	chargée de recherche	LMFA	CNRS/ECL
LEBOEUF Francis	professeur	LMFA	ECL
PERKINS Richard	professeur	LMFA	ECL
ROGER Michel	professeur	LMFA	ECL
SCOTT Julian	professeur	LMFA	ECL
SHAO Liang	directeur de recherche	LMFA	CNRS/ECL
SIMOENS Serge	chargé de recherche	LMFA	CNRS/ECL
TREBINJAC Isabelle	maître de conférences	LMFA	ECL

Nbre LMFA 23

BENAYOUN Stéphane	professeur	LTDS	ECL
CAMBOU Bernard	professeur	LTDS	ECL
COQUILLET Bernard	maître de conférences	LTDS	ECL
DANESCU Alexandre	maître de conférences	LTDS	ECL
FOUVRY Siegfrid	chargé de recherche	LTDS	CNRS/ECL
GEORGES Jean-Marie	professeur émérite	LTDS	ECL
GUERRET Chrystelle	chargé de recherche	LTDS	CNRS/ECL
HERTZ Dominique	past	LTDS	ECL
ICHCHOU Mohamed	professeur	LTDS	ECL
JEZEQUEL Louis	professeur	LTDS	ECL
JUVE Denyse	ingénieur de recherche	LTDS	ECL
KAPSA Philippe	directeur de recherche	LTDS	CNRS/ECL
LE BOT Alain	directeur de recherche	LTDS	CNRS/ECL
LOUBET Jean-Luc	directeur de recherche	LTDS	CNRS/ECL
MARTIN Jean-Michel	professeur	LTDS	ECL
MATHIA Thomas	directeur de recherche	LTDS	CNRS/ECL
MAZUYER Denis	professeur	LTDS	ECL
PERRET-LIAUDET Joël	maître de conférences	LTDS	ECL
SALVIA Michelle	maître de conférences	LTDS	ECL
SIDOROFF François	professeur	LTDS	ECL
SINOU Jean-Jacques	professeur	LTDS	ECL
STREMSDOERFER Guy	professeur	LTDS	ECL

THOUVEREZ Fabrice	*professeur*	LTDS	ECL
TREHEUX Daniel	*professeur*	LTDS	ECL
VINCENS Eric	*maître de conférences*	LTDS	ECL

Nbre LTDS 25

Total HdR ECL	91

To my loving parents
for their
unconditional love, understanding and moral support

Acknowledgements

This thesis is the conclusion of my three-year researches at the department of Laboratoire de Tribologie et Dynamique des Systèmes (LTDS) and Laboratoire Ampère of Ecole Centrale de Lyon (ECL). Many people have helped me over the past three years and it is my great pleasure to take this opportunity to express my sincere gratitude to them all.

First and foremost, I would like to express my heartfelt appreciation and gratitude to my supervisors, Professor Mohammed Ichchou, Professor Gérard Scorletti and Doctor Fabien Mieyeville, for their constant guidance and invaluable supports throughout my researches in ECL. Professor Mohamed Ichchou outlines the direction of my research and always encourages me. Without him, I could not have the opportunity to finish my thesis in ECL and have a clear direction for my research. I am also very grateful to Professor Gérard Scorletti, it is him who gives me the chance to work with him in his office and his comprehensive knowledge, rigorous scholarship and open mind deeply influence me. He is always full of ideas and open for new ideas. He also tolerates my poor French and my English with a Chinese accent. I have already got used to the very strong coffee he usually invites me. These are all one student can expect and ask from his supervisors. There is no way to pay back for their admirable, inspirational and immeasurable dedication, but at least I can promise that I will follow their spirits in my future study and work.

I would also like to thank the members of LTDS and Ampère for providing an enjoyable working environment of mutual interest in each others' research in which many problems could be discussed and solved

in a quick and informal manner. Thank you all. I also feel extremely lucky to have some of the most interesting Chinese at ECL. I appreciate for their sincere help and friendship: Dr. Wenjin Zhou, Dr. Tianli Huang, Changwei Zhou, Yonghua Wang, Xingrong Huang and many others.

On a more personal note, I would like to thank my family and girl friend for their supports. Their love, care, help and encouragements for so many years have made this thesis possible. I want to thank them for being so supportive over these years despite my choices in life.

Finally, I gratefully acknowledge Chinese Scholarship Council (CSC). It provides the funding source to support my Ph.D work.

致谢

首先我要感谢我的导师Mohammed Ichchou 教授和Gérard Scorletti 教授。感谢他们在我博士期间的细心指导。没有他们的帮助我很难顺利的完成博士课题。感谢Mohamed Ichchou 教授让我有机会来到里昂中央理工大学攻读博士学位，并帮助我规划了博士期间的科研方向。感谢 Gérard Scorletti 教授，他学识渊博、治学严谨、对工作充满热情。他那拥挤的办公室是我工作效率最高的地方。他是我遇见过的最忙碌的导师，但他依然帮助我反复修改每一篇论文的每一句话，查证每一条参考文献，即使是因为重感冒说话都困难的时候。感谢两位风格不同的导师，从他们身上我不仅学到了相关的专业知识，更领会了科研工作者的情趣和严谨。和他们一起工作是一件非常幸运的事情，他们对我科研以及生活的影响会让我终身受益。

里昂中央理工是一个让人温暖的地方，我会永远怀恋这三年在操场上肆意的奔跑，在篮球场上尽情释放的激情以及在健身房挑战自我的挥汗如雨。我会永远珍惜与各位朋友的真挚友谊。感谢周文晋博士、于航博士和黄天力博士对我学习和生活上的帮助，感谢王永华，周常伟，黄行蓉，高峰，李喆，黄刚，张陆，陈旭，石柳等，谢谢你们对我支持、鼓励与包容。我不会忘记午餐后与大家的咖啡时间，以及和大家共同度过的快乐时光。在里昂中央理工我不仅仅完成了博士课题，更有幸地与大家相识相知，真心地希望我们的友谊日久天长！

我要对我的父母和我的女朋友说一句谢谢，在我追逐梦想的人生道路上，我需要你们，我爱你们！同时我也要感谢其他的亲人对我在法国留学期间的关心、支持和鼓励。最后，我要感谢国家留学基金委博士期间的全额资助。

Abstract

Flexible structures are increasingly used in various applications such as aerospace, automotive and so on. Since they are lightly damped and susceptible to vibrations, active vibration control is desirable. In practice, in addition to achieving effective vibration reduction, we have also to consider the required control energy to avoid the energy insufficiency, the control input to avoid control saturation and reduce the effects of measurement noises. On the other hand, as flexible structures have infinite number of resonant modes and only the first few can be employed in the system modeling and the controller design, there always exist neglected high-frequency dynamics, which can induce the spillover instability. Furthermore, the parametric uncertainties on modal parameters can degrade the control performances and even destabilize the closed-loop system. In this context, a quantitative robust control methodology for active vibration control of flexible structure is proposed in this thesis. Phase and gain control polices are first proposed to enforce frequency-dependent phase and gain requirements on the controller, which can be realized by the output feedback H_∞ control design. The phase and gain control polices based H_∞ control can make a trade-off among the complete set of control objectives and offer a qualitative robust controller. Especially, the LPV H_∞ control is used to reduce the required control energy for LPV systems. The generalized polynomial chaos (gPC) framework with finite element analysis is employed for uncertainty quantification. It allows us to investigate the effects of structural property uncertainties on natural frequencies and achieve their probabilistic information. Then, in the presence of parametric and dynamic uncertainties, μ/ν analysis and the random algorithm using Monte Carlo Method

are used to quantitatively ensure the closed-loop stability and performance robustness properties both in deterministic and probabilistic senses. The proposed quantitative robust control methodology is thus developed by employing various techniques from automatic control and mechanical engineering, thus reducing the gap between them for robust vibration control of flexible structures. Its effectiveness are verified by numerical simulations and experimental validation on LTI and LPV non-collocated piezoelectric cantilever beams.
Keywords: Phase and gain control policies, uncertainties, robustness analysis, LPV control, piezoelectric actuator, gPC framework

Résumé

Les structures flexibles sont de plus en plus utilisées dans des domaines variés comme l'aérospatiale, l'automobile, etc.. Les avantages du contrôle actif des vibrations sont son faible amortissement et sa sensibilité aux vibrations. Dans la réalité, en plus des exigences de réduction effective des vibrations, il faut également prendre en compte la quantité d'énergie nécessaire pour le contrôle, les entrées du contrôle pour éviter la saturation de commande, ainsi que la réduction des effets des bruits de mesure. D'autre part, comme les structures flexibles ont une infinité de modes de résonance et que seuls les premiers modes peuvent être utilisés dans la modélisation du système et dans la conception de contrôleur, les dynamiques négligées en hautes fréquences peuvent induire une instabilité dite "spill over". De plus, les incertitudes sur les paramètres modaux peuvent dégrader les performances de contrôle et même déstabiliser le système en boucle fermée. Dans ce contexte, on propose dans cette thése une méthodologie quantitative de contrôle actif et robuste des vibrations des structures flexibles. Des stratégies de contrôle de la phase et du gain sont d'abord proposées pour assurer des spécifications dépendant de la fréquence sur la phase et le gain du contrôleur. Ces spécifications peuvent être réalisées par la conception du contrôleur par la méthode H_∞ . Le contrôle H_∞ basé sur ces stratégies permet d'obtenir un compromis entre l'ensemble des objectifs de contrôle et d'offrir un contrôleur robuste qualitatif. En particulier, nous avons utilisé le contrôle LPV H_∞ pour réduire l'énergie nécessaire au contrôle du système LPV. Le cadre généralisé du chaos polynomial (gPC) avec analyse par éléments finis, qui permet l'étude des effets des incertitudes de propriétés structurelles sur les fréquences naturelles et qui permet d'obtenir leurs informations probabilistes, est employé pour la quantification des incertitudes. Ensuite, en présence des incertitudes paramétriques et dynamiques, nous avons utilisé l'analyse μ/ν et l'algorithme aléatoire en utilisant la méthode de Monte-Carlo pour assurer en méme temps la stabilité en boucle

fermée et les propriétés de robustesse de la performance à la fois dans le sens déterministe et le sens probabiliste. La méthodologie de contrôle robuste quantitatif proposée est donc développée en employant des techniques diverses du contrôle automatique et du génie mécanique, et ainsi permet de réduire l'écart entre eux pour le contrôle robuste de la vibrations pour des structures flexibles. Son efficacité est vérifiée par des simulations numériques et la validation expérimentale sur des poutres é équipées de piézoélectriques non-colocalisés, LTI et LPV.

Mots clés: stratégies de contrôle de la phase et du gain, incertitudes, analyse de la robustesse, contrôle LPV, actionneurs piézoélectriques, chaos polynomial généralisé

Contents

Nomenclature

Roman Symbols

E Young's Modulus

I Identity matrix of compatible dimensions

Greek Symbols

$\mu_\Delta(M)$ Structured singular value of matrix M with respect to the structrued uncertainty Δ

$\rho(A)$ The spectral radius of matrix A

$\bar{\sigma}(A)$ Largest singular value of matrix A

Other Symbols

$\mathbb{C}$ Field of complex numbers

$\mathbb{C}^{m\times n}$ Field of complex matrices of dimension $m \times n$

$\det(A)$ Determinant of matrix A

$\mathcal{F}_l(N, K)$ Lower LFR

A^* Complex conjugate transpose of matrix A

$A > 0$ Hermitian matrix $A^* = A$ with strictly positive eigenvalues

$\mathbb{R}$ Field of real numbers

$\mathcal{RH}_\infty^{m\times n}$ Proper real-rational stable transfer function matrices of dimension $m \times n$

Nomenclature

$\text{diag}(A_1, A_2, \ldots, A_n)$ Block-diagonal matrix with element A_i on the main diagonal

$\Re(s)$ Real part of $s \in \mathbb{C}$

$\Im(s)$ Imaginary part of $s \in \mathbb{C}$

Acronyms

FEM Finite Element Method

LFR Linear Fractional Transformation

LHP Left-Half Plane

LMI Linear Matrix Inequality

LPV Linear Parameter-Varying

LTI Linear Time-Invariant

MIMO Multi-Input-Multi-Output

RHP Right-Half Plane

RP Robust Performance

RS Robust Stability

SISO Single-Input-Single-Output

Chapter 1

Introduction

This chapter first introduces the motivation of this research. The research objectives and the research approaches are then briefly discussed. Finally, an outline of the remaining chapters is provided.

1.1 Motivation of this research

With more advanced technologies and materials in industries, lightweight components are widely implemented in practice for miniaturization and efficiency such as in aerospace and automotive ones. Due to the lightweight components, the structures become more flexible and more susceptible to vibration, which may cause unpleasant noises, unwanted stress, malfunction and even structural failure. As a result, the flexible structures have naturally become suitable candidates for vibration reduction and many researchers have sought various methods for this purpose. Recently active vibration control technologies have drawn attention because active control methods are becoming cost efficient due to rapid development of electronic technologies. One more reason is the appearance of new actuator-sensor concepts, namely, piezoelectric actuators and sensors incorporated into host structures.

Normally, designing effective controllers necessitates having accurate models of the realistic system. However, in practice due to various sources of uncertainty, it is very difficult (or perhaps even impossible) to obtain mathematical models

that are identical to the physical plants, regardless of whether the models are derived from the first principles, through the finite element method or through the system identification. Some major sources of model uncertainties are as follows:

- **Unmodelled dynamics:** usually the controller design requires model descriptions of reasonable size and complexity. In many cases, linear time-invariant models of a reduced order are used for the controller design. Particularly, as flexible structures have infinite number of resonant modes, the existence of neglected high frequency dynamics is unavoidable in the system modeling, and thus the associated spillover problem [1] has to be investigated (Balas, 1978a,b), since it could severely degrade the control performance and even destabilize the closed-loop system. In addition, considering the nonlinearities in practical systems, the linearization in system modeling may also lead to imperfections in the models.

- **Parametric errors:** even if the models include all dynamics of the real structures, there will always exist errors on the modal parameters, *e.g.* the natural frequencies and damping ratios. These errors may be due to practical limitations of identification hardwares and associated identification algorithms or due to the inaccuracy in the structural properties used in the finite element method and the analytical formulations, *e.g.* structural material and geometrical variations (Choi et al., 2004a).

- **Varying loads and external forces:** plant dynamics change depending on their load conditions or external forces. For example, the inertia and the position of center of gravity of an aircraft change depending on the distribution of passengers, cargo and fuel; even sometimes the plant dynamics are fixed, the position of external forces may vary and affect the disturbance dynamics, which can be termed as position dependent dynamics (Symens et al., 2004; Paijmans et al., 2006; Paijmans, 2007). This varying dynamics could have considerable effects on the final control performances and are desirable to be considered in the system modeling and the control designs.

[1] the sensor outputs are contaminated by the neglected dynamics, which we called observation spillover, and the feedback control excites the neglected dynamics, which is termed as control spillover

- **Time variance:** plant dynamics undergo changes during operation. Varying environmental conditions such as the temperature changes or the wear caused by aging could significantly influence the plant dynamics (Hegewald and Inman, 2001; Shimon and Hurmuzlu, 2007; Gupta et al., 2012). Besides, Li et al. (2009) investigate temperature dependence of piezoelectric coefficients and demonstrate that they increase with an increase in temperature.

- **Manufacturing variance**: If we consider a series of plants, the controller design is usually performed for one or several prototypes of them. However, in a series production there will always be manufacturing variances between the individual plants and the controller must cope with all of them (Hecker, 2006). For instance, defects such as micro cracks, holes and so on may arise during the manufacturing of piezoelectric materials. This could significantly change the electromechanical properties of piezoelectric sensors/actuators (Umesh and Ganguli, 2013).

In literature, the model uncertainties are investigated with several techniques from various disciplines. From the mechanical community, several numerical methods are proposed for the uncertainty quantification (UQ). The UQ is the science about the uncertainty that quantitatively identifies where are the sources of the uncertainty, characterizes which kind of forms the uncertainty is, investigates the evolvement of the uncertainty during simulations, analyzes the effects of the uncertainty on the system outputs, determines which uncertainty is most dominant and reduces the number of different uncertainties. Monte Carlo Simulation (MCS) is a well-known technique in this field, which provides the entire probability density function of any random variable (Liu, 2008). Being an interesting alternative, the generalized polynomial chaos (gPC) framework is gaining in popularity and has been applied to various engineering problems such as stochastic finite elements, the estimation of response variability, probabilistic robust control and so on (Ghanem and Spanos, 1991; Polyak and Tempo, 2001; Xiu and Karniadakis, 2002; Choi et al., 2004b; Hou et al., 2006; Templeton et al., 2012).

From the automatic control community, the presence of model uncertainties has always been a critical issue in control theory and applications. Linear

quadratic Gaussian (LQG) control and Kalman filtering are proposed to deal with the uncertainty based on a stochastic approach (Athans, 1971). With these methods, the uncertainty is only considered in the form of exogenous disturbances having a stochastic characterization and the plant models are assumed to be exactly known. To overcome this paradigm, since the early 1980s, a successful attempt is achieved to directly introduce the model uncertainties, which can be cast into parametric and dynamic uncertainties. Parametric uncertainties correspond to the variations in the parameters of mathematical models of the physical plants, and a dynamic uncertainty corresponds to unmodeled or neglected high frequency dynamics that are not taken into account in the system modeling or the control designs. The design objective is to determine solutions that are guaranteed against all possible uncertain models, that is, the controller is designed with the aim of guaranteeing a specified performance for all possible models even in the worst case although it may occur rarely. This control can thus be regarded to be robust with respect to the parametric and dynamic uncertainties. A major stepping stone in the robust control is the work of Zames (1981) that first proposes the method to consider a specific control performance using weighting functions, that is, the weighted sensitivity function. Afterwards, in the so-called H_∞ control (Zhou et al., 1996), various control specifications can be translated as constraints simultaneously, defined by weighting functions, on the magnitude of corresponding weighted closed-loop transfer functions. The controller design boils down to the optimization on the H_∞ norm of the weighted closed-loop transfer functions (Glover and Doyle, 1988). This formulation surmounts some drawbacks of classical optimal control, such as the lack of guaranteed margins of LQG. It is notable that many control designs, *e.g.* the H_∞ control, only use the nominal reduced models and usually treat the model uncertainties in an incomplete or heuristic way. Based on the structured singular value also known as the μ theory (Packard and Doyle, 1993), μ synthesis is proposed to explicitly account for the information and structure of the model uncertainties. The motivation of μ synthesis is attractive and a great deal of effort has been devoted to this subject, but μ synthesis is still difficult to be implemented in practice since its synthesis is not convex and it is not easy to control the order of the resulting controller (Skogestad and Postlethwaite, 2005).

1.1 Motivation of this research

As known, even if the model uncertainties are not explicitly considered in many control designs, the closed-loop system may still be robust to a certain level of uncertainties. In this context, the focus is to efficiently verify the robust stability and the robust performance with a given controller. Many methods can be used for this purpose depending on the natural and structure of the uncertainties such as Kharitonov theorem (Kharitonov, 1978; Bhattacharyya et al., 1995), the small gain theorem (Zames, 1966) and the μ theory (Zhou et al., 1996). These robustness analysis methods are deterministic since they provide a definite answer to the closed-loop robustness properties. As a complementary method, in several practical cases, probabilistic robustness analysis could also be used to take into account the probabilistic information of parametric uncertainties and enlarge the robust issue to the probabilistic sense, for example, probabilistic robustness bounds can be computed at the expense of a probabilistic risk of failure, which are usually larger than the corresponding deterministic ones and thus claimed to be practically less conservative in Tempo et al. (2005).

In the presence of parametric and dynamic uncertainties, besides the robustness properties of the closed-loop system, for active vibration control of flexible structures a complete set of control objectives have to be considered simultaneously. The set of control objectives include the vibration reduction of every controlled resonant mode with a corresponding a priori determined level, the moderate control energy to avoid the controller saturation and exceeding the actuator operated voltage, and the constraints on the effects of the measurement noise. As these control objectives usually have conflicting requirements on the controller, a trade-off among them has to be made in control designs over corresponding frequency ranges in a rational and systematic way (Balas and Doyle, 1994). Based on the extensive literature review in the subsequent chapter, it is demonstrated that in spite of a large number of control methods for active vibration control, a general control methodology which allows us to systematically design a quantitative robust controller that satisfies the complete set of control objectives has to be proposed. In this research, to achieve this goal, a bridge among several techniques from mechanical engineering and automatic control is built to make full advantages of these techniques and reduce the gap between them for quantitative robust control of flexible structures.

1.2 Approaches of this research

As discussed above, considering the complete set of control objectives involved in active vibration control, to avoid some drawbacks of existing control methods such as the classical ones, the usual H_∞ control and the μ synthesis, a general and systematic quantitative robust control methodology has to be developed. For this purpose, in this research, a positive frequency dependent function is introduced to determine the controlled resonant modes and explicitly define the specification of vibration reduction. In the presence of parametric and dynamic uncertainties, phase and gain control policies are first proposed to impose qualitative frequency dependent gain and phase requirements on the controller:

- When the specification of vibration reduction is not satisfied for the open-loop system, the phase control policy requires the gain of the controller to be large enough for effective vibration reduction. Meanwhile, it enforces the phase requirement on the controller such that around the controlled resonant frequencies the open-loop transfer function stays in the right half plane on Nyquist plot. This phase property provides adequate stability robustness to parametric uncertainties. The phase requirement is in contrast with the passivity theorem (Khalil, 1996) and the negative-imaginary approach (Lanzon and Petersen, 2008) which impose more strict phase requirements on the plant and the controller, and thus can only be applied to collocated systems.

- When the specification of vibration reduction is satisfied for the open-loop system, the gain control policy requires the gain of the controller to be as small as possible to limit the control energy and reduce the effects of the measurement noise. Based on the small gain theorem, it also provides a certain level of stability robustness to a generalized dynamic uncertainty including neglected high frequency dynamics and other dynamics when the phase control policy is not used. As no parametric uncertainty is considered with the small gain theorem, the associated conservatism could be reduced.

Phase and gain control policies can be applied to explain some existing classical control designs, *e.g.* the critically damped method (Goh and Yan, 1996) and the

cross-over point method (Bayon de Noyer and Hanagud, 1998a) for acceleration feedback control (AFC). For several specific single-input-single-output (SISO) cases, phase and gain control policies can be realized by some classical control methods such as AFC, direct velocity feedback (DVF) control, positive position feedback (PPF) control and so on, despite the fact this realization is not achieved deliberately by these methods. Obviously, it is desirable to have a more rational and systematic way to realize phase and gain control policies for both SISO and multiple-input-multiple-output (MIMO) systems. The dynamic output feedback H_∞ control is a competitive solution to this problem due to its inherent characteristics, for example, the H_∞ control allows defining the design specifications in the frequency domain and the dynamic output feedback H_∞ control designs can be accomplished efficiently using polynomial-time algorithms, thus providing a stabilizing controller with a reasonable order (Doyle et al., 1989; Gahinet and Apkarian, 1994). As a result, phase and gain control policies are used in the dynamic output feedback H_∞ control to incorporate necessary weighting functions and determine them in a rational and systematic way. Meanwhile, with the appropriate weighting functions, efficient H_∞ control algorithms can automatically realize phase and gain control policies and generate a satisfactory H_∞ controller that makes a trade-off among various control objectives. In general, this robust control methodology is developed by well employing phase and gain control policies in the H_∞ control. It can be used for both SISO and MIMO systems with collocated or non-collocated sensors and actuators.

It is notable that, although the phase and gain control policies are quite qualitative, when they are employed in the H_∞ control, due to the features of the H_∞ control, the proposed robust control methodology can ensure quantitative nominal vibration reduction defined by the positive frequency dependent function. In addition, this control methodology can also quantitatively ensure the modulus margin which is, in some extend, related to the robustness properties of the closed-loop system in a qualitative way. As a result, in the presence of parametric and dynamic uncertainties, to quantitatively verify the robustness properties of the closed-loop system using the designed H_∞ controller, reliable and efficient robustness analysis is conducted in this research, *e.g.* the structured singular value (μ) analysis (Skogestad and Postlethwaite, 2005). Specifically, to

investigate the effects of structural uncertainties, *e.g.* material and geometrical uncertainties, on the system responses, *e.g.* the natural frequencies, the generalized polynomial chaos (gPC) framework is employed for the uncertainty quantification (UQ). The UQ allows us to translate the structure uncertainties, which are often considered in mechanical designs, into parametric uncertainties, which can be directly investigated in robustness analysis. The UQ provides the intervals and the probabilistic information of parametric uncertainties due to distributed structural uncertainties. Based on the information of parametric and dynamic uncertainties, both deterministic and probabilistic robustness analyses can be performed to quantitatively verify the robustness properties of the closed-loop system. They complement and compare each other to provide reliable and comprehensive investigations of the robustness properties in the deterministic sense and the probabilistic one. In addition, with linear matrix inequality (LMI) optimization, the proposed quantitative robust control methodology can also be applied to linear parameter varying (LPV) systems and offer a parameter dependent H_∞ controller, for instance, the designed controller can not only satisfy the complete set of control objectives and the closed-loop robustness properties, but also take into account the energy saving for LPV systems. In conclusion, the proposed quantitative robust control methodology is mainly achieved by two steps: first phase and gain control policies based LTI/LPV H_∞ control provides a H_∞ controller which guarantees quantitative nominal vibration reduction and qualitative robustness properties of the closed-loop system, and then both deterministic and probabilistic robustness properties using the designed controller are verified. This control methodology is very general and able to supply enough flexibility to make a trade-off among various control objectives .

1.3 Organization of this dissertation

This dissertation consists of six chapters and is organized as follows:

Chapter 2: Backgrounds

This chapter provides the backgrounds for the research. An extensive literature review is firstly conducted for related techniques such as the employment of

smart materials for active vibration control, the H_∞ active vibration control and the uncertainty quantification with polynomial chaos expansion. Then some backgrounds of the H_∞ control and deterministic and probabilistic robustness analyses are given for the sake of completeness. This chapter ends with active vibration control of a simple mass-damper-spring (MDS) system, which is used to illustrate the main design processes of the H_∞ control and deterministic robustness analysis, and emphasize some considerable problems for the following research.

Chapter 3: Phase and gain control policies based H_∞ control
This chapter first proposes the control problem to consider a complete set of control objectives in the area of robust active vibration of flexible structures. Then to solve this control problem, phase and gain control policies are proposed to impose frequency dependent gain and phase requirements on the controller. These control policies can be used to explain some classical control designs, and more importantly they can be well employed in the dynamic output feedback H_∞ control to develop a general and systematical robust control methodology which ensures quantitative nominal vibration reduction and qualitative robustness properties of the closed-loop system. Both numerical simulations and experimental results are used to demonstrate the effectiveness of this control methodology for active vibration control of a non-collocated piezoelectric cantilever beam.

Chapter 4: Robustness analysis of flexible structures
Based on chapter 3, this chapter mainly focuses on extending the previous qualitative robust control methodology to the quantitative one using deterministic and probabilistic robustness analyses. This quantitative robust control methodology utilizes effective uncertainty quantification, *i.e.* the generalized polynomial chaos (gPC) framework, to have parametric uncertainties from the structural uncertainties with the finite element analysis. The achieved probabilistic information of parametric uncertainties can then be directly considered in various robustness analyses to achieve quantitative robustness properties of the closed-loop system. The effectiveness of this control methodology is numerically

validated on a non-collocated piezoelectric cantilever beam with uncertainties on structural material properties.

Chapter 5: Quantitative robust active vibration control of LPV system
This chapter extends the proposed quantitative robust control methodology for linear parameter varying (LPV) system modeling with position-dependent dynamics. First, a brief introduction of LPV system modeling and LPV control using linear fractional representations (LFR) is given. Then phase and gain control policies are employed in LPV H_∞ control design to have a parameter dependent LPV H_∞ controller by solving a finite dimensional LMI optimization. Both the worst-case H_∞ controller and the AFC one are designed and compared with the LPV H_∞ controller. The numerical simulations demonstrate the effectiveness and advantages of the LPV control design for quantitative robust active vibration of a non-collocated cantilever beam which is excited by a position varying external force.

Chapter 6: Conclusions and future research
This chapter summaries the research and outlines potential directions for future research.

Chapter 2

Backgrounds

The purpose of this chapter is to provide backgrounds for the research. The first part of this chapter provides an extensive literature review on several fields closely related to this research: the employment of smart materials for active vibration control, the H_∞ based active vibration control and the uncertainty quantification with the generalized polynomial chaos framework. The second part of this chapter simply introduces the backgrounds of the H_∞ control and the outlines of deterministic and probabilistic robustness analyses. Finally, a simple mass-damper-spring system is used to illustrate the main processes of the H_∞ control and the deterministic robustness analysis, and emphasize some useful remarks for the subsequent research.

2.1 Literature review

2.1.1 Smart materials for active vibration control

The piezoelectric effect is first discovered by the Curie brothers in 1880 (Mason, 1981; Ballato, 1996). Specifically, they find that squeezing certain materials (*piezein* is the Greek word for squeeze) results in an electric charge; this effect enables the use of piezoelectric materials in strain sensors. On the other hand, the use of piezoelectric materials as actuators exploits the converse effect, that is, the application of an electric voltage results in a mechanical strain. This converse effect is credited to Lippmann's theoretical predictions, which are also experimen-

tally verified by the Curie brothers. Due to the direct and converse piezoelectric effects, piezoelectric materials can be used as sensors and actuators for structural control. Considering their mechanical simplicity, lightweight, small volume, and ability to be easily integrated into applications with flexible structures, piezoelectric materials have found many applications in vibration control (Moheimani and Fleming, 2006; Wang and Inman, 2011). This research field has witnessed an explosive growth in recent years.

Flexible structures have been widely used in a variety of industrial, scientific as well as defence applications (Cannon and Schmitz, 1984; Garcia et al., 1992; Dd et al., 1993; Han et al., 1999a; Wu et al., 2000; Tokhi et al., 2001). One of the most significant characteristics of flexible structures is their highly resonant modes due to the inherently small dissipation of kinetic and strain energy, which is reflected by a relatively small structural damping. Such flexible structures may suffer from considerable vibrations when they are excited by external disturbances around the resonant frequencies. The vibrations may lead to unpleasant noises, unwanted stresses, positioning errors and in severe cases, failure due to fatigue. This has motivated a huge amount of research in the broad field of vibration control of flexible structures (Vaillon and Philippe, 1999; Salapaka et al., 2002; Benosman and Vey, 2004). Particularly, during the past few decades, there has been considerable interest in the area of the active control of structural vibrations by using piezoelectric sensors and actuators due to the fact that they can be easily bonded on or imbedded into conventional structures, and can be easily manufactured in the desired shapes. Meanwhile, they are lightweight and have higher actuating force and lower power consumption characteristics (Han et al., 1999b; Qiu et al., 2009).

To design piezoelectric smart structures for efficient active vibration control, both structural dynamics and control methods have to be considered. A lot of research effort concerning modeling of the piezoelectric materials incorporated into flexible structures with the finite element method (FEM) or the system identification can be founded in Crawley and de Luis (1987); Hagood et al. (1990); Tzou and Tseng (1990); Lee (1990); Balas and Doyle (1990); Benjeddou (2000); Chang et al. (2002); Dong et al. (2006). Meanwhile, after the classical survey paper by Balas (Balas, 1982), a large effort has been spent by the researchers in the auto-

matic control in order to deal with vibration reduction by using active feedback control. For this purpose, various control structures and control methods are employed for linear time-invariant (LTI) systems, *e.g.* PID control (Juntao, 2005; Khot et al., 2012), velocity feedback control (Balas, 1979; Wang et al., 2001a; Aoki et al., 2008), positive position feedback (PPF) control (Hegewald and Inman, 2001; Fanson and Caughey, 1990; Friswell and Inman, 1999; Qiu et al., 2007), acceleration feedback control (Goh and Yan, 1996; Qiu et al., 2009), pole placement control (Zhang and Li, 2013), linear quadratic gaussian (LQG) (Han et al., 1999b; Xu and Koko, 2004), linear quadratic regulator (LQR) (Trindade et al., 2001; Bhattacharya et al., 2002; Dong et al., 2013), fuzzy control (Takawa et al., 2000; Zhong et al., 2004; Zorić et al., 2013), sliding mode control (Pai and Sinha, 2007; Bandyopadhyay et al., 2007; Wu and Zheng, 2009), model predictive control (Wills et al., 2008; Takács and Rohal-Ilkiv, 2012), adaptive control (Valoor et al., 2001; Ma and Ghasemi-Nejhad, 2005), neural control (Jha and Rower, 2002; Jha and He, 2002), independent modal space control (Baz et al., 1992), resonant control (Pota et al., 2002; Moheimani and Vautier, 2005), integral resonant control (Aphale et al., 2007), μ synthesis (Boulet et al., 2001; Li et al., 2003; Li and Ma, 2013), H_∞ control (Smith et al., 1994; Seto and Kar, 2000; Barrault et al., 2007; Iorga et al., 2008) and linear parameter varying control (Caigny et al., 2010; Onat et al., 2011), which can be used for LTI systems depending on time-varying parameters.

2.1.2 H_∞ based active vibration control of flexible structures

Motivated by the work of Zames (1981), which incorporates weighting functions to synthesize stabilizing controllers with guaranteed performances (sensitivity function minimization), the H_∞ control is introduced into the control theory. To make full use of H_∞ control, the control problem has to be expressed as a mathematical optimization problem and then finds the controller to solve this problem. The H_∞ control has the advantage over classical control methods in that it is readily applicable to both the SISO and MIMO systems. It is also demonstrated that carefully designed H_∞ controllers can provide satisfactory robustness properties

in the presence of parametric and dynamic uncertainties (Crassidis et al., 2000; Zhang et al., 2001, 2009a), which are not easy or even possible to obtain with PID, LQR or H_2 control. Due to the property of the H_∞ norm, the H_∞ control naturally allows defining the specification of vibration reduction in the frequency domain. Furthermore, the state and dynamic output feedback H_∞ control designs can be accomplished efficiently using polynomial-time algorithms, thus providing a stabilizing controller with a reasonable order (Doyle et al., 1989; Gahinet and Apkarian, 1994). Due to these features, the H_∞ control is receiving intense interest in the control literature and has been successfully applied to a wide variety of practical problems (Jabbari et al., 1995; Dosch et al., 1995). However, despite these promising features, the practical use of H_∞ based active vibration control remains limited mainly due to its drawbacks such as how to incorporate necessary weighting functions and appropriately determine them. In the following, we have an extensive review of the H_∞ control designs for robust active vibration control:

- The mixed sensitivity design is most usually adopted in H_∞ control, *e.g.* Chang et al. (2002); Seto and Kar (2000); Sadri et al. (1999); Kar et al. (2000a); Liu et al. (2004); Xie et al. (2004); Zhang et al. (2009b); Kilicarslan (2010); Douat et al. (2011); Douat (2011); Kumar (2012). However, this H_∞ control structure may necessarily lead to the pole-zero cancellation between the designed H_∞ controller and the nominal plant (Sefton and Glover, 1990). This pole-zero cancellation should be avoided for lightly damped flexible structures, especially in the presence of parametric uncertainties (Scorletti and Fromion, 2008a).

- The definition of the specification of vibration reduction is critical in H_∞ control. A frequency-dependent weighting function $W(s)$ or a matching model $M(s)$ can be used to this end (Forrai et al., 2001a; Rao et al., 2007). However, it is not explained clearly how to choose $W(s)$ or $M(s)$ and if several resonant modes have to be controlled, $W(s)$ and $M(s)$ could be very complicated and have a high order. This results in a high-order H_∞ controller, which requires extensive online computations imposing limitations on the sample rate for real-time implementation and precluding observation and control of high frequency resonant modes.

In addition to the vibration reduction performance, the H_∞ control should also impose constraints on the control energy and reduce the effects of the measurement noise. But these control objectives are often neglected, *e.g.* Seto and Kar (2000); Liu et al. (2004); Xie et al. (2004); Forrai et al. (2001a); Kar et al. (2000b). Sometimes, constant weighting functions are used to this end, *e.g.* Zhang et al. (2001); Huo et al. (2008). However, as they are frequency-independent and cannot represent suitable requirements on the controller over various frequency ranges, the measurement noise may have significant adverse effects on the control performances and the closed-loop system may even not work properly in real-time implementation due to the control saturation problem.

- In H_∞ control, a set of control objectives have to be reflected as the constrains on the H_∞ norm of corresponding weighted closed-loop transfer functions. This requires us to incorporate necessary and appropriate weighting functions in H_∞ control. Naturally, the selection of weighting functions is critical in H_∞ control and has considerable effects on the final control performance with the designed controller. It is even regarded to be the main drawback of H_∞ control by Zhang et al. (2001). As claimed in Crassidis et al. (2000), the selection of weighting functions cannot be explicitly related to the control objectives in a straightforward manner and trial and error iterations are required to determine the weighting functions. Inappropriate weighting functions may neglect some control objectives and fail to have a satisfactory H_∞ controller. Usually, constant, low-pass, high-pass and band-stop/pass filters are employed as weighting functions with trial and errors, *e.g.* Crassidis et al. (2000); Liu et al. (2004); Rao et al. (2007); Shimon et al. (2005). In these studies, although for investigated cases these weighting functions can provide an H_∞ controller to satisfy certain control objectives, a general and systematical selection of weighting functions is required for H_∞ control where a set of control objectives can be considered simultaneously.

- To consider the stability robustness to parametric and dynamic uncertainties, a norm bounded additive or multiplicative perturbation has been

widely used in H_∞ control. These perturbations can represent neglected high frequency dynamics related to the spillover instability, *e.g.* Chang et al. (2002); Zhang et al. (2001); Sadri et al. (1999); Xie et al. (2004); Kar et al. (2000b); Font et al. (1994); Carrere et al. (1997); Moreira et al. (2001); Yaman et al. (2001, 2002); Caracciolo et al. (2005). They can also include all possible uncertain models due to parametric uncertainties as performed in Chang et al. (2002); Crassidis et al. (2000); Xie et al. (2004); Forrai et al. (2001a); Filardi et al. (2003). Based on the unstructured uncertainty, the small gain theorem (Desoer and Vidyasagar, 1975) is then applied to ensure the closed-loop stability.

It is notable that, in H_∞ control due to the presence of parametric uncertainties, the employed unstructured uncertainty inevitably introduces considerable conservatism in the robustness properties of the closed-loop system (Morris et al., 1992). To reduce this conservatism, mixed H_2/H_∞ control together with pole placement is used to guarantee the stability robustness to parametric uncertainties (Hong et al., 2006). The controller is synthesized from a system of Linear Matrix Inequality (LMI), however, the stability robustness is not investigated. Furthermore, the regulated variables in H_2/H_∞ control are not clearly specified and there may exist considerable conservatism in the multi-objective state feedback synthesis. In Wang et al. (2001b); Wang (2003), assuming matched form of parametric uncertainties, the singular value decomposition and H_2 control are proposed to consider parametric uncertainties such that the phase margin keeps larger than 60° for all possible models. However, the matching condition could often be violated in practice (Stalford, 1987) and the desired phase or gain margin expected by H_2 control is no longer guaranteed when the Kalman filter is used for the state estimation (Doyle, 1978). Sometimes, only a dynamic uncertainty is explicitly considered in H_∞ control and parametric uncertainties are considered with the μ analysis to verify the robustness properties with the designed controller, *e.g.* Yaman et al. (2001, 2002); Iorga et al. (2009). Collocated sensors and actuators are also used in H_∞ to have prominent stability robustness, *e.g.* Dosch et al. (1995); Hong et al. (2006); Bai and Grigoriadis (2005); Demetriou et al. (2009).

In few cases, neither dynamic nor parametric uncertainty is explicitly considered, *e.g.* Filardi et al. (2003); Chen et al. (2010). A slightly modified H_∞ control is used in (Halim and Moheimani, 2002) based on the definition of a spatial H_∞ norm of the transfer function from the piezoelectric actuator to the deflections of the points on a beam.

Besides the H_∞ control designs, to reduce the conservatism in the presence of parametric uncertainties or several dynamic uncertainties, Doyle (1982) proposed the concept of structured singular value (μ) and employed the structured uncertainty $\underline{\boldsymbol{\Delta}}$ to investigate structural characteristics of all uncertainties. Based on $\underline{\boldsymbol{\Delta}}$, μ synthesis is developed to design a robust stabilizing controller such that the robustness properties of the closed-loop system are ensured with respect to the defined $\underline{\boldsymbol{\Delta}}$ (Doyle, 1985; Fan et al., 1991). The motivation of μ synthesis is attractive, unfortunately, there is no direct method to synthesize such μ robust controllers. Normally, μ synthesis involves the use of H_∞ optimization for the controller synthesis and μ analysis for the robustness properties verification with the designed controller, for instance, the widely used DK-iteration (Doyle et al., 1991). But even for a given controller, the accurate μ computation is in general NP-hard[1] (Braatz et al., 1994; Blondel and Tsitsiklis, 2000). Therefore, lower and upper bounds of μ are usually calculated to approximate its accurate value with frequency gridding method (Young and Dolye, 1990; Young et al., 1992). This method requires a sufficiently fine frequency gridding to have reliable results. In the case of lightly damped flexible structures, the critical frequency could be neglected and the robustness properties are thus overestimated (Freudenberg and Morton, 1992). In addition to the problem introduced by μ analysis, DK-iteration fails to generate a μ upper bound optimal controller due to its inherent non-convexity and only provides a μ upper bound sub-optimal controller, which largely depends on the selection of initial parameters. The order of this controller increases in every DK-iteration and tends to be very large. Therefore, as claimed in (Skogestad and Postlethwaite, 2005), whilst the structured singular value is a useful analysis tool for assessing designs, μ synthesis is sometimes difficult to use and often too complex for the practical problem at hand. In its full generality, the

[1] given any algorithm to compute μ, there will be problems for which the algorithm cannot find the answer in polynomial time.

μ synthesis problem is not yet solved mathematically; where solutions exist the controllers tend to be of very high order; the algorithms may not always converge and design problems are sometimes difficult to formulate directly. As a result, although in literature μ synthesis has been applied to structural control (Li et al., 2003; Qiu and Tani, 1995; Tani et al., 1995; Karkoub et al., 2000; Gáspár et al., 2002, 2003), from a practical point of view, μ synthesis (DK-iteration) is not suitable for active vibration control of flexible structures.

2.1.3 Polynomial chaos expansion for uncertainty quantification

As discussed above, a substantial number of papers demonstrate the effectiveness of H_∞ control for active vibration control. However, it is notable that either the H_∞ control or μ synthesis is based on the most pessimistic value of performance among the possible ones, usually referred to as the worst-case. This worst-case performance is usually realized only by a single member of the uncertain model set and by a particular input signal. No information is provided regarding the likelihood that this worst-case will ever occur in practice (Crespo and Kenny, 2005). This implies that in some practical cases we have to require more knowledge than just simple bounds on parametric uncertainties, as is typically used in the worst-case control designs. Thus, a computationally efficient approach of estimating probabilistic information of parametric uncertainties is required in this research. For this purpose, the uncertainty quantification (UQ) can be used. UQ builds a bridge between practical sources of the uncertainty and the typical parametric uncertainties to be considered in robust control designs. It allows considering the uncertainty from the beginning of the system design but not after the controller design. For example, UQ can quantitatively determine the effects of various structural material or geometrical uncertainties on the system natural frequencies, and thus provide bounded parametric uncertainties with the probabilistic information that is available for both robust control designs and various robustness analysis.

There exist several numerical techniques for UQ such as probability theory (Ang and Tang, 1984), fuzzy theory (Wood et al., 1992), evidence the-

ory (Shafer, 1976), Bayesian theory and convex model theory (Soundappan et al., 2004) and information gap decision theory under severe uncertainty (Ben-Haim, 2001). The common issue among these theories is how to determine the degree to which uncertain events are likely to occur, and there are distinct differences between the various approaches as to how this is achieved (Manan and Cooper, 2010). Among these techniques, the generalized polynomial chaos (gPC) framework is used in this research for UQ due to its computational efficiency and adequate accuracy compared to traditional MCS methods (Xiu and Karniadakis, 2002). The development of gPC started with the seminal work on polynomial chaos (PC) by Ghanem and co-workers. Inspired by the theory of Winner-Hermite homogeneous chaos (Wiener, 1938), Ghanem employed Hermite polynomials as orthogonal basis to represent random processes and applied the technique to solutions of many engineering problems with success, *e.g.* Spanos and Ghanem (1989); Ghanem (1998, 1999). To solve convergence and probability approximations for non-Gaussian problems, the gPC is proposed in Xiu and Karniadakis (2002): by using the Winer-Asker family of orthogonal polynomials, the gPC provides corresponding orthogonal polynomials as basis depending on the probability distribution of random inputs. Optimal convergence can thus be achieved by choosing theses proper basis. The effectiveness of gPC has been proved by many engineering applications such as Choi et al. (2004a); Hou et al. (2006); Manan and Cooper (2010); Sudret (2008); Kishor et al. (2011); Nechak et al. (2011). In practical application of gPC, it is critical to determine the coefficients of the gPC polynomials. Besides the Galerkin projection and collocation methods (Babuška et al., 2004; Xiu and Hesthaven, 2005), Choi et al. (2004a) provides the first application of a least squares based hybrid approach using a Latin Hypercube sampling (LHS) technique (Mckay et al., 1979) applied in a non-intrusive way. The regression approach and variance analysis are used to find the dominant polynomial coefficients. This method is also utilized by the work of Umesh and Ganguli (2013); Manan and Cooper (2010); Kishor et al. (2011) and this research. The in-depth treatment of gPC framework and associated mathematical backgrounds can be found in Ghanem and Spanos (1991); Xiu (2010) and references therein.

2.2 Backgrounds of H_∞ control

Extensive investigation of the H_∞ control design procedures are available in the literature, *e.g.* (Zhou et al., 1996). Here the optimal and suboptimal H_∞ control problems are introduced and the design procedures are briefly reviewed.

2.2.1 H_∞ control problem

To consider a set of control objectives with various control methods, the most general feedback control structure can be used, as illustrated in Figure 2.1, where $N(s)$ is the general plant, $K(s)$ the stable controller to be designed, $u(s)$ the control signal, $v(s)$ the input signal to $K(s)$, $p(s)$ the external signals, which could consist of the disturbance signal $d(s)$ and the measurement noise $n(s)$, and $q(s)$ the regulated signals to be minimized, which could consist of the system output $y(s)$ and the control signal $u(s)$. By partitioning $N(s)$ according to the sizes of the signals, the system is described as

$$\begin{bmatrix} q(s) \\ v(s) \end{bmatrix} = N(s) \begin{bmatrix} p(s) \\ u(s) \end{bmatrix} = \begin{bmatrix} N_{qp}(s) & N_{qu}(s) \\ N_{vp}(s) & N_{vu}(s) \end{bmatrix} \begin{bmatrix} p(s) \\ u(s) \end{bmatrix} \tag{2.1}$$

$$u(s) = K(s)v(s) \tag{2.2}$$

where $N_{qp}(s)$ represents the open-loop transfer function matrix from $p(s)$ to $q(s)$. The closed-loop transfer function matrix from p to q is given by the lower Linear Fractional Transformation (LFT) $\mathcal{F}_l(N, K)$ (Hecker, 2006):

$$\mathcal{F}_l(N, K)(s) = N_{qp}(s) + N_{qu}(s)K(s)(I - N_{vu}(s)K(s))^{-1}N_{vp}(s) \tag{2.3}$$

Elementary operations on LFT (addition, product, etc.) are defined in Zhou et al. (1996). Denote $T(s) = \mathcal{F}_l(N, K)(s)$, the closed-loop transfer function from the disturbance $d(s)$ to $y(s)$ or $u(s)$ can thus be represented by $T_{yd}(s)$ or $T_{ud}(s)$.

Naturally, the prerequisite for the controller $K(s)$ in Equation (2.2) is to internally stabilize the plant $N(s)$. Moreover, a proper controller $K(s)$ is said to be admissible if it internally stabilizes $N(s)$ (Zhou et al., 1996). The internal stability is an important property of any feedback system, as it ensures that

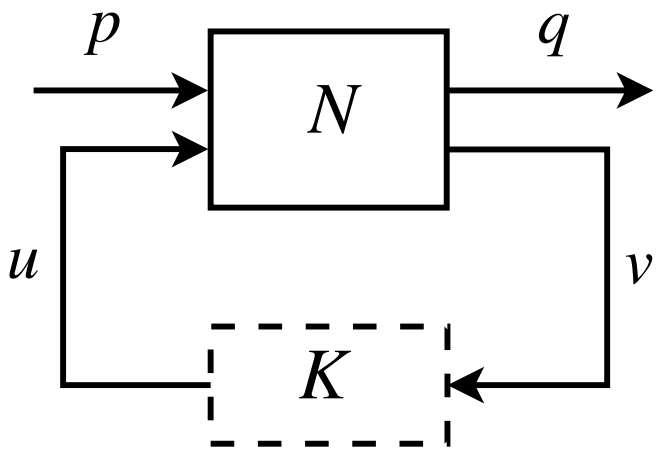

Figure 2.1: The most general feedback control structure

all internal signals are of bounded energy whenever the exogenous signals have bounded energy. Besides, the internal stability can be understood that, in the absence of exogenous perturbations, the states of $N(s)$ and $K(s)$ eventually converge to zero for any set of initial conditions. On the other hand, we have to define a measure how good the stabilizing $K(s)$ is. In H_∞ control theory, this measure is chosen in terms of the H_∞ norm of $T(s)$, that is,

$$||T(s)||_\infty = \sup_{\Re(s)>0} \bar{\sigma}(T(s)) = \sup_{\omega} \bar{\sigma}(T(j\omega)),\ \forall\omega \in \mathbb{R} \tag{2.4}$$

where $\mathbb{R}$ denotes the fields of real numbers, $\Re(s)$ represents the real part of the complex variable s and $\bar{\sigma}(A)$ the largest singular value of the matrix A defined as

$$\bar{\sigma}(A) = \max(\sigma_1, \sigma_2, \ldots, \sigma_n)$$

where σ_i is the singular value of the matrix A, which is defined as the square roots of the eigenvalues of the matrix A^*A, that is, $\sigma_i = \sqrt{\lambda_i(A^*A)}$. As for the SISO cases, there exists only one singular value being equivalent to $\sqrt{A(j\omega)^*A(j\omega)}$, the H_∞ norm represents the maximum gain of the transfer function, for example,

$$||T_{yd}(s)||_\infty = \sup_{\omega} |T_{yd}(j\omega)| \tag{2.5}$$

The illustration of a typical sensitivity transfer function $S(s)$ is shown in Fig-

ure 2.2. For the MIMO cases, $||T_{yd}(s)||_\infty$ can also be explained as

$$||T_{yd}(s)||_\infty = \sup_{\omega\in\mathbb{R}} \bar{\sigma}(T_{yd}(j\omega)) = \sup_{||d(j\omega)||\neq 0} \frac{||y(j\omega)||_2}{||d(j\omega)||_2} \tag{2.6}$$

with $y(j\omega) = T_{yd}(j\omega)d(j\omega)$.

Based on the definition of H_∞ norm, some useful properties of the H_∞ norm are introduced as follows. Let $G(s)$ and $H(s)$ be any transfer function matrices with appropriate dimensions. Then we have the following inequalities:

$$||G(s)H(s)||_\infty \leq ||G(s)||_\infty ||H(s)||_\infty \tag{2.7}$$

and

$$\begin{aligned} \left\| \begin{bmatrix} G(s) \\ H(s) \end{bmatrix} \right\|_\infty &\geq \|G(s)\|_\infty & \left\| \begin{bmatrix} G(s) \\ H(s) \end{bmatrix} \right\|_\infty &\geq \|H(s)\|_\infty \\ \left\| \begin{bmatrix} G(s) & H(s) \end{bmatrix} \right\|_\infty &\geq \|G(s)\|_\infty & \left\| \begin{bmatrix} G(s) & H(s) \end{bmatrix} \right\|_\infty &\geq \|H(s)\|_\infty \end{aligned} \tag{2.8}$$

The interpretations of H_∞ norm and its associate properties make the H_∞ norm useful in academical and engineering applications.

As defined in Zhou et al. (1996), the optimal H_∞ control problem is stated as follows

Optimal H_∞ Control: find an admissible controller $K(s)$ such that $||T(s)||_\infty$ is minimized.

In essence, this is a minimum optimization problem

$$\inf_{K \ stabilizing} ||T(s)||_\infty \tag{2.9}$$

subject to the constraint Equation (2.1) and (2.2). This provides a justification of the H_∞ control through the argument that minimizes the peak of $T_{yd}(j\omega)$, which necessarily renders the magnitude of $T_{yd}(j\omega)$ small at all frequencies. By incorporating appropriate weighting functions into $T_{yd}(j\omega)$, the H_∞ control can emphasize the frequency-dependent control requirements. This improvement of

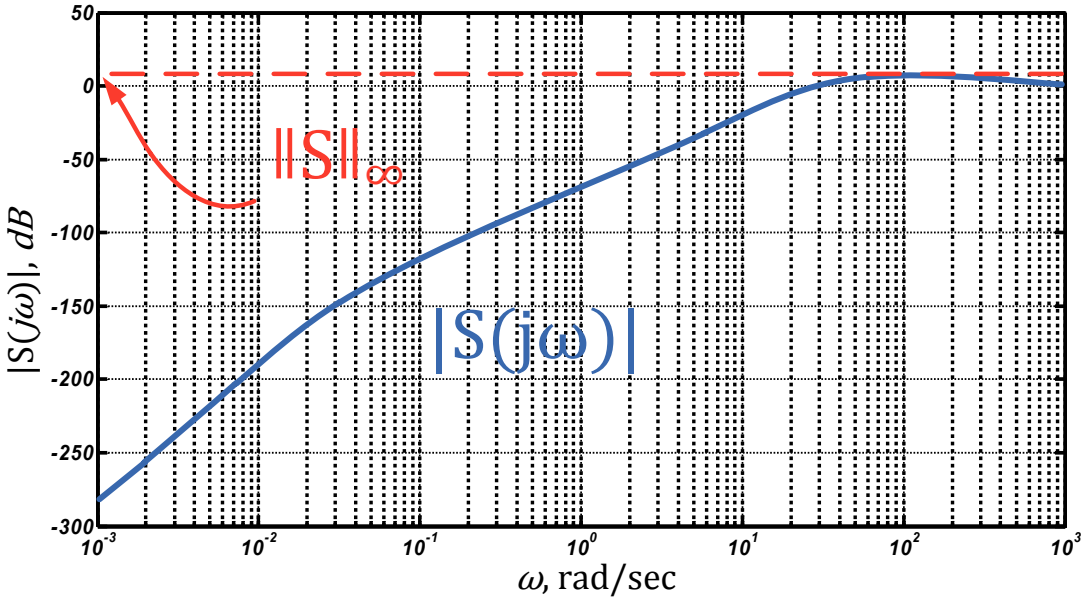

Figure 2.2: The H_∞ norm of the transfer function $S(j\omega)$ for the SISO cases (Korniienko, 2011)

the worst-case scenario in the frequency domain is very useful for active vibration control and particularly attractive for lightly damped flexible strictures with piezoelectric actuators since their limited available actuation power makes the piezoelectric actuators impossible to achieve effective vibration reduction for all resonant modes. As a result, a frequency-dependent positive function is practically required to define the controlled resonant modes with corresponding levels of vibration reduction (Zhang et al., 2013a).

However, it is notable that the optimal H_∞ control problem as defined above is often both numerically and theoretically complicated (Glover and Doyle, 1989). As claimed in (Zhou et al., 1996), knowing the achievable optimal (minimum) H_∞ norm may be useful theoretically since it sets a limit on what we can achieve. However, in practice, it is often not necessary and sometimes even undesirable to design an optimal controller, and it is usually much cheaper to obtain controllers that are very close in the norm sense to the optimal ones, which will be termed as suboptimal controllers. A suboptimal controller may also have other better properties than the optimal ones such as lower bandwidth.

Suboptimal H_∞ Control: Given $\gamma > 0$ find an admissible controller $K(s)$ such that

$$||T(s)||_\infty < \gamma \tag{2.10}$$

subject to the constraint Equation (2.1) and (2.2). The suboptimal design can be refined through an iterative search technique to obtain a value of γ as close to the minimum achievable $\gamma_{opt} := \min\{||T(s)||_\infty : \ K(s) \text{ admissible}\}$ as desired.

2.2.2 Augmented system with weighting functions

In H_∞ control, according to the set of control objectives, necessary and appropriate input and output weighting functions are required to account for the relative magnitude of various signals, their frequency dependence and relative importance. In addition, since we normally have frequency-dependent control objectives, which are closely related to the magnitudes of some closed-loop transfer functions, the weighting functions have to reflect such frequency-dependent upper bounds on the magnitudes of these closed-loop transfer functions. For example, as illustrated in Figure 2.3, the bound $\ell_{\text{trk}}(\omega)$ on the magnitude of the tracking error transfer function $H_{\text{trk}}(j\omega)$, *i.e.* $|H_{\text{trk}}(j\omega)| \leq \ell_{\text{trk}}(j\omega), \ \forall\omega$, ensures that the tracking error transfer function is below 20dB at frequencies below 10Hz and rolls off below 1Hz. To reflect this frequency-dependent requirement on $H_{\text{trk}}(j\omega)$, appropriate weighting functions $W_{\text{cmd}}(j\omega)$ and $W_{\text{trk}}(j\omega)$ are used and $\ell_{\text{trk}}(\omega) = \gamma|W_{\text{cmd}}(j\omega)W_{\text{trk}}(j\omega)|^{-1}$. For this SISO case, based on the basic property of H_∞ norm, we have

$$||W_{\text{trk}}(s)H_{\text{trk}}(s)W_{\text{cmd}}(s)||_\infty \leq \gamma \Leftrightarrow |H_{\text{trk}}(j\omega)| \leq \ell_{\text{trk}}(\omega), \ \forall\omega \tag{2.11}$$

Note that the selection of weighting functions considerably determines the effectiveness of the H_∞ control design, *e.g.* which control objective can be considered with H_∞ control and how to make a trade-off among various control objectives (Balas and Doyle, 1994).

The weighting functions are then incorporated into the general control structure $N(s)$ to construct the general H_∞ control structure, as shown in Figure 2.4, where $P(s)$ is the augmented plant, $w(s)$ the exogenous input signals, $z(s)$ the

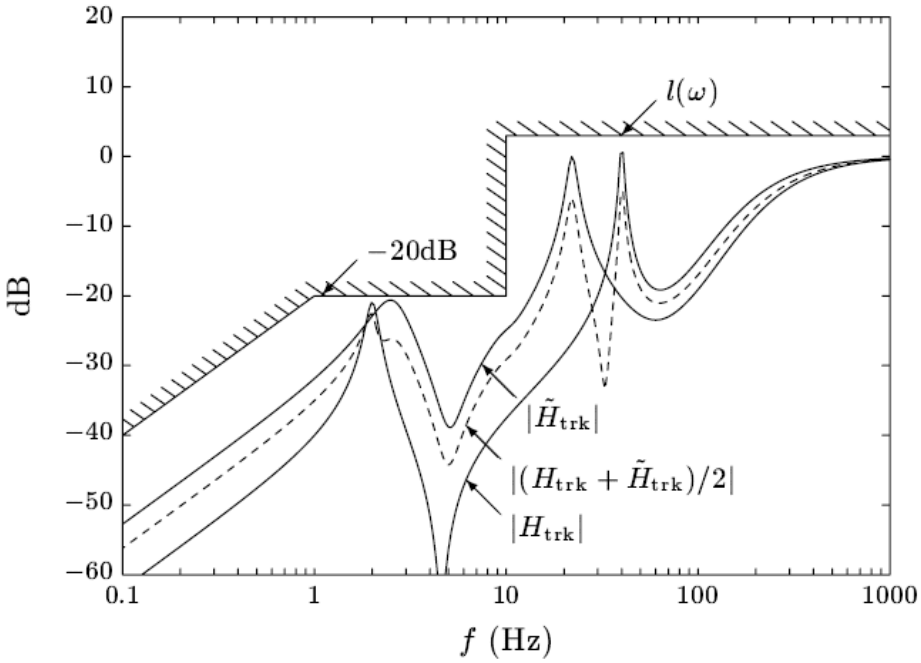

Figure 2.3: Upper bounds on frequency response magnitude of $H_{\rm trk}(j\omega)$. Two transfer functions $H_{\rm trk}(j\omega)$ and $\bar{H}_{\rm trk}(j\omega)$ that satisfy the specification of (2.11) are shown together with their average (on page 185 of Boyd and Barratt (1992))

weighted regulated signals. Compared to the general control structure of Figure 2.1, the input weighting function matrix $W_{\rm in}(s)$ with appropriate dimensions provides the relationship between the external signal $p(s)$ and the new exogenous input $w(s)$, that is, $p(s) = W_{\rm in}(s)w(s)$. Similarly, the output weighting function matrix $W_{\rm out}(s)$ with appropriate dimensions provides the relationship between the regulated signal $q(s)$ and the new weighted one $z(s)$, that is, $z(s) = W_{\rm out}(s)q$. Naturally, we have $P(s) = W_{\rm out}(s)N(s)W_{\rm in}(s)$ and, by partitioning $P(s)$ according to the sizes of the signals, the augmented system is described as

$$\begin{bmatrix} z(s) \\ v(s) \end{bmatrix} = P(s) \begin{bmatrix} w(s) \\ u(s) \end{bmatrix} = \begin{bmatrix} P_{zw}(s) & P_{zu}(s) \\ P_{vw}(s) & P_{vu}(s) \end{bmatrix} \begin{bmatrix} w(s) \\ u(s) \end{bmatrix} \tag{2.12}$$

$$u(s) = K(s)v(s) \tag{2.13}$$

The weighted closed-loop transfer function matrix $T_{zw}(s)$ from w to z is given by

the lower Linear Fractional Transformation $\mathcal{F}_l(P, K)$, that is,

$$T_{zw}(s) = \mathcal{F}_l(P, K)(s) = P_{zw}(j\omega) + P_{zu}(j\omega)K(j\omega)(I - P_{vu}(j\omega)K(j\omega))^{-1}P_{vw}(j\omega)$$

For the augmented system, the suboptimal H_∞ control problem is formulated to find a controller $K(s)$ such that $||T_{zw}(s)||_\infty < \gamma$ subject to Equation (2.12) and (2.13). According to the property of the H_∞ norm as expressed in Equation (2.8), $||T_{zw}(s)||_\infty < \gamma$ ensures the $||T_{z_i w_j}(s)||_\infty < \gamma$ for every i and j. For example, using suitable weighting functions $W_{\text{in}}(s)$ and $W_{\text{out}}(s)$, γ can be chosen to one and thus a set of control objectives represented by the constraints on $||T_{z_i w_j}(s)||_\infty < 1$ can be satisfied simultaneously by the designed $K(s)$, *e.g.* the H_∞ control design provides us the mechanisms into $K(s)$ that achieves effective vibration reduction as desired and also provides moderate control energy to avoid the control saturation problem and the excessive wear of actuators. For the sake of simplicity, with the augmented plant $P(s)$ one solution to the H_∞ controller synthesis is presented in Appendix A.

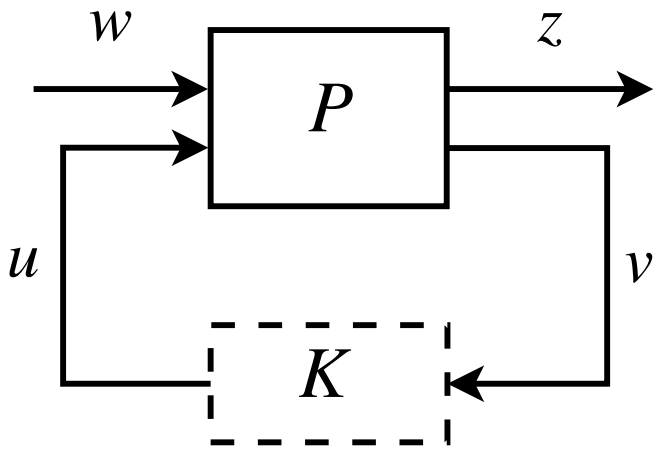

Figure 2.4: The general H_∞ control structure

2.3 Outlines of the robustness analysis

It is notable that the above mentioned H_∞ control design is based on the augmented mathematical model of the plant, which is constructed by incorporating

weighting functions into the general model $N(s)$. However, $N(s)$ is derived with the analytical formulations or the finite element method (FEM), where various assumptions and simplifications are used, *e.g.* linear elasticity, perfect bonding of the actuators, neglecting high frequency dynamics of the plant, and ignoring the sensor and actuator dynamics, or $N(s)$ is obtained by the system identification, which can only provide dynamical models with the finite frequency dynamics and a certain level of parameter errors due to the hardware limitations or the problems of the identification algorithms. As a result, $N(s)$ can only be a nominal representation of the practical controlled plant. As the controller is designed based on the nominal $N(s)$, the robustness analysis is desirable to verify the robustness properties of the closed-loop systems with respect to the model uncertainties. The following terms are extensively used in the literature (Skogestad and Postlethwaite, 2005):

- Nominal stability (NS): the system is stable with no model uncertainty;
- Nominal performance (NP): the system satisfies the performance specifications with no model uncertainty;
- Robust stability (RS): the system is stable for all perturbed plants about the nominal model up to the worst-case model uncertainty;
- Robust performance (RP): the system satisfies the performance specifications for all perturbed plants about the nominal model up to the worst-case model uncertainty.

2.3.1 Deterministic robustness analysis

In the deterministic robustness analysis, the worst case is investigated such that the robustness properties of the closed-loop system can be verified for any possible models in the presence of allowable uncertainties. Two cases with respect to the uncertainties can be considered in the deterministic robustness analysis: the sources and the characteristics of the uncertainties are not considered, in which case some general class of unstructured uncertainty representations such as an additive uncertainty is used and the small gain theorem (Zames, 1966) is then

applied to check the robustness properties; in other design situations, the sources and the characteristics of the uncertainties are precisely known, in which case a structured uncertainty representation can be used and the μ analysis (Packard and Doyle, 1993) is recommendable.

Several versions of the small gain theorem are available in the literature. The version presented here is sufficient to illustrate its importance and links well with the robust performance theorem for μ analysis. Let $\mathcal{RH}_\infty^{n\times n}$ denote proper real-rational stable transfer function matrices and the transfer function matrix $M(s) \in \mathcal{RH}_\infty^{n\times n}$ includes the designed controller based on the nominal dynamical models. If the uncertainty $\Delta \in \mathcal{RH}_\infty^{n\times n}$ is allowed to be any H_∞ norm bounded complex transfer function matrix, it is usually referred to as unstructured uncertainty, for example, the unstructured uncertainty Δ only represents a dynamic uncertainty. On the other hand, if parametric uncertainty or several dynamic uncertainties have to be considered, the structured uncertainty $\Delta \in \mathcal{RH}_\infty^{n\times n}$ is desirable, which can consider various sources of uncertainties by a diagonal block, *i.e.* $\Delta = \text{diag}(\Delta_1, \Delta_2, \cdots, \Delta_n)$ (Skogestad and Postlethwaite, 2005).

Theorem 2.3.1. (**Small gain theorem**) *Consider the feedback interconnection depicted in Figure 2.5, suppose $M \in \mathcal{RH}_\infty^{n\times n}$ and let $\gamma > 0$. Then this feedback control structure is internally stable for any unstructured uncertainty $\Delta \in \mathcal{RH}_\infty^{n\times n}$ with $||\Delta||_\infty \leq 1/\gamma$ $(< 1/\gamma)$ if and only if $||M||_\infty < \gamma$ $(\leq \gamma)$ (Skogestad and Postlethwaite, 2005).*

It can be shown that the above small gain condition is sufficient to guarantee internal stability even if Δ is a nonlinear time-varying stable operator, given an appropriately defined stability notion (Desoer and Vidyasagar, 1975). As above stated, although the small gain theorem can be used directly to derive robust stability and performance results, it may be very conservative for systems with structured uncertainty. The exact stability and performance analysis for such systems requires the definition of another matrix function called the structured singular value, denoted by μ.

In the case that the sources of uncertainty are explicitly known, the structured uncertainty Δ has to be used and M can always be chosen so that Δ is block

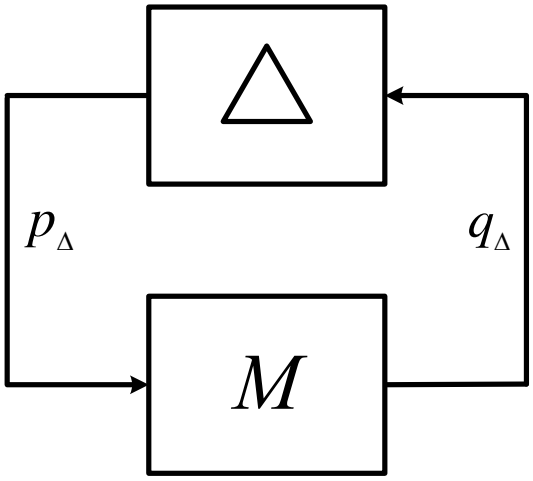

Figure 2.5: General $M - \Delta$ feedback configuration

diagonal, that is, $\Delta \in \underline{\boldsymbol{\Delta}}$

$$\underline{\boldsymbol{\Delta}} \triangleq \{\text{diag } \left(\delta_1^r I_{t_1}, \ldots, \delta_V^r I_{t_V}, \delta_{V+1}^c I_{r_1}, \ldots, \delta_{V+S}^c I_{r_S}, \Delta_{V+S+1}, \ldots, \Delta_{V+S+F}\right) : \\ \delta_k^r \in \mathbb{R},\ \delta_{V+i}^c \in \mathbb{C},\ \Delta_{V+S+j} \in \mathbb{C}^{m_j \times m_j}, 1 \leq k \leq V,\ 1 \leq i \leq S, 1 \leq j \leq F\}$$

where $\mathbb{R}$ and $\mathbb{C}$ denote the fields of real and complex numbers, δ_k^r represents the k^{th} real scalar parametric uncertainty with t_k repetition, δ_{V+i}^c represents the i^{th} repeated complex scalar uncertainty with r_i repetition and Δ_{V+S+j} represents the j^{th} full dynamic uncertainty with size $m_j \times m_j$. Note that to apply μ analysis, various original parametric uncertainties such as material or geometrical uncertainties on the structures have to be reflected by δ_k^r and the neglected dynamics of the system can be represented by δ_{V+i}^c or Δ_{V+S+j}. In practice, by incorporating suitable normalization functions in N, we have $\delta_k^r \in [-1, 1]$, $|\delta_i^c| \leq 1$ and $\bar{\sigma}(\Delta_j) \leq 1$ and the notation $\boldsymbol{B}_\Delta$ is introduced for the norm bounded diagonal uncertainty block, that is,

$$\boldsymbol{B}_\Delta := \{\Delta \in \underline{\boldsymbol{\Delta}} :\ \bar{\sigma}(\underline{\boldsymbol{\Delta}}) \leq 1\} \tag{2.14}$$

Based on the structured uncertainty set $\underline{\boldsymbol{\Delta}}$, the structured singular value of constant matrices is defined as

Definition 2.3.1. *Suppose $M \in \mathbb{C}^{m \times n}$ and let $\underline{\boldsymbol{\Delta}}$ be a specifical set which deter-*

mines the structure of the uncertainty Δ. *Then the structured singular value of* M *with respect to the structured uncertainty* Δ *is defined by*

$$\mu_{\Delta}(M) := \frac{1}{\min\{\bar{\sigma}(\Delta) |\ \det(I - M\Delta) = 0,\ \Delta \in \underline{\mathbf{\Delta}}\}} \tag{2.15}$$

if no $\Delta \in \underline{\mathbf{\Delta}}$ *makes* $\det(I - M\Delta) = 0$ *singular, in which case* $\mu_{\Delta}(M) = 0$.

Conceptually, the structured singular value is nothing but a straightforward generalization of the singular values for constant complex matrices. To be more specific, consider again the robust stability problem depicted in Figure 2.5, where both $M(s)$ and $\Delta(s)$ are stable. One critical point is to calculate how large Δ can be (in the sense of $||\Delta||_{\infty}$) without destabilizing the feedback system. Since the closed-loop poles are given by the values of Δ such that $\det(I - M(s)\Delta(s)) = 0$, the feedback system becomes unstable if $\det(I - M(s)\Delta(s)) = 0$ for some s at the closed right-half plane. Now, let $k > 0$ be a sufficiently small number so that the closed-loop system is internally stable for all $\Delta \in \mathcal{RH}_{\infty}^{n \times n}$ with $||\Delta||_{\infty} < k$. Then, start increasing the value k until the closed-loop system just becomes unstable. Denote the value of k which just makes the loop unstable by k_m. Based on the small gain theorem, it is obvious that if Δ is unstructured

$$||M(s)||_{\infty} := \sup_{\omega} \bar{\sigma}(M(j\omega)) = \frac{1}{k_m} \tag{2.16}$$

Therefore, according to the Theorem 2.3.1, for any ω, $\bar{\sigma}(M(j\omega))$ can be written as

$$\bar{\sigma}(M(j\omega)) = \frac{1}{\min\{\bar{\sigma}(\Delta(j\omega)) |\ \det(I - M\Delta) = 0,\ \Delta \text{ is unstructured}\}}$$

In other words, the reciprocal of the largest singular value of $M(s)$ is a measure of the smallest unstructured uncertainty that causes instability of the feedback system. Then, the following theorem is a natural extension of the small gain theorem to the structured uncertainty case (Packard and Doyle, 1993):

Theorem 2.3.2. (**Robust stability**) *Consider the feedback interconnection depicted in Figure 2.5, suppose* $M \in \mathcal{RH}_{\infty}^{n \times n}$ *and let* $\gamma > 0$. *Then this feedback control structure is internally stable for any structured uncertainty* $\Delta \in \mathcal{RH}_{\infty}^{n \times n}$

with $||\Delta||_\infty \leq 1/\gamma$ $(< 1/\gamma)$ *if and only if* $\sup_\omega \mu_\Delta(M(j\omega)) < \gamma$ $(\leq \gamma)$, *where the set* $\underline{\mathbf{\Delta}}$ *determines the structure of* Δ.

As $\mu_\Delta(M(j\omega))$ is a function of the frequency ω, their relationship is usually illustrated by the μ-plot over the frequency range of interest. This theorem implies that the peak value of the μ-plot of $M(j\omega)$ determines the size of the perturbations that the loop is robustly stable against. Therefore, a great deal of attention has to be paid to the critical frequencies to have reliable $\mu_\Delta(M(s))$.

Usually, the stability is not the only problem of a closed-loop system that must be robust to the model uncertainties. In most cases, long before the closed-loop system is destabilized, the closed-loop performance becomes unacceptable, for instance, the vibration reduction of a controlled resonant mode is not satisfied with respect to the a priori defined specification of vibration reduction. Therefore, the robust performance has also to be considered. With Linear Fractional Transformation (LFT), both robust stability and robust performance can be investigated in a unified framework. Based on the unit framework, the following theorem gives the robust performance analysis test (Packard and Doyle, 1993):

Theorem 2.3.3. (**Robust performance**) *Consider the feedback interconnection depicted in Figure 2.6, suppose* $\bar{N} \in \mathcal{RH}_\infty$ *and let* $\gamma > 0$. *Then this feedback control structure is internally stable and satisfies* $||\mathcal{F}_u(\bar{N}, \Delta)(s)||_\infty < \gamma$ *for any structured uncertainty* $\Delta \in \mathcal{RH}_\infty$ *with* $||\Delta||_\infty \leq 1/\gamma$ *if and only if*

$$\sup_\omega \mu_{\hat{\Delta}}(\bar{N}(j\omega)) < \gamma$$

where $\mathcal{F}_u(\bar{N}, \Delta)(s)$ is the closed-loop transfer function from $p(s)$ to $q(s)$ as defined in Equation (2.18), the augmented uncertainty $\hat{\Delta}$ belongs to the set $\underline{\hat{\mathbf{\Delta}}} := \{\text{diag}(\Delta, \Delta_{Perf}) : \Delta \in \underline{\mathbf{\Delta}}, \Delta_{Perf} \in \mathbb{C}^{m\times n}\}$, the set $\underline{\mathbf{\Delta}}$ determines the structure of Δ and the m, n are the dimensions of p and q.

This theorem is important to verify the robust performance and shows that the robust performance is equivalent to the robust stability with the augmented uncertainty $\underline{\hat{\mathbf{\Delta}}}$, *e.g.* compared to Figure 2.5 a fictitious uncertainty Δ_{Perf} is added in Figure 2.6. By partitioning $\bar{N}(s)$ compatibly with the dimension of Δ we have

$$\begin{bmatrix} q_\Delta \\ q \end{bmatrix} = \begin{bmatrix} \bar{N}_{11} & \bar{N}_{12} \\ \bar{N}_{21} & \bar{N}_{22} \end{bmatrix} \begin{bmatrix} p_\Delta \\ p \end{bmatrix} \tag{2.17}$$

Obviously, the $M(s)$ of Figure 2.5 for robust stability analysis is $\bar{N}_{11}(s)$. The closed-loop transfer function from $p(s)$ to $q(s)$ is represented by the upper LFT, $\mathcal{F}_u(\bar{N}, \Delta)$ (Hecker, 2006),

$$q(s) = \mathcal{F}_u(\bar{N}, \Delta)p(s) = (\bar{N}_{22} + \bar{N}_{21}\Delta(I - \bar{N}_{11}\Delta)^{-1}\bar{N}_{12})p(s) \tag{2.18}$$

In practice, before applying the theorems outlined above to verify the robustness properties of the closed-loop system, the model uncertainties are usually normalized and corresponding weighting functions are incorporated into $\bar{N}$ to make $||\Delta||_\infty \leq 1$. Besides, as discussed above, to reflect the frequency-dependent control objectives, a performance weighting function $W_{\text{perf}}(s)$ has to be incorporated into $\bar{N}$, which also normalizes $||\Delta_{\text{perf}}||_\infty \leq 1$. The notation $\boldsymbol{B}_{\underline{\hat{\boldsymbol{\Delta}}}}$ is thus introduced for the unit normalized diagonal augmented uncertainty, that is,

$$\boldsymbol{B}_{\hat{\Delta}} := \{\hat{\Delta} \in \underline{\hat{\boldsymbol{\Delta}}} : \ \bar{\sigma}(\underline{\hat{\boldsymbol{\Delta}}}) \leq 1\}$$

Therefore, for any $\hat{\Delta} \in \boldsymbol{B}_{\underline{\hat{\Delta}}}$, the robust performance can be transformed to $||\mathcal{F}_u(\bar{N}, \hat{\Delta})(s)||_\infty < 1$ and Theorem 2.3.3 provides the condition for the robust performance:

$$\sup_\omega \mu_{\hat{\Delta}}(\bar{N}(j\omega)) < 1 \tag{2.19}$$

This implies that unit normalized structured uncertainty Δ and the $|W_{\text{perf}}(j\omega)|$ can be simultaneously enlarged by $1/\sup_\omega \mu_{\hat{\Delta}}(\bar{N}(j\omega))$ before the closed-loop performance is violated. In addition, for any $\Delta \in \boldsymbol{B}_\Delta$, Theorem 2.3.2 provides the condition for the robust stability:

$$\sup_\omega \mu_\Delta(M(j\omega)) < 1 \tag{2.20}$$

This implies that the unit normalized structured uncertainty Δ can be enlarged by the robustness stability margin $k_m = 1/\sup_\omega \mu_\Delta(M(j\omega))$ before the closed-loop system is destabilized.

2.3 Outlines of the robustness analysis

In deterministic robustness, the general LFT framework of Figure 2.6 can be used for both the robust stability and the robust performance. In addition, since the structure of $N - \Delta$ is very general, various sources of uncertainty, such as parametric, dynamic, structured and unstructured, can be easily taken into account by the general uncertainty Δ. For these reasons, the LFT framework is a valuable tool for both practitioners and theoreticians by applying the above theorems. However, this classical worst-case robustness analysis has also shown some limitations when the control system is affected by general structured uncertainty structures, especially for uncertainties entering in a nonlinear fashion into the control system. To investigate these limitations, a great research effort focuses on complexity issues of feedback system such as Poljak and Rohn (1993); Nemirovskii (1993); Coxson and DeMarco (1994). These researches demonstrate that the above deterministic robustness analysis is NP-hard (Braatz et al., 1994; Blondel and Tsitsiklis, 2000), and thus lower and upper bounds of μ are usually calculated to approximate its accurate value (Young and Dolye, 1990; Young et al., 1992; Ferreres et al., 2003). It also implies that the deterministic robustness could be practically intractable, unless the number of uncertainties entering into the feedback system is very limited (Calafiore et al., 2000). To avoid this drawback, many other contributions attack the same problem following a parallel line of research, with the goal of computing upper and lower bounds (instead of the accurately true value) of the robustness margins for a very general structured Δ, for instance, Matlab Robust Control Toolbox R2012 makes use of the results from Young and Dolye (1990) and Young et al. (1992), where the frequency gridding is used over frequency ranges of interest. With these methods, the nice point is that the upper bound of μ which evaluates the closed-loop robustness properties can be computed via convex optimization such as the interior point methods (Boyd et al., 1994). Note that despite these efforts, the conservatism involved in deterministic robustness analysis is still present. On the other hand, for lightly damped flexible structures, the critical frequencies could be neglected and thus the robustness margins could be also overestimated (Freudenberg and Morton, 1992). Another remarkable feature of the deterministic robustness analysis is that all uncertainties are always assumed to be deterministic, for example, just simple bounds on parametric uncertainties are used. However, in many prac-

tical cases, there is also probabilistic information of parametric uncertainty to be considered.

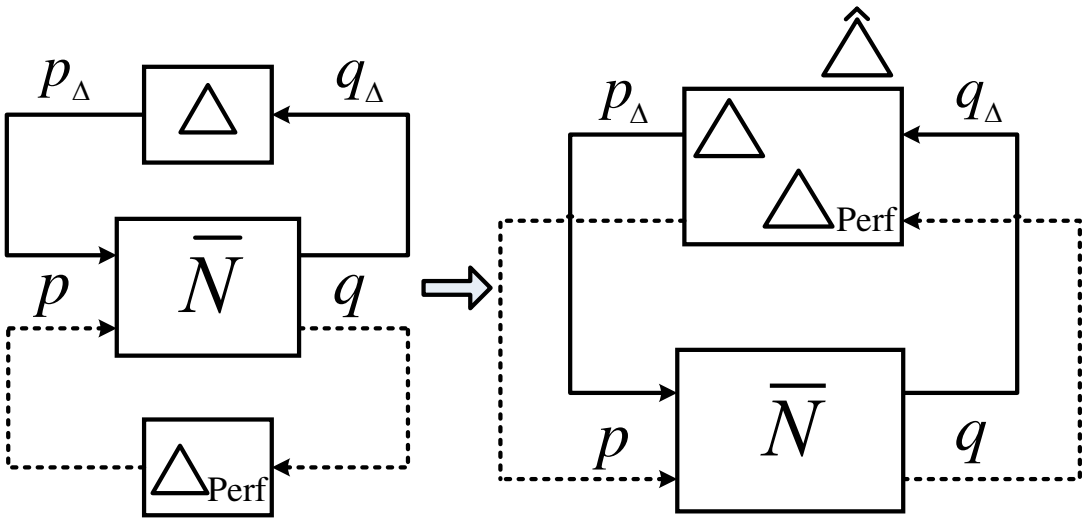

Figure 2.6: A general LFT framework for robust performance analysis

2.3.2 Probabilistic robustness analysis

In order to overcome the difficulties involved in deterministic robustness analysis as discussed previously, the probabilistic robustness analysis has been developed as an effective tool to deal with the general uncertainty. For an in-depth understanding of this method, the reader may refer to the books Tempo et al. (2005); Calafiore and Dabbene (2002, 2006). The motivation of these methods is to assume that the uncertainty affecting the system has a probabilistic nature. This assumption appears to be natural in many practical applications especially when parametric uncertainties are considered. The objective is then to verify the probabilistic robustness properties of the closed-loop system such as the probabilistic robustness margins and the probability degradation function. In other words, a given control performance, *e.g.* $||\mathcal{F}_u(N,\Delta)(s)||_\infty < 1$, is robustly satisfied in a probabilistic sense if it is guaranteed against most, although not all, possible uncertainty models, and one accepts the risk of a system property being violated by a set of uncertainties with a small probability measure. Such systems are claimed to be practically robust from an engineering point of view (Calafiore et al., 2011).

2.3 Outlines of the robustness analysis

In spite of the interesting features of the probabilistic robustness analysis, it must be noted that the probabilistic robustness analysis does not mean a simplification of the problem. Actually, sometimes estimating the probabilistic robustness properties may be even computationally harder than establishing the deterministic ones, since it requires the computation of multidimensional probability integrals (Calafiore et al., 2011). These integrals can be evaluated exactly only in very special cases of limited practical interest. To solve the computational problem, several randomized techniques can be used. They have been used extensively in various branches of science and engineering to tackle difficult problems that are too hard to be treated via exact deterministic methods, for instance, the Monte Carlo Simulation used in computational physics, simulations, financial risk analysis, and the Las Vegas techniques employed in computer science. Some specific techniques are developed for generating random samples of the structured uncertainty acting on the system (Tempo et al., 2005). The probability is estimated using a finite number of random samples, and tail inequalities are used to bound the estimation error. One nice point of the sampling number is that it is independent on the number of the controller and the uncertainty considered in the closed-loop system (Tempo et al., 1997). The resulting algorithms are called randomized algorithms (RAs), *i.e.* algorithms that make random choices during execution to produce a result. It has been demonstrated that, in the context of systems and control, RAs have low complexity and are associated with the robustness bounds which are less conservative than the classical ones, obviously at the expense of a probabilistic risk (Tempo et al., 2005).

This probabilistic robustness analysis is not an alternative to the deterministic robustness analysis that performs the worst-case analysis, but it provides useful and complementary information to the deterministic robustness analysis. In some extend, it can be applied to verify the reliability of the deterministic robustness margins and used in conjunction with the deterministic robustness analysis to obtain additional information such as the probabilistic degradation of the system stability and the control performance when the uncertainty level goes beyond the deterministic robustness margins. In essence, the definitions of robustness properties used in probabilistic robustness analysis are different from those defined in deterministic robustness analysis. These definitions determine corresponding

characteristics and advantages of deterministic and probabilistic analysis. Therefore, to make full use of these robustness analysis, they are desirable to be used simultaneously to compare and complement each other.

2.4 A simple example of H_∞ control design

2.4.1 H_∞ control design

In this section, to illustrate the basic design processes of H_∞ control and the robustness analysis as discussed above, we consider the design of robust controllers for active vibration of a simple and typical mechanical system, namely a mass-damper-spring (MDS) system, and also investigate the robustness properties of the closed-loop system. The MDS system is a common experimental device frequently used in mechanical and control laboratories. Since it is a second-order system, it can represent a specifical resonant mode of flexible structures and only parametric uncertainties have to be considered in the robustness analysis.

The active vibration control of a second-order MDS system is illustrated in Figure 2.7 and using Newton's second law, the dynamics of such a system can be described by the following differential equation,

$$m\ddot{x}(t) + c\dot{x}(t) + kx(t) = F(t)$$

where m, c, k are the physical mass, damping and spring constants of the system, $x(t)$ is the displacement of the mass block from the equilibrium position, $F(t)$ is the external force acting on the mass. Applying Laplace transformation and assuming zero initial conditions, the transfer function $G(s)$ representing the dynamics from $F(s)$ to $X(s)$ is

$$G(s) = \frac{X(s)}{F(s)} = \frac{1/m}{s^2 + c/ms + k/m} = \frac{g}{s^2 + 2\zeta\omega_n s + \omega_n^2} \tag{2.21}$$

where $g = 1/m$, $\zeta = \frac{c}{2\sqrt{km}}$, $\omega_n = \sqrt{k/m}$ are the gain, the damping ratio and the natural frequency of the system, which are usual modal parameters to define vibration characteristics of the system (Meirovitch, 1986). It is notable that, for

effective vibration control of practical structures, the modal parameters such as ζ and ω_n are most important and more available to be identified by different methods, *e.g.* the modal test (Ewins, 2000), the system identification (Ljung, 1999) and so on.

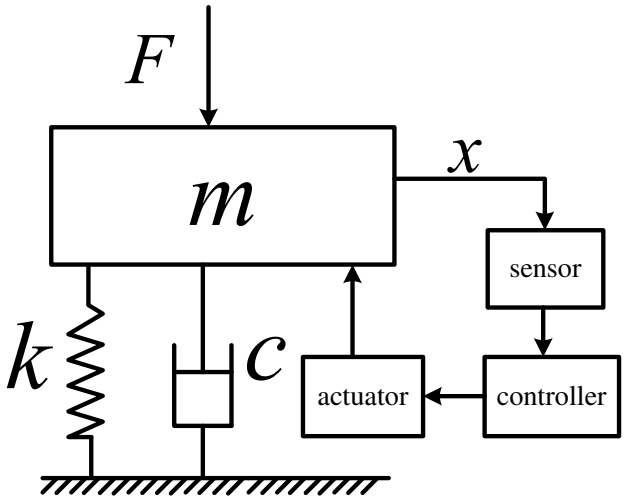

Figure 2.7: Active vibration control of a second-order mass-damper-spring system

For this MDS example, a stabilizing controller $K(s)$ is required to have desired specification of vibration reduction and enforce constraints on the control energy. As illustrated in Zhang et al. (2013a), the sensitivity transfer $S(s)$ function can be used to define the specification of vibration reduction and the constraints on the closed-loop transfer function $K(s)S(s)$ allow us to limit the control power due to that fact that (Scorletti and Fromion, 2008a)

$$\begin{aligned}\lim_{T\to\infty}\frac{1}{T}\int_{-\frac{T}{2}}^{+\frac{T}{2}}||u(t)||^2dt &= \frac{1}{2\pi}\int_{-\infty}^{+\infty}\mathcal{S}_u(j\omega)d\omega \\ &\leq \frac{1}{2\pi}\int_{-\infty}^{+\infty}\bar{\sigma}(T_{ud}(j\omega))\mathcal{S}_d(j\omega)d\omega\end{aligned}$$

where $\mathcal{S}_d(j\omega)$ represents the power spectral density of the disturbance signal $d(s)$ and $T_{ud}(j\omega) = K(j\omega)S(j\omega)$. This demonstrate that by limiting the singular value of $K(j\omega)S(j\omega)$ the control energy is also limited.

Besides, as discussed above, the requirements on these closed-loop transfer

functions are usually frequency-dependent. Therefore, as shown in Figure 2.8, the common mixed sensitivity control structure is constructed, where $d(s)$ is the disturbance signal such the initial displacement of the mass, $y(s)$ the system output, $v(s)$ and $u(s)$ the input and output signals to the controller $K(s)$, and $W_i(s)$ represents related weighting function to represent the frequency characteristics of these signals and the control performances related to $S(s)$ and $K(s)S(s)$. This control structure allows us to impose frequency-dependent requirements on $S(s)$ and $K(s)S(s)$ simultaneously. According to the nominal values of m, k, we have the only natural frequency of the MDS system, *i.e.* $\omega_n = \sqrt{k/m}$ and then the weighting functions can be tuned to provide a suitable cross-over frequency of $S(s)$ such that a satisfactory vibration reduction is obtained in the frequency range of interest.

Naturally, the original H_∞ control objectives of this MDS system are to find a stabilizing controller $K(s)$ such that

$$||W_y(s)S(s)W_d(s)||_\infty \leq 1 \tag{2.22}$$

$$||W_u(s)K(s)S(s)W_d(s)||_\infty \leq 1 \tag{2.23}$$

However, there does not exist an efficient algorithm to solve this control problem. Motivated by the property of the H_∞ norm, we can design a controller $K(s)$ such that

$$\left\| \begin{bmatrix} W_y(s)S(s)W_d(s) \\ W_u(s)K(s)S(s)W_d(s) \end{bmatrix} \right\|_\infty \leq 1 \tag{2.24}$$

Fortunately, the Equation (2.24) can guarantee the original control objectives and can be solved using efficient polynomial-time algorithms as implemented in Matlab Robust Toolbox.

As described in the general H_∞ control structure of Figure 2.4, we have

$$d(s) = W_d(s)w(s),\ z(s) = \begin{bmatrix} z_1(s) \\ z_2(s) \end{bmatrix} = \begin{bmatrix} W_y(s) & 0 \\ 0 & W_u(s) \end{bmatrix} \begin{bmatrix} y(s) \\ u(s) \end{bmatrix}$$

and the augmented plant $P(s)$ can be partitioned appropriately as

$$P_{zw}(s) = \begin{bmatrix} W_d(s)W_y(s) \\ 0 \end{bmatrix} \quad P_{zu}(s) = \begin{bmatrix} G(s)W_v(s) \\ W_u(s) \end{bmatrix}$$
$$P_{vw}(s) = W_d(s) \qquad P_{vu}(s) = G(s)$$

As performed in Scorletti and Fromion (2008a), to reduce the complexity and the order of $P(s)$ being equal to the order of the designed H_∞ controller, $P(s)$ is reformulated as

$$P(s) = \begin{bmatrix} W_d(s)W_y(s) & G(s)W_y(s) \\ 0 & W_u(s) \\ W_d(s) & G(s) \end{bmatrix} = \begin{bmatrix} 0 & W_y(s) \\ I & 0 \\ 0 & I \end{bmatrix} \begin{bmatrix} 0 & W_u(s) \\ W_d(s) & G(s) \end{bmatrix}$$

where all the elements occur just one time. With $P(s)$, $K(s)$ is ready to be obtained and satisfy the control objectives as described in Equation (2.22) and (2.23).

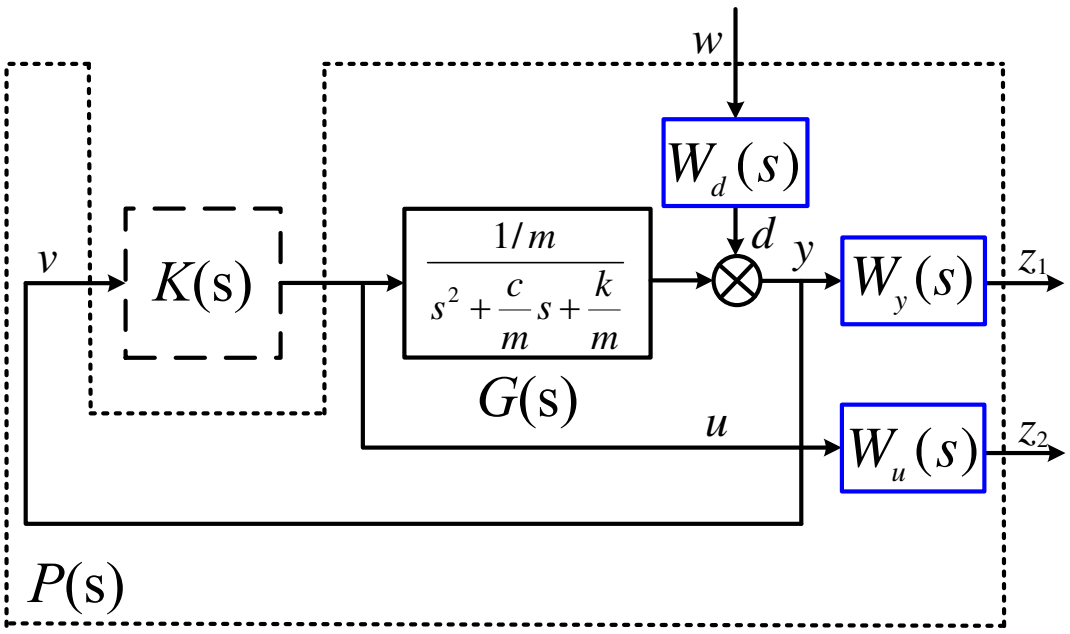

Figure 2.8: Mixed sensitivity design structure for the MDS system

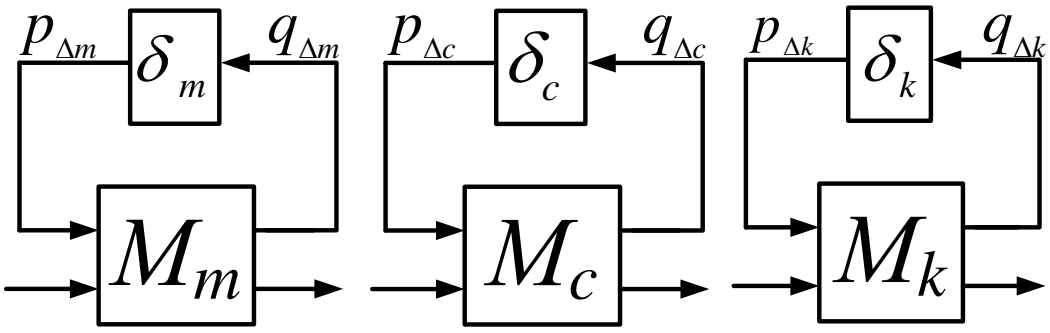

Figure 2.9: LFRs of parametric uncertainties

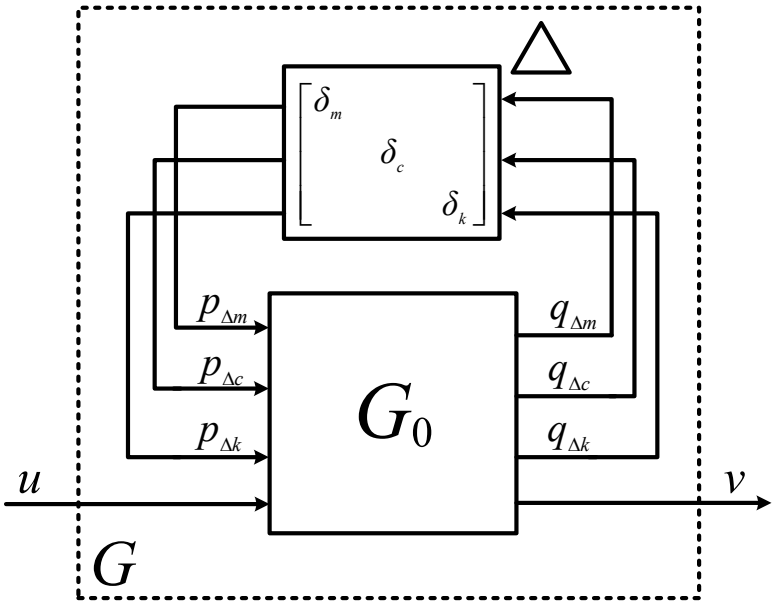

Figure 2.10: LFR of uncertain $G(s)$ with parametric uncertainties

2.4.2 Robustness analysis

As discussed above, there usually exist variations in the modal parameters g, ζ, ω_n, which are not known exactly but can be assumed to be within certain intervals. These variations may be due to the errors in the system identification if the system is identified or due to the measurement errors of the physical

parameters used in the system modeling, for instance,

$$\begin{aligned} m &= \bar{m}(1+p_m\delta_m), \quad 0<p_m<1, \ |\delta_m|\le 1 \\ c &= \bar{c}(1+p_c\delta_c), \quad\ \ 0<p_c<1, \ \ |\delta_c|\le 1 \\ k &= \bar{k}(1+p_k\delta_k), \quad\ \ 0<p_k<1, \ \ |\delta_k|\le 1 \end{aligned}$$

where $\bar{m},\ \bar{c},\ \bar{k}$ are nominal values of $m,\ c,\ k$ and $p_m,\ p_c,\ p_k,\ \delta_m,\ \delta_c,\ \delta_k$ represent the relative variations on these parameters, *e.g.* $p_m = 0.5$ means that there exists 50% uncertainty in the mass. As discussed above, using an upper LFT we can represent these parametric uncertainties systematically, that is,

$$m = \mathcal{F}_u(M_m, \delta_m),\ c = \mathcal{F}_u(M_c, \delta_c),\ k = \mathcal{F}_u(M_k, \delta_k)$$

where

$$M_m = \begin{bmatrix} 0 & \bar{m} \\ p_m & \bar{m} \end{bmatrix},\ M_c = \begin{bmatrix} 0 & \bar{c} \\ p_c & \bar{c} \end{bmatrix},\ M_k = \begin{bmatrix} 0 & \bar{k} \\ p_k & \bar{k} \end{bmatrix}$$

These LFRs can be illustrated in Figure 2.9, where the uncertainties $\delta_m,\ \delta_c,\ \delta_k$ have corresponding inputs $p_{\delta m},\ p_{\delta c},\ p_{\delta k}$ and outputs $q_{\delta m},\ q_{\delta c},\ q_{\delta k}$. Based on these LFRs of parametric uncertainties and the dynamics of MDS system as described in Equation (2.21), we have the uncertain $G(s) = \mathcal{F}_u(G_0(s), \Delta)$, as shown in Figure 2.10, where $G_0(s)$ denotes the nominal input/output dynamics of MDS system and $\Delta = \text{diag}(\delta_m,\ \delta_c,\ \delta_k)$ is the diagonal parametric uncertainty matrix pulled out from $G(s)$. Note that as in this example only a second-order $G(s)$ is considered, no dynamic uncertainty on $G(s)$ is considered.

As discussed in section 2.3.1, based on theorem 2.3.2, the uncertain $G(s)$, the designed controller $K(s)$ and Δ are used to develop $M-\Delta$ feedback structure for deterministic robust stability analysis as illustrated in Figure 2.11, where $p_\Delta = [p_{\Delta m},\ p_{\Delta c},\ p_{\Delta k}]^T$, $q_\Delta = [q_{\Delta m},\ q_{\Delta c},\ q_{\Delta k}]^T$ and $M = \mathscr{F}_l(G, K)$. For robust performance analysis, $N-\hat{\Delta}$ feedback structure is developed based on theorem 2.3.2, where a performance weighting function $W_{\text{perf}}(s)$ is incorporated into $\bar{N}$ to make $\hat{\Delta} = \text{diag}(\Delta, \Delta_{\text{Perf}}) \in \boldsymbol{B}_{\underline{\hat{\Delta}}}$. Unlike the mixed sensitivity design, deterministic robust performance analysis about the performance criterion

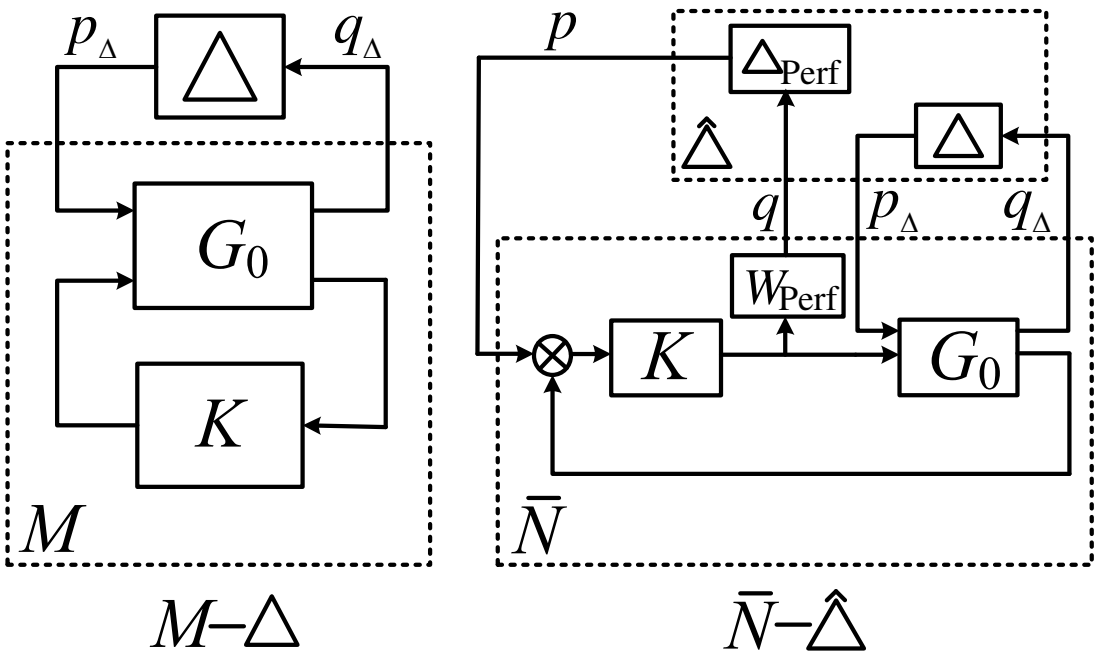

Figure 2.11: $M-\Delta$ and $N-\hat{\Delta}$ feedback structures for robustness analysis of the closed-loop MDS system

$S-KS$ can be performed individually to reduce associated conservatism. For instance, to ensure that, in the presence of Δ, $|(1+K(j\omega)\mathcal{F}_u(G_0(j\omega),\Delta))^{-1}| \leq |W_d(j\omega)W_y(j\omega)|^{-1}$, $\forall\omega$, $|W_{\text{perf}}(s)|$ can just be selected as $|W_d(s)W_y(s)|$. In addition to deterministic robustness analysis, to consider the probabilistic information of the variations on m, c, k and $(g,\ \zeta,\ \omega_n)$, the probabilistic robustness analysis can also be performed to obtain probabilistic robustness properties, but for the sake of simplicity, only deterministic robustness analysis is used for this MDS example.

2.4.3 Numerical applications

To numerically illustrate the design of H_∞ control and the deterministic robustness analysis, below are the parameters used in the MDS example (Gu et al.,

2005):

$$\begin{aligned} \bar{m} &= 3, \quad \bar{c} = 1, \quad \bar{k} = 2 \\ p_m &= 0.4, \; p_c = 0.2, \; p_k = 0.3 \end{aligned}$$

with $|\delta_m| \leq 1$, $|\delta_c| \leq 1$, $|\delta_k| \leq 1$. This means that there exists 40% uncertainty on the mass, 20% uncertainty on the damping coefficient and 30% uncertainty on the spring stiffness, that is, $1.8 \leq m \leq 4.2$, $0.8 \leq c \leq 1.2$, $1.4 \leq k \leq 2.6$. The nominal modal parameters of this numerical example is $g_0 = 0.33$, $\zeta_0 = 0.20$, $\omega_{n0} = 0.82$ and the nominal model of this MDS system is

$$G_0(s) = \frac{0.33}{s^2 + 0.33s + 0.67}$$

Based on $\omega_{n0} = 0.82$rad/sec, to have effective vibration reduction for $G_0(s)$, the magnitude of the nominal sensitivity transfer function $|S_0(j\omega)| = |(1 + K(j\omega)G_0(j\omega))^{-1}|$ is desirable to be less than one below 1rad/sec. With the mixed sensitivity control structure of Figure 2.8, as used in Gu et al. (2005), this frequency-dependent requirement on $|S_0(j\omega)|$ can be represented by a constant weighting function $W_d(s)$ and a second-order weighting function $W_y(s)$, for instance,

$$W_y(s) = 0.85 \times \frac{s^2 + 1.8s + 10}{s^2 + 8.0s + 0.01}, \; W_d(s) = 1, \; W_u(s) = 0.01$$

where $W_u(s) = 0.01$ also specifies the requirement on $K(s)S_0(s)$, that is, $|K(j\omega)S_0(j\omega)| \leq 40$dB has to be satisfied for any frequency, as illustrated in Figure 2.12. With this set of weighting functions, as performed in section 2.4.1, we have the H_∞ controller $K_\infty(s)$:

$$K_\infty(s) = \frac{-4.65(s - 239.5)(s^2 + 0.33s + 0.67)}{(s + 1.25 \times 10^{-3})(s + 8.00)(s^2 + 7.02s + 24.08)}$$

As shown in Figure 2.12, $K_\infty(j\omega)$ ensures that the magnitudes of $|K_\infty(j\omega)S_0(j\omega)|$ and $|S_0(j\omega)|$ are smaller than their determined upper bounds at any frequency,

that is, $K_\infty(s)$ satisfies the nominal control performances:

$$\begin{aligned} \left\| 0.85 \frac{s^2 + 1.8s + 10}{s^2 + 8.0s + 0.01} S_0(s) \right\|_\infty &\leq 1 \\ ||K_\infty(s) S_0(s)||_\infty &\leq 100 \end{aligned}$$

It is notable that the second-order $W_y(s)$ as employed in Gu et al. (2005) is neither the only nor the best choice to define the frequency-requirement on $S(j\omega)$, and a first-order low-pass filter $W_y(j\omega)$ could be more suitable in terms of its reduced order, while enforcing the constraints on $|S_0(j\omega)|$.

Although the stabilizing controller $K_\infty(s)$ satisfies the nominal control objectives, in the presence of parametric uncertainties, it is necessary to verify the robustness properties of the closed-loop system using $K_\infty(s)$. For this MDS example, only the deterministic robustness analysis as discussed in section 2.4.2 is used. As shown in Figure 2.13, usual μ analysis with frequency gridding method is conducted over the frequency range of interest and we have the robustness properties of the closed-loop system:

- For the robust stability, from the top part of Figure 2.13, the maximum value of the upper bounds of μ is $0.76 < 1$ around 0.80rad/sec. Based on Equation (2.20), $\sup_\omega \mu_\Delta(M(j\omega)) = 0.76 < 1$ means that the closed-loop system using $K_\infty(s)$ achieves satisfactory robust stability in the presence of the assumed parametric uncertainties and this structured uncertainty can be enlarged by $1/0.76 = 1.32$ before the closed-loop system is destabilized[1], that is, we have the stability robustness to the parametric uncertainties $1.416 \leq m \leq 4.584$, $0.736 \leq c \leq 1.264$ and $1.208 \leq k \leq 2.792$.

- For the robust performance in terms of $S(s)$, *i.e.* to verify if

$$\left\| 0.85 \frac{s^2 + 1.8s + 10}{s^2 + 8.0s + 0.01} (1 + K_\infty(s) \mathcal{F}_u(G_0(s), \Delta))^{-1} \right\|_\infty \leq 1$$

  is also satisfied in the presence of assumed parametric uncertainties,

[1] Since the upper and lower bounds of μ do not coincide well around 0.80rad/sec, there could exist a certain level of conservatism in the calculated 1.32.

from the bottom part of Figure 2.13, the maximum value of the upper bounds of μ is $1.64 > 1$ around 0.87rad/sec. Based on Equation (2.19), $\sup_{\omega} \mu_{\hat{\Delta}}(\bar{N}(j\omega)) = 1.64 > 1$ means that the robust performance could be violated due to the assumed parametric uncertainties Δ, *e.g.* the requirement that $|(1 + K_\infty(j\omega)\mathcal{F}_u(G_0(j\omega), \Delta))^{-1}| < 1,\ \forall\omega \leq 1$rad/sec cannot be satisfied.

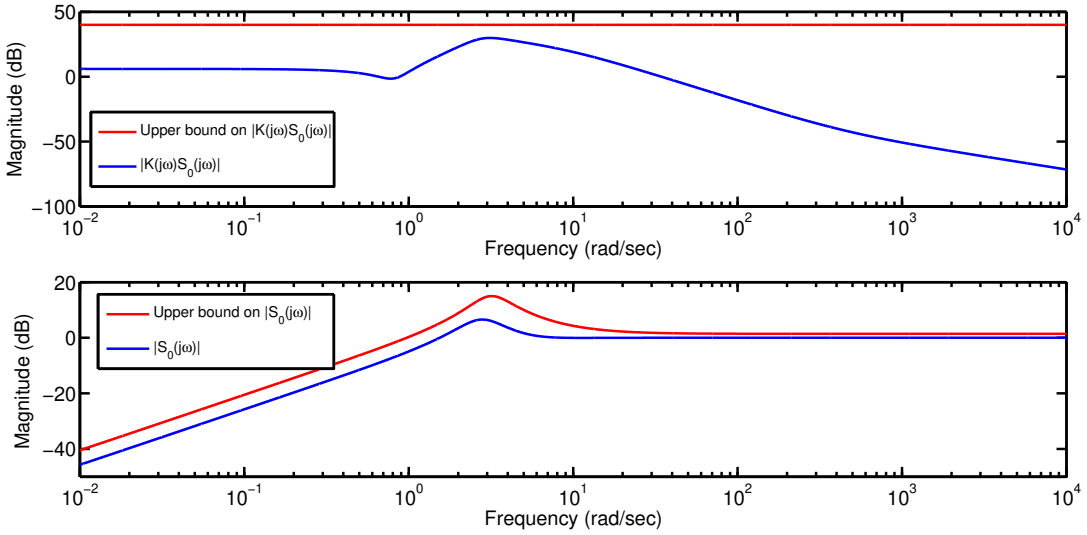

Figure 2.12: Upper bounds on the magnitudes of $|K(j\omega)S_0(j\omega)|$ and $|S_0(j\omega)|$

2.4.4 Remarks for the numerical applications

With the numerical applications, the main procedures of the H_∞ control design and the robustness analysis are illuminated in a clear way. Besides, we have some useful remarks from these numerical applications:

- As known, the selection of weighting functions is very important to the design of H_∞ control. Usually, according to a set of control objectives, frequency-dependent weighting functions are required such as $W_y(s)$ used in the MDS example. To emphasize this point, if all the weighting functions are constant, *e.g.* $W_y(s) = 1,\ W_u(s) = 0.01,\ W_d(s) = 1$, using the mixed sensitivity control structure, the obtained controller has zero gain, that is,

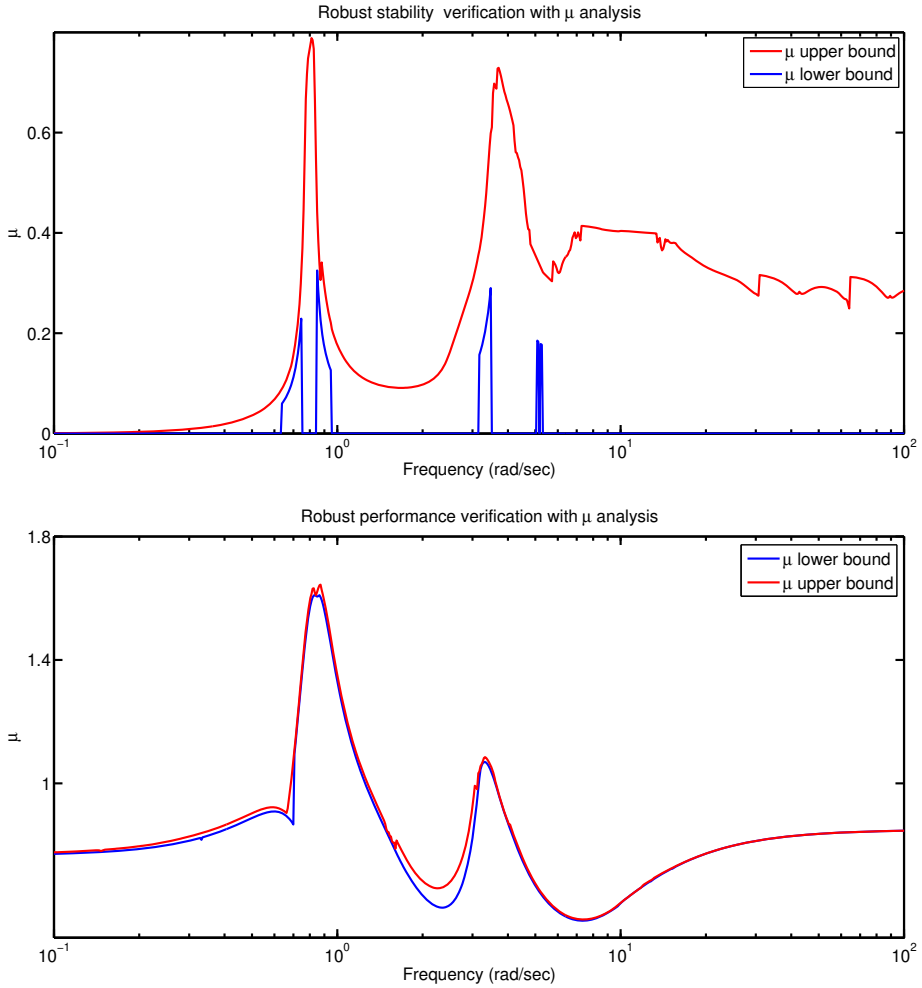

Figure 2.13: The μ-plot against the frequency range of interest for robust stability analysis (top) and robust performance analysis (bottom) using $K_\infty(s)$

no controller is actually required according to the suboptimal H_∞ control algorithm. This result is reasonable since $G_0(s)$ is stable and the controller $K(s) = 0$ can ensure the closed-loop system to be stable and provide $\|S(s)K(s)\|_\infty = 0$ and $\|S(s)\|_\infty = 1$, which is the best solver we can achieve with respect to the optimization problem. However, such optimization does not make any sense for practical control designs. This fact confirms that, to satisfy practical control objectives, frequency-dependent weighting functions have to be appropriately determined. In addition to the control objectives, the selection of weighting functions also has considerable effects

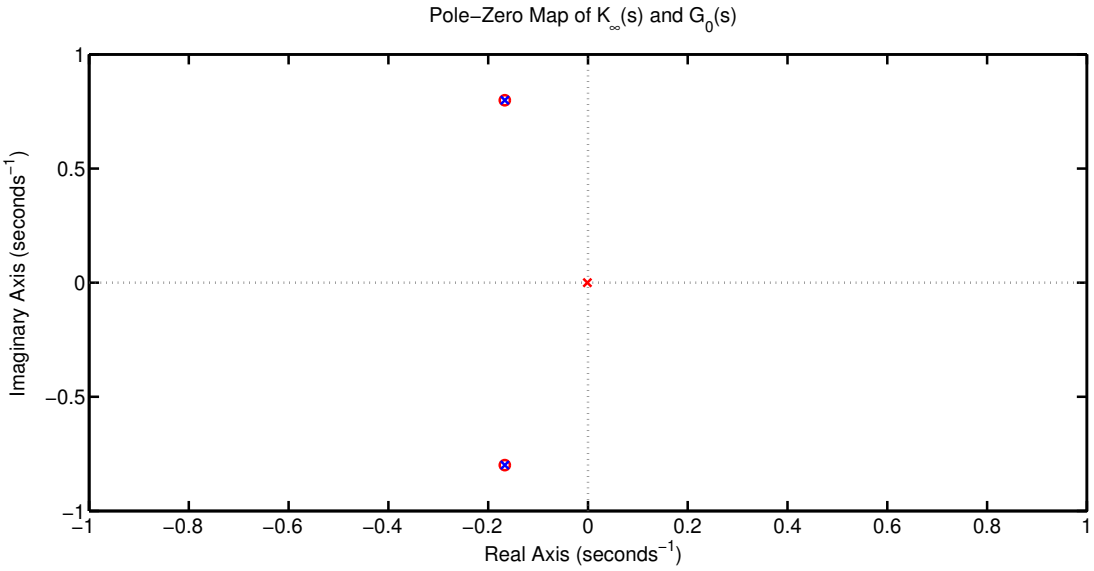

Figure 2.14: The pole-zero map of $K_\infty(s)$ and $G_0(s)$: the blue crosses are the poles of $G_0(s)$ and the red circles are the zeros of $K_\infty(s)$

on the closed-loop robustness to parametric and dynamic uncertainties, for example, to avoid spillover instability, the synthesized H_∞ controller has to roll over at high frequencies using suitable weighting functions. In this research, the weighting functions are selected based on the principle of phase and gain control policies proposed in next chapter, which allows to consider not only a complete set of control objectives such as the specification of vibration reduction, the moderate control energy and so on, but also the closed-loop stability and performance robustness to parametric and dynamic uncertainties.

- Although the employed mixed sensitivity control design is widely used, we have to focus considerable attention on its significant drawback, *i.e.* the pole-zero cancellation between the designed H_∞ controller $K(s)$ and the nominal model $G_0(s)$. This cancellation is shown in the pole-zero map of Figure 2.14, where some other poles and zeros of $K(s)$ and $G_0(s)$ are neglected. Naturally, in the presence of parametric uncertainties, such pole-zero cancellation could significantly degrade the control performances, for instance, the robust performance is not satisfied for this MDS example

with $K_\infty(s)$. To avoid the pole-zero cancellation, as illustrated in Scorletti and Fromion (2008a) on page 108, the 4-block H_∞ control structure can be used to enforce frequency-dependent upper bounds on the magnitude of the transfer function $G_0(j\omega)S_0(j\omega)$ by associated weighting functions. To have the same nominal control performances as $K_\infty(s)$ does, using the 4-block H_∞ control structure and suitable weighting functions, a new stabilizing H_∞ controller is obtained:

$$K_{n\infty}(s) = \frac{48.41(s+8.20)(s^2+1.25s+1.10)}{(s+1.20\times 10^{-3})(s+8.00)(s+5.71)}$$

As expected, the pole-zero cancellation between $K_{n\infty}(s)$ and $G_0(s)$ is avoided, as shown in the pole-zero map of Figure 2.15. The μ analysis is used to verify the robustness properties of the closed-loop system using $\bar{K}_\infty(s)$, as shown in Figure 2.16. It is demonstrated that $K_{n\infty}(s)$ can satisfy not only the nominal control performances but also provide better robustness properties compared to $K_\infty(s)$: $\sup_\omega \mu_\Delta(M(j\omega)) = 0.4$ means that the structured uncertainty can be enlarged by $1/0.4 = 2.50$ before the closed-loop system is destabilized, that is, we have the stability robustness to the parametric uncertainties $0 < m \leq 6.00$, $0.20 \leq c \leq 1.80$ and $0.50 \leq k \leq 3.50$; $\sup_\omega \mu_{\hat{\Delta}}(\bar{N}(j\omega)) = 0.97 < 1$ means that the robust performance is also ensured, *i.e.* $|(1+K_{n\infty}(j\omega)\mathcal{F}_u(G_0(j\omega),\Delta))^{-1}| < 1,\ \forall\omega \leq 1$. Compared to Figure 2.13, it is clear that with $K_{n\infty}(s)$ there is a dramatic improvement of the robustness properties.

- Flexible structures have an infinite number of resonant modes, and sometimes effective vibration control is required for several resonant modes simultaneously. Therefore, to suitably reflect the frequency-dependent specification of vibration reduction, complicated weighting functions such as $W_y(s)$ have to be used. The complexity of weighting functions may induce the order of $P(s)$ high, thus leading to a too high-order $K(s)$, which is usually equal to the order of $P(s)$. To reduce this complexity, $G(s)$ is desirable to be decomposed appropriately such that several simple constant weighting functions can be used to appropriately reflect the specification of

vibration reduction on every interested resonant mode (Font et al., 1994). In addition, to explicitly enforce the constraints on the control energy, some frequency-dependent weighting functions associated with $K(s)S(s)$ such as $W_u(s)$ have to be used.

- For this MDS system, the relationship between the physical parameters and the modal ones can be directly obtained based on the analytical formulations, *e.g.* the natural frequency $\omega_n = \sqrt{k/m}$. These formulations are useful for the uncertainty quantification (UQ), for instance, the deterministic or the probabilistic information of the mass can be easily reflected into that of ω_n, which can be considered in various robustness analysis. However, for practical systems such analytical formulations do not exist and even they do exist for some specifical structures such as the natural frequencies of a simple cantilever beam, the placement of sensors and actuators may have considerable effects on the natural frequencies. In such cases, efficient UQ, *e.g.* the gPC framework, is required to quantitatively determine the effects of mechanical uncertainties on the modal ones in an efficient way.

- Even for a simple system such as the MDS example, analytical derivations of LFRs of the parametric uncertainties and uncertain models are not straightforward and could be very complicated. Therefore, for flexible structures consisting of an infinite number of resonant modes, it is necessary to employ efficient tools to develop the LFR of the uncertain system. To this end, a graphical toolbox has to be developed in the Matlab-Simulink R2012 environment, where the enhanced LFR toolbox (Hecker et al., 2005) could be used to have the LFR of the uncertain system. Compared to the usual script programming, the graphical toolbox can achieve the augmented plant $P(s)$, the $M-\Delta$ structure and the $\hat{N}-\hat{\Delta}$ structure in a more convenient and systematic way, thus facilitating the H_∞ control design and the robustness analysis for practically complicated systems.

- For usual robust control designs and robustness analysis, both parametric and dynamic uncertainties are assumed to be norm bounded but not measurable in real-time. However, in some practical cases, some sources of

system uncertainties can be measured in real-time. The time-varying information of uncertainties is desirable to be considered in the control design to obtain improved control objectives, *e.g.* saving the control energy and, in some extend, reducing the magnitude of the control signal to avoid control saturation. This control problem can be investigated with linear parameter varying (LPV) system modeling and control designs, *e.g.* Scorletti and Fromion (1998); Dinh et al. (2005).

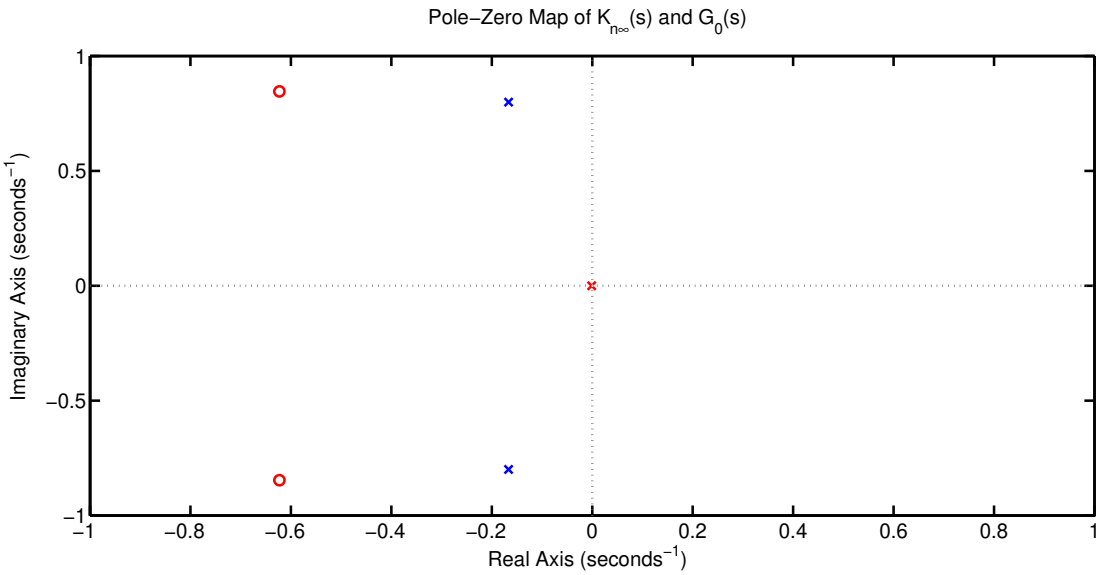

Figure 2.15: The pole-zero cancellation between $K_{n\infty}(s)$ and $G_0(s)$ is avoided: the blue crosses are the poles of $G_0(s)$ and the red circles are the zeros of $K_\infty(s)$

2.5 Summary

This chapters has an extensive literature review on related research fields and focus on the introduction of the H_∞ control and the robustness analysis. These techniques play an very important role in this research. This chapter ends with a simple MDS example. It is notable that the main motivation of this representative MDS example is neither to design the best H_∞ controller for the particular system nor to employ the most efficient techniques for robustness analysis, but to

illustrate the main processes of the H_∞ control design and the robustness analysis, and to emphasize the possibly involved problems for robust vibration control, which have to be fully considered in the subsequent chapters.

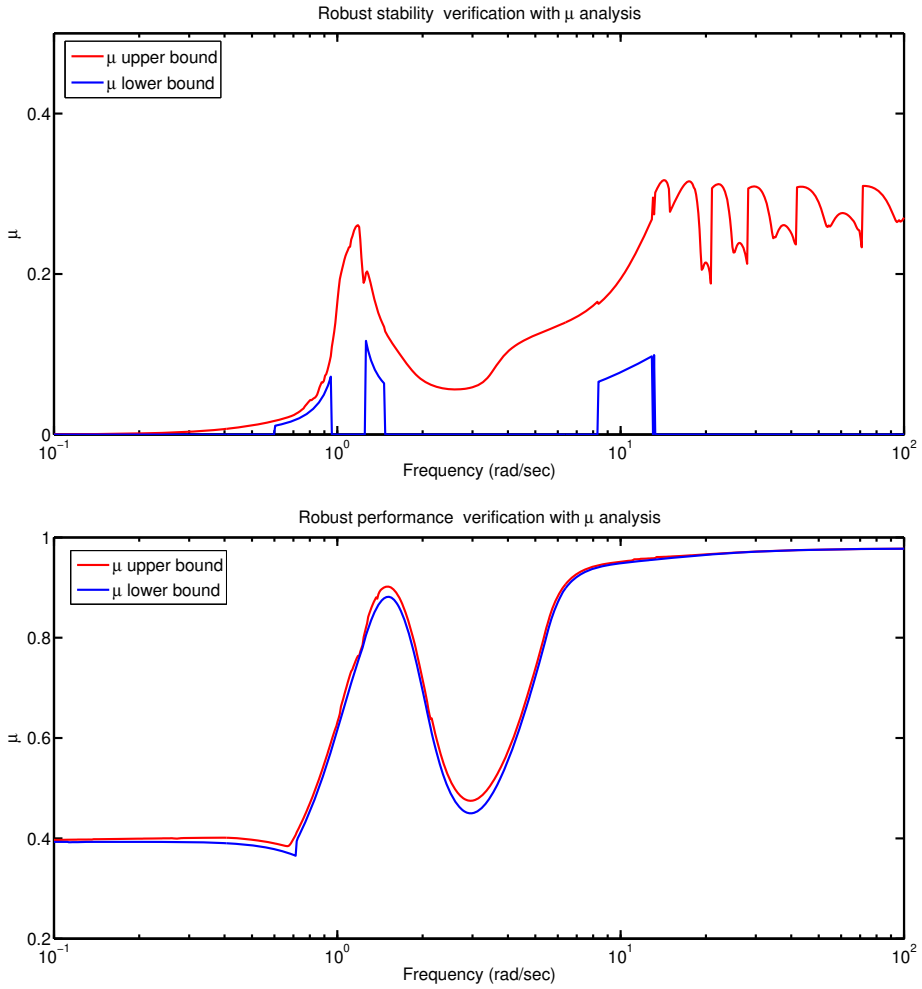

Figure 2.16: The μ-plot against the frequency range of interest for robust stability analysis (top) and robust performance analysis (bottom) using $K_{n\infty}(s)$

Chapter 3

Phase and gain control policies based H_∞ control

This chapter first emphasizes a complete set of control objectives in the area of robust active vibration of flexible structures. When the set of control objectives is considered, phase and gain control policies are proposed to impose frequency-dependent gain and phase requirements on the controller in order to achieve these specifications. They can be used to explain some classical control designs such as the acceleration feedback control, and more important, they are employed in the dynamic output feedback H_∞ control to develop a general and systematical robust control methodology which can ensure quantitative nominal vibration reduction defined by a positive frequency-dependent function and the qualitative robustness properties of the closed-loop system. The effectiveness of this control methodology is validated on a non-collocated piezoelectric cantilever beam with numerical simulations and experimental results.

3.1 Problem statement

As known, one of the most significant characteristics of flexible structures is their highly resonant modes due to the inherently small dissipation of kinetic and strain energy, which is reflected by a relatively small structural damping. Such flexible structures may suffer from considerable vibrations when they are excited around

the resonant frequencies. Although, there exist many control designs for active vibration control as reviewed in section 2.1, a general control methodology to systematically consider the complete set of control objectives has to be proposed, *e.g.* the vibration reduction of every controlled resonant mode with corresponding a priori determined level, the constraints on the control energy, the reduction of effects of the measurement noise and the robustness properties to parametric and dynamics uncertainties. Besides, as these control objectives usually have conflicting requirements on the controller, the control design must achieve a trade-off among them in a rational and systematic way.

To obtain effective vibration reduction, it is desirable to design a controller for the resonance reduction, that is, the controller should effectively reduce the frequency response magnitudes around the controlled resonant frequencies and have limited effects elsewhere. To determine the controlled resonant frequencies and quantitatively define the specification of vibration reduction, a positive frequency-dependent function $U(\omega)$ and the most general feedback control structure of Figure 2.1 in section 2.2.1 are introduced. As above described, the transfer function $T_{yd}(j\omega)$ represents the closed-loop transfer function from the disturbance d to the system output y, the specification of vibration reduction can thus be defined as

$$|T_{yd}(j\omega)| \leq U(\omega), \ \forall \ \omega \in \mathbb{R} \tag{3.1}$$

For the SISO systems, this specification can be illustrated in Figure 3.1, where the solid curve $N_{yd}(j\omega)$ represents the open-loop transfer function from d to y. Obviously, for this particular case, the first two resonant modes have to be controlled.

In practice, in addition to the specification of vibration reduction, several other control objectives have to be simultaneously considered, *e.g.* the closed-loop stability, the moderate control energy, the effects of the measurement noise and the stability robustness to parametric and dynamic uncertainties. In the control design, the complete set of control objectives can be translated into the requirements on the corresponding transfer function matrices. The typical vibration control structure of Figure 5.1 is introduced for the SISO systems, where $G_d(s)$ and $G_p(s)$ represent disturbance and plant dynamical models respectively (Pota

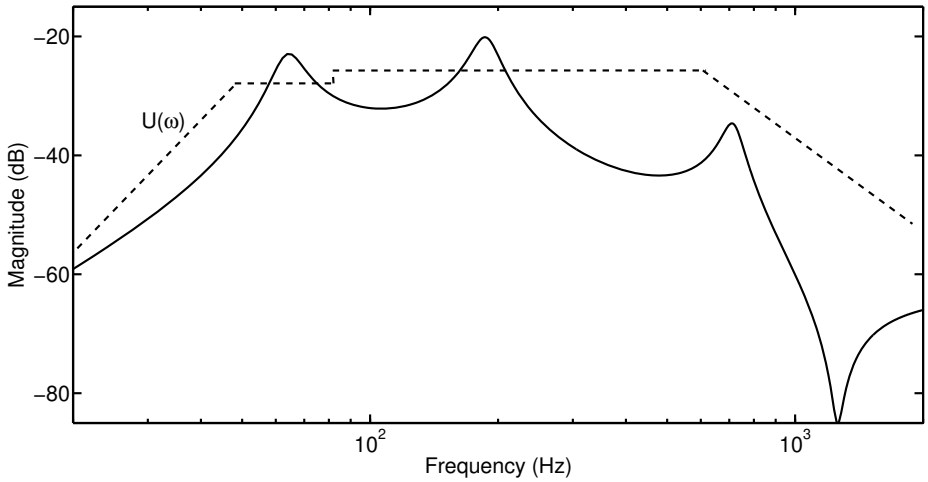

Figure 3.1: A specification of vibration reduction for flexible structures

et al., 1999). Obviously, this is a specific case of the most general control structure of Figure 2.1 in that the system output y can be measured and directly fed back to the controller $K(s)$, that is,

$$\begin{aligned} y &= G_d d + G_p u \\ u &= Kv \\ v &= y + n \end{aligned}$$

Based on the control structure of Figure 5.1, the closed-loop stability can be investigated with the Nyquist stability criterion in terms of the open-loop transfer function $L(j\omega) = K(j\omega)G_p(j\omega)$. The modulus margin M_m represents the smallest distance from $L(j\omega)$ to the critical point $-1 + j0$ on Nyquist plot (Bourlès and Kwan, 2010),

$$M_m = \inf_{\omega} |1 + L(j\omega)| = \frac{1}{\sup_{\omega} \frac{1}{|1+L(j\omega)|}} = \frac{1}{\sup_{\omega} |S(j\omega)|}, \forall \omega \in \mathbb{R} \tag{3.2}$$

where $S(j\omega) = (1+L(j\omega))^{-1}$ is the sensitivity function of the closed-loop system. Based on the Nyquist stability criterion, for the stability robustness, the larger M_m, the better. In addition, $M_m^{-1} = M_s = \sup_{\omega} |S(j\omega)|$, $\forall \omega \in \mathbb{R}$ is the maximum

peak of the sensitivity function and is closely related to the gain margin (GM) and the phase margins (PM): when the Nyquist plot of $L(j\omega)$ crosses the negative real axis between -1 and 0, we have the (upper) gain margin $\mathrm{GM}_U > 1$ and

$$\mathrm{GM}_U \geq \frac{M_s}{M_s - 1} \text{ and } \mathrm{PM} \geq 2\arcsin\left(\frac{1}{2M_s}\right) \geq \frac{1}{M_s}[\mathrm{rad}] \tag{3.3}$$

for instance, $M_m = 0.5$ ensures $\mathrm{GM}_U \geq 2$ and $\mathrm{PM} \geq 29.0°$; for an unstable plant, when the Nyquist plot of $L(j\omega)$ crosses the negative real axis between $-\infty$ and -1, we have the lower gain margin $\mathrm{GM}_L < 1$ and

$$\mathrm{GM}_L \leq \frac{M_s}{M_s + 1} \tag{3.4}$$

The detailed derivations of Equation (3.3) and (3.4) can be found in Skogestad and Postlethwaite (2005) and Šebek and Hurák (2009). These equations imply that the application of M_s can implicitly take into account the GM and PM, which, in some extend, are related to the robustness properties, but have been proved to be insufficient indicators for the system performance and stability robustness (Zhou et al., 1996). One application of M_s is the parameters tuning of PID controllers (Garcia et al., 2004; Jones and Tham, 2006). However, as claimed in Zhao et al. (2011), the parameters tuning method based only on M_s is still deficient and inadequate in some cases.

The beneficial effects of $K(s)$ on the vibration reduction are represented by $|T_{yd}(j\omega)| = |G_d(j\omega)S(j\omega)|$ and the associated control energy can be investigated through the transfer function $|T_{ud}(j\omega)| = |G_d(j\omega)K(j\omega)S(j\omega)|$. The effects of the measurement noise on the control energy and the system output are respectively represented by $|T_{un}(j\omega)| = |K(j\omega)S(j\omega)|$ and $|T_{yn}(j\omega)| = |1 - S(j\omega)| = |T(j\omega)|$ where $T(s)$ is the complimentary sensitivity function. Hence, these control objectives are equivalent to reducing the magnitudes of related closed-loop transfer functions.

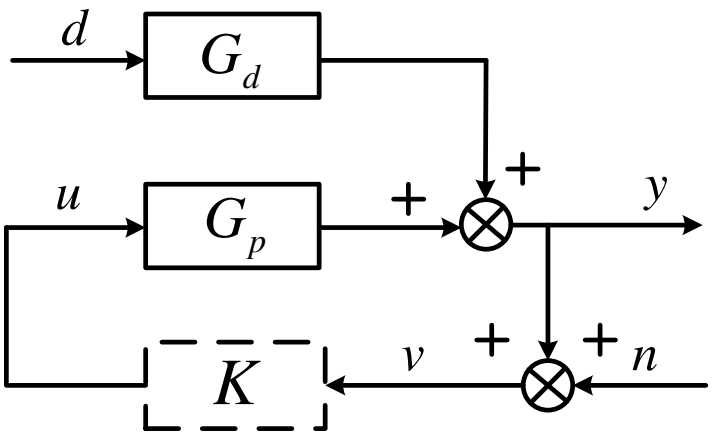

Figure 3.2: A typical feedback control structure for active vibration control

3.2 Phase and gain control policies

To design a controller $K(s)$ satisfying above mentioned control objectives, it is desirable to translate the control objectives into frequency-dependent requirements on $K(j\omega)$. The relationships between the control objectives and the closed-loop transfer functions are used to this end, especially, when $|L(j\omega)| \gg 1$ and $|L(j\omega)| \ll 1$, these closed-loop transfer functions can be simplified with respect to $K(j\omega)$ as summarized in Table 3.1. This simplification allows the investigation of the relationships between the control objectives and $|K(j\omega)|$.

$\lvert L(j\omega)\rvert$	$\gg 1$	$\ll 1$
$\lvert T_{yd}(j\omega)\rvert$	$\approx \left\lvert \frac{G_d(j\omega)}{L(j\omega)} \right\rvert$	$\approx \lvert G_d(j\omega)\rvert$
$\lvert T_{yn}(j\omega)\rvert$	≈ 1	$\approx \lvert L(j\omega)\rvert$
$\lvert T_{ud}(j\omega)\rvert$	$\approx \left\lvert \frac{G_d(j\omega)}{G_p(j\omega)} \right\rvert$	$\approx \lvert K(j\omega)G_d(j\omega)\rvert$
$\lvert T_{un}(j\omega)\rvert$	$\approx \left\lvert \frac{1}{G_p(j\omega)} \right\rvert$	$\approx \lvert K(j\omega)\rvert$

Table 3.1: Relationships between closed-loop transfer functions and the controller

For efficient vibration reduction, $|T_{yd}(j\omega)|$ is focused and Table 3.1 implies that at frequencies where $|G_d(j\omega)| > U(\omega)$, *i.e.* the specification of vibration

reduction is not satisfied, $|K(j\omega)|$ is required to be large enough, for example,

$$|L(j\omega)| \gg 1 \text{ and } |K(j\omega)| \geq \frac{|G_d(j\omega)|}{|G_p(j\omega)U(\omega)|} \tag{3.5}$$

On the other hand, at frequencies where $|G_d(j\omega)| \leq U(\omega)$, *i.e.* the specification of vibration reduction is satisfied, no control energy is needed and the ideal controller should be $|K(j\omega)| = 0$. For moderate control energy, $|T_{ud}(j\omega)|$ has to be limited, however, when $|L(j\omega)| \gg 1$ the control energy is nearly independent on $K(j\omega)$ and thus it cannot be limited by any $K(j\omega)$. In contrast, when $|L(j\omega)| \ll 1$ the control energy can be limited by making $|K(j\omega)|$ as small as possible. In addition, when $|L(j\omega)| \ll 1$ the effects of the measurement noise $|T_{yn}(j\omega)|$ and $|T_{un}(j\omega)|$ can also be reduced with small $|K(j\omega)|$. In conclusion, $|K(j\omega)|$ is required to be large enough around the controlled resonant frequencies and beyond these frequencies $|K(j\omega)|$ has to be as small as possible. Above analysis provides available and quite qualitative frequency-dependent requirements on $|K(j\omega)|$. Subsequently, the stability robustness to parametric and dynamic uncertainties is considered and the phase requirement on $K(j\omega)$ is enforced.

3.2.1 The phase control policy

3.2.1.1 Principle of the phase control policy

The frequency responses of flexible structures are mainly dominated by the behavior around their resonant frequencies. As shown in Figure 3.3, these frequency responses seem to be circular to some extent on Nyquist plot. The effects of parametric uncertainties on $L(j\omega)$ can also be illustrated on Nyquist plot: when the i^{th} damping ratio ζ_i is decreasing or the i^{th} gain R_i is increasing, the modulus of the i^{th} 'circle' becomes larger; when the i^{th} resonant frequency ω_i is changing, the orientation of the i^{th} 'circle' changes. Due to these parametric uncertainties, not only the closed-loop stability but also the stability robustness has to be investigated. Implied by the Nyquist stability criterion, when $L(j\omega)$ is stable and stays in the left-half plane (LHP) on Nyquist plot, the effects of parametric uncertainties are critical to the closed-loop stability, particularly, around the controlled resonant frequencies where $|L(j\omega)|$ has to be large enough for effective

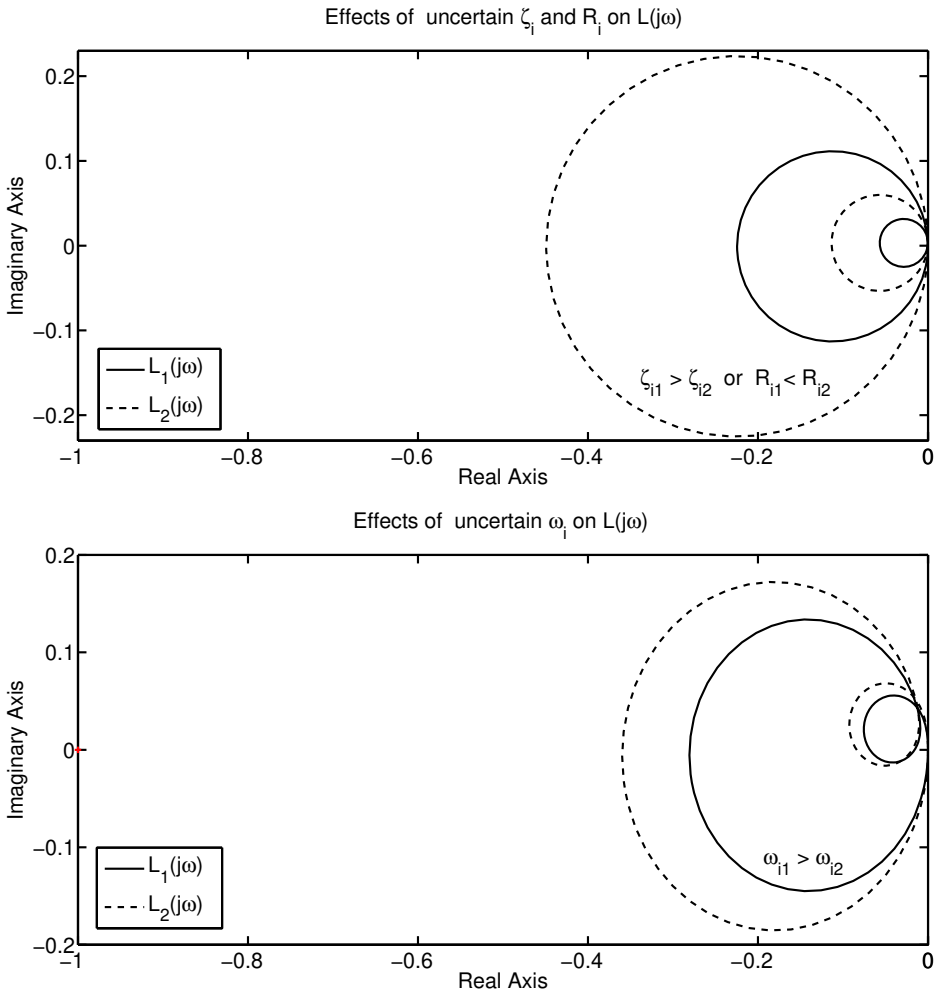

Figure 3.3: The effects of parametric uncertainties on $L(j\omega)$

vibration reduction and thus $L(j\omega)$ may well encircle the critical point $-1+j0$. To solve this problem, the phase control policy is proposed: around the controlled resonant frequencies, $|K(j\omega)|$ has to be large enough to satisfy the specification of vibration reduction, meanwhile, the stability robustness to parametric uncertainties is guaranteed by enforcing the phase requirement on $K(j\omega)$ such that $\angle L(j\omega) = [\angle K(j\omega) + \angle G_p(j\omega)] \in [-90°, +90°]$, that is, around the controlled resonant frequencies $L(j\omega)$ stays in the right-half plane (RHP) on Nyquist plot,

$$\Re(L(j\omega)) \geq 0,\ \omega \in [\omega_{ci} - \delta_{\omega_{ci}},\ \omega_{ci} + \delta_{\omega_{ci}}],\ \delta_{\omega_{ci}} > 0 \tag{3.6}$$

where $\Re(L(j\omega))$ represents the real part of $L(j\omega)$ and ω_{ci} is the i^{th} controlled resonant frequency. The Equation (3.6) guarantees that $L(j\omega)$ cannot intersect the negative real axis on Nyquist plot around ω_{ci} even there exist a certain level of parametric uncertainties. Necessarily, $L(j\omega)$ cannot encircle the critical point $-1 + j0$ around ω_{ci} and thus adequate stability robustness to parametric uncertainties is achieved. This phase requirement on $L(j\omega)$ can be regarded as a generalization of the direct velocity feedback control (Balas, 1979), which requires $L(j\omega)$ to stay in RHP at any frequency,

$$\Re(L(j\omega)) \geq 0, \ \forall\omega \in \mathbb{R}.$$

3.2.1.2 Comparisons with the passivity theorem and the NI approach

For the SISO systems, the classical passivity theorem (Khalil, 1996) and the negative-imaginary (NI) approach first proposed in (Lanzon and Petersen, 2008, 2007) can also be interpreted by the phase requirement on $L(j\omega)$. Compared to the phase control policy, more strict phase requirements on the the plant dynamical model $G_p(j\omega)$ and the controller $K(j\omega)$ are enforced by these methods to guarantee the closed-loop stability, for instance, $G_p(j\omega)$ has to be positive-real or negative-imaginary. The definitions of positive-real systems and negative-imaginary systems are as follows. Let G^* be the be the complex conjugate transpose of a matrix the matrix G.

Definition 3.2.1. *(Zhou et al., 1996)*
Let the set of positive-real transfer function matrices be defined as

$$\mathscr{P} := \{G \in \mathcal{RH}_\infty^{n\times n} : [G(j\omega) + G^*(j\omega)] \geq 0, \forall\omega \in \mathbb{R}\}.$$

and the set of strictly positive-real transfer function matrices be defined as

$$\mathscr{P}_s := \{G \in \mathcal{RH}_\infty^{n\times n} : [G(j\omega) + G^*(j\omega)] > 0, \forall\omega \in \mathbb{R}\}.$$

where $\mathcal{RH}_\infty$ denotes the set of all proper real-rational stable transfer function matrices and the superscript $G(j\omega)^*$ denotes the complex conjugate transpose of $G(j\omega)$.

Definition 3.2.2. *(Lanzon and Petersen, 2008)*
Let the set of negative-imaginary transfer function matrices be defined as

$$\mathscr{I} := \{G \in \mathcal{RH}_\infty^{n\times n} : j[G(j\omega) + G^*(j\omega)] \geq 0, \forall\omega \in (0,\infty)\}.$$

and the set of strictly negative-imaginary transfer function matrices be defined as

$$\mathscr{I}_s := \{G \in \mathcal{RH}_\infty^{n\times n} : j[G(j\omega) + G^*(j\omega)] > 0, \forall\omega \in (0,\infty)\}.$$

For the SISO systems, definition 3.2.1 implies that positive-real transfer function matrices have a phase lag between $-90°$ and $+90°$ for any frequency, that is, $G(\omega)$ lies in RHP on the Nyquist plot

$$\Re(G(j\omega)) \geq 0, \forall\omega \in \mathbb{R}$$

Definition 3.2.2 implies that negative-imaginary transfer function matrices have a phase lag between $-180°$ and $0°$ in the frequency interval $(0,\infty)$, that is, $G(j\omega)$ lies in the low-half plane on the Nyquist plot

$$\Im(G(j\omega)) \leq 0, \forall\omega \in (0,\infty)$$

where $\Im(G(j\omega))$ represents the imaginary part of $G(j\omega)$.

Based on the above definitions we have the following theorems to investigate internal stability of a negative/positive feedback interconnection of transfer function matrices $G(s)$ and $K(s)$, as shown in Figure 3.4.

Theorem 3.2.1. *Given $G(s) \in \mathscr{P}$ and $K(s) \in \mathscr{P}_s$. Then then the* negative *feedback connection of $G(s)$ and $K(s)$ is internally stable (Khalil, 1996).*

Theorem 3.2.2. *Given $G(s) \in \mathscr{I}$ and $K(s) \in \mathscr{I}_s$, and suppose $G(\infty)K(\infty) = 0$ and $K(\infty) \geq 0$. Then the*positive *feedback connection $G(s)$ and $K(s)$ is internally stable if and only if the eigenvalues of the matrix $G(0)K(0)$ are strictly less than* 1 *(Lanzon and Petersen, 2008).*

Above theorems can be used in classical control design to ensure the closed-loop stability of collocated systems. With velocity sensors, $G_p(j\omega) \in \mathscr{P}$ and a

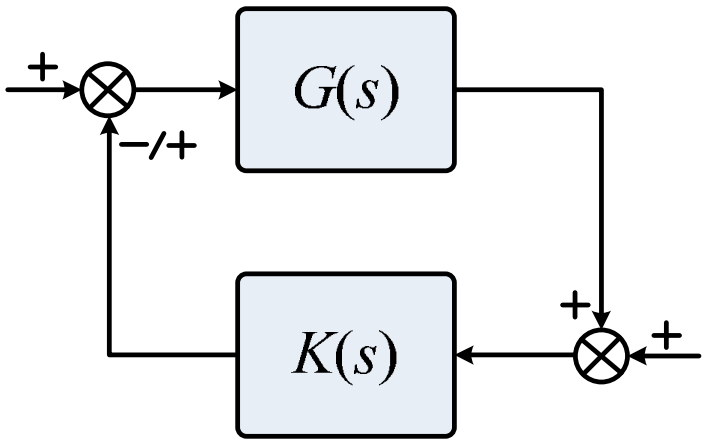

Figure 3.4: A negative/positive feedback interconnection of $G(s)$ and $K(s)$

controller $K(j\omega) \in \mathscr{P}_s$ can ensure the closed-loop stability with negative feedback control, *e.g.* the direct velocity feedback control (Balas, 1979). With position sensors, $G_p(j\omega) \in \mathscr{I}_s$ and a controller $K(j\omega) \in \mathscr{I}$ can ensure the closed-loop stability with positive feedback control if the eigenvalues of $G_p(0)K(0)$ are strictly less than one, *e.g.* the positive position feedback control (PPF) (Goh and Caughey, 1985) and the resonant control (Pota et al., 2002; Moheimani and Vautier, 2005). Similarly, with acceleration sensors, $G_p(j\omega) \in \mathscr{I}$ and a controller $K(j\omega) \in \mathscr{I}_s$ can ensure the closed-loop stability with positive feedback control if eigenvalues of $G_p(0)K(0)$ are strictly less than 1, *e.g.* the acceleration feedback control (AFC) (Sim and Lee, 1993).

In SISO cases, these closed-loop stability conditions can be explained with the Nyquist stability criterion. When $G_p(j\omega) \in \mathscr{P}$ and $K(j\omega) \in \mathscr{P}_s$, we have $\angle G_p(j\omega) \in [-90°, +90°]$, $\forall\omega$ and $\angle K(j\omega) \in (-90°, +90°)$, $\forall\omega$. As a result, the open loop transfer function $L(j\omega)$, $\angle L(j\omega) = \angle G_p(j\omega)K(j\omega) = [\angle G_p(j\omega) + \angle K(j\omega)] \in (-180°, +180°)$, $\forall\omega$. This shows that $L(j\omega)$ cannot intersect the negative real axis on Nyquist plot. Necessarily, $L(j\omega)$ cannot encircle the critical point $s = -1 + j0$ and the negative feedback interconnection of $G_p(j\omega)$ and $K(j\omega)$ is stable from the Nyquist stability criterion. When $G_p(j\omega) \in \mathscr{I}_s$ and $K(j\omega) \in \mathscr{I}$, we have $\angle G_p(j\omega) \in (-180°, 0°)$, $\forall\omega \in (0, \infty)$ and $\angle K(j\omega) \in$

$[-180°, 0°]$, $\forall\omega \in (0, \infty)$. Therefore, $\angle L(j\omega) \in (-360°, 0°)$, $\forall\omega \in (0, \infty)$ and $L(j\omega)$ can intersect the positive real axis on Nyquist plot only at $\omega = 0$ since $G_p(j\infty)K(j\infty) = 0$. From the Nyquist stability criterion, the positive feedback interconnection of $G_p(j\omega)$ and $K(j\omega)$ is stable if $G_p(0)K(0) < 1$ such that $L(j\omega)$ does not encircle the critical point $s = 1 + j0$. The explanation of the positive feedback interconnection of $G_p(j\omega) \in \mathscr{I}$ and $K(j\omega) \in \mathscr{I}_s$ is similar.

It is notable that, to apply the above theorems for the closed-loop stability, $G_p(j\omega)$ must be positive-real or imaginary-negative for all frequencies in the presence of various uncertainties. However, from a practical point of view, it is not necessary and difficult to satisfy these phase requirements, for instance, $\Re(G_p(j\omega)) \geq 0$, $\forall\omega \in \mathbb{R}$ or $\Im(G_p(j\omega)) \leq 0$, $\forall\omega \in \mathbb{R}$ can be frequently destroyed by neglected high frequency dynamics or time delays (Rohrs et al., 1985; Griggs et al., 2007). Moreover, these phase requirements cannot be satisfied in the case of non-collocated sensors and actuators, that is, at some frequencies $\angle G_p(j\omega) \in (+90°, +180°)$. In practice, non-collocated sensors and actuators are often unavoidable due to installation convenience or are even recommendable for high degrees of observability and controllability (Bayon de Noyer and Hanagud, 1998a; Kim and Oh, 2013). In such case, the passivity theorem and the negative-imaginary approach cannot be used, for instance, *e.g.* direct velocity feedback (DVF) control shows severe instability problem for the non-collocated systems (Cannon Jr and Rosenthal, 1984). Thus, the uncertainties and non-collocated systems pose challenging problems for the control design and the robustness analysis, which are proposed based on these methods, *e.g.* Balas (1979); Pota et al. (2002); Aphale et al. (2007); Goh and Caughey (1985); Sim and Lee (1993); Gatti et al. (2007); Petersen and Lanzon (2010); Song et al. (2010); Engelken et al. (2010); Bhikkaji et al. (2012); Song et al. (2012). In addition, based on the theorem 3.2.2, $G_p(0)$ has to be calculated to verify the Theorem 3.2.1, but for flexible structures $G_p(s)$ has infinite number of resonant modes and it is not easy to have accurate $G_p(0)$. On the other hand, both positive-real and negative-imaginary approaches only consider the closed-loop stability, however, to consider a trade-off between the stability and the performance, sometimes even $G_p(j\omega) \in \mathscr{P}_s$ a controller $K(j\omega) \notin \mathscr{P}$ may be used for better control performance. The above discussion highlights the benefits of the phase control policy,

that is, it has no phase requirement on $G_p(j\omega)$ and the gain and phase requirement on $K(j\omega)$ is enforced only around ω_{ci}. These features of the phase control policy allow the application of the phase control policy to both collocated and non-collocated systems to consider not only the stability robustness to parametric uncertainties and but also the specification of vibration reduction. Although here the phase control policy is interpreted with the SISO systems, a good point is that it can be readily employed in H_∞ control which can be used for both SISO and MIMO systems. Therefore, the phase control policy can be used for both SISO and MIMO systems with collocated or non-collocated sensors and actuators. To some extent, the phase control policy is related to the concepts of finite frequency positive-real (Iwasaki et al., 2003) and finite frequency negative-imaginary (Xiong et al., 2012).

3.2.2 The gain control policy

As discussed above, when the specification of vibration reduction is satisfied, *i.e.* $|G_d(j\omega)| \leq U(\omega)$, the ideal case is $|K(j\omega)| = 0$. However, this is practically impossible and thus the stability robustness to the dynamic uncertainty on $G_p(j\omega)$ has to be investigated. Usually, a norm bounded additive or multiplicative perturbation can be used to represent the dynamic uncertainty,
additive perturbation:

$$G_p(j\omega) = G_{p0}(j\omega) + \Delta_a(j\omega), \quad |\Delta_a(j\omega)| \leq |W_a(j\omega)|, \ \forall\omega \in \mathbb{R} \tag{3.7}$$

multiplicative perturbation:

$$G_p(j\omega) = (1 + \Delta_m(j\omega))G_{p0}(j\omega), \ |\Delta_m(j\omega)| \leq |W_m(j\omega)|, \ \forall\omega \in \mathbb{R} \tag{3.8}$$

where $G_{p0}(j\omega)$ and $G_p(j\omega)$ are the nominal and perturbed plant dynamical models; $W_a(j\omega)$ and $W_m(j\omega)$ are the norm bounded transfer functions used as upper bounds on the magnitudes of the additive and multiplicative dynamic uncertainties respectively.

From the small gain theorem (Zhou et al., 1996), the necessary and sufficient conditions for the stability robustness to the additive and multiplicative dynamic

uncertainties are
additive perturbation:

$$|T_{un}(j\omega)| = |K(j\omega)S_0(j\omega)| < \frac{1}{|W_a(j\omega)|} \leq \frac{1}{|\Delta_a(j\omega)|}, \ \forall\omega \in \mathbb{R} \tag{3.9}$$

multiplicative perturbation:

$$|T_{yn}(j\omega)| = |T_0(j\omega)| < \frac{1}{|W_m(j\omega)|} \leq \frac{1}{|\Delta_m(j\omega)|}, \ \forall\omega \in \mathbb{R} \tag{3.10}$$

where $S_0(j\omega) = (1 + K(j\omega)G_{p0}(j\omega))^{-1}$ and $T_0(j\omega) = K(j\omega)G_{p0}(j\omega)S_0(j\omega)$. The smaller $|T_{un}(j\omega)|$ and $|T_{yn}(j\omega)|$ are, the larger $|W_a(j\omega)|$ and $|W_m(j\omega)|$ can be, that is, the closed-loop system can tolerate a larger dynamic uncertainty. From Table 3.1, when $|L(j\omega)| \ll 1$, $|T_{un}(j\omega)| \approx |K(j\omega)|$ and $|T_{yn}(j\omega)| \approx |L(j\omega)|$. Hence, the above conditions can be reflected by the requirements on $|K(j\omega)|$,
additive perturbation:

$$|K(j\omega)| < \frac{1}{|W_a(j\omega)|}, \ \forall\omega \in \mathbb{R} \tag{3.11}$$

multiplicative perturbation:

$$|K(j\omega)| < \frac{1}{|G_{p0}(j\omega)W_m(j\omega)|}, \ \forall\omega \in \mathbb{R} \tag{3.12}$$

Based on the above analysis, the gain control policy is proposed: at the frequencies where the specification of vibration reduction is satisfied, $|K(j\omega)|$ has to be as small as possible to limit the control energy and reduce the effects of the measurement noise. Based on the small gain theorem, the gain control policy also provides a certain level of stability robustness to a generalized dynamic uncertainty including usual neglected high frequency dynamics and other dynamics when the phase control policy is not used, *e.g.* the low and middle frequency dynamics in (Barrault et al., 2007, 2008). In addition, as only the dynamic uncertainty is considered with the small gain theorem, the associated conservatism could be reduced.

The proposed phase and gain control policies impose frequency dependent

requirements on $|K(j\omega)|$ and $\angle K(j\omega)$ to consider a complete set of control objectives in the presence of parametric and dynamic uncertainties. It is notable that phase and gain control policies are quite qualitative, for instance, the $\delta_{\omega_{ci}}$ in Equation (3.6) is not explicitly specified and related formulation derivations are not rigorous. As it is practically difficult to change $|K(j\omega)|$ or $\angle K(j\omega)$ dramatically over a very small frequency range, there always exist transition frequency ranges for $K(j\omega)$ to switch from one control policy to the other one. The transition frequency ranges are most critical to control design especially when the resonant modes are closely spaced and the phase control policy has to be used over the middle frequency ranges. As a result, to make full use of phase and gain control policies, great attention should be paid to their realization and the trade-off among various control objectives. Although for several specific SISO cases, phase and gain control policies could be realized by some classical control methods such as AFC and so on, it is desirable to have a more rational and systematic way to realize them for more general cases. The dynamic output feedback H_∞ control is a competitive solution to this problem due to its inherent characteristics.

3.2.3 Comparisons with phase margin and gain margin

Before the application of phase and gain control policies, their main features are summarized and compared to those of phase margin (PM) and gain margin (GM). The gain and phase margins are recalled Skogestad and Postlethwaite (2005):

- The gain margin GM is defined as $\text{GM} = 1/|L(j\omega_{180})|$, where $L(j\omega) = G_p(j\omega)K(j\omega)$ is the open-loop transfer function and ω_{180} is the phase crossover frequency at which the Nyquist curve of $L(j\omega)$ crosses the negative real axis, that is, $\angle L(j\omega_{180}) = -180°$. The GM is the factor by which the loop gain $|L(j\omega)|$ may be increased before the closed-loop system becomes unstable. The GM is thus a direct safeguard against steady-state gain uncertainty.

- The phase margin PM is defined as $\text{PM} = \angle L(j\omega_c) + 180°$, where ω_c is the gain crossover frequency at which $|L(j\omega)|$ first crosses 1 from above, that

is, $|L(j\omega_c)| = 1$. The PM tells how much negative phase (phase lag) we can add to $L(j\omega)$ at frequency ω_c before the phase at this frequency becomes $-180°$, which corresponds to the closed-loop instability. The PM is a direct safeguard against time delay uncertainty and the system becomes unstable if we add a time delay of $\theta_{\max} = \text{PM}/\omega_c$.

As discussed above, the main motivation of phase and gain control policies is to provide qualitative frequency dependent requirements on the controller $K(j\omega)$ to consider a complete set of control objectives:

- When the specification of vibration reduction is not satisfied, the phase control policy requires $|K(j\omega)|$ to be large enough for efficient vibration reduction. Besides, it enforces the phase requirement on $K(j\omega)$, that is, $\angle L(j\omega) = [\angle K(j\omega) + \angle G_p(j\omega)] \in [-90°, +90°]$ around the controlled resonant frequencies. This means that $L(j\omega)$ stays in the right half plane on Nyquist plot around the controlled resonant frequencies,

$$\Re(L(j\omega)) \geq 0,\ \omega \in [\omega_{ci} - \delta_{\omega_{ci}},\ \omega_{ci} + \delta_{\omega_{ci}}],\ \delta_{\omega_{ci}} > 0 \tag{3.13}$$

  where $\Re(L(j\omega))$ represents the real part of $L(j\omega)$ and ω_{ci} is the i^{th} controlled resonant frequency. This guarantees that $L(j\omega)$ cannot intersect the negative real axis on Nyquist plot around ω_{ci} even there exist a certain level of parametric uncertainties. Necessarily, $L(j\omega)$ cannot encircle the critical point $s = -1 + j0$ around ω_{ci} and thus adequate stability robustness to parametric uncertainties is achieved.

- When the specification of vibration reduction is satisfied, the gain control policy requires $|K(j\omega)|$ to be as small as possible to limit the control energy and reduce the effects of the measurement noise. From the small gain theorem Desoer and Vidyasagar (1975), the gain control policy also provides a certain level of stability robustness to a generalized dynamic uncertainty including both usual neglected high frequency dynamics relate to spillover instability and other dynamics when the phase control policy is not used such as the low and middle frequency dynamics in Barrault et al. (2007, 2008). This implies that the control energy has to be only advertently

supplied to the controlled resonant modes.

Then a general and systematic robust control methodology is developed by employing phase and gain control policies in the dynamic output feedback H_∞ control: according to the set of control objectives, phase and gain control policies incorporate necessary weighting functions and determine them in a rational and systematic way; on the other hand, with the appropriate weighting functions, efficient H_∞ control algorithms can automatically realize phase and gain control policies and generate a satisfactory H_∞ controller. The proposed control methodology can be used for both SISO and MIMO systems with collocated or non-collocated sensors and actuators.

From the above analysis, we can find the main advantages of phase and gain control policies over the GM and PM:

- With respect to the stability robustness, the GM and PM can only consider two specific uncertainties on $L(j\omega)$: the steady-state gain uncertainty and the time delay one. In contrast, the phase control policy provides adequate stability robustness to various parametric uncertainties such as the natural frequency ω_k, the damping ratio ζ_k and the gain R_k for every controlled resonant modes. These uncertainties cannot be explicitly considered by the GM or PM. The gain control policy also considers the stability robustness to a generalized dynamic uncertainty which can consider various kinds of uncertainties.

  Besides, the simple GM and PM proposed for SISO systems do not generalize easily to MIMO systems. In comparison, the gain control policy employs the small gain theorem and can be used for both SISO and MIMO systems. Although the phase control policy is interpreted with SISO systems, it is employed in H_∞ control and the nice point is that the H_∞ control can be also used for the control design of MIMO systems. Therefore, phase and gain control policies are more general and more powerful than GM and PM for the study of stability robustness. They can be used for both SISO and MIMO systems with collocated or non-collocated sensors and actuators.

- The purposes of GM and PM are to consider the stability robustness to specific uncertainties. But the purposes of phase and gain control policies

are to consider a set of control objectives including the vibration reduction performance, the stability to parametric and dynamic uncertainties and so on.

Obviously, the proposed phase and gain control policies are more efficient with respect to robust active vibration control.

3.3 Application of phase and gain control policies

3.3.1 Explanation of classical control designs

The principle of phase and gain control policies can explain several classical control designs. In addition to direct velocity feedback control as discussed in section 3.2.1.1, acceleration feedback control and positive position feedback can also be explained as follows.

3.3.1.1 Explanation of AFC

The basic idea of acceleration feedback control (AFC) is to pass the acceleration signal through some second order compensators with suitable parameters and generate a force feedback proportional to the output of the controller (Bayon de Noyer and Hanagud, 1998a). If n resonant modes of a flexible structure $G(s)$ have to be controlled simultaneously, the AFC controller $K_{AFC}(s)$ has to include n compensators in parallel

$$G(s) = \sum_{i=1}^{n} \frac{R_i s^2}{s^2 + 2\zeta_{si}\omega_{si}s + \omega_{si}^2} \tag{3.14}$$

$$K_{AFC}(s) = \sum_{i=1}^{n} \frac{\gamma_i \omega_{ci}^2}{s^2 + 2\zeta_{ci}\omega_{ci}s + \omega_{ci}^2} \tag{3.15}$$

where ω_{si}, ζ_{si} and R_i are the natural frequency, the damping ratio and the gain of i^{th} controlled resonant mode of the flexible structure; ω_{ci}, ζ_{ci} and γ_i are the corresponding parameters of $K_{AFC}(s)$. The principle structure of AFC is shown

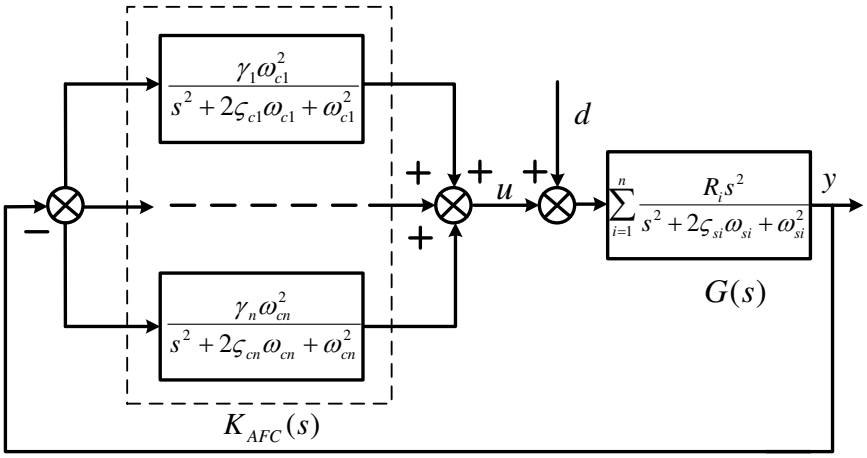

Figure 3.5: The principle of AFC for n controlled resonant modes

in Figure 3.5, where each compensator is just tuned to a controlled resonant mode. This control structure is a specific case of the general control structures since the regulated system output y can be measured and directly fed back to the controller. In addition, the disturbance d and the plant input u are assumed to be exerted at the same position. The structure of $K_{AFC}(s)$ is fixed and the focus of AFC is to determine the parameters of $K_{AFC}(s)$ for every controlled resonant mode.

According to the phase control policy, $\omega_{ci} \approx \omega_{si}$ and appropriate ζ_{ci}, γ_i are used to ensure $|K_{AFC}(j\omega)|$ large enough around ω_{si}. In this case, $L(j\omega)$ can be approximated as

$$L(j\omega) = G(j\omega)K_{AFC}(j\omega) \approx \frac{\gamma_i R_i}{4\zeta_{ci}\zeta_{si}},\ \omega \in [\omega_{si} - \delta_{\omega_{si}},\ \omega_{si} + \delta_{\omega_{si}}] \tag{3.16}$$

This implies that, around ω_{si}, $\gamma_i R_i > 0$ ensures $\Re(L(j\omega)) > 0$ and $|L(j\omega)|$ is proportional to γ_i/ζ_{ci}. Therefore, the selection of ζ_{ci} and γ_i has significant effects on the vibration reduction performance. Due to the fixed structure of $K_{AFC}(j\omega)$, the gain control policy can only be used after ω_{sn} where $K_{AFC}(j\omega)$ begins to roll off.

The above design method of $K_{AFC}(s)$ with phase and gain control policies are consistent with the methods in literature, *e.g.* the critically damped method (Goh

and Yan, 1996), the cross-over point method (Bayon de Noyer and Hanagud, 1998a) and the H_2 optimized method (Bayon de Noyer and Hanagud, 1998b). All of these methods require $\omega_{ci} = \omega_{si}$ and $\gamma_i R_i > 0$.

3.3.1.2 Explanation of PPF

The technique of positive position feedback (PPF) is first introduced by Caughey and Goh (1982), several researches have employed and modified this technique in their own studies. Goh and Caughey (1985) also published a study comparing collocated velocity feedback to PPF. They derived a stability criterion and showed that PPF stability is not dependent on the damping ratios of flexible structures (Preumont, 2011). The PPF is used in Fanson and Caughey (1990) to control the first six bending modes of a cantilever beam, which is proved to be simple to implement and have global stability conditions even in the presence of actuator dynamics. The PPF controllers $K_{PPF}(s)$ are basically a special form of second order compensators. The principle structure of PPF is shown in Figure 3.5, which is similar to that of AFC, and each compensator is tuned to its controlled resonant mode.

$$G(s) = \sum_{i=1}^{n} \frac{R_i}{s^2 + 2\zeta_{si}\omega_{si}s + \omega_{si}^2} \tag{3.17}$$

$$K_{PPF}(s) = \sum_{i=1}^{n} \frac{g_i\omega_{pi}^2}{s^2 + 2\zeta_{pi}\omega_{pi}s + \omega_{pi}^2} \tag{3.18}$$

The effectiveness of vibration control with PPF depends on the accuracy of the modal parameters of the plant model $G_p(s)$ used in the control design (Goh and Lee, 1991). Besides, as any narrow band active control design, $K_{PPF}(s)$ achieves its best results if tuned properly to the targeted controlled resonant mode. As proposed in (Goh and Lee, 1991), the parameters of $K_{PPF}(s)$, *i.e.* g_i, ω_{pi} and ζ_{pi}, have to be decided on the structural damping ratios and natural frequencies, *i.e.* ζ_{si} and ω_{si}, to achieve the maximum amount of damping. Most researchers suggest $\omega_{pi} \approx \omega_{si}$ or ω_{pi} to be lightly larger than ω_{si}, except that $\omega_{pi} = 1.3\omega_{si}$ is chosen in Dosch et al. (1992); Baillargeon and Vel (2005) and $\omega_{pi} = 1.45\omega_{si}$ in Fagan (1993). The range for ζ_{pi} found in the literature reaches from 0.01

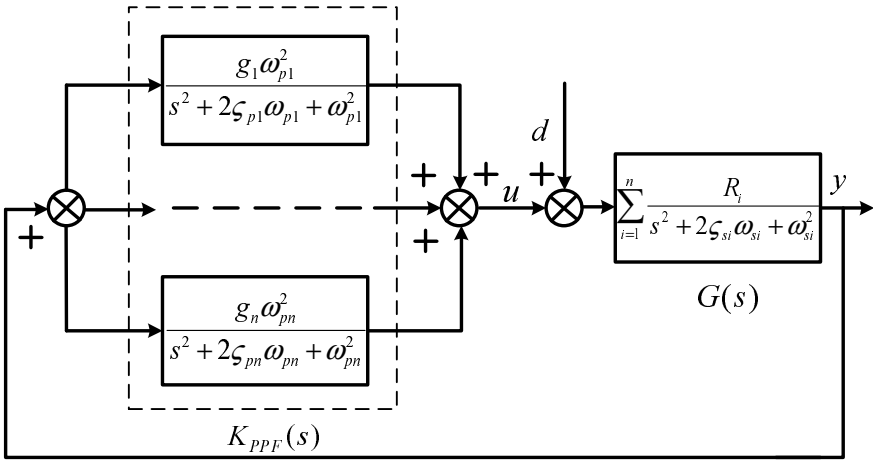

Figure 3.6: The principle of PPF for n controlled resonant modes

to 0.5 to have a compromise between the vibration reduction and the stability robustness (Hegewald and Inman, 2001; Sethi et al., 2006). The values of g_i is closely related to the closed-loop stability as claimed in Preumont (2011). Sometimes, the parameters of $K_{PPF}(s)$ are determined with a trial and error technique experimentally such as in Dosch et al. (1992); Fanson and Chen (1986). Based on the NI approach, simple and analytical stability conditions are derived in Pereiraa and Aphaleb (2013) to determine these parameters, where the sensor dynamics at low frequencies are also considered.

3.3.2 The proposed qualitative robust control methodology

As the classical control designs cannot ensure that the designed controllers are optimal with respect to a set of control objectives simultaneously, in this chapter, a general and systematic robust control methodology is developed by employing phase and gain control policies in the dynamic output feedback H_∞ control. As shown in the H_∞ control structure of Figure 3.7, according to the control objectives, the augmented plant $P(s)$ is built by incorporating necessary weighting functions W_i into the typical feedback control structure. The weighting functions account for the relative magnitude of signals, their frequency dependence and relative importance. Two exogenous input signals $w = [w_1, w_2]^T$ and three

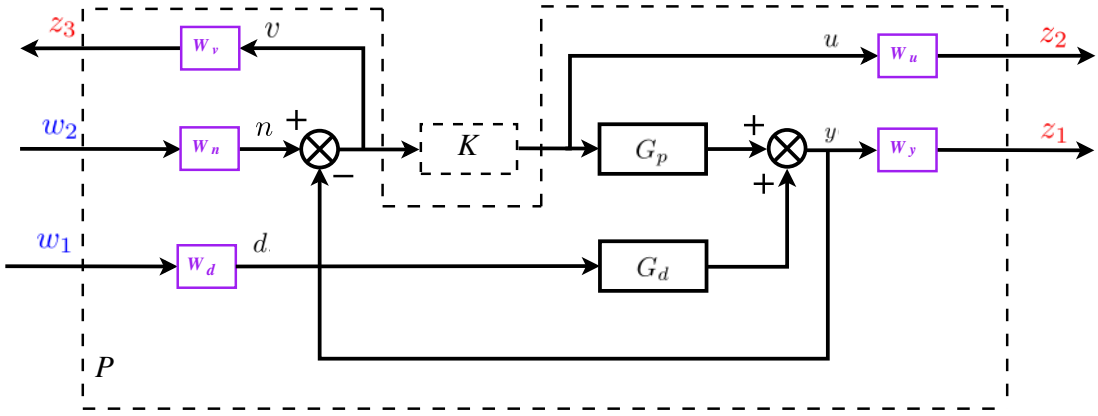

Figure 3.7: H_∞ control structure

regulated signals $z = [z_1, z_2, z_3]^T$ are employed, where $d = W_d w_1$, $n = W_n w_2$, $z_1 = W_y y$, $z_2 = W_u u$ and $z_3 = W_v v$. By partitioning $P(s)$ according to the size of signals, the system is described as

$$\begin{bmatrix} z(s) \\ v(s) \end{bmatrix} = P(s) \begin{bmatrix} w(s) \\ u(s) \end{bmatrix} = \begin{bmatrix} P_{zw}(s) & P_{zu}(s) \\ P_{vw}(s) & P_{vu}(s) \end{bmatrix} \begin{bmatrix} w(s) \\ u(s) \end{bmatrix} \tag{3.19}$$

$$u(s) = K(s)v(s) \tag{3.20}$$

where

$$P_{zw}(s) = \begin{bmatrix} W_d(s)G_d(s)W_y(s) & 0 \\ 0 & 0 \\ -W_d(s)G_d(s)W_v(s) & W_n(s)W_v(s) \end{bmatrix}, \quad P_{zu}(s) = \begin{bmatrix} G_p(s)W_y(s) \\ W_u(s) \\ -G_p(s)W_v(s) \end{bmatrix}$$

$$P_{vw}(s) = \begin{bmatrix} -W_d(s)G_d(s) & W_n(s) \end{bmatrix}, \qquad P_{vu}(s) = \begin{bmatrix} -G_p(s) \end{bmatrix}$$

The standard H_∞ control problem is to achieve a stabilizing controller $K(j\omega)$ which minimizes the H_∞ norm of the augmented closed-loop transfer function matrix $F_l(P, K)(s)$ defined as

$$\|F_l(P, K)(s)\|_\infty = \sup_\omega \bar{\sigma}(F_l(P, K)(j\omega))$$

where $F_l(P,K)(j\omega) = P_{zw}(j\omega) + P_{zu}(j\omega)K(j\omega)(I - P_{vu}(j\omega)K(j\omega))^{-1}P_{vw}(j\omega)$. Let $\gamma_{\min}$ be the minimum value of $\|F_l(P,K)(s)\|_\infty$ over all stabilizing controllers. The H_∞ sub-optimal control problem is: given a $\gamma > \gamma_{\min}$, find all stabilizing controllers such that $\|F_l(P,K)(s)\|_\infty \leq \gamma$. This optimization can be solved efficiently and by reducing γ iteratively an optimal solution is achieved (Doyle et al., 1989). With appropriate weighting functions, $\gamma = 1$ can be used and a complete set of control objectives are transformed to the constraints on the corresponding weighted closed-loop transfer functions, *e.g.* $\|T_{z_1w_1}(s)\|_\infty \leq 1$ represents the specification of vibration reduction. Due to the property of H_∞ norm, $\|F_l(P,K)(s)\|_\infty \leq 1$ ensures $\|T_{z_jw_i}(s)\|_\infty \leq 1$, that is, these control objectives are satisfied simultaneously with the designed H_∞ controller.

As known, in H_∞ control the selection of weighting functions is quite important to achieve a satisfactory $K(s)$. Fortunately, according to a set of control objectives, phase and gain control policies can incorporate necessary weighting functions in H_∞ control and determine them in a rational and systematic way:

- To define the specification of vibration reduction, $W_d(j\omega)$ and $W_y(j\omega)$ should be used and satisfy

$$|W_d(j\omega)W_y(j\omega)U(\omega)| \geq 1, \forall\omega \in \mathbb{R}. \tag{3.21}$$

  then $\|T_{z_1w_1}(s)\|_\infty = \|W_d(s)G_d(s)S(s)W_y(s)\|_\infty \leq 1$ ensures $|T_{yd}(j\omega)| = |G_d(j\omega)S(j\omega)| \leq U(\omega), \forall\omega \in \mathbb{R}$. Depending on the shape of $U(\omega)$, sometimes complicated $W_d(j\omega)$ and $W_y(j\omega)$ may be required and thus decomposed H_∞ control structure is recommendable in such cases (Font et al., 1997).

- To impose the requirements on $K(j\omega)$ according to phase and gain control policies, $|K(j\omega)S(j\omega)|$ can be investigated since it is a good indicator of $|K(j\omega)|$ when $|L(j\omega)| \ll 1$, as shown in Table 3.1. When the phase control policy is used, $|K(j\omega)|$ has to be large enough for effective vibration reduction. From the Equation (3.5), $W_n(j\omega)$ and $W_u(j\omega)$ should be used and satisfy

$$|W_n(j\omega)W_u(j\omega)G_d(j\omega)| < |G_p(j\omega)U(j\omega)|, \forall\omega/\ |G_d(j\omega)| > U(\omega) \tag{3.22}$$

The phase requirement on $K(j\omega)$ can be automatically fulfilled by the H_∞ control algorithm with a stable stabilizing $K(s)$. This provides adequate stability robustness to parametric uncertainties. When the gain control policy is used, $|K(j\omega)|$ has to be as small as possible to have moderate control energy and reduce the effects of the measurement noise. Besides, the gain control policy has to provide a certain level of stability robustness to a dynamic uncertainty. For this purpose, with the additive dynamic uncertainty $\Delta_a(s)$, $W_n(j\omega)$ and $W_u(j\omega)$ should be used and satisfy

$$|W_n(j\omega)W_u(j\omega)| > |W_a(j\omega)|, \ \forall\omega \in \mathbb{R} \tag{3.23}$$

then $\|T_{z_2w_2}(s)\|_\infty = \|W_n(s)K(s)S(s)W_u(s)\|_\infty \leq 1$ ensures the stability robustness to $\Delta_a(s)$ based on Equation (3.9); with the multiplicative dynamic uncertainty $\Delta_m(s)$, $W_n(j\omega)$ and $W_y(j\omega)$ should be used and satisfy

$$|W_n(j\omega)W_y(j\omega)| > |W_m(j\omega)|, \ \forall\omega \in \mathbb{R} \tag{3.24}$$

then $\|T_{z_1w_2}(s)\|_\infty = \|W_n(s)T(s)W_y(s)\|_\infty \leq 1$ ensures the stability robustness to $\Delta_m(s)$ based on Equation (3.10).

- To have a modulus margin $M_m > \lambda \in (0,1)$, $W_n(j\omega)$ and $W_v(j\omega)$ should be used and satisfy

$$|W_n(j\omega)W_v(j\omega)| > \lambda, \forall\omega \in \mathbb{R} \tag{3.25}$$

This can be derived from Equation (5.12) and the constraints on $|S(j\omega)|$

$$\|T_{z_3w_2}(s)\|_\infty = \|W_n(s)S(s)W_v(s)\|_\infty \leq 1$$

For instance $\lambda = 0.5$ implies that $\sup_\omega |S(j\omega)|$ must be less than 2 and thus it is required $|W_n(j\omega)W_v(j\omega)| > 0.5, \forall\omega \in \mathbb{R}$.

As shown above, according to the set of control objectives, phase and gain control policies can be used in H_∞ control to incorporate necessary weighting functions and determine them in a rational and systematic way. On the other

hand, with the appropriate weighting functions, efficient H_∞ control algorithms can automatically realize phase and gain control policies and generate a satisfactory H_∞ controller to make a trade-off among various control objectives. Although the phase control policy is interpreted with the SISO systems, a nice point is that the H_∞ control can be also used for the control design of MIMO systems. As a result, a general and systematic robust control methodology for active vibration control of flexible structures is developed by well employing phase and gain control policies in the dynamic output feedback H_∞ control. This control methodology can guarantee quantitative nominal vibration reduction defined by the positive frequency dependent function and qualitative robustness properties of the closed-loop system. It can be used for both SISO and MIMO systems with collocated or non-collocated sensors and actuators.

3.4 Numerical simulations and experimental results

3.4.1 System modeling

To illustrate the effectiveness of the proposed control methodology, active vibration control of a non-collocated piezoelectric cantilever beam is investigated, as shown in Figure 3.8, where a piezoelectric actuator is mounted near the fixed end and an accelerometer near the free end. Based on the modal analysis approach (Meirovitch, 1986) and the modeling of piezoelectric actuators (Moheimani and Fleming, 2006), applying Laplace transformation and assuming zero initial conditions, the plant dynamical model $G_p(s)$ representing the dynamics from the voltage applied on the piezoelectric actuator $V_a(x_a, s)$ to the beam acceleration $\ddot{Y}(x, s)$ is

$$G_p(s) = \frac{\ddot{Y}(x, s)}{V_a(x_a, s)} = \sum_{i=1}^{\infty} \frac{R_i s^2}{s^2 + 2\zeta_i \omega_i s + \omega_i^2} \tag{3.26}$$

Similarly, the disturbance dynamical model $G_d(s)$ representing the dynamics from the disturbance $d(x_d, s)$ to the beam acceleration $\ddot{Y}(x, s)$ is

$$G_d(s) = \frac{\ddot{Y}(x,s)}{d(x_d,s)} = \sum_{j=1}^{\infty} \frac{R_j s^2}{s^2 + 2\zeta_j \omega_j s + \omega_j^2} \tag{3.27}$$

where $R_{i/j}$, $\zeta_{i/j}$ and $\omega_{i/j}$ are the modal parameters to be identified.

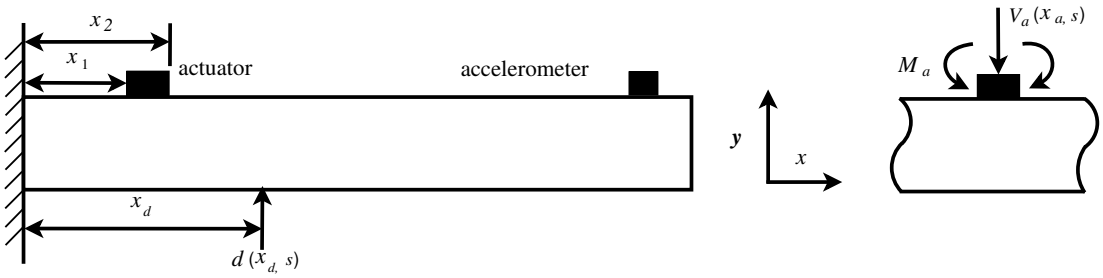

Figure 3.8: The piezoelectric cantilever beam

The experimental set-up for the parameter identification is illustrated in Figure 3.9, where the dSPACE generates and acquires the input signal $x(t)$, pseudo random binary sequence (PRBS), and acquire the output signal $y(t)$ from the accelerometer. Experimental frequency responses are estimated by $T_{xy}(\omega)$, being the quotient of the cross power spectral density of $x(t)$ and $y(t)$, $S_{xy}(\omega)$, and the power spectral density of $x(t)$, $S_{xx}(\omega)$ (Bendat and Piersol, 1980),

$$T_{xy}(\omega) = \frac{S_{xy}(\omega)}{S_{xx}(\omega)}, \ \omega \in \{\omega_1, \omega_2, \ldots, \omega_M\} \tag{3.28}$$

where M is the number of estimated frequency points. For $G_p(s)$, PRBS is sent to the piezoelectric actuator with no input to the shaker. Similarly, PRBS is sent to the shaker for $G_d(s)$ and the signal to the piezoelectric actuator is set to zero. To avoid aliasing problem, the sampling frequency of dSPACE is set at 10 kHz. The Hanning window and twenty averages are employed to have reliable experimental frequency responses, as shown in Figure 3.10.

With $T_{xy}(\omega)$, $G_d(s)$ and $G_p(s)$ can be estimated as a ratio of two polynomials in the Laplace variable s based on Equation (3.26) and (3.27) with the user-defined number of poles and zeros. The best curve fitting is performed to deter-

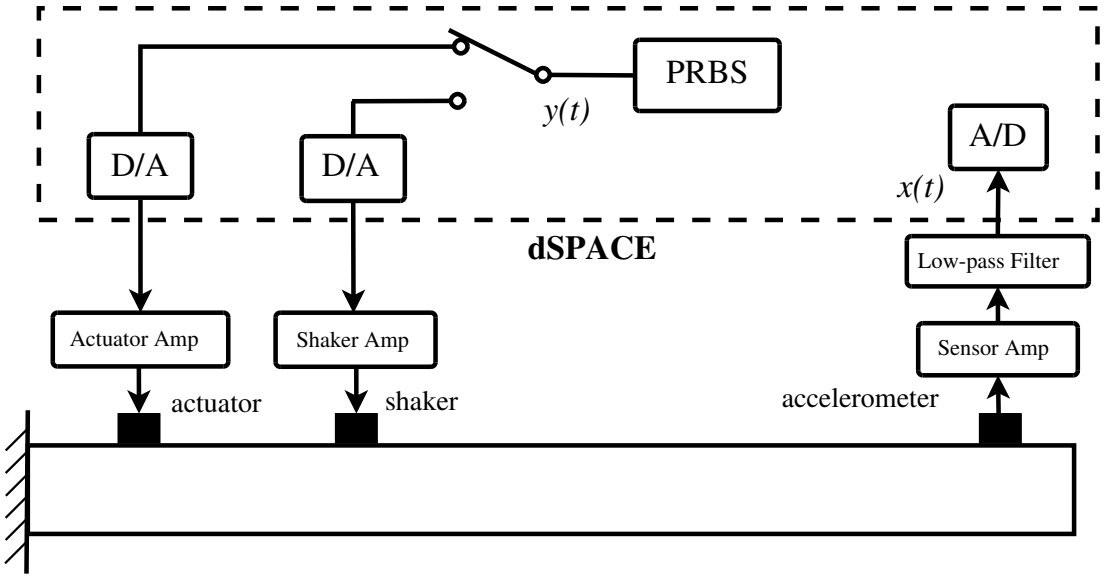

Figure 3.9: Experimental set-up for parameter identification

mine the values of poles, zeros and gains with a least squares method (Schoukens and Pintelon, 1991),

$$\min_{P} \sum_{k=1}^{M} \varphi(\omega(k)) |T_{xy}(\omega(k)) - G(\omega(k))|^2, \ k \in \{1, 2, \ldots, M\} \tag{3.29}$$

where P represents all the modal parameters of $G(j\omega)$ to identify and $\varphi(\omega(k))$ is a frequency dependent weighting function to emphasize the importance over different frequency ranges. The above parameter identification procedure can be realized in Matlab R2012 with a graphical user interface. This helps us to obviously observe the contribution of every resonant mode to the whole dynamics. The dynamics of the shaker, the piezoelectric actuator, the accelerometer, the filters and other hardwares are all incorporated into the identified $G_d(s)$ and $G_p(s)$:

$$G_d(s) = \frac{-1.2 \times 10^{-2} s^2}{s^2 + 65.8s + 1.6 \times 10^5} + \frac{1.4 \times 10^{-2} s^2}{s^2 + 172.9s + 1.4 \times 10^6} + \frac{-2.1 \times 10^{-3} s^2}{s^2 + 505.3s + 2.0 \times 10^7}$$

$$G_p(s) = \frac{-3.6 \times 10^{-4} s^2}{s^2 + 65.6s + 1.6 \times 10^5} + \frac{-2.8 \times 10^{-4} s^2}{s^2 + 153.0s + 1.5 \times 10^6} + \frac{3.3 \times 10^{-3} s^2}{s^2 + 609.1s + 1.7 \times 10^7}$$

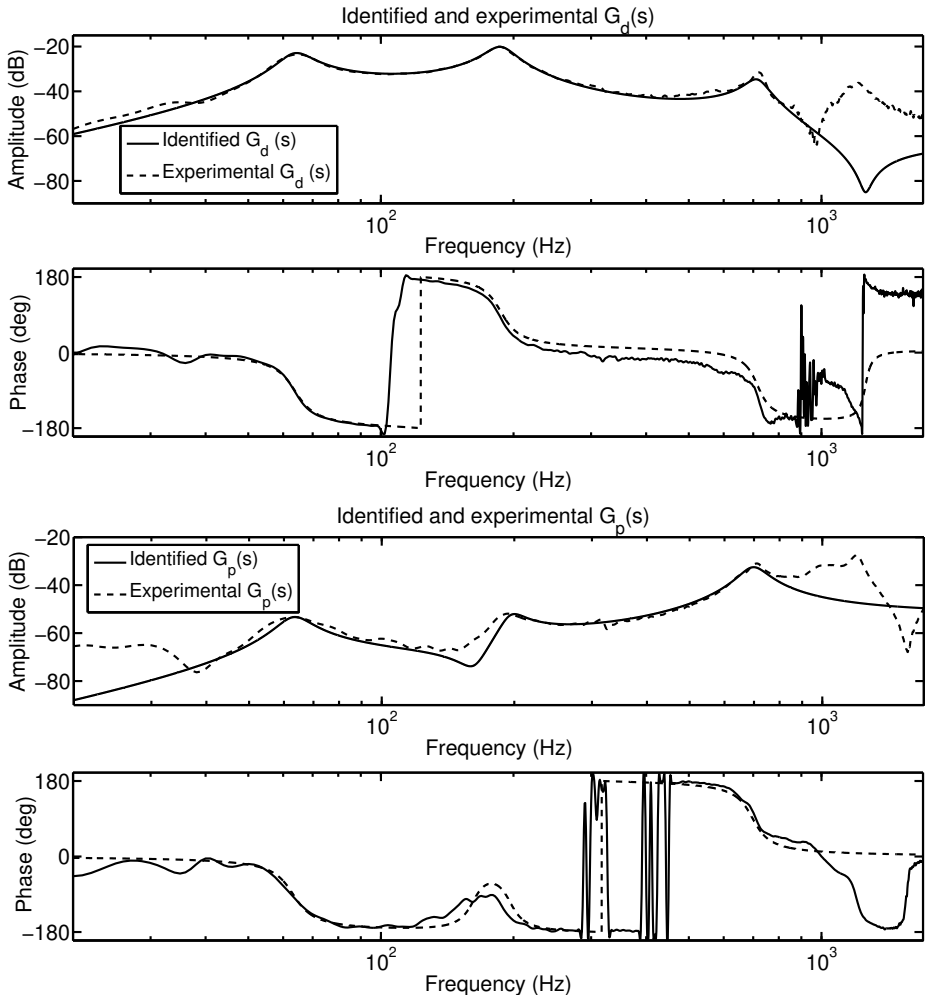

Figure 3.10: Identified and experimental $G_d(j\omega)$ and $G_p(j\omega)$

As illustrated in Figure 3.10, the identified frequency responses of $G_d(s)$ and $G_p(s)$ are in good agreement with the experimental ones over the frequency range of interest. It is notable that either from analytical or finite element method (Moheimani and Fleming, 2006; Piefort, 2001) different transfer functions associated with the same structure should have identical poles, but due to the errors in the system identification, the poles of identified $G_d(s)$ and $G_p(s)$ are not exactly the same. Based on the specification of vibration reduction as illustrated in Figure 3.1, the phase control policy has to be applied to the first two resonant modes and the gain control policy to the others.

3.4.2 Design of AFC

Based on the cross-over point method (Bayon de Noyer and Hanagud, 1998a), the parameters of $K_{AFC}(s)$ are determined as $\omega_{ci} = \omega_{si}$, $\zeta_{ci} = 2\zeta_{fi} - \zeta_{si}$ and $\gamma_i = \frac{(\zeta_{ci}-\zeta_{si})^2}{R_i}$. The ζ_{fi} is a user-defined final damping ratio of the i^{th} controlled resonant mode and the final frequency $\omega_{fi} = \sqrt{\omega_{si}\omega_{ci}} = \omega_{si}$. Based on the above identified $G_p(s)$, with $\zeta_{f1} = 0.3$ and $\zeta_{f2} = 0.2$, $K_{AFC1}(s)$ and $K_{AFC2}(s)$ are designed for the first resonant mode and the first two respectively,

$$\begin{aligned} K_{AFC1}(s) &= \frac{-8.4 \times 10^7}{s^2 + 410.8s + 1.6 \times 10^5} \\ K_{AFC2}(s) &= \frac{-8.4 \times 10^7}{s^2 + 410.8s + 1.6 \times 10^5} + \frac{-4.1 \times 10^8}{s^2 + 831.9s + 1.5 \times 10^6} \end{aligned}$$

The numerical simulations with $K_{AFC1}(s)$, $K_{AFC2}(s)$ and the identified models are illustrated in Figure 3.11. As required by the phase control policy around the controlled resonant frequencies ω_{ci}, $|K_{AFC1}(j\omega)|$ and $|K_{AFC2}(j\omega)|$ are large enough for effective vibration control and $L(j\omega)$ stays in RHP to have the stability robustness to parametric uncertainties. On the other hand, as required by the gain control policy, $K_{AFC1}(j\omega)$ and $K_{AFC2}(j\omega)$ roll off after ω_{c1} and ω_{c2} respectively to have a certain level of stability robustness to the dynamic uncertainty.

3.4.3 Design of the proposed control methodology

Considering the fact that $G_d(s)$ and $G_p(s)$ should have the same poles and motivated by the work in (Font et al., 1994), for this particular case, $G_p(s)$ can be decomposed as $G_p(s) = G_{p12}(s)G_{p3}(s)$, where $G_{p12}(s) \approx G_{d1}(s) + G_{d2}(s)$. The phase control policy is applied to $G_{p12}(s)$ and the gain control policy is applied to other dynamics. Moreover, to simplify $W_d(j\omega)$ and $W_y(j\omega)$ required to reflect the specification of vibration reduction, $G_{p12}(s)$ is decomposed as illustrated in Figure 3.12. With this decomposition, the constant $W_d(j\omega)$, $W_{y1}(j\omega)$ and $W_{y2}(j\omega)$ can be used to represent the specification of vibration reduction

$$\|T_{z_{11}w_1}(s)\|_\infty = \|W_d(s)G_{p1}(s)S(s)W_{y1}(s)\|_\infty \leq 1$$

$$\|T_{z_{12}w_1}(s)\|_\infty = \|W_d(s)G_{p2}(s)S(s)W_{y2}(s)\|_\infty \leq 1$$

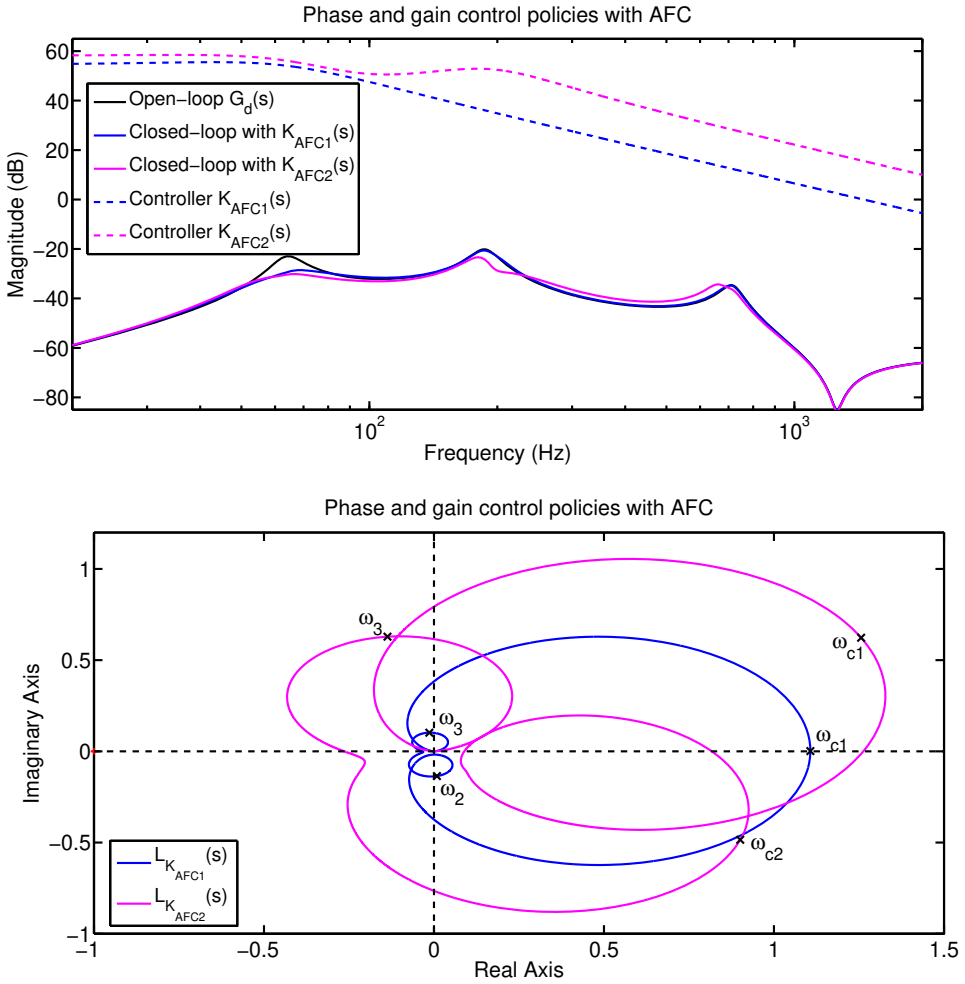

Figure 3.11: Phase and gain control policies with AFC: ω_{ci} represents the i^{th} controlled resonant frequency

It is notable that $W_d(j\omega)$, $W_{y1}(j\omega)$ and $W_{y2}(j\omega)$ can also explicitly prevent the pole-zero compensation between $G_p(j\omega)$ and $K(j\omega)$ at ω_1 and ω_2 (Scorletti and Fromion, 2008a). These decompositions reduce the order of H_∞ controller, being the total order of all involved plants and weighting functions. For the sake of simplicity, $W_y(j\omega)$ is no longer used in the decomposed H_∞ control structure and thus only the additive dynamic uncertainty is explicitly considered with $W_n(j\omega)$ and $W_u(j\omega)$.

For this particular case, the proposed control methodology generates the con-

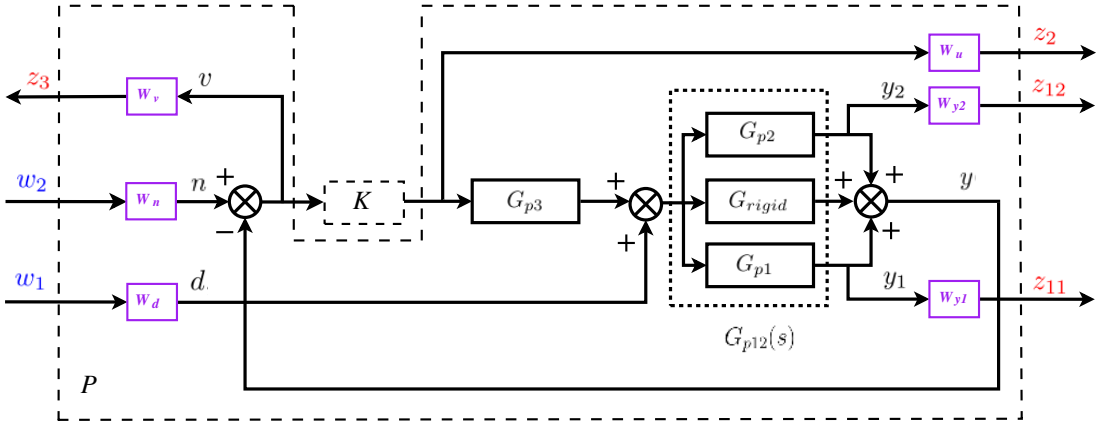

Figure 3.12: Decomposed H_∞ control structure

troller $K_\infty(s)$ using all constant weighting functions and the popular balanced truncation method (Gu et al., 2005) is used to have $K_{r\infty}(s)$ with a reduced order for easier real-time implementation,

$$K_\infty(s) = \frac{1268.4(s-4.3\times10^5)(s^2-67.8s+2.5\times10^5)(s^2+609.1s+1.9\times10^7)}{(s^2+408.9s+3.2\times10^5)(s^2+950.4s+9.0\times10^5)(s^2+4167s+1.6\times10^7)}$$

$$K_{r\infty}(s) = \frac{45134(s-1.1\times10^4)(s^2-70.2s+2.5\times10^5)}{(s^2+354.5s+2.0\times10^5)(s^2+682s+8.7\times10^6)}$$

The numerical simulations with $K_\infty(s)$, $K_{r\infty}(s)$ and the identified models are illustrated in Figure 3.11. As required by the phase control policy around ω_{c1} and ω_{c2}, $|K_\infty(j\omega)|$ and $|K_{r\infty}(j\omega)|$ are large enough for effective vibration control and $L(j\omega)$ stays in RHP to have the stability robustness to parametric uncertainties. On the other hand, as required by the gain control policy, $K_\infty(j\omega)$ and $K_{r\infty}(j\omega)$ roll off after ω_{c2} to have a certain level of stability robustness to the dynamic uncertainty.

3.4.4 Comparisons between AFC and proposed control methodology

From the numerical simulations, it is shown that for this particular case both AFC and the proposed control methodology achieve the vibration reduction of their controlled resonant modes. However, the specification of vibration reduc-

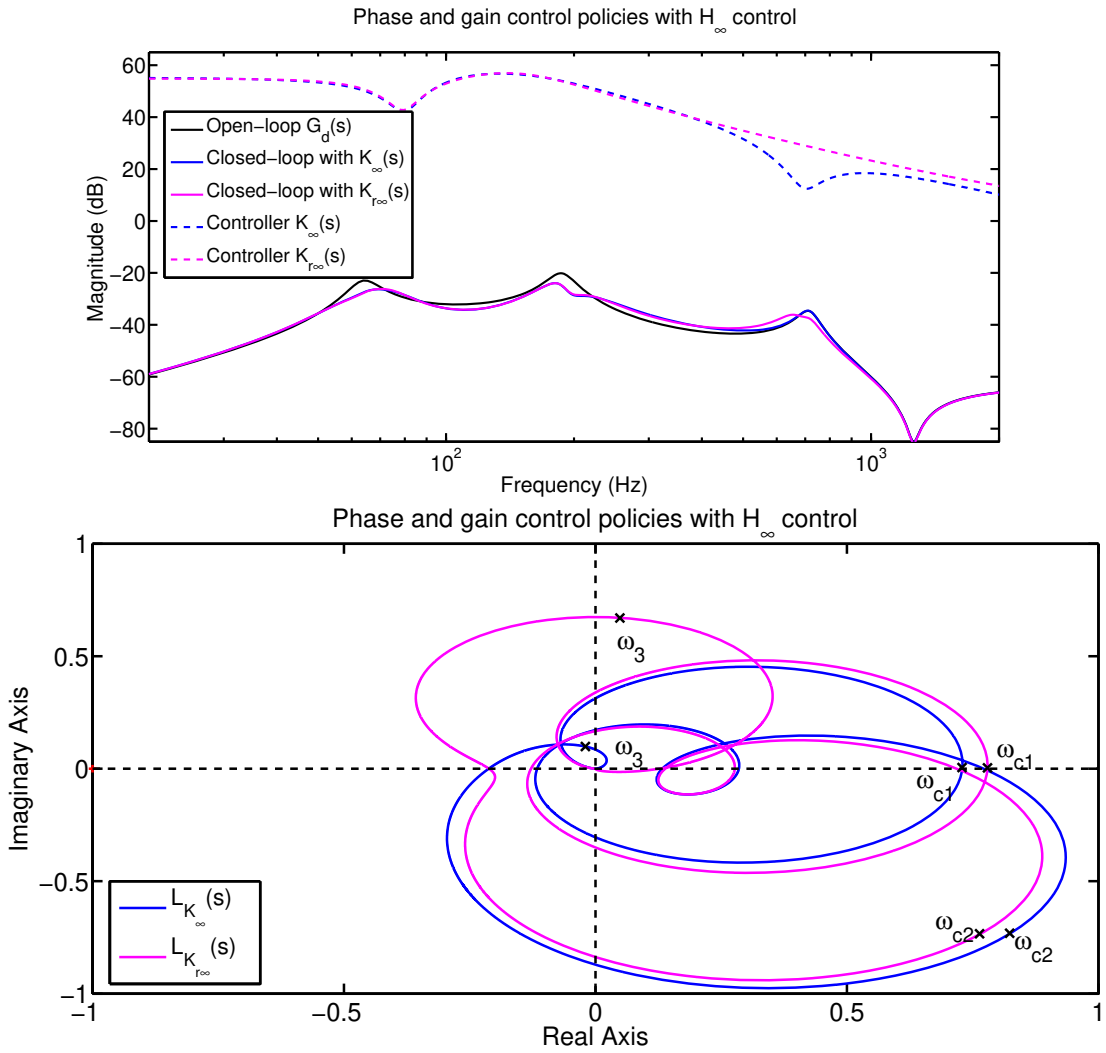

Figure 3.13: Phase and gain control policies with H_∞ control: ω_{ci} represents the i^{th} controlled resonant frequency

tion is not directly considered by AFC. It is reflected by the user-defined damping ratios such as $\zeta_{f1} = 0.3$ and $\zeta_{f2} = 0.2$, which are closely related to the magnitude of the open-loop transfer function. On the other hand, the parametric uncertainties could have considerable detrimental effects on the practically obtained damping ratios. Besides, when the controlled resonant modes are closely spaced, it is not easy to determine the parameters of $K_{AFC}(j\omega)$ and a large amount of time and energy could be required to meet the specification of vibration reduction. Sometimes, even a lot of efforts are put into the parameter selection, no

satisfactory $K_{AFC}(j\omega)$ is obtained. This may lead to the question: with respect to the specification of vibration reduction, whether there exists a satisfactory $K_{AFC}(j\omega)$ or not. Fortunately, the proposed control methodology has no such question and a trade-off among various control objectives can be achieved by tuning the weighting functions.

The comparisons in terms of the main design processes between H_∞ control design and classical control designs that shape the open-loop transfer function are illustrated in Figure 3.14. It clearly shows that the classical open-loop shaping control methods consider the control objectives, which are defined in the frequency or time domain, with the relationship between the closed-loop transfer functions and the open-loop transfer function. However, for the time-domain control objectives such as the setting time, the transformations from the control objectives to the closed-loop transfer functions are not accurate and sometimes could be very complicated especially for high-order systems. In addition, if the control objectives are defined in the frequency domain, it is desirable to consider them by enforcing the constrains on the related closed-loop transfer functions directly. For example, to satisfy the specification of vibration reduction $|G_d(j\omega)(1 + L(j\omega))^{-1}| \leq U(\omega),\ \forall\omega$, the proposed control methodology employs suitable weighting functions to enforce quantitative constraints on $|G_d(j\omega)(1 + L(j\omega))^{-1}|$, however, the classical open-loop shaping control methods achieve this by appropriate shaping of $|L(j\omega)|$, which does not consider $G_d(j\omega)$ and could be very time consuming. Even sometimes, for a selected control structure, *e.g.* AFC, PPF and PID, the control objectives cannot be achieved by any selection of the controller parameters.

In real-time implementation, due to the physical limitations, it is necessary to enforce an upper bound on $U_{\max} = \max_t |u(t)|,\ \forall t \in \mathbb{R}$ to avoid the controller saturation and exceeding the actuator operated voltage. It is normally difficult to enforce the constraint on $U_{\max}$ directly in H_∞ control, however, from a practical point of view, $U_{\max}$ can be limited by restricting $|K(j\omega)|$ in the frequency domain. Due to the fixed structure of $K_{AFC}(j\omega)$, it can only roll off after the last controlled resonant mode even the gain control policy is indeed required at lower frequencies. This means that AFC has little flexibility to make a trade-off between the vibration reduction performance and the control energy. An unnecessarily

large $U_{\max}$ may be produced. In contrast, the proposed control methodology can provide more flexibility and explicitly limit $|K(j\omega)|$ with frequency dependent weighting functions, for instance, the controller $K'_\infty(j\omega)$ is obtained with a first order low-pass $W_u(j\omega)$,

$$K'_\infty(s) = \frac{2.78\times10^5(s-2431)(s+1)(s^2-228.2s+2.8\times10^5)}{(s+963.8)(s^2+607.4s+1.23\times10^5)(s^2+413.6s+6.23\times10^5)} \times \frac{(s^2+609.1s+1.92\times10^7)}{(s^2+3280s+1.91\times10^7)}$$

As shown in Figure 3.15, compared to $K_\infty(j\omega)$ obtained with all constant weighting functions, $|K'_\infty(j\omega)| \approx |K_\infty(j\omega)|$ around the controlled resonant frequencies for effective vibration reduction and $|K'_\infty(j\omega)| \ll |K_\infty(j\omega)|$ at low frequencies. As illustrated in Figure 3.16, the numerical simulations demonstrate that $K'_\infty(j\omega)$ produces a smaller $U_{\max}$ than $K_\infty(j\omega)$ and $K_{AFC2}(j\omega)$ do.

The above analysis implies that the proposed control methodology may be not the best choice for some specific SISO cases. Sometimes, other simpler control designs such as AFC can also satisfy the control objectives. But the proposed control methodology is more general and more systematic. It can be used for both SISO and MIMO systems to consider a complete set of control objectives and provide enough flexibility to make a trade-off among them.

3.4.5 Experimental implementation

The experimental set-up for real-time implementation is depicted in Figure 3.17. The designed continuous controllers are discretized using bilinear transform and compiled to obtain the digital controller codes to upload dSPACE DS1104 rapid prototyping digital controller board together with Matlab/Simulink R2012 and ControlDesk 4.1. The analog-to-digital (A/D) and digital-to-analog (D/A) converters are included in dSPACE hardware. The sampling frequency of dSPACE is set at 10 kHz, which is high enough to avoid the aliasing problem. The vibration signal measured by the accelerometer is first through a low-pass filter and then enters the A/D converter. A high-voltage amplifier, capable of driving highly capacitive loads, is used to supply necessary voltage to the piezoelectric actuator. Disturbance signal PRBS with suitable magnitude is generated by dSPACE

and sent to a shaker to excite the beam. The offset of the measurement noise is acquired and compensated by adding an external signal with Simulink. It is notable that all amplifies have to keep the same amplification factor as used in the system identification process.

Not surprisingly, the output of $K_{AFC2}(s)$ is saturated. As shown in Figure 3.18, $K_{AFC1}(s)$, $K_{\infty}(s)$ and $K_{r\infty}(s)$ achieve 8 dB reduction for the first resonant mode. $K_{\infty}(s)$ and $K_{r\infty}(s)$ also achieve 11 dB reduction for the second one. The spillover instability due to the neglected high frequency dynamics is avoided. Compared to the numerical results calculated with the identified $G_d(s)$ and $G_p(s)$, the experimental vibration reduction performances are better. To our best understanding, this performance discrepancy is mainly due to the errors in the system identification, which result in parametric uncertainties on $G_d(s)$ and $G_p(s)$, *e.g.* the poles of the identified $G_d(s)$ and $G_p(s)$ are not the same and the realistic $|G_p(s)|$ is indeed larger than the identified one. To have good agreements between numerical and experimental results, more accurate system modeling is desirable. The experimental results also demonstrate that, when the phase control policy is used, the variation in $|L(j\omega)|$ due to parametric uncertainties does not destabilize the system but has considerable effects on the vibration reduction performances. In addition, when the gain control policy is used, $|L(j\omega)|$ should be small enough, otherwise the disturbance signal may be amplified. This problem is most critical over transition frequency ranges, for instance, with $K_{\infty}(s)$ and $K_{r\infty}(s)$ this amplification occurs between the second and third resonant frequencies. As shown in Figure 3.15, $|K_{AFC1}(j\omega)| \ll |K_{\infty}(j\omega)|$ over the transition frequency range and this disturbance amplification is avoided with $K_{AFC1}(s)$. Therefore, to avoid the disturbance amplification, more accurate system modeling is beneficial and the controller has to roll off quickly enough over the transition frequency ranges. With the proposed control methodology, this roll-off requirement on the controller can be reflected by the corresponding weighting functions such as $W_n(s)$ and $W_u(s)$ of Figure 3.7. It is also notable that a trade-off among various control objectives must be considered in the selection of weighting functions.

3.5 Summary

The main contribution of this chapter is to propose a general and systematic robust control methodology for active vibration control of flexible structures such that the complete set of control objectives can be investigated. To achieve this goal, phase and gain control policies are proposed to impose qualitative frequency dependent requirements on the controller over the corresponding frequency ranges. By well employing phase and gain control policies in the dynamic output feedback H_∞ control, a general and systematic robust control methodology is developed: phase and gain control policies incorporate the necessary weighting functions and determine them in a rational and systematic way; on the other hand, with the appropriate weighting functions, efficient H_∞ control algorithms can automatically realize phase and gain control policies and generate a satisfactory H_∞ controller. The proposed control methodology makes full use of phase and gain control policies and the H_∞ control, thus guaranteeing quantitative nominal vibration reduction defined by the positive frequency dependent function and qualitative robustness properties of the closed-loop system. This control methodology can be used for both SISO and MIMO systems with collocated or non-collocated sensors and actuators. In this chapter, this control methodology is validated on the non-collocated SISO piezoelectric cantilever beam. Both numerical simulations and experimental results demonstrate the effectiveness of the proposed control methodology.

Since the proposed control methodology is general and systematic, it can be applied to more complicated and practical structures, *e.g.* the suspension systems (Zhong et al., 2010) where several sensors and actuators can be used. To quantitatively verify the robustness properties of the closed-loop system with the designed H_∞ controller, deterministic and probabilistic robustness analyses can be employed, as shown in chapter 4. In chapter 5, with the finite dimensional LMI optimization (Scorletti, 1996), the proposed control methodology can also be extended to linear parameter varying systems to have a quantitative robust parameter-dependent H_∞ controller.

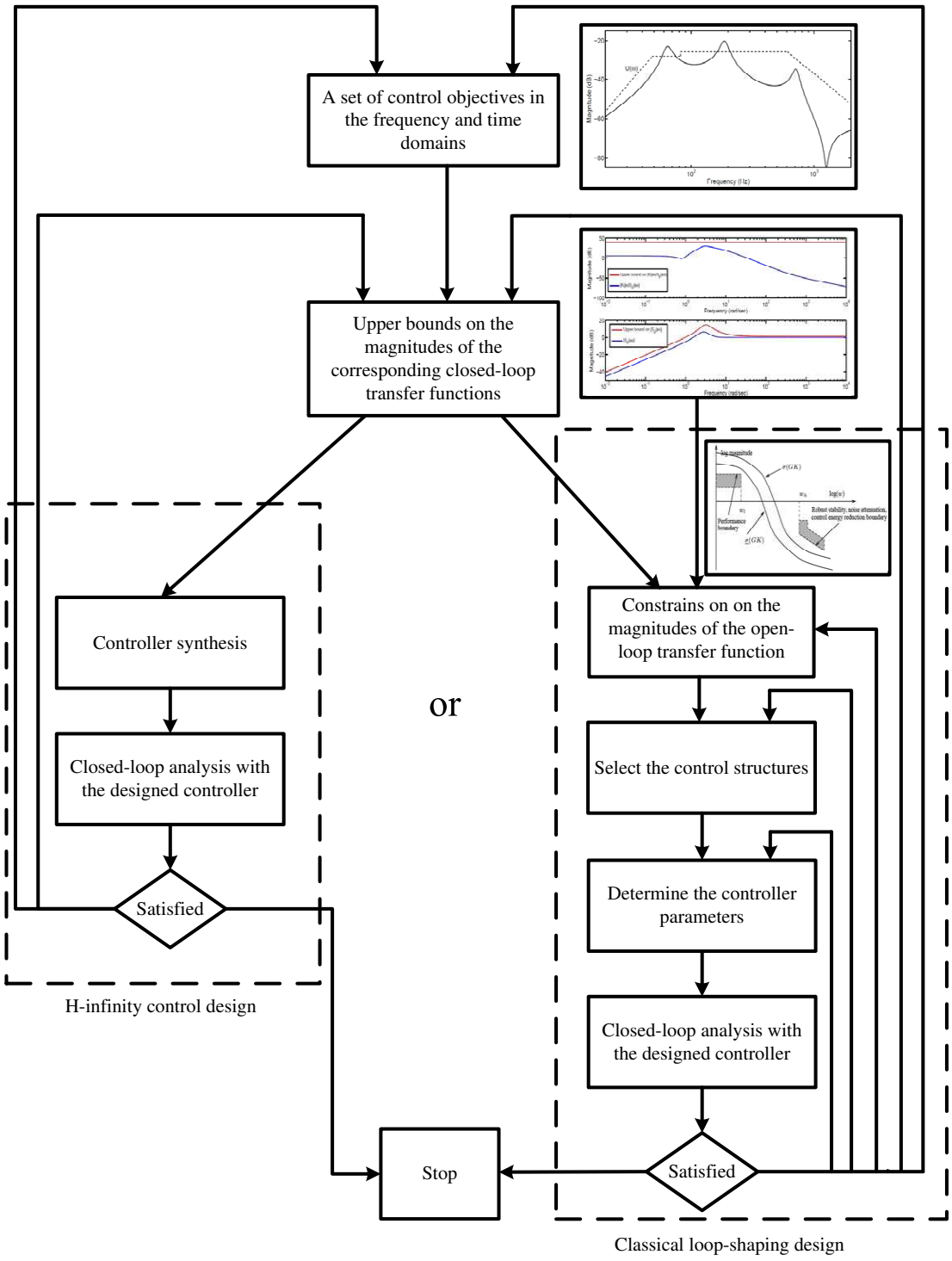

Figure 3.14: Comparisons between classical control and proposed control method (Scorletti and Fromion, 2008a)

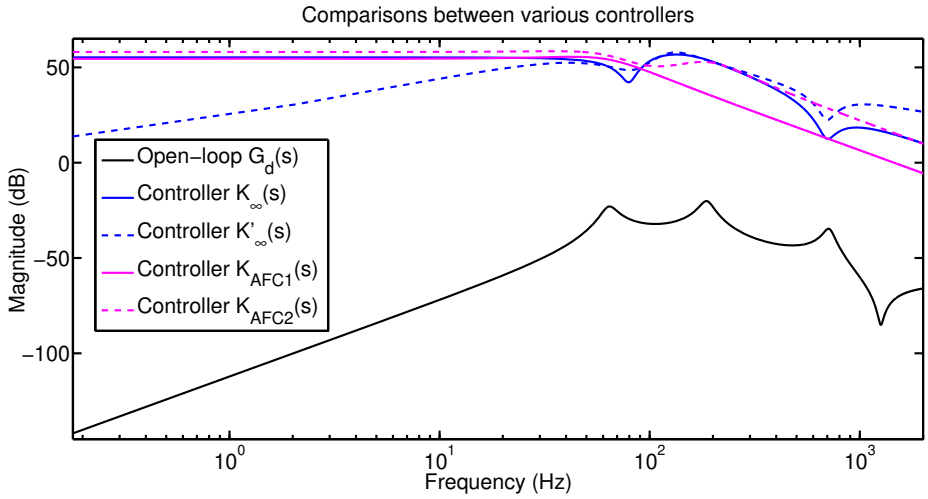

Figure 3.15: Comparisons between various controllers

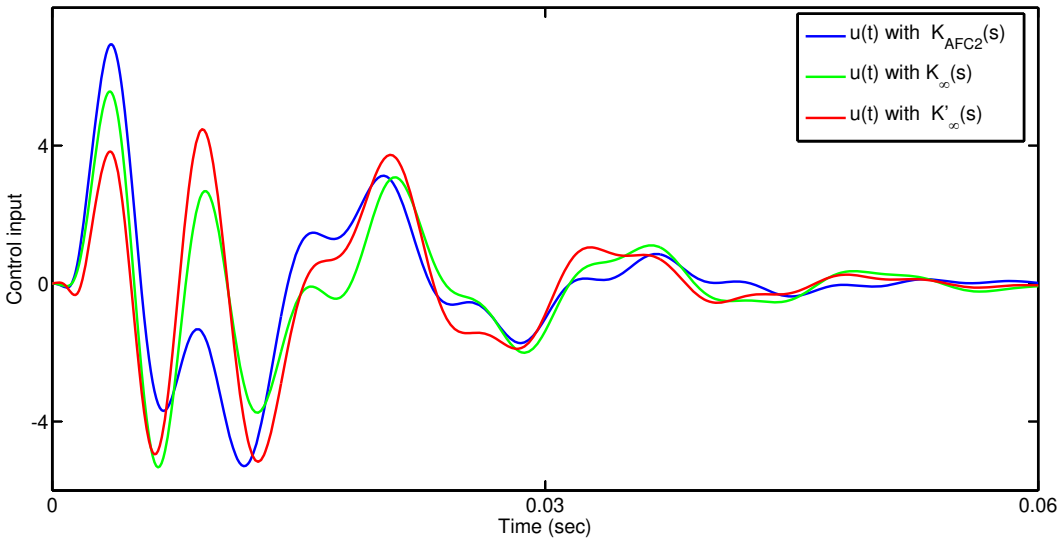

Figure 3.16: Comparisons of $U_{\max}$ required by various controllers

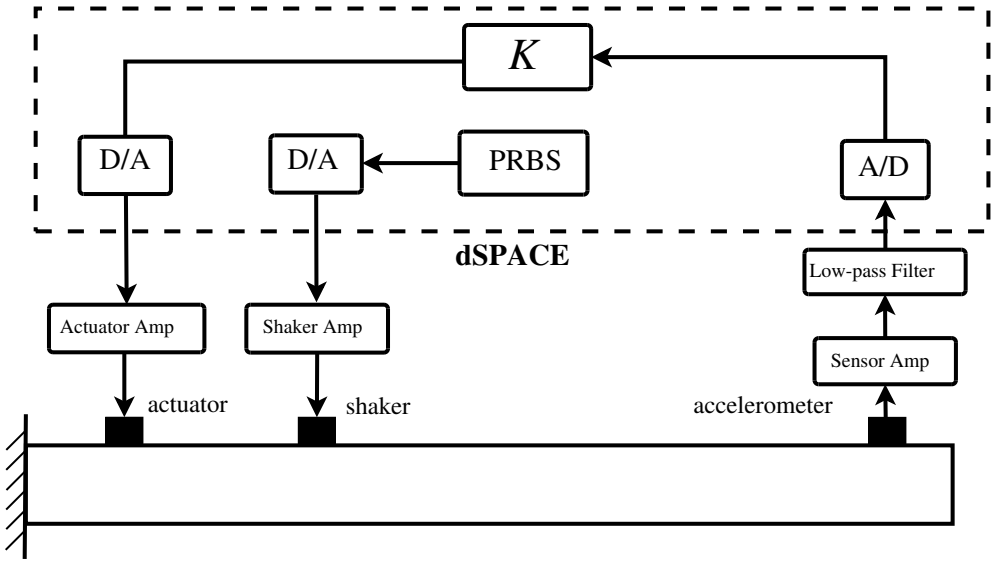

Figure 3.17: Experimental set-up for active vibration control

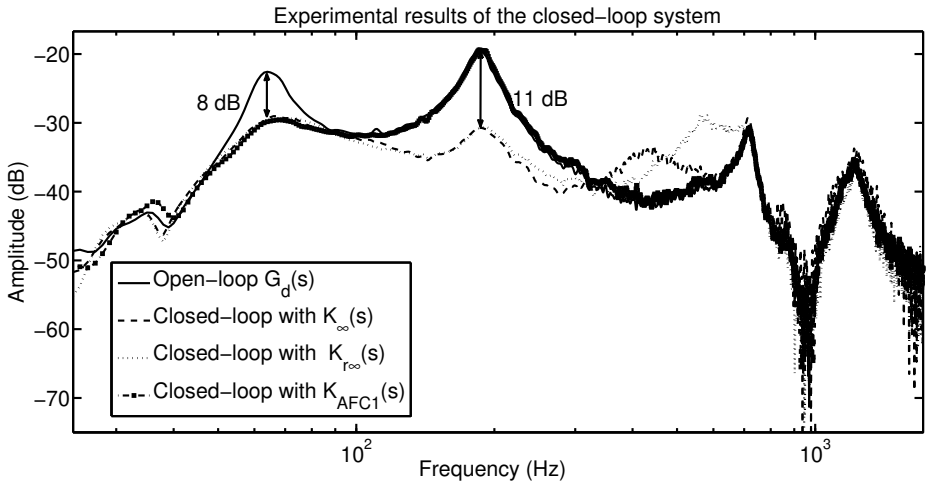

Figure 3.18: Experimental results of the closed-loop system

Chapter 4

Robustness analysis of flexible structures

As described in chapter 2, the obtained dynamical models inevitably have parametric uncertainties due to random variations in structural properties that are employed in the analytical formulations and the finite element analysis, or due to the identification errors. Besides, a dynamic uncertainty has to be considered to represent neglected high frequency dynamics which may lead to the spillover instability. In the presence of parametric and dynamic uncertainties, phase and gain control policies based H_∞ output feedback control is proposed in the previous chapter. However, it can only provide qualitative robustness properties of the closed-loop system. Furthermore, no probabilistic information of the parametric uncertainties can be considered, *e.g.* every uncertain natural frequency is assumed to be independent and have the uniform distribution within a given range. This assumption could be very conservative from a practical point of view. Therefore, this chapter focuses on extending the previous qualitative robust control methodology to the quantitative one. First, the probabilistic information of parametric uncertainties can be obtained with the uncertainty quantification methods such as the generalized polynomial chaos (gPC) framework. Then, the robustness properties of the closed-loop system using the designed H_∞ controller are quantitatively verified both in the deterministic sense and the probabilistic one. The effectiveness of this control methodology is numerically validated on a

non-collocated piezoelectric cantilever beam with structural material uncertainty.

4.1 Problem statement

Considering structural complexity and manufacturing or measuring errors, structural properties of practical piezoelectric flexible structures usually have substantial levels of uncertainty, which may have considerable effects on the system natural frequencies that are critical in many control designs, for instance, a lot of AFC and PPF methods require their frequencies to be equal to the system natural frequencies. However, normally no analytical formulation relating structural properties to the natural frequencies is available for complex piezoelectric flexible structures. As a result, several numerical methods are proposed to investigate the effects of structural property uncertainties on the natural frequencies and thus achieve their probabilistic distributions. This is usually referred to as uncertainty quantification and Monte Carlo Simulation (MCS) (Liu, 2008) is a traditional technique in this field to have entire probability density function (PDF) of any random variable, but the computation cost is usually expensive since a large number of samples are required for reasonable accuracy. The generalized polynomial chaos (gPC) framework is gaining in popularity and can be applied to various engineering problems (Templeton, 2009). It has been proved that gPC based uncertainty propagation methods are computationally far superior to traditional MCS methods (Xiu and Karniadakis, 2002). In Manan and Cooper (2010) and Kishor et al. (2011), Latin Hypercube Sampling (LHS) is employed in gPC framework to compute the polynomial chaos coefficients using the regression and variance analysis.

To take into account probabilistic information of parametric uncertainties in the control design, the probability theory is incorporated into classical robust and optimal control such as scenario approach based probabilistic robust control and probabilistic LQR design (Tempo et al., 2004). Besides, gPC framework is recently employed to solve this problem (Templeton et al., 2012; Hover and Triantafyllou, 2006; Fisher and Bhattacharya, 2009; Duong and Lee, 2010). The central idea and main interest of the gPC based probabilistic robust control are to substitute random variables into the original stochastic system by truncated

polynomial chaos expansion according to their distributions. This generates a finite set of deterministic differential equations in a higher-dimensional space and estimates every original state $x_i(t, \Delta)$ with its truncated polynomial chaos expansion $\hat{x}_i(t)$.

In this chapter, the previous qualitative robust control methodology is extended to the quantitative one by building a bridge among multi-discipline techniques. This is can be used to solve the above mentioned probabilistic robust control in some extend. Firstly, reduced nominal dynamical models are obtained with the finite element analysis and the modal parameter identification. The gPC framework with LHS is used to propagate structural property uncertainties into the natural frequencies. Then, in the presence of parametric and dynamic uncertainties, phase and gain control policies based dynamic output feedback H_∞ control is used for the controller design to satisfy a set of predetermined control objectives. With the designed controller, reliable deterministic and probabilistic robustness analyses are conducted with μ/ν analysis and random algorithms respectively (Zhou et al., 1996; Calafiore et al., 2000). They take into account the probabilistic information of parametric uncertainties and quantitatively verify the robustness properties both in the deterministic sense and the probabilistic one. Lastly, according to the results of the robustness analysis, if necessary, the weighting functions used in H_∞ controller can be retuned and a risk-adjusted trade-off could be made among various control objectives.

Compared to the proposed quantitative robust control methodology, where phase and gain control policies based H_∞ output feedback control and reliable various robustness analysis are conducted separately, the μ synthesis such as widely used DK-iteration has some remarkable problems, *e.g.* the computational convergence and reliable estimation of μ upper bound for flexible structures. These problems indeed limit the realistic use and the effectiveness of μ synthesis (Skogestad and Postlethwaite, 2005). Moreover, the proposed control methodology avoids the estimation of state $x_i(t, \Delta)$, which is required by gPC based probabilistic robust control. Actually, this estimation is only suited in a limited short time and has no guaranteed accuracy. Additionally, no dynamic uncertainty can be represented with the gPC framework and thus it is impossible to apply gPC based control in the presence of a dynamic uncertainty. The computational cost

of the gPC based control is also a problem in its practical application. With respect to the specifications of vibration reduction normally defined in the frequency domain, neither gPC based control (Duong and Lee, 2010; Smith et al., 2006) nor probabilistic LQR is suitable in that they are mainly to design an optimal H_2 or LQR controller with state feedback for minimizing a cost function or for the reference tracking specified in the time domain. These comparisons provide us confidence to believe that the proposed control methodology control is the most appropriate for efficient active vibration control of piezoelectric flexible structures, where the probabilistic information of parametric uncertainties can be investigated and the robustness properties of the closed-loop system have to be quantitatively ensured both in the deterministic sense and the probabilistic one.

4.2 System analysis

4.2.1 Deterministic system modeling

Based on the finite element modeling of piezoelectric flexible structures (Piefort, 2001), it is known that the plant transfer function $G_p(s)$ from the voltage $V(s)$ exerted on one piezoelectric actuator to the acceleration output $\ddot{Y}(x_s, s)$ at location x_s has the form

$$G_p(s) = \frac{\ddot{Y}(x_s, s)}{V(s)} = \sum_{k=1}^{\infty} G_{pk}(s) = \sum_{k=1}^{\infty} \frac{R_k s^2}{s^2 + 2\zeta_k \omega_k s + \omega_k^2} \tag{4.1}$$

Similarly, the disturbance transfer function $G_d(s)$ from the external disturbance force $F(x_d, s)$ at location x_d to $\ddot{Y}(x_s, s)$ is

$$G_d(s) = \frac{\ddot{Y}(x_s, s)}{F(x_d, s)} = \sum_{k=1}^{\infty} G_{dk}(s) = \sum_{k=1}^{\infty} \frac{Q_k s^2}{s^2 + 2\zeta_k \omega_k s + \omega_k^2} \tag{4.2}$$

These models have an infinite number of resonant modes, however, in practice only the first few resonant modes can be employed in the controller design and the neglected high frequency dynamics are represented by a dynamic uncertainty. To identify the modal parameters of $G_p(s)$ and $G_d(s)$, their frequency responses

$T_{xy}(G_p(j\omega))$ and $T_{xy}(G_d(j\omega))$ can be computed with the commercial software COMSOL over interested frequency ranges. This can be regarded to be analogous to performing realistic experimental investigations as conducted in Dong et al. (2006); Nestorović et al. (2012). Then, best curve fitting is performed to have those modal parameters (Schoukens and Pintelon, 1991). It is notable that $G_p(s)$ and $G_d(s)$ should have the same natural frequencies despite the errors in the curve fitting.

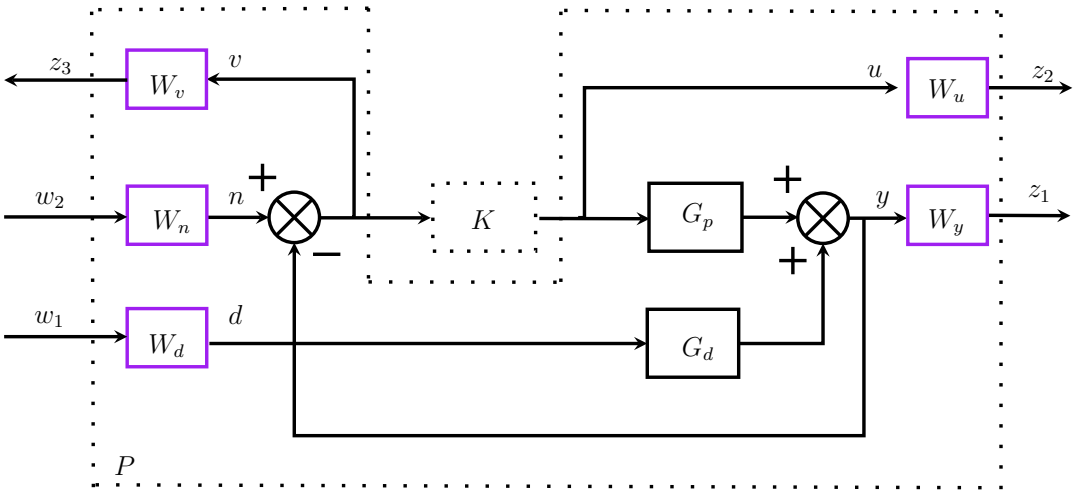

Figure 4.1: H_∞ control structure

4.2.2 Uncertainty quantification with gPC framework

In this research, the generalized polynomial chaos (gPC) framework, *i.e.* Wiener-Askey polynomial chaos, is used to propagate structural property uncertainties into the natural frequency ω_k and to achieve its probabilistic information. According to the gPC framework, we have the correspondence between the choice of the distribution of random variable ξ and the orthogonal polynomials $\Gamma_i(\xi)$ as summarized in Table 4.1 (Xiu and Karniadakis, 2002). For example, if Young's Modulus E of the flexible structure is assumed to have Gaussian distribution, *i.e.* $E \sim N(\mu_E, \sigma_E^2)$, 1−D Hermite polynomials can be used for ω_k

$$\omega_k = \beta_{0k} + \beta_{1k}\xi_1 + \beta_{2k}(\xi_1^2 - 1) + \beta_{3k}(\xi_1^3 - 3\xi_1) + \beta_{4k}(\xi_1^4 - 6\xi_1^2 + 3) + \dots \quad (4.3)$$

where $\xi_1 = \frac{E-\mu_E}{\sigma_E}$ is a normalized random variable. Similarly, to consider independent variables, *e.g.* the Young's Modulus $E \sim N(\mu_E, \sigma_E^2)$ and the density of the flexible structure $\rho \sim N(\mu_\rho, \sigma_\rho^2)$, 2−D Hermite polynomials can be used

$$\omega_k = \beta_{0k} + \beta_{1k}\xi_1 + \beta_{2k}\xi_2 + \beta_{3k}(\xi_1^2 - 1) + \beta_{4k}\xi_1\xi_2 + \beta_{5k}(\xi_2^2 - 1) + \dots \qquad (4.4)$$

where $\xi_2 = \frac{\rho-\mu_\rho}{\sigma_\rho}$. The coefficients β can be determined using sampling scheme Latin Hypercube Sampling (LHS) with the regression and analysis of variance (Choi et al., 2004a).

Random variable ξ	$\Gamma_i(\xi)$ of the Wiener-Askey scheme
Gaussian	Hermite
Uniform	Legendre
Gamma	Laguerre
Beta	Jacobi

Table 4.1: The correspondence between choice of the distribution of random variable ξ and polynomials $\Gamma_i(\xi)$ (Xiu and Karniadakis, 2002)

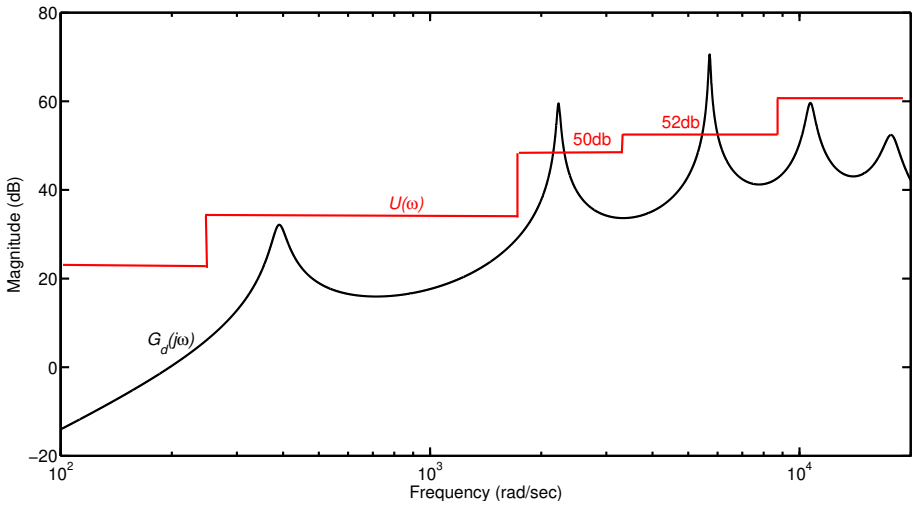

Figure 4.2: The specification of vibration control: $U(\omega)$

4.3 The proposed quantitative robust control design

4.3.1 Phase and gain control policies based H_∞ controller design

The phase and gain control policies based dynamic output feedback H_∞ control is used her for the controller design. The typical H_∞ control framework for active vibration control is recalled here, as shown in Figure 3.7, where G_p and G_d represent reduced nominal plant and disturbance dynamical models respectively, K the controller to be designed, d the disturbance signal, n the measurement noise, y the output from the accelerometer, u the control energy, v the input signal to K. By incorporating weighting functions W_i, we have the exogenous input signals w and the regulated variable z. Appropriate selection of W_i is critical in H_∞ control to account for the relative magnitude of signals, their frequency dependence and their relative importance. The proposed phase and gain control policies can offer available guidelines for the selection of W_i according to the specification of vibration reduction for flexible structures, for example, as illustrated in Figure 4.2, where the modulus of the frequency response of the transfer function between the disturbance input and the system output must be smaller than a user defined positive frequency-dependant function $U(\omega)$. By employing phase and gain control policies to the H_∞ control, a set of weighting functions can be appropriately determined such that all the predetermined control objectives are satisfied simultaneously.

4.3.2 Deterministic and probabilistic robustness analysis

Although phase and gain control policies based H_∞ control can ensure quantitative vibration reduction, it only qualitatively accounts for parametric and dynamic uncertainties. Therefore, it is desirable to perform deterministic and probabilistic robustness analysis to consider probabilistic information of parametric uncertainties and quantitatively ensure robustness properties of the closed-loop system both in the deterministic sense and the probabilistic one.

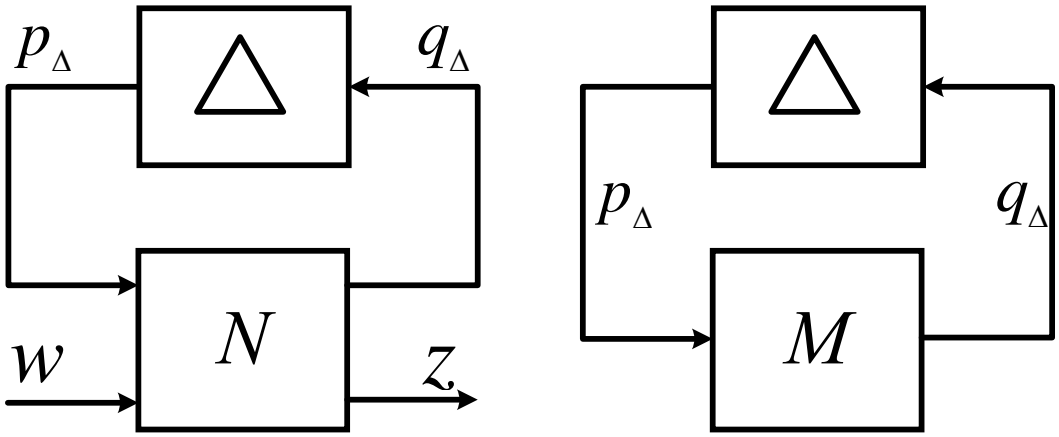

Figure 4.3: General LFT framework

4.3.2.1 Deterministic robustness analysis

To perform deterministic robustness analysis, the original stochastic system with parametric and dynamic uncertainties has to be rearranged by the structured uncertainty block Δ and the nominal augmented plant N, as shown in Figure 4.3 (Zhou et al., 1996), where $w(s)$ consists of exogenous input signals and $z(s)$ consists of regulated variables. By partitioning $N(s)$ compatibly with the dimension of $\Delta(s)$ we have

$$\begin{bmatrix} q_\Delta \\ z \end{bmatrix} = \begin{bmatrix} N_{11} & N_{12} \\ N_{21} & N_{22} \end{bmatrix} \begin{bmatrix} p_\Delta \\ w \end{bmatrix} ; \; M = N_{11} \tag{4.5}$$

The closed-loop transfer function from $w(s)$ to $z(s)$ is represented by an upper linear fractional transformation (LFT), $\mathscr{F}_u(N, \Delta)$,

$$z(s) = \mathscr{F}_u(N, \Delta)w(s) = (N_{22} + N_{21}\Delta(I - N_{11}\Delta)^{-1}N_{12})w(s) \tag{4.6}$$

Based on general LFT framework, the definition of the structured singular value $\mu_\Delta(M)$ can be expressed as

$$\mu_\Delta(M) \triangleq \frac{1}{\min\{k_m | \; \det(I - k_m M\Delta) = 0, \; \Delta \in \boldsymbol{B}_\Delta\}} \tag{4.7}$$

where $\boldsymbol{B}_\Delta$ is the norm bounded diagonal uncertainty block as defined on 29. The closed-loop robust stability is then determined by the following theorem (Zhou et al., 1996)

Theorem 4.3.1. *Assume that the nominal system M and the perturbation Δ are stable. Then the $M-\Delta$ is stable for any $\Delta \in \boldsymbol{B}_\Delta$ if and only if*

$$\mu_\Delta(M(j\omega)) < 1, \ \forall\omega \tag{4.8}$$

Besides the robust stability, the worst-case performance of the closed-loop system has to be investigated. Let us denote $\Delta_1 = \text{diag}(\Delta_{\text{Para}}, \ \Delta_{\text{Dyn}}) \in \boldsymbol{B}_{\Delta_1}$ and define the worst-case performance λ_{wc} as

$$\lambda_{wc}(\omega) \triangleq \sup_{\Delta_1 \in \boldsymbol{B}_{\Delta_1}} \bar{\sigma}(\mathscr{F}_u(N, \Delta_1)(j\omega)), \ \forall\omega \tag{4.9}$$

then skewed μ (ν) analysis is performed using a norm bounded fictitious performance uncertainty $\Delta_2 = \Delta_{\text{Perf}}(j\omega)$, *i.e.* $\bar{\sigma}(\Delta_2) \leq 1$, and a corresponding performance normalization function $W_{\text{Perf}}(j\omega) = \frac{1}{U(\omega)}$. According to the definition of $\nu(\hat{N})$ (Ferreres and Fromion, 1999)

$$\nu(\hat{N}) \triangleq \frac{1}{\min\{k_n | \ \det(I - k_n\hat{N}\Delta) = 0, \ \Delta = \text{diag}(\Delta_1, \ k_n\Delta_2), \ \Delta_i \in \boldsymbol{B}_\Delta\}} \tag{4.10}$$

we have

$$\nu(\hat{N}(j\omega)) \leq 1 \Leftrightarrow \lambda_{wc}(\omega) \leq U(\omega), \forall\omega \tag{4.11}$$

Compared to the original N in Equation (4.5) for classical μ analysis, $\hat{N}$ also incorporates $W_{\text{Perf}}(j\omega)$. In addition, with ν analysis, we can calculate the largest gain $\gamma_{\text{perf}}(\omega)$, which represents how much the normalized parametric and dynamic uncertainties can be enlarged simultaneously before the worst-case performance is violated,

$$\gamma_{\text{perf}}(\omega) \triangleq \sup_{\gamma} \sup_{\Delta_1 \in \gamma\boldsymbol{B}_{\Delta_1}} \bar{\sigma}(\mathscr{F}_u(N, \Delta_1)(j\omega)) \leq U(\omega), \forall\omega \tag{4.12}$$

As $U(\omega)$ is a frequency-dependent function, $\gamma_{\text{perf}}(\omega)$ also depends on ω. In the following γ_{perf} is used for the sake of simplicity.

As the accurate calculation of the value of $\mu_\Delta(M)$ is NP-hard (Braatz et al., 1994), lower and upper bounds of $\mu_\Delta(M)$ are usually computed. The reciprocal of the upper bound of $\mu_\Delta(M)$ is referred to as deterministic robustness margin

$$k_{\mathrm{DRM}} = \frac{1}{\max \mu_\Delta(M)} \tag{4.13}$$

It means how much the normalized parametric and dynamic uncertainties can be enlarged simultaneously before the closed-loop system gets instable. The lower bound of $\mu_\Delta(M)$ provides a destabilizing perturbation and reflects the conservatism in the upper bound. To compute the upper and lower bounds of $\mu_\Delta(M)$, Matlab Robust Control Toolbox R2012 makes use of the results from Young and Dolye (1990) and Young et al. (1992), where the frequency gridding is used over frequency ranges of interest. However, in the case of lightly damped flexible systems, narrow and high peaks on $\mu_\Delta(M(j\omega))$ plot commonly exist around resonant frequencies (Freudenberg and Morton, 1992). This implies that if the frequency gridding is not sufficient enough and neglects the critical frequency at which $\mu_\Delta(M(j\omega))$ is maximal, the robustness properties are overestimated. Therefore, in this research besides the ordinary frequency gridding method as used in Iorga et al. (2009), a frequency interval method (Ferreres et al., 2003) is applied to have more reliable results, *i.e.* they are neither conservative nor overestimated. Similarly, for reliable $\nu(\hat{N})$ calculation for lightly damped flexible systems, both Matlab R2012 built-in function 'wcgain' and the general skewed mu toolbox (SMT) (Ferreres et al., 2004) can be used, which respectively employs the frequency gridding method and the frequency interval method. The frequency interval method calculates upper bounds of $\mu_\Delta(M(j\omega))$ for some frequency ranges of interest, that is, it provides the upper bound of $\mu_{\Delta i}(M(j\omega)), \forall\omega \in [\underline{\omega}_i, \overline{\omega}_i], i = 1, 2, \cdots, n$. Therefore, a stair step function of the upper bound of $\mu_\Delta(M(j\omega))$ against the whole frequency range of interest is obtained.

4.3.2.2 Probabilistic robustness analysis

In the context of probabilistic robustness analysis, the uncertainty Δ is indeed bounded within a given set but it is also a random matrix with support $\mathcal{B}_{\mathbb{D}}(\rho) =$

$\{\Delta : \Delta \in \rho \boldsymbol{B}_\Delta\}$ having given distribution (Tempo et al., 2004). In this research, probabilistic robustness margin k_{PRM} and probabilistic worst-case performance are computed with a randomized algorithm, *i.e.* Monte Carlo Simulation (MCS).

Based on an associated positive level γ, the probability of k_{PRM} is represented by $p(\gamma)$ defined as

$$p(\gamma) \triangleq P_R\{k_{\text{PRM}} \leq \gamma\} \tag{4.14}$$

This means that with the probability $p(\gamma)$, we have $k_{\text{PRM}} \leq \gamma$. As exact computation of $p(\gamma)$ is in general very difficult, $p(\gamma)$ is usually estimated by its empirical probability $\hat{p}_n(\gamma)$. For every value of γ, the random sampling generates the uncertainties as $\Delta^1, \Delta^2, \ldots, \Delta^n \in \mathcal{B}_{\mathbb{D}}(\gamma)$ and thus $\hat{p}_n(\gamma)$ is

$$\hat{p}_n(\gamma) = \frac{1}{n}\sum_{i=1}^{n} I(\Delta^i),\ \Delta^i \in \mathcal{B}_{\mathbb{D}}(\gamma) \tag{4.15}$$

where $I(\Delta^i)$ is a indicator to the stability of the closed-loop system: $I(\Delta^i) = 1$ means that the closed-loop system is stable, otherwise, $I(\Delta^i) = 0$. The sampling number n is based on Chernoff bound (Tempo et al., 1997), that is, for any $\epsilon \in (0, 1)$ and $\delta \in (0, 1)$,

$$n \geq \frac{1}{2\epsilon^2}\log\frac{2}{\delta} \tag{4.16}$$

Obviously, this sampling number n is independent on the number of uncertainties. It ensures that with the probability $1 - \delta$, we have

$$|\hat{p}_n(\gamma) - p(\gamma)| \leq \epsilon.$$

To perform probabilistic worst-case performance for the specification of vibration reduction, denote $J(\Delta^i) = \bar{\sigma}(\mathcal{F}_u(N, \Delta^i)(j\omega)),\ \forall\omega$ and define $\lambda_{wc}(\rho)$ for every interested ρ,

$$\lambda_{wc}(\rho) \triangleq \sup_{\Delta^i \in \mathcal{B}_{\mathbb{D}}(\rho)} (J(\Delta^i)) \tag{4.17}$$

As exact computation of $\lambda_{wc}(\rho)$ is very difficult, it is usually estimated by its empirical probability $\bar{\lambda}_m(\rho)$ defined as

$$\bar{\lambda}_m(\rho) = \max_{\substack{\Delta^i \in \mathcal{B}_{\mathbb{D}}(\rho),\\ i=1,2\ldots,m}} J(\Delta^i) \tag{4.18}$$

where the uncertainties $\Delta^1, \Delta^2, \ldots, \Delta^m \in \mathcal{B}_{\mathbb{D}}(\rho)$ are randomly generated and the sampling number m is determined based on log-over-log bound (Tempo et al., 1997), that is, for any $\epsilon \in (0,1)$ and $\delta \in (0,1)$,

$$m \geq \frac{\log \frac{1}{\delta}}{\log \frac{1}{1-\epsilon}} \tag{4.19}$$

This sampling number m ensures that with the probability $1-\delta$, we have

$$P_R\{\lambda_{wc}(\rho) > \bar{\lambda}_m(\rho)\} \leq \epsilon.$$

From the definition of γ_{perf} in Equation (4.12), ρ can be regarded as risked adjusted $\tilde{\gamma}_{\text{perf}}$ in a probabilistic sense.

With given $\epsilon \in (0,1)$ and $\delta \in (0,1)$, the focus of probabilistic robustness analysis is to compute $\hat{p}_n(\gamma)$ and $\bar{\lambda}_m(\rho)$ for interested γ and ρ, which are associated with k_{PRM} and $\tilde{\gamma}_{\text{perf}}$. On the one hand, k_{PRM} and $\tilde{\gamma}_{\text{perf}}$ can be used to verify the conservatism and the overestimation in k_{DRM} and γ_{perf} in a nearly deterministic sense. On the other hand, to some extent, they can be used to reflect the conservatism in k_{DRM} and γ_{perf} in a probabilistic sense. Obviously, the above deterministic and probabilistic robustness analysis complement and compare each other and can provide reliable and comprehensive investigation of the closed-loop robustness properties.

4.4 Numerical case study

4.4.1 System modeling

The design process and the effectiveness of the proposed control methodology are illustrated by robust active vibration control of a non-collocated piezoelectric cantilever beam consisting of one piezoelectric actuator and one accelerometer, as shown in Figure 4.4. Although, for this simple piezoelectric cantilever beam, we have analytical formulations for the system modeling (Moheimani and Fleming, 2006; Qiu et al., 2009), the effects of the bounded piezoelectric actuator on the system dynamics such as the natural frequencies could be significant and have to be considered (Dhuri and Seshu, 2007a,b, 2009). Therefore, to take into account

such effects and ensure that the proposed method can be used for general structures where no analytical modes exist, in this research, finite element analysis (FEA) is employed in the system modeling and the subsequent uncertainty quantification. With nominal structural properties, FEA is performed in COMSOL 3.5a, and then the parameter identification is used to acquire the corresponding plant and dynamical models $G_p(s)$ and $G_d(s)$ for the first five resonant modes. Their frequency responses are well consistent with those from FEA, as shown in Figure 4.5. As expected, the poles of $G_p(s)$ are the same as those of $G_d(s)$ and their damping ratios are also assumed to be the same,

$$\begin{aligned} G_d(s) &= \frac{-3.2s^2}{s^2+31.2s+1.5\times10^5} + \frac{19.0\times10^{-1}s^2}{s^2+44.5s+5.0\times10^6} + \frac{-40.6s^2}{s^2+68.5s+3.3\times10^7} \\ &+ \frac{48.1s^2}{s^2+321.1s+1.1\times10^8} + \frac{-37.6s^2}{s^2+1597.0s+3.1\times10^8} \end{aligned}$$

$$\begin{aligned} G_p(s) &= \frac{3.4\times10^{-2}s^2}{s^2+31.2s+1.5\times10^5} + \frac{-1.5\times10^{-1}s^2}{s^2+44.5s+5.0\times10^6} + \frac{2.1\times10^{-1}s^2}{s^2+68.5s+3.3\times10^7} \\ &+ \frac{-3.8\times10^{-3}s^2}{s^2+321.1s+1.1\times10^8} + \frac{-4.5\times10^{-1}s^2}{s^2+1597.0s+3.1\times10^8} \end{aligned}$$

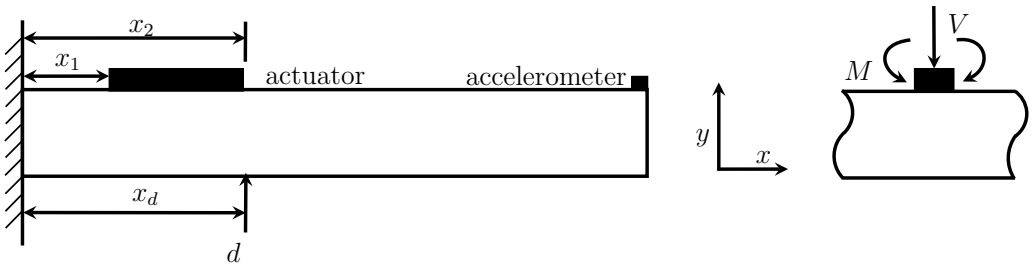

Figure 4.4: The piezoelectric cantilever beam

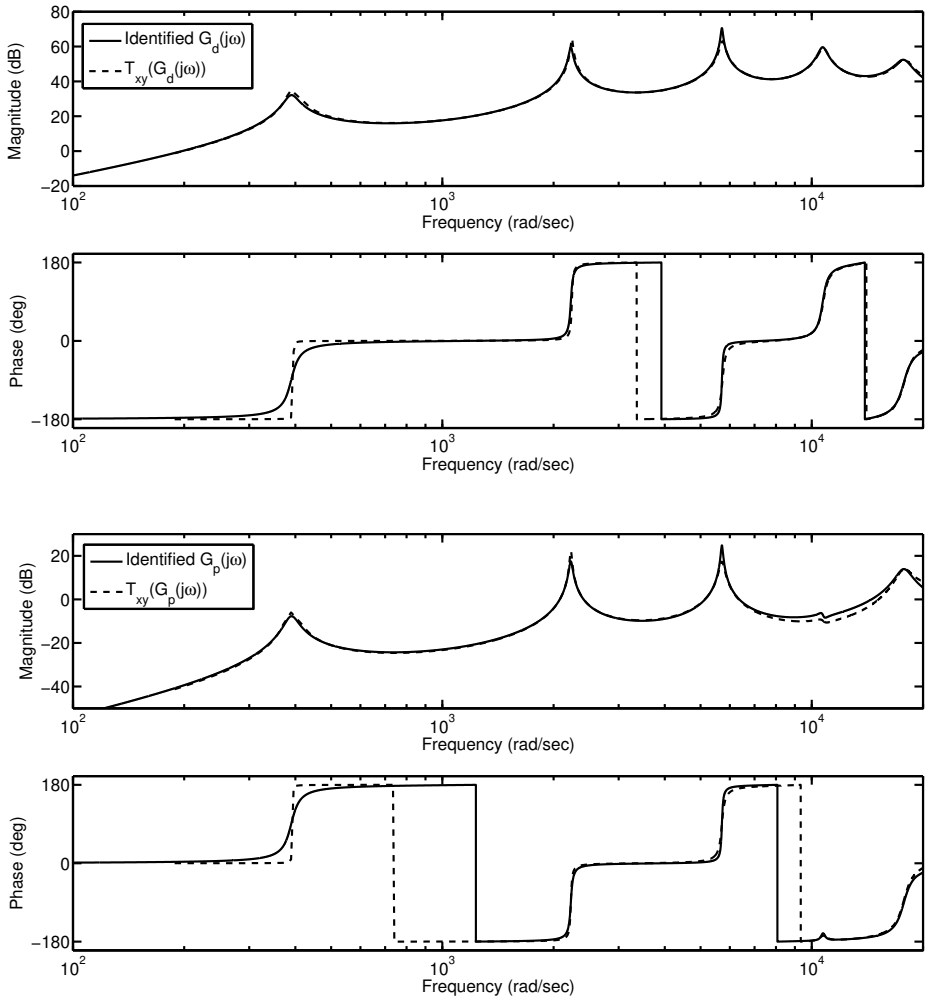

Figure 4.5: FEA and identified frequency responses of $G_d(j\omega)$ and $G_p(j\omega)$

4.4.2 Uncertainty quantification for natural frequencies with PCE

According to the specification of vibration reduce illustrated in Figure 4.2 and the principle of phase and gain control polices, only the first three resonant modes are necessary to employ in H_∞ control and thus the effects of structural properties on $\omega_i,\ i = 1, 2, 3$ have to investigated. Other higher resonant modes are represented by a dynamic uncertainty. In this chapter, E and ρ of the cantilever beam are assumed to have Gaussian distributions, that is, $E \sim N(\mu_E, \sigma_E^2)$ and $\rho \sim N(\mu_\rho, \sigma_\rho^2)$

with $\mu_E = 50$ Gpa, $\sigma_E = 1.67$ Gpa and $\mu_\rho = 2500$ kg/m^3, $\sigma_\rho = 250$ kg/m^3. If only uncertain E is considered, with gPC framework and eigenvalues analysis in COMSOL, 1−D PCE models are developed using 30 LHS and 10000 MCS samples, for example,

$$\begin{aligned} \omega_1 &= 219.0 + 3.46E; \text{ MCS} \\ \omega_1 &= 219.2 + 3.46E; \text{ PCE} \end{aligned}$$

Similarly when both uncertain E and ρ are investigated we have

$$\begin{aligned} \omega_1 &= 418.2 + 3.49E - 0.0798\rho; \text{ MCS} \\ \omega_1 &= 414.2 + 3.45E - 0.0773\rho; \text{ PCE} \end{aligned}$$

where the units of ω and E are rad/sec and Gpa. This approximated linear relationship can also be explained from Taylor series expansions of theoretical ω_k without considering the effects of piezoelectric actuators (Qiu et al., 2009), that is, $\omega_k = g_k\sqrt{\frac{E}{\rho}}$, where g_k is an constant associated to structural properties. With the first-order Taylor series expansions for E, we have the comparisons of Figure 4.6, which demonstrate that the gPC based uncertainty quantification has sufficient accuracy and great improvement in efficiency compared to MCS. It is also shown that, for this particular case, although the analytical relationship between ω_k and E without considering the piezoelectric actuator is available, the effects of the bounded piezoelectric actuator on ω_k are considerable and must be taken into account in the system modeling and the uncertainty quantification. As ω_k is more sensitive to the variation of E compared to that of ρ, for the sake of simplicity, only uncertain E is considered in the subsequent robustness analysis.

4.4.3 H_∞ control design

In the H_∞ control design and the robustness analysis, the relationship between $G_{dk}(s)$ and $G_{pk}(s)$ is considered with the scale constant g_k as illustrated in the decomposed H_∞ control structure of Figure 4.7. This decomposition can reduce the achieved H_∞ controller order and allow us to make a trade-off among the vibration reduction for every controlled mode. When the phase control policy

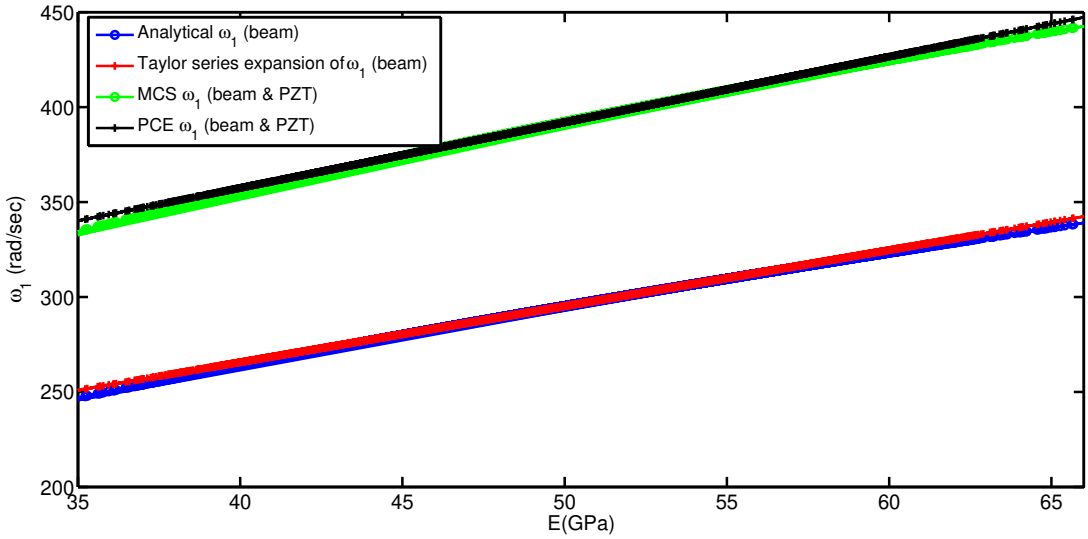

Figure 4.6: Theoretical, Taylor series expansion, MCS and PCE for ω_1

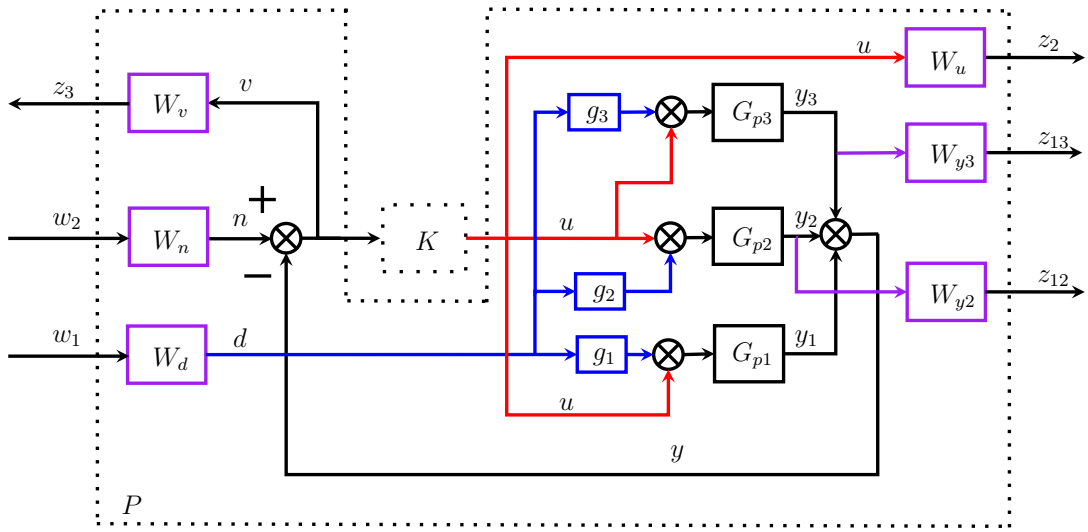

Figure 4.7: The decomposed H_∞ control structure

is used $L(j\omega)$ has to be large enough and $|K(j\omega)(1 + L(j\omega))^{-1}| \approx |K(j\omega)|$. This implies that the requirements on $|K(j\omega)|$ can be approximately reflected by $\|T_{w_2 \to z_2}(s)\|_\infty \leq 1$, *i.e.* $|K(j\omega)| \leq \frac{1}{|W_n(j\omega)W_u(j\omega)|}$. Normally the larger $|K(j\omega)|$ is, the better the control performance is, however, this could degrade the robust

stability of the closed-loop system in the presence of parametric and dynamic uncertainties and increase the control effort (Balas and Doyle, 1994). As a result, trade-offs among those control objectives have to be considered in the selection of W_i. In this particular case, it is apparent from Figure 4.2 that the phase control policy has to be applied to the second and third resonant modes and the gain control policy has to be applied to the first resonant mode and the neglected high frequency ones. Therefore, a second order $W_u(s)$ is used

$$W_u(s) = k\frac{s + M\omega_B^*}{s + \epsilon}\frac{s + fM\omega_B^*}{s + 0.1fM^2\omega_B^*} \tag{4.20}$$

where the parameters $k,\ \epsilon,\ M,\ f$ and ω_B^* are determined based on phase and gain control policies such that the requirements on $|K(j\omega)|$ are satisfied among different frequency ranges.

The following set of W_i is employed for this case: $W_n = 5, W_v = \frac{1}{50}, W_d = \frac{1}{100}, W_{y2} = \frac{1}{3.2}, W_{y3} = \frac{1}{4.0}$ and $k = 1,\ \epsilon = 10^{-6},\ M = 1000,\ f = 2,\ \omega_B^* = 3$. With these weighting functions, we have the corresponding controller $K_\infty(s)$. As expected and illustrated in Figure 4.8, with $K_\infty(s)$ the phase control policy is applied to the second and third resonant modes, *i.e.* around $\omega_{2/3}$ $|K_\infty(j\omega)|$ is large enough and $L(j\omega) = G_p(j\omega)K_\infty(j\omega)$ stays in RHP; the gain control policy is applied to the first resonant mode and the neglected high frequency ones, *i.e.* around ω_1 $|K_\infty(j\omega)|$ is small and at high frequencies $K_\infty(j\omega)$ rolls off quickly, which ensures $|L(j\omega)|$ small enough at these frequencies. Although the analysis implies that with $K_\infty(s)$ qualitative robustness properties of the closed-loop system can be achieved, reliable robustness analysis has to be performed subsequently to obtain quantitative robustness properties.

4.4.4 Robustness analysis

Based on above parametric uncertainty quantification with PCE, assuming $E \in [45, 55] = 50 + 5\delta_E,\ |\delta_E| \leq 1$, we have

$$\omega_k = \omega_{k0} + \omega_{k1}\delta_E;\ |\delta_E| \leq 1, k = 1, 2, 3$$

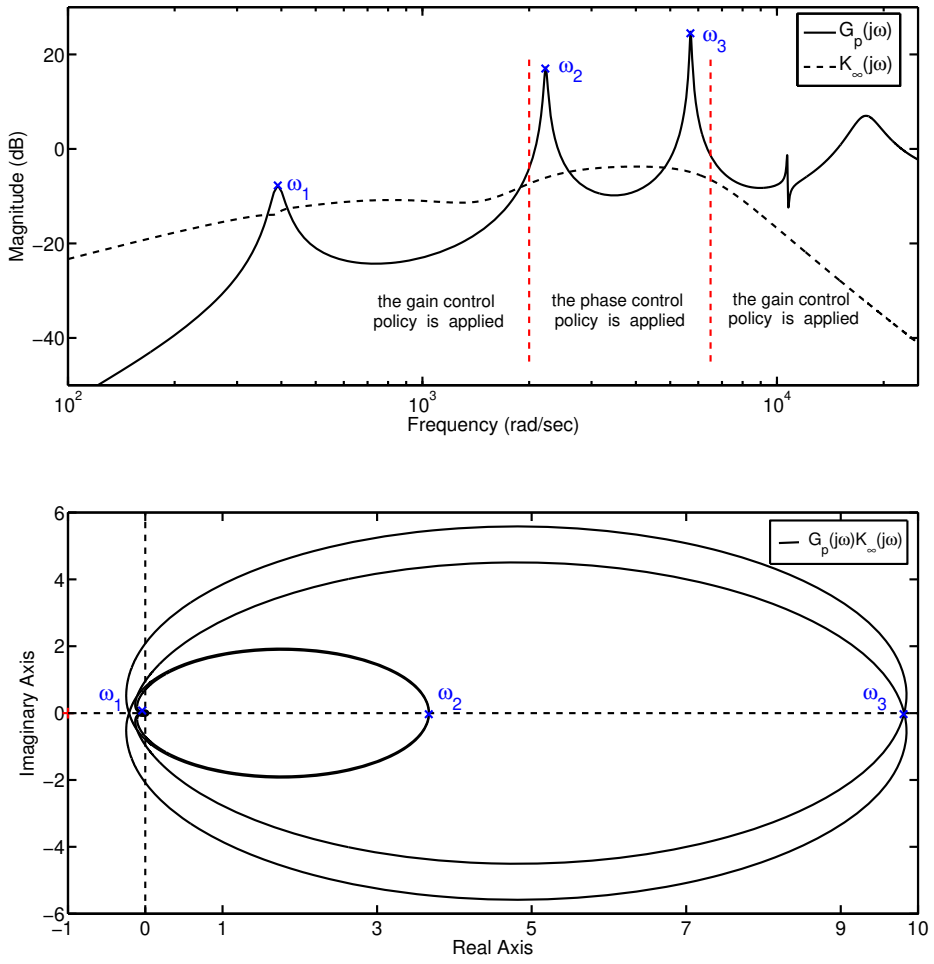

Figure 4.8: Phase and gain control polices with $K_\infty(s)$

This transformation from δ_{ω_k} to δ_E allows us to consider the probabilistic information of ω_k due to distributed E and the relationship among every ω_k. Uncertain ζ_k can be assumed to have certain deviation such as 20% about its nominal value

$$\zeta_k = \zeta_{k0} + \zeta_{k1}\delta_{\zeta_k};\ |\delta_{\zeta_k}| \leq 1, \zeta_{k1} = 0.2\zeta_{k0}, k = 1, 2, 3$$

To represent dynamic and fictitious performance uncertainties, norm bounded uncertainty $\Delta_{\text{Dyn}}(j\omega)$ and $\Delta_{\text{Perf}}(j\omega)$ are used with suitable dynamic normalization functions $W_{\text{Dyn}}(j\omega)$ and $W_{\text{Perf}}(j\omega)$. With Simulink modeling, the fact that $G_p(s)$ and $G_d(s)$ have the same natural frequencies is considered and

the nominal augmented plant N' and the corresponding structured uncertainty $\Delta' = \text{diag}(\Delta'_1,\ \Delta'_2) \in \boldsymbol{B}_\Delta$ are developed, where $\Delta'_1 = \text{diag}(\Delta_{\text{Para}},\ \Delta_{\text{Dyn}})$ and $\Delta'_2 = \Delta_{\text{Perf}}$, especially, $\Delta_{\text{Para}} = \text{diag}\ (\delta_E I_6, \delta_{\zeta 1}, \delta_{\zeta 2}, \delta_{\zeta 3})$.

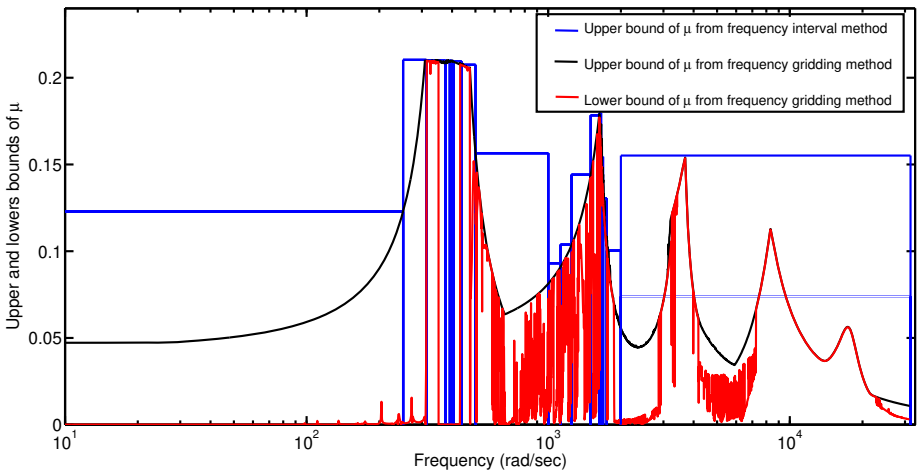

Figure 4.9: Deterministic robust stability analysis with $\zeta_{k1} = 0.2\zeta_{k0}$

4.4.4.1 Deterministic robustness analysis

With the obtained N' and Δ', the above mentioned frequency gridding and frequency interval methods are used for deterministic robustness analysis without considering any probabilistic information of ω_k or ζ_k. When $\zeta_{k1} = 0.2\zeta_{k0}$ the deterministic robust stability analysis of Figure 4.9 shows that the upper and lower bounds of μ from the frequency gridding method coincide well around the resonant frequencies and they are also consistent well with the upper bound of μ from the frequency interval method. This means that the estimated μ and the corresponding $k_{\text{DRM}} = 4.76$ are reliable, in other words, the closed-loop system remains stable for any $\Delta \in 4.76\Delta'_1$. With ν analysis the results of deterministic worst-case performance are illustrated in Figure 4.10, which show that the upper and lower bounds of the worst-case performance from the frequency gridding method ('wcgain') coincide and they are also well consistent with the results from the frequency interval method (SMT). These results ensure that the obtained $\gamma_{\text{perf}} = 1.70$ is reliable, that is, the specification of vibration reduction is

fulfilled for any $\Delta \in 1.70\Delta_1'$. It is notable that as every ω_k depends on δ_E, the worst-case performances for the second and third resonant modes cannot happen at the same time.

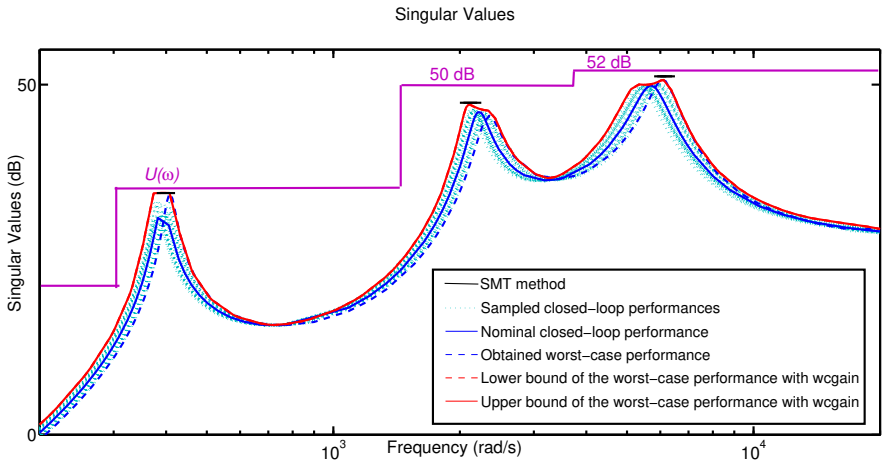

Figure 4.10: Deterministic worst-case performance analysis with $\zeta_{k1} = 0.2\zeta_{k0}$ and $\Delta \in 1.70\Delta_1'$

Uniformly distributed E	Gaussian distributed E
$\hat{p}_n(4.76) = 100\%$	$\hat{p}_n(4.76) = 100\%$
$\hat{p}_n(4.98) = 98.20\%$	$\hat{p}_n(4.98) = 98.22\%$

Table 4.2: Probabilistic stability analysis: $\epsilon = 0.01, \delta = 0.02, \zeta_{k1} = 0.2\zeta_{k0}$

4.4.4.2 Probabilistic robustness analysis

Probabilistic robustness analysis is performed to consider probabilistic information of ω_k and ζ_k and provide complements and comparisons to the above deterministic robustness analysis. In this numerical case, both the uniformly and Gaussian distributed E are considered and ζ_k is assumed to have uniform distribution. When $\zeta_{k1} = 0.2\zeta_{k0}$ the results from probabilistic stability analysis are illustrated in Table 4.2 with $\epsilon = 0.01, \delta = 0.02$. It verifies that with probability $1 - \delta = 98\%$ for either uniformly or Gaussian distributed ω_k, the closed-loop system remains stable for all sampled $\Delta \in 4.76\Delta_1'$. Additionally, a few destabilizing perturbations $\Delta_{\text{des}} \in 4.77\Delta_1'$ are found. It is reasonable to conclude that

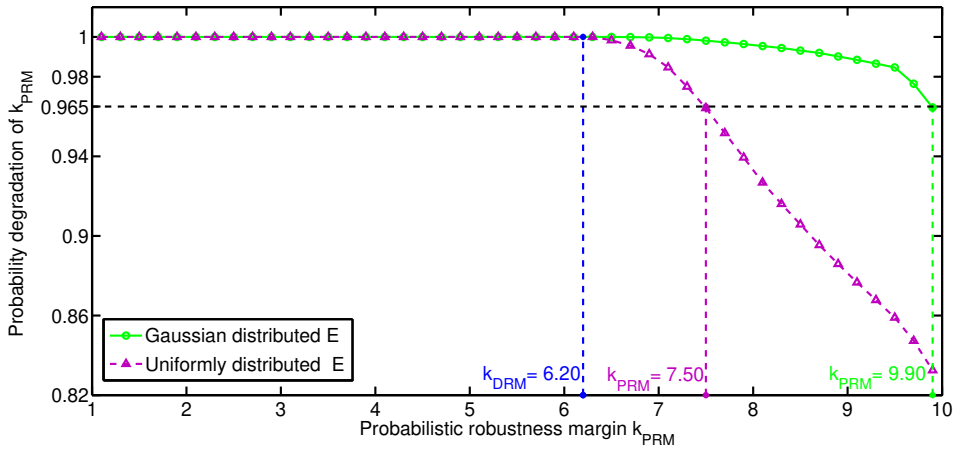

Figure 4.11: Probabilistic robust stability analysis with $\zeta_{k1} = 0.1\zeta_{k0}, \epsilon = 0.01, \delta = 0.02$

$k_{\mathrm{DRM}} = 4.76$ from μ analysis is neither conservative nor overestimated. Probabilistic stability analysis also shows that for uniformly distributed E if a 1.80% loss of probabilistic robust stability is tolerated, the corresponding $k_{\mathrm{PRM}} = 4.98$ is increased by 5.96% with respect to its deterministic counterpart $k_{\mathrm{DRM}} = 4.76$.

The above probabilistic stability analysis is based on the normalization $\zeta_{k1} = 0.2\zeta_{k0}$, *i.e.* ζ_k has 20% deviation of its nominal value. This limits k_{DRM} and k_{PRM} smaller than 5 to guarantee $\zeta_k > 0$ and explains why this is no significant difference between $k_{\mathrm{DRM}} = 4.76$ and $k_{\mathrm{PRM}} = 4.98$. To more clearly reveal the interest of k_{PRM} from a probabilistic point of view, ζ_k is assumed to have 10% deviation of its nominal value, *i.e.* $\zeta_{k1} = 0.1\zeta_{k0}$, but the normalization of other uncertainties is not changed. This enlarges the allowable k_{DRM} and k_{PRM} to 10 and reduces the relative normalization of ζ_k with respect to that of other uncertainties as illustrated by red rectangles in Figure 4.12. When $\zeta_{k1} = 0.1\zeta_{k0}$, we have $k_{\mathrm{DRM}} = 6.20$ and the probability degradation function of k_{PRM} of Figure 4.11. This shows that with probability 98%, if a 3.50% loss of probabilistic robust stability is tolerated, for Gaussian distributed E $k_{\mathrm{PRM}} = 9.9$, which is increased by 59.7% with respect to its deterministic counterpart $k_{\mathrm{DRM}} = 6.20$ and increased by 32.0% with respect to the result for uniformly distributed E. The results are summarized in Table 4.3. Compared to Table 4.2, the difference between k_{DRM}

and k_{PRM} is more significant. With this normalization, we have $\gamma_{\mathrm{perf}} = 2.0$. The effects of relative normalization of ζ_k with respect to that of other uncertainties on k_{DRM} and γ_{perf} are illustrated in Figure 4.12, where the zero point corresponds to the nominal values of the uncertainties.

Uniformly distributed E	Gaussian distributed E
$\hat{p}_n(6.20) = 100\%$	$\hat{p}_n(6.20) = 100\%$
$\hat{p}_n(7.50) = 96.5\%$	$\hat{p}_n(9.90) = 96.5\%$

Table 4.3: Probabilistic stability analysis: $\epsilon = 0.01$,$\delta = 0.02$, $\zeta_{k1} = 0.1\zeta_{k0}$

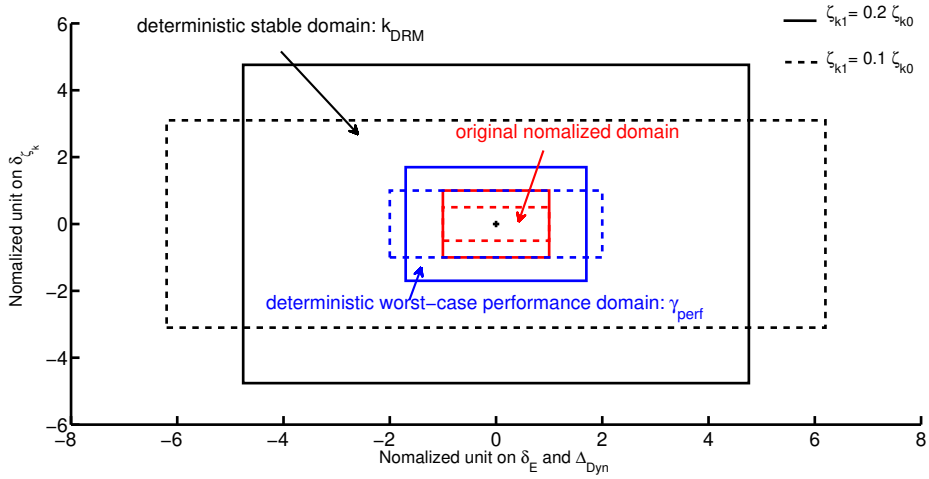

Figure 4.12: Deterministic robust domains in the space of uncertainties

Probabilistic worst-case performance analysis is also performed. When $\zeta_{k1} = 0.2\zeta_{k0}$, the results are summarized in Table 4.4 and Table 4.5. On the one hand, from Table 4.4 it is demonstrated that with probability 98%, the specification of vibration reduction is fulfilled for all sampled $\Delta_1' \in 1.70\boldsymbol{B}_{\Delta_1}$, but when $\Delta_1' \in 1.72\boldsymbol{B}_{\Delta_1}$ a few perturbations can be found to violate the specification of vibration reduction for uniformly distributed E. These results verify that $\gamma_{\mathrm{perf}} = 1.70$ from ν calculation is neither conservative nor overestimated. On the other hand, from Table 4.5 it is demonstrated that with probability 90%, the risk adjusted $\tilde{\gamma}_{\mathrm{perf}} = 2.21$ for Gaussian distributed E. This is increased by 30.0% with respect to its deterministic counterpart $\gamma_{\mathrm{perf}} = 1.70$ and increased by 15.1% with respect to the result for uniformly distributed E. The effects of various distributed E

on the worst-case performance are also of significance in statistics meaning as illustrated in Figure 4.13 with $\epsilon = 0.001, \delta = 0.1, \zeta_{k1} = 0.2\zeta_{k0}$ and $\Delta_1' \in 2.10\boldsymbol{B}_{\Delta_1}$.

Targeted resonant mode	Uniformly distributed E	Gaussian distributed E
The second mode	$\bar{\lambda}_m(1.70) = 48.30\text{dB} < 50.00\text{dB}$ $\bar{\lambda}_m(1.72) = 49.04\text{dB} < 50.00\text{dB}$	$\bar{\lambda}_m(1.70) = 48.02\text{dB} < 50.00\text{dB}$ $\bar{\lambda}_m(1.72) = 48.70\text{dB} < 50.00\text{dB}$
The third mode	$\bar{\lambda}_m(1.70) = 51.67\text{dB} < 52.00\text{dB}$ $\bar{\lambda}_m(1.72) = 52.50\text{dB} > 52.00\text{dB}$	$\bar{\lambda}_m(1.70) = 51.50\text{dB} < 52.00\text{dB}$ $\bar{\lambda}_m(1.72) = 51.94\text{dB} < 52.00\text{dB}$

Table 4.4: Probabilistic worst-case performance analysis: $\epsilon = 0.001, \delta = 0.02, \zeta_{k1} = 0.2\zeta_{k0}$

Targeted resonant mode	Uniformly distributed E	Gaussian distributed E
The second mode	$\bar{\lambda}_m(1.92) = 48.72\text{dB}$	$\bar{\lambda}_m(2.21) = 48.83\text{dB}$
The third mode	$\bar{\lambda}_m(1.92) = 52.00\text{dB}$	$\bar{\lambda}_m(2.21) = 52.00\text{dB}$

Table 4.5: Probabilistic worst-case performance analysis: $\epsilon = 0.001, \delta = 0.1, \zeta_{k1} = 0.2\zeta_{k0}$

The deterministic and probabilistic robustness analyses provide reliable and comprehensive investigations of the closed-loop robustness properties both in the deterministic sense and the probabilistic one. They demonstrate that, for lightly damped flexible systems, the employed calculation methods of μ and ν are reliable, that is, we have neither conservative nor overestimated deterministic robustness properties, *i.e.* k_{DRM} and γ_{perf}. On the other hand, the probabilistic robustness properties, *i.e.* k_{PRM} and $\tilde{\gamma}_{\text{perf}}$, allow us to consider the probabilistic information of parametric uncertainties. The robustness analysis also demonstrates that with the proposed control methodology we can have attractive robustness properties of the closed-loop system both in the deterministic sense and the probabilistic one. However, it is notable that the main purpose of the proposed control methodology is not only to design a good controller for active vibration control, which is sometimes easy to achieve with simpler control methods such as the velocity feedback control, the acceleration feedback control and so on, but also to offer a general and systematic way to achieve several trade-offs between conflicting objectives, *e.g.* the robust stability and robust performance, the vibration reduction for every targeted resonant mode and the deterministic and probabilistic robustness properties.

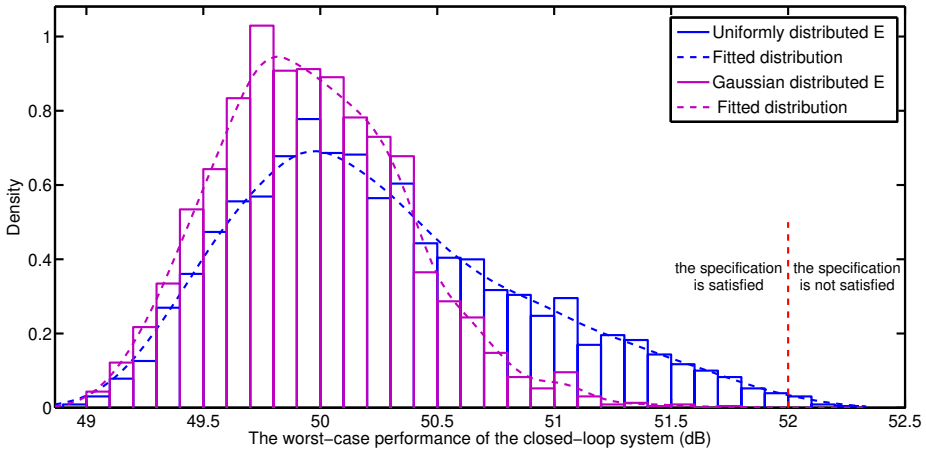

Figure 4.13: Probabilistic worst-case performance analysis in statistics meaning

4.5 Summary

This chapter focuses on applying efficient robustness analysis to the development of the quantitative robust active vibration control methodology. This is achieved by building a bridge among several techniques from various disciplines. The proposed control methodology employs the phase and gain control policies based H_∞ control to have a qualitative robust controller, and investigates the effects of structural properties on natural frequencies with the gPC based uncertainty quantification. It allows to directly consider the structural properties in various robustness analysis and to quantitatively verify the robustness properties of the closed-loop system both in the deterministic sense and the probabilistic one. In this chapter, the design processes and the effectiveness of the proposed control methodology are illustrated by active vibration control of a non-collocated piezoelectric cantilever beam with neglected high frequency dynamics and the uncertainties on its structural properties.

Chapter 5

Quantitative robust active vibration control of LPV systems

The purpose of this chapter is to extend the proposed phase and gain control policies for linear parameter varying (LPV) systems to reduce the control energy and, in some extend, the amplitude of the control signal, while satisfying the complete set of control objectives. First, the LPV system and LPV control problem are briefly introduced. Then, phase and gain control policies are employed in the LPV H_∞ control design to obtain a parameter dependent H_∞ controller using convex optimization involving Linear Matrix Inequality. The numerical simulations demonstrate the effectiveness of the LPV control design for robust active vibration of a non-collocated cantilever beam which is excited by a position varying external force. Compared to the acceleration feedback control and classical worst-case H_∞ control, the proposed quantitative robust LPV control can take into account the real-time information of varying parameters and thus reduce the required control energy and, in some extend, the magnitude of the control signal.

5.1 Problem statement

As discussed in chapter 4, the proposed quantitative robust control methodology is applied to linear time-invariant (LTI) plants where linear dynamical models are used to represent the physical dynamics and uncertain parameters are as-

sumed to be bounded but not achievable in real-time. However, in practice, some plants have time-varying parameters that can be measured. Recently, Linear Parameter Varying (LPV) systems have received a rapidly increasing attention to model the dynamics of these plants, due to the fact that they can provide an interesting framework for gain-scheduling control by means of convex optimization (Rugh and Shamma, 2000; Boyd and Vandenberghe, 2004). The LPV systems constitute a class of linear systems whose dynamics usually depend on physical time-varying parameters, which are not known a priori but assumed to be measurable in real-time. Such parameters are restricted to vary in predetermined sets and can be used as extra information in the control designs to generate parameter-dependent controllers, thus leading to increased control performance when contrasted with some robust control designs. The LPV paradigm has been used for system modeling and control designs in a variety of applications such as the flight control and missile autopilots (Balas et al., 1997; Tan et al., 2000), the aeroelasticity (Jadbabaie and Hauser, 2002), the magnetic bearings (Witte et al., 2010), the turbofan engines (Balas, 2002), the vibration and noise control (Caigny et al., 2010; Ballesteros and Bonn, 2011), the tool machines with position-dependent dynamics (Paijmans, 2007; Symens et al., 2008), the automotive systems (Fialho and Balas, 2002) and so on.

In general, in the presence of parametric and dynamic uncertainties, there exist two approaches to the design of robust controllers for LPV systems: the controllers that do not depend on the variation of the changing parameter, but guarantee the control objectives for all possible dynamical models, *e.g.* the classical robust or the worst-case controllers as used for LTI systems; the controllers that change according to the variations of the changing parameters, *i.e.* the parameter-dependent controllers are designed. Using worst-case control designs, the dynamics of LPV systems are modeled with norm bounded uncertainties and no exact knowledge of the uncertain parameters can be considered, even it is available. In contrast, with LPV control designs, the time-varying parameters are assumed to be measured on-line and used in the LPV controller synthesis, which could provide better control performances. It is notable that, for some particular cases as investigated in this chapter, both the worst-case controller and the LPV one can satisfy the specification of vibration reduction and a certain level

of robustness properties. But, in addition to these normal control objectives, the designed controllers are required to consume as little control energy as possible for their practical implementations (Skogestad and Postlethwaite, 2005), since in some applications very little energy is available for active control, yet passive and semi-active methods cannot meet the control objectives, especially when the control energy is obtained from harvesting systems, *e.g.* Ichchou et al. (2011); Wang and Inman (2013a,b), and/or low-power storage devices (batteries or super capacitors) as often desirable in aerospace systems, *e.g.* Moreira et al. (2001); Yang and Sun (2002). As a result, if the control energy is not well considered or even totally neglected in the control designs, the active vibration control systems may eventually be powered off of harvested energy and/or low power storage devices. Moreover, due to the hardware limitations, the control input must be restricted by a prescribed upper bound to avoid the controller saturation and exceeding the actuator operated voltage, *e.g.* Saberi et al. (2000); Materazzi and Ubertini (2012). Exceeding the upper bound could cause unexpected behavior of the closed-loop system such as actuator damages, large overshoots, loss of control effectiveness or even a dynamic instability. In addition, as claimed in Assadian (2002), usually the vibration control capability of various controllers is measured using their effects on the sensitivity transfer function in the frequency domain. This fails to provide the control designers a physical measure for comparisons, but ranking controllers based on their energy requirements or control inputs provides an supplement and important physical measure for the controller selection.

Therefore, an important constraint in practical active vibration control designs is the required control energy and the control input. To achieve effective robust controllers, this constraint is critical and really deserves enough attention. In the following, we have an extensive review of various techniques for saving the control energy and reducing the control input:

- Kondoh et al. (1990) propose an optimization criterion for the location selection of actuators and sensors to obtain effective vibration reduction and minimize the control energy. Bardou et al. (1997) focus on physical parameter optimization of the plate and the locations of the excitation and the actuator forces to minimize the control energy. In Lee et al. (1996) and Baz and Poh (1988), to reduce the required control energy for active vibration

control of flexible structures, an optimal direct velocity feedback (DVF) control and a modified independent modal space control are respectively used to determine the optimal locations of the actuators and sensors and the control gains. Kumar and Narayanan (2008) numerically reveal that, by optimal placement of collocated piezoelectric actuators and sensors, the designed linear quadratic regulator (LQR) optimal controller can achieve effective vibration reduction of the flexible beam, while requiring a smaller control input compared to DVF control. For vibration control of a thin-walled composite beam, Zorić et al. (2013) employ the fuzzy optimization strategy to determine the size and the location of piezoelectric actuators and sensors. The particle swarm optimization (PSO) based LQR controller is then designed to maximize the closed-loop damping ratios and minimize the control input. Besides, a literature review about optimal placement of piezoelectric actuators and sensors for minimizing the control energy can be found in Gupta et al. (2010).

- Assadian (2002) computes the control energy for active vibration control of an vibratory system and investigates the effects of control methods on the control energy, where nonoptimal DVF control, classical H_∞ control and LQR control are compared. The trade-off curves of the control energy versus the closed-loop control performance are investigated. P. Van Phuoc et al. (2009) employ a genetic algorithm for the parameter optimization of a positive position feedback (PPF) controller to minimize the control energy for active vibration reduction of a flexible robot manipulator. Similarly, Chen et al. (2011) use PSO to determine the parameters of the proportional-integral-derivative (PID) controller such that the control energy for a mass-damper-spring system is minimized.

  Wang and Inman (2011) introduce a reduced energy control (REC) law by employing a saturation control to switch the control system from one state to another one, providing conventional active controllers with a limited voltage boundary. Both experimental and numerical comparisons are performed in terms of the control energy and the setting time with PPF control, PID control, nonlinear control and LQR control. The REC law is then imple-

mented in Wang and Inman (2013a,b) to improve unmanned aerial vehicle performance in wind gusts and reduce the control energy which is limited and harvested from ambient wing vibration. In Kumar et al. (2006), for active vibration control of an inverted L structure, the LQR based adaptive controller achieves robust performance and requires smaller control input compared to the pole placement method. Materazzi and Ubertini (2012) employ the 'State-dependent Riccati Equation' to reduce the control input, which consists of solving online the LQR problem with adaptive weighting functions and system matrices. In Qiu (2013), nonlinear controllers are proposed for active vibration control of a piezoelectric cantilever plate, where the control gains are computed with three nonlinear functions to adapt to the measured vibration amplitudes and regulate the control input in real-time for effective vibration reduction and avoiding the control saturation.

- With classical H_∞ control, related weighting functions are used to tune the bandwidth of the H_∞ controller, thus imposing constraints on the control energy, *e.g.* the frequency-independent weighting functions are used in Zhang et al. (2001); Huo et al. (2008), and the frequency-dependent ones are used in Zhang et al. (2013a); Sivrioglu et al. (2004); Zhang et al. (2013b). Based on H_∞ loop shaping designs, Reinelt (1999, 2000, 2001) investigates active control of multivariable systems with hard bounded control input to avoid the control saturation. This control method assumes the reference signal and its first derivative to be norm bounded, and focuses on the selection of weighting functions which are explicitly related to the upper bound on the control input. The selection procedure is fulfilled until the prescribed upper bound is met and indeed user iterative as performed in Forrai et al. (2001b) and Forrai et al. (2003) for active vibration control of a three-storey flexible structure. In Kumar (2012), LQR control, classical mixed sensitivity H_∞ control, H_∞ loop shaping design and μ synthesis are used for active vibration control of a flexible beam with variable boundary conditions. These controllers are compared in terms of the required control energy and the closed-loop robust performance evaluated with μ analysis (Skogestad and Postlethwaite, 2005). It shows that, for this

specifical case, the H_∞ loop shaping based controller outperforms others in terms of the control energy utilization.

Above literature review proves that, for practical active vibration control designs, it is critical to consider the constraint on the control energy and the control input. It is also shown that, in most of these researches, the constraint is achieved by kinds of optimizations of the placement and sizing of the actuators and sensors, the structural parameters, and the parameters of fixed controllers such as DVF, PID and PPF. However, as claimed in Darivandi et al. (2013), these optimization methods are generally non-convex and the dynamical models of flexible structures usually have a large number of degrees of freedom. Consequently, these optimization based methods could be inaccurate or computationally impractical. Furthermore, due to physical and installation limitations, sometimes there exists little flexibility for such optimization, for instance, although non-collocated actuators and sensors are not desirable for the closed-loop robust stability, they are unavoidable due to installation restrictions and even recommendable for high degrees of observability and controllability (Bayon de Noyer and Hanagud, 1998a; Kim and Oh, 2013). Besides, the measurement of all state variables required by LQR is not always practically available, and the specification of vibration reduction and the robustness properties cannot be quantitatively investigated with DVF, PPF, LQR, PID or nonlinear controllers.

On the other hand, the H_∞ loop shaping designs do not directly consider the control energy and only enforce the constraint on the control signal with the following inequality (Reinelt, 2000):

$$\|u(s)\|_\infty \leq 2n\|T_{ud}(s)\|_\infty\|d(s)\|_\infty \tag{5.1}$$

where, as shown in Figure 5.1, $T_{ud}(s)$ is the closed-loop transfer function form the disturbance signal $d(s)$ to the control signal $u(s)$, $\|u(s)\|_\infty$ represents the maximum amplitude of $u(s)$ and n denotes the McMillan degree of $T_{ud}(s)$ (Saberi et al., 2000). This inequality shows that decreasing $\|T_{ud}(s)\|_\infty$ reduces the upper bound for the maximum control input. Therefore, the weighting functions such as $W_1(s)$ and $W_2(s)$ are used in the H_∞ loop shaping design to adjust the open-loop transfer function $L(s) = G_p(s)K(s)$ so as to reduce $\|T_{ud}(s)\|_\infty$ according the

following relationship:

$$\begin{aligned} |T_{ud}(j\omega)| &= |G_d(j\omega)K(j\omega)(1+G_p(j\omega)K(j\omega))^{-1}| \\ &\approx |G_d(j\omega)K(j\omega)|, \text{ at frequency } |L(j\omega)| = |G_p(j\omega)K(j\omega)| \ll 1 \\ &= |G_d(j\omega)W_1(j\omega)\hat{K}_\infty(j\omega)W_2(j\omega)| \end{aligned}$$

where the controller $\hat{K}_\infty(s)$ is designed based on the shaped plant dynamical model $\hat{G}_p(s) = W_2(s)G_p(s)W_1(s)$.

These formulations provide a relationship between the upper bound for the maximum control input and related weighting functions. However, in many H_∞ loop shaping designs, *e.g.* Forrai et al. (2001b, 2003), the magnitudes of related weighting functions, *e.g.* $|W_1(j\omega)|$ and $|W_2(j\omega)|$, are tuned in the whole frequency range, that is, the selection is frequency-independent. This selection is relatively simpler than the phase and gain control polices based frequency-dependent selection (Zhang et al., 2013a). But, the gain of the corresponding controller could be very small not only at high frequencies for avoiding the spillover problem and saving the control energy, but also around the controlled resonant frequencies, thus failing to have effective vibration reduction. This implies that the frequency-independent weighting functions cannot provide a good trade-off among various control objectives.

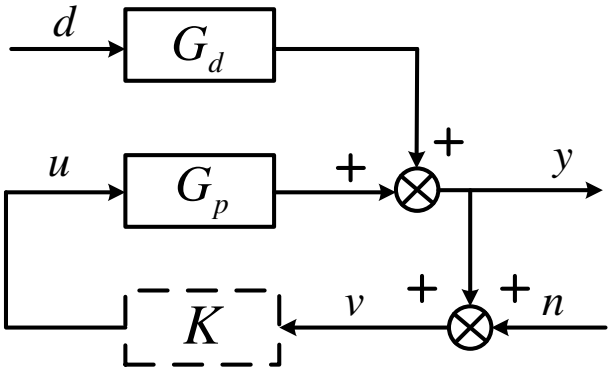

Figure 5.1: A typical feedback control structure for active vibration control

It is also notable that, in addition to the conservatism involved in the equality of Equation (5.1), the assumption that $|L(j\omega)| = |G_p(j\omega)K(j\omega)| \ll 1$ is not

satisfied in the crossover regions where $|L(j\omega)| \approx 1$, and thus one cannot infer anything about $|T_{ud}(j\omega)|$ or $\|u(s)\|_\infty$ from $|L(j\omega)|$. Compared to classical H_∞ control designs, the H_∞ loop shaping designs cannot directly enforce constraints on the closed-loop transfer functions related to the set of control objectives, but just approximate these closed-loop requirements by enforcing the constraints on $|L(j\omega)|$ as some traditional control designs do. Since this approximation is not direct, there may exist considerable errors in this approximation over certain frequency ranges. Particularly, as previously discussed, if the control performance is explicitly defined in the frequency domain such as $|T_{yd}(j\omega)|$ for the vibration reduction, this approximation is actually not necessary. Besides, the H_∞ loop shaping designs do not explicitly consider the disturbance dynamical model $G_d(s)$, which indeed has significant effects on the set of control objectives. It is also notable that, although the LPV control techniques have been used widely, the application of LPV system modeling and associated LPV control techniques to reduce the control energy or the control input has not been specifically addressed in previous researches.

Based on above discussions, in order to tackle these drawbacks, the main focus of this chapter is placed on the application of LPV control techniques to develop a quantitative robust active vibration control method for flexible structures such that the complete set of control objectives are satisfied, particularly the required control energy and the control input could be reduced. In Section **??**, to develop this control method, the Linear Fractional Representation (LFR) (Hecker, 2006; Hecker et al., 2005) is used to give a systematical approach for the LPV system modeling, where the scheduled variables, parametric and dynamic uncertainties can be considered uniformly. As proposed in Dinh et al. (2005); Dinh (2005), for a LTI plant considering a set of performance trade-offs parameterized by a scalar θ, several weighting functions depending on θ are incorporated into the LTI plant to develop an augmented LPV system, and an trade-off dependent H_∞ controller is synthesized by solving the finite dimensional Linear Matrix Inequality (LMI) optimization problem. In this chapter, an LPV plant with position-dependent dynamics has to be considered, and to save the control energy, some weighting functions have to be parameter-dependent. Based on the phase and gain control policies, the weighting functions can be appropriately determined, thus develop-

ing the augmented LPV system. Then, an efficient LPV H_∞ control technique, *e.g.* Dinh et al. (2005); Scorletti and L. EI Ghaoui (1998), is used to synthesize a qualitative robust parameter-dependent H_∞ controller such that the complete set of control objectives are satisfied, especially the required control energy is reduced. To quantitatively verify the robustness properties of the closed-loop system, various robustness analyses are conducted (Zhang et al., 2013b). The design processes and the effectiveness of the proposed control method are illustrated by active vibration control of a non-collocated piezoelectric cantilever beam, where the considered scheduled variable is the position of the external force. This is representative of the systems with parameter-dependent dynamics as investigated in Paijmans et al. (2006); Wood (1995), which could be modeled as LPV systems. In addition to the LPV H_∞ control, classical robust H_∞ control is also used for this numerical case. Their nominal control performances and the robustness properties are compared. The effectiveness of these controllers is compared in terms of the control energy, the control input and the system output in the time domain, which is difficult to be translated precisely to anything tractable in the frequency domain (Boyd and Barratt, 1992) and are not fully investigated in previous active vibration control designs (Kumar, 2012).

5.2 Preliminaries of LPV control

5.2.1 LPV systems

An LPV system is a linear system whose dynamics, *e.g.* defined by a state space representation, depend on time-varying exogenous parameters whose trajectories are a priori unknown. Nevertheless, some information is available such as the intervals to which the parameters and sometimes their derivative belong to. More formally, an LPV system can be defined as following (Scorletti and Fromion, 2008b):

Definition 5.2.1. *LPV system*
Let the set $\Theta_t \in \mathbb{R}^{n_\theta}$ *be a compact set,* Θ *be a set of measurable functions from*

$[0, \infty)$ *to* $\mathbb{R}^{n_\theta}$ *such that for* $\theta(\cdot) \in \Theta$, *for all* $t \geq 0$, $\theta(t) \in \Theta_t$ *and*

$$\begin{bmatrix} A(\theta) & B(\theta) \\ C(\theta) & D(\theta) \end{bmatrix} \tag{5.2}$$

be a continuous matrix function defined from $\Theta_t \in \mathbb{R}^{(n+n_o)\times(n+n_i)}$. *A Linear Parameter Varying (LPV) system is defined as*

$$q = \Sigma_{LPV}(p) \begin{cases} \dot{x}(t) = A(\theta(t))x(t) + B(\theta(t))p(t) \\ q(t) = C(\theta(t))x(t) + D(\theta(t))p(t) \ , \ \exists \theta(\cdot) \in \Theta \\ x(t_0) = x_0 \end{cases} \tag{5.3}$$

where $x(t) \in \mathbb{R}^n$ *is the state vector,* $p(t) \in \mathbb{R}^{n_i}$ *the disturbance input,* $q(t) \in \mathbb{R}^{n_o}$ *the output and* $\theta(t) \in \mathbb{R}^{n_\theta}$ *the exogenous parameter vector assumed to be measured on-line:* $\theta(t) = [\theta(t), \cdots, \theta_{n_\theta}(t)]^T$.

An LPV system is thus defined by the Equation (5.2) and a set Θ. The LPV systems usually under consideration can be classified along the class of the set Θ and the class of the state space matrix functions of $\sum_{LPV}$ on θ. In this chapter, we focus on one class of state space matrices.

Set Θ: The compact set Θ_t is usually a polytope (more precisely an hyperrectangle):

$$\Theta_t = \left\{ \theta = [\theta_1, \cdots, \theta_{n_\theta}]^T \mid \forall i = 1, \ldots, n_\theta, \right\}$$

The set Θ is defined from Θ_t. Three cases are usually considered as discussed in (Scorletti and Fromion, 2008b) and in this research, unbounded parameter rates of variation is used (Scorletti and L. EI Ghaoui, 1998; Scherer, 2001):

$$\Theta = \{\theta(\cdot) \mid \text{for all } t \geq 0, \ \theta(t) \in \Theta_t\}$$

There are mainly two kinds of state space matrices dependence on θ (Scorletti and Fromion, 2008b): one is that the state space matrices are affine functions of θ and the other one is that the state space matrices are rational functions of θ. The later one is focused in this research:

Any rational matrix function in Θ has an LFT realization: there exists four

matrices A_Σ, B_Σ, C_Σ and D_Σ of compatible dimensions such that

$$\begin{bmatrix} A(\theta) & B(\theta) \\ C(\theta) & D(\theta) \end{bmatrix} = D_\Sigma + C_\Sigma \Delta_\Sigma(\theta(t))(I - A_\Sigma \Delta_\Sigma(\theta(t)))^{-1} B_\Sigma$$

with

$$\Delta_\Sigma(\theta(t)) = \begin{bmatrix} \theta_1(t) I_{r1} & 0 & \cdots & \cdots & 0 \\ 0 & \ddots & \ddots & & \vdots \\ \vdots & \ddots & \theta_i(t) I_{r_i} & \ddots & \vdots \\ \vdots & & \ddots & \ddots & 0 \\ 0 & \cdots & \cdots & 0 & \theta_{n_\theta}(t) I_{r_{n_\theta}} \end{bmatrix}$$

for some $r_i, i = 1, ..., n_\theta$. Such LPV systems are referred to as LFT systems. An important subcase is the case when the state space matrices are polynomial functions of Θ (Bliman, 2003). Other dependences can also be introduced such as any continuous dependence (Becker, 1995; Wu et al., 1996), piecewise affine dependence (Lim, 1999) and spline dependence (Scherer, 1998). The detailed classes of LPV systems can be found in Scorletti and Fromion (2008b).

5.2.2 The LPV control problem

Let us consider the augmented LPV plant P_{LPV} defined as

$$\begin{bmatrix} z \\ y \end{bmatrix} = P_{au} \left(\begin{bmatrix} w \\ u \end{bmatrix} \right) \begin{cases} \dot{x}(t) = A(\theta(t))x(t) + B_w(\theta(t))w(t) + B_u(\theta(t))u(t) \\ z(t) = C_z(\theta(t))x(t) + D_{zw}(\theta(t))w(t) + D_{zu}(\theta(t))u(t) \\ y(t) = C_y(\theta(t))x(t) + D_{yw}(\theta(t))w(t) \end{cases} \quad (5.4)$$

where $x(t) \in \mathbb{R}^{n_p}$ is the state vector, $u(t) \in \mathbb{R}^{n_u}$ the control input, $y(t) \in \mathbb{R}^{n_y}$ the measured output, $z(t) \in \mathbb{R}^{n_z}$ the weighted regulated output, $w(t) \in \mathbb{R}^{n_w}$ the exogenous input. The state space matrices of $P_{au}(s, \theta)$ are assumed to be rational functions of θ. Based on the definition of $P_{au}(s, \theta)$, we consider the LPV control problem:
Design an LPV controller $u = K_{LPV}(y)$ such that with the closed-loop system of Figure 5.2 denoted by the lower LFT $\mathcal{F}_l(P_{au}, K_{LPV})$ (Zhou et al., 1996):

- $\mathcal{F}_l(P_{au}, K_{LPV})$ is asymptotically stable;

- $\mathcal{F}_l(P_{au}, K_{LPV})$ satisfies a performance specification, for example, $\mathcal{F}_l(P_{au}, K_{LPV})$ has an $\mathcal{L}_2$ gain less than a given γ, where the $\mathcal{L}_2$ gain is defined as the smallest γ such that for any input w, $\int_0^T z(t)^T z(t)dt \leq \gamma^2 \int_0^T w(t)^T w(t)dt$, $\forall T \geq 0$. For LTI systems, the $\mathcal{L}_2$ gain is equal to the H_∞ norm. Moreover, if the $\mathcal{L}_2$ gain of $\mathcal{F}_l(P_{au}, K_{LPV})$ is no larger than γ, necessarily we have $\|\mathcal{F}_l(P_{au}(s,\theta_i), K_{LPV}(s,\theta_i))\|_\infty \leq \gamma, \forall \theta_i$.

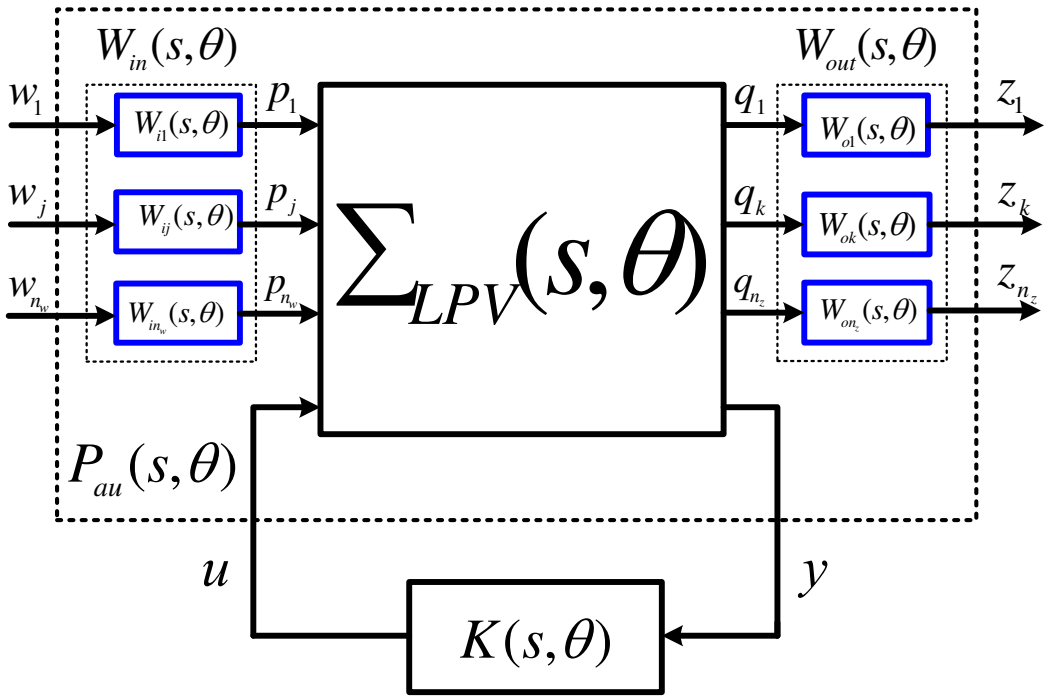

Figure 5.2: Augmented LPV plant $P_{au}(s,\theta)$

Evidently, the weighting functions representing the complete set of control objectives are critical to have an efficient $K_{LVP}(s,\theta)$ and have to be appropriately determined. The phase and gain control policies proposed in Zhang et al. (2013a) are useful for the selection. As above discussed, an LPV controller is usually designed for a plant defined as an LPV system. Numerous LPV controller design approaches have been proposed since last 90's with different levels of conservatism or numerical efficiency. A classification of LPV controllers can be obtained based on the following features: the controller parameters, the feedback structure and the dependence of the state matrices of the controller on the pa-

rameters. The detailed classification of existing LPV controller, different cases of parameter dependence and available feedback structures can be found in Scorletti and Fromion (2008b). In this research, the used controller state space matrices only depend on $\theta(t)$ and the output feedback control is used, that is, the output $y(t)$ of the plant $P_{au}(s,\theta)$ is assumed to be measured in real-time:

$$u = K_{LPV}(y) \begin{cases} \dot{x}_K(t) = A_K(\theta(t))x_K(t) + B_K(\theta(t))y(t) \\ u(t) = C_K(\theta(t))x_K(t) + D_K(\theta(t))y(t) \end{cases} \tag{5.5}$$

where $x_K(t) \in \mathbb{R}^{n_K}$ and the matrices $A_K(\theta(t))$, $B_K(\theta(t))$, $C_K(\theta(t))$, $D_K(\theta(t))$ have to be synthesized. In this case, we obtain the following state space representation for the closed-loop system

$$\begin{bmatrix} A_{cl}(\theta(t)) & B_{cl}(\theta(t)) \\ C_{cl}(\theta(t)) & D_{cl}(\theta(t)) \end{bmatrix} = \begin{bmatrix} A(\theta(t)) & 0 & B_w(\theta(t)) \\ 0 & 0 & 0 \\ C_z(\theta(t)) & 0 & D_{zw}(\theta(t)) \end{bmatrix} +$$

$$\begin{bmatrix} 0 & B_u(\theta(t)) \\ I_n & 0 \\ 0 & D_{zu}(\theta(t)) \end{bmatrix} \begin{bmatrix} A_K(\theta(t)) & B_K(\theta(t)) \\ C_K(\theta(t)) & D_K(\theta(t)) \end{bmatrix} \begin{bmatrix} A_K(\theta(t)) & I_n & 0 \\ C_y(\theta(t)) & 0 & D_{yw}(\theta(t)) \end{bmatrix}$$

It is notable that the order of the output feedback controller is a priori enforced to be equal to the order of the augmented LPV plant $P_{au}(s,\theta)$. Considering the conservatism and computational efficiency, the LPV control technique proposed in Scorletti (1996); Scorletti and L. EI Ghaoui (1998) is employed for the LPV controller synthesis, which can be solved with LMI constraints as briefly presented in B.1.

With the designed LPV controller, reliable deterministic and probabilistic robustness analyses have to be conducted with μ/ν analysis and the random algorithm respectively (Zhou et al., 1996; Calafiore et al., 2000). They can take into account the probabilistic information of parametric uncertainties and quantitatively verify the robustness properties both in the deterministic sense and the probabilistic one. According to the results of the robustness analyses, if necessary, the weighting functions used in the control design can be retuned and a trade-off

could be made among various control objectives. The LPV system modeling, the LPV controller design and the robustness analyses consist of the proposed quantitative robust LPV control method, which is general and allows to satisfy the complete set of control objectives. In this chapter, the design processes and effectiveness of the control method are subsequently illustrated with active vibration control of a piezoelectric cantilever beam excited by an external position-varying force, which has position-dependent dynamics and is modeled as an LPV system.

5.3 Application of the proposed control method

The proposed quantitative robust LPV control is applied to active vibration of a piezoelectric cantilever beam, as shown in Figure 5.3. It is excited by an external position-varying force $F(t, x_f)$, *i.e.* x_f is varying within a bounded range and assumed to be measurable in real-time. This is representative of the systems with parameter-dependent dynamics and could be modeled as an LPV system.

Based on the above discussion, some main steps are outlined for the design of a quantitative robust LPV H_∞ controller:

Step 1: Focus on the LPV system modeling to determine the schedule parameter θ and develop the LPV model $\Sigma_{LPV}(s, \theta)$ for the position-dependent dynamics using LFR.

Step 2: According to the complete set of control objectives such as the fixed specification of vibration reduction and the modulus margin, necessary weighting functions are appropriately employed based on phase and gain control policies. Especially, to fully employ the information of θ and improve some control objectives, one or several weighting functions have to depend on θ, for instance, the gain of $W_i(s, \theta)$, *i.e.* $k_{W_i}(\theta)$, depends on θ to reduce the control energy. It is critical to determine $k_{W_i}(\theta)$ in the controller design: first a finite number of allowable θ_j are chosen, which provides the corresponding LTI plant $\Sigma_{LPV}(s, \theta_j)$. Based on $\Sigma_{LPV}(s, \theta_j)$, the corresponding $k_{W_i}(\theta_j)$ and other weighting functions are selected to develop $P_{au}(s, \theta_j)$. Then one LTI H_∞ controller $K_\infty(s, \theta_j)$ is achieved to satisfy these control objectives, *e.g.* $\|\mathcal{F}_l(P_{au}(s, \theta_j), K_\infty(s, \theta_j))\|_\infty \leq 1$. Lastly, based on the chosen θ_j and the selected $k_{W_i}(\theta_j)$, the interpolation of $k_{W_i}(\theta)$ can be obtained using least mean square method to have $k_{W_i}(\theta)$ for the infinite number

of allowable θ.

Step 3**:** Based on $\Sigma_{LPV}(s,\theta)$ and the weighting functions, the augmented LPV plant $P_{au}(s,\theta)$ is well developed using LFR. Then with the employed LPV control technique, the LPV controller $K_{LPV}(s,\theta)$ can be synthesized, that is, the matrices $A_K(\theta(t))$, $B_K(\theta(t))$, $C_K(\theta(t))$, $D_K(\theta(t))$ of Equation (5.5) are achieved.

Step 4**:** Verify that the complete set of control objectives are satisfied with the designed $K_{LPV}(s,\theta)$ for any allowable value of θ. With the weighting functions, these control objectives are reduced to $\|\mathcal{F}_l(P_{au}(s,\theta), K_{LPV}(s,\theta))\|_\infty \leq 1, \forall\theta$. As above discussed, when the $\mathcal{L}_2$ gain of $\mathcal{F}_l(P_{au}(s,\theta), K_{LPV}(s,\theta))$ is no larger than one, necessarily we have $\|\mathcal{F}_l(P_{au}(s,\theta), K_{LPV}(s,\theta))\|_\infty \leq 1, \forall\theta$, that is, the set of control objectives are satisfied with $K_{LPV}(s,\theta)$. Besides, in the presence of parametric and dynamic uncertainties, the robustness properties of the closed-loop system using $K_{LPV}(s,\theta)$ are quantitatively verified with deterministic and probabilistic robustness analyses. If some control objectives are not satisfied, return to Step 2 to make a better trade-off among various control objectives by adjusting the weighting functions and employ more values of θ_j for a better interpolation of $k_{W_i}(\theta)$.

5.3.1 LPV modeling of the position-dependent dynamics

As shown in Figure 5.3, the location of the accelerometer sensor and that of the piezoelectric actuator are determinant, but the location of the external force is varying within a certain range, *i.e.* x_s and x_a are fixed and the scheduled variable θ can be introduced for x_f such that

$$x_f = \theta L_{\text{beam}},\ \theta \in [\theta_{\min},\ \theta_{\max}],\ 0 < \theta_{\min} < \theta_{\max} < 1$$

where L_{beam} is the total length of the cantilever beam and $\theta_{\min}$, $\theta_{\max}$ determine the allowable position of the force.

Based on modal analysis approach (Meirovitch, 1986) and the modeling of piezoelectric actuators (Moheimani and Fleming, 2006), applying Laplace transformation and assuming zero initial conditions, for the first n resonant modes we have the formulations of the disturbance dynamical model $G_d(s)$ representing the dynamics from $F(s,x_f)$ to the beam acceleration $\ddot{Y}(x,s)$, and the plant dy-

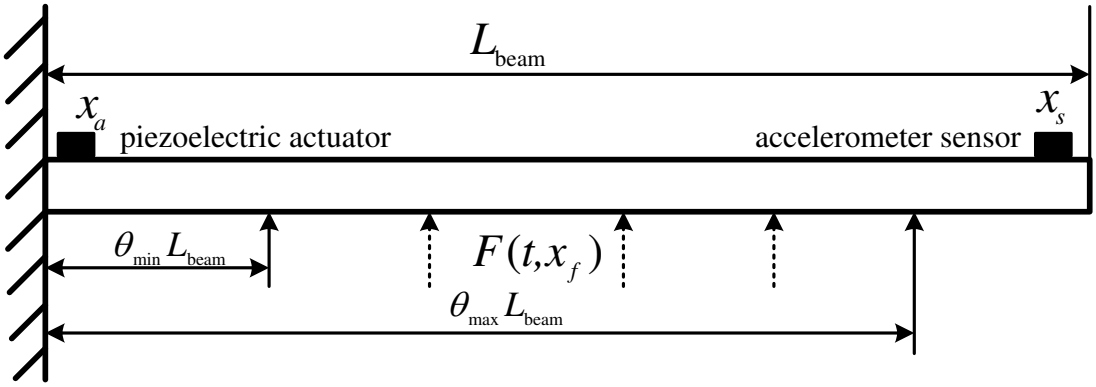

Figure 5.3: A piezoelectric cantilever beam with position-dependent dynamics

namical model $G_p(s)$ representing the dynamics from the voltage applied on the piezoelectric actuator $V_a(x_a, s)$ to the beam acceleration $\ddot{Y}(s, x_s)$, that is,

$$G_d(s) = \frac{\ddot{Y}(s,x_s)}{F(s,x_f)} = \sum_{i=1}^{n} G_{di}(s) = \sum_{i=1}^{n} \frac{k_{di}(x_s,x_f)s^2}{s^2+2\zeta_i\omega_i+\omega_i^2}$$

$$G_p(s) = \frac{\ddot{Y}(s,x_s)}{V_a(s,x_a)} = \sum_{i=1}^{n} G_{pi}(s) = \sum_{i=1}^{n} \frac{k_{pi}(x_s,x_a)s^2}{s^2+2\zeta_i\omega_i+\omega_i^2}$$

To determine $G_d(s)$ and $G_p(s)$, we have to obtain the modal parameters such as the damping ratio ζ_i, the natural frequency ω_i and the gain $k_{pi/di}$. Based on the analytical formulations for the Euler-Bernoulli beam bounded with piezoelectric actuators (Moheimani and Fleming, 2006), ω_i and k_{pi} depend on x_s, x_a and the structural properties, *e.g.* the material properties and the geometrical dimensions. Since these elements are fixed in this case, $G_p(s)$ is determined and independent on θ. On the other hand, k_{di} depends on $x_f = \theta L_{\text{beam}}$, that is,

$$k_{di}(\theta) = g_i[\sinh(\lambda_i\theta) - \sin(\lambda_i\theta)] + h_i[\cosh(\lambda_i\theta) - \cos(\lambda_i\theta)] \tag{5.6}$$

where g_i, λ_i, h_i depend on the determinant structural properties. As shown in Figure 5.4, for $i = 1, 2, 3$, the gain $k_{di}(\theta)$ has particularly severe dependence on θ such that small variations in θ can generate large variations in the magnitude

and the phase of $G_{di}(s)$.

Note that, for a given structure, $G_{di}(s,\theta)$ and $G_{pi}(s)$ have the same ω_i, and for the sake of simplicity, their damping ratio ζ_i is also assumed to be the same. To consider this fact and be readily employed in the control design, for the i^{th} resonant mode, it is desirable to consider the transfer function vector $[G_{di}(s,\theta),\ G_{pi}(s)]$ with the state space form:

$$\begin{aligned} A_i &= \begin{bmatrix} -2\zeta_i\omega_i & 1 \\ -\omega_i^2 & 0 \end{bmatrix} \in \mathbb{R}^{2\times 2},\ B_i(\theta) = \begin{bmatrix} -2\zeta_i\omega_i \\ -\omega_i^2 \end{bmatrix} [k_{di}(\theta)\ k_{pi}] \in \mathbb{R}^{2\times 2} \\ C_i &= \begin{bmatrix} 1 & 0 \end{bmatrix} \in \mathbb{R}^{1\times 2}, \qquad D_i(\theta) = [k_{di}(\theta)\ k_{pi}] \in \mathbb{R}^{1\times 2} \end{aligned}$$

Naturally, when the first n resonant modes of $[G_d(s,\theta),\ G_p(s)]$ have to be investigated, we have the state space matrices:

$$\begin{aligned} A(\theta) &= \begin{bmatrix} A_1 & \mathbf{0} & \cdots & \mathbf{0} \\ \mathbf{0} & \ddots & \ddots & \vdots \\ \vdots & \ddots & \ddots & \mathbf{0} \\ \mathbf{0} & \cdots & \mathbf{0} & A_n \end{bmatrix} \in \mathbb{R}^{2n\times 2n} \\ B(\theta) &= \begin{bmatrix} B_1(\theta) \\ \vdots \\ B_n(\theta) \end{bmatrix} = \begin{bmatrix} b_1 & \mathbf{0} & \cdots & \mathbf{0} \\ \mathbf{0} & \ddots & \ddots & \vdots \\ \vdots & \ddots & \ddots & \mathbf{0} \\ \mathbf{0} & \cdots & \mathbf{0} & b_n \end{bmatrix} \begin{bmatrix} k_d(\theta) & k_p \end{bmatrix} \in \mathbb{R}^{2n\times 2} \\ C(\theta) &= \begin{bmatrix} C_1, & \cdots & , C_n \end{bmatrix} \in \mathbb{R}^{1\times 2n} \\ D(\theta) &= [1, \cdots, 1] \begin{bmatrix} k_d(\theta), & k_p \end{bmatrix} \in \mathbb{R}^{1\times 2} \end{aligned} \tag{5.7}$$

where $\mathbf{0}$ represents the zero matrix of a compatible dimension, $k_p = [k_{p1}, \cdots, k_{pn}]^T \in \mathbb{R}^{n\times 1}$, $k_d(\theta) = [k_{d1}(\theta), \cdots, k_{dn}(\theta)]^T \in \mathbb{R}^{n\times 1}$ and $b_i = \begin{bmatrix} -2\zeta_i\omega_i \\ -\omega_i^2 \end{bmatrix} \in \mathbb{R}^{2\times 1}$.

To appropriately consider the dependence of $k_d(\theta)$ on θ, the LFR of $k_d(\theta)$ is

used:

$$k_d(\theta) = [k_{d1}(\theta), \cdots, k_{dn}(\theta)]^T = \theta\star \left[\begin{array}{c|c} A_{k_d} & B_{k_d} \\ \hline C_{k_d} & D_{k_d} \end{array}\right] \tag{5.8}$$

where $\star$ is the Redheffer star product (Zhou et al., 1996), the matrices $A_{k_d} \in \mathbb{R}^{m\times m}$, $B_{k_d} \in \mathbb{R}^{m\times 1}$, $C_{k_d} \in \mathbb{R}^{n\times m}$ and $D_{k_d} \in \mathbb{R}^{n\times 1}$ have to be determined, and m is the necessary fractional order for $k_d(\theta)$. Actually, based on the definition of LFR, Equation (5.8) represents

$$k_d(\theta) = D_{k_d} + C_{k_d}\theta(I_m - A\theta)^{-1}B_{k_d}$$

Since the Equation (5.6) reveals that $k_{di}(\theta)$ is not a rational function of θ, in order to obtain the LFR of $k_d(\theta)$, it is necessary to approximate $k_d(\theta)$ by a rational function. For this purpose, enough samples of $\theta_j \in [\theta_{\min}, \theta_{\max}]$ are used to have the corresponding values of $k_d(\theta_j)$, and then the least mean square method is used for the interpolation of $k_d(\theta), \theta \in [\theta_{\min}, \theta_{\max}]$. With the Equation (5.7) and Equation (5.8), we have the LFR of $[G_d(s,\theta),\ G_p(s)]$, that is,

$$\begin{aligned}[G_d(s,\theta),\ G_p(s)] &= \frac{1}{s}\star \left\{ \left[\begin{array}{cccc|cccc} A_1 & \mathbf{0} & \cdots & \mathbf{0} & b_1 & \mathbf{0} & \cdots & \mathbf{0} \\ \mathbf{0} & \ddots & \ddots & \vdots & \mathbf{0} & \ddots & \ddots & \vdots \\ \vdots & \ddots & \ddots & \mathbf{0} & \vdots & \ddots & \ddots & \mathbf{0} \\ \mathbf{0} & \cdots & \mathbf{0} & A_n & \mathbf{0} & \cdots & \mathbf{0} & b_n \\ \hline C_1, & \cdots & \cdots & , C_n & 1, & \ldots & \ldots & , 1 \end{array}\right] \left[\begin{array}{c|c} I & \mathbf{0} \\ \hline \mathbf{0} & [k_d(\theta),\ k_p] \end{array}\right] \right\} \\ &= (\frac{1}{s}, \theta)\star \left[\begin{array}{c|c} \hat{A} & \hat{B} \\ \hline \hat{C} & \hat{D} \end{array}\right] \end{aligned} \tag{5.9}$$

where I represents the identity matrix of a compatible dimension, the constant matrices $\hat{A} \in \mathbb{R}^{(2n+m)\times(2n+m)}$, $\hat{B} \in \mathbb{R}^{(2n+m)\times 2}$, $\hat{C} \in \mathbb{R}^{1\times(2n+m)}$ and $\hat{D} \in \mathbb{R}^{1\times 2}$. It is notable that the vector $[k_d(\theta),\ k_p]$ in both $B(\theta)$ and $D(\theta)$ has to be pulled out to have the simplest LFR of $[G_d(s,\theta),\ G_p(s)]$ (Scorletti and Fromion, 2008a). This is desirable for the controller synthesis and the robustness analysis.

For this particular case, using $x_a = 3.5$mm, $x_s = 223.2$mm and the structural properties listed in Table 5.1, we have the nominal modal parameters for the first

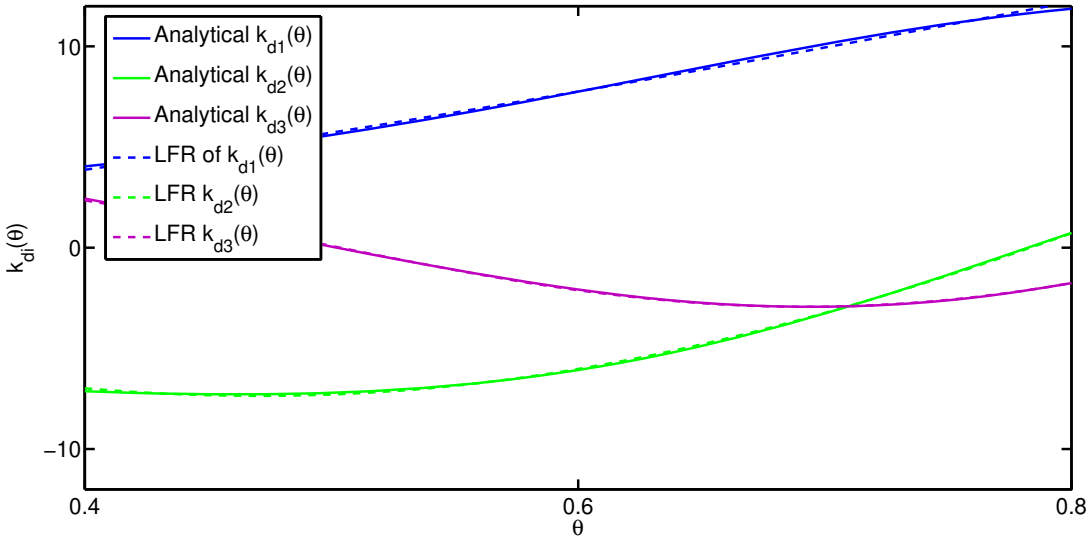

Figure 5.4: Analytical and LFR of $k_{di}(\theta),\ \theta \in [0.4, 0.8],\ i = [1, 2, 3]$

three resonant modes:

$$\begin{aligned} \omega_i &= [295.2, 1850.1, 5180.2], && i = 1, 2, 3 \\ k_{pi} &= [-8.9 \times 10^{-3}, 20.0 \times 10^{-3}, -10.4 \times 10^{-3}], && i = 1, 2, 3 \\ \zeta_i &= [20.0 \times 10^{-3}, 8.0 \times 10^{-3}, 5.0 \times 10^{-3}], && i = 1, 2, 3 \end{aligned}$$

With $\theta_{\min} = 0.4$ and $\theta_{\max} = 0.8$, the corresponding matrices for the LFR of $k_d(\theta),\ \theta \in [0.4, 0.8]$ are

$$A_{k_d} = \begin{bmatrix} 2.10 & -1.41 \\ 1.00 & 0 \end{bmatrix},\ B_{k_d} = \begin{bmatrix} 4.00 \\ 0 \end{bmatrix}$$

$$C_{k_d} = \begin{bmatrix} 0.32 & 0.47 \\ -1.87 & 2.74 \\ -2.24 & 1.90 \end{bmatrix},\ D_{k_d} = \begin{bmatrix} 1.926 \\ -3.941 \\ 8.594 \end{bmatrix}$$

with the fractional order $m = 2$ for enough accuracy. As shown in Figure 5.4, this LFR of $k_d(\theta)$ has a good agreement with the analytical $k_d(\theta)$ for the first three resonant modes.

Property	Beam	PZT	Unit
E	50.0	140.0	Gpa
l	248.0	45.0	mm
w	20.5	20.5	mm
t	4.0	1.5	mm
ρ	2500.0	/	kg/m^3
k_{d31}	/	-1.23×10^{-10}	/

Table 5.1: Nominal geometrical and mechanical properties of the piezoelectric cantilever beam

5.3.2 LPV and LTI H_∞ control designs

Both the proposed LPV H_∞ control design and the worst-case H_∞ control design as employed in Zhang et al. (2013a) are used to achieve the same fixed specification of vibration reduction defined by a frequency-dependent function $U(\omega)$. In this case, for the sake of simplicity, $U(\omega) = 40\text{dB},\ \forall\ \omega \in \mathbb{R}$, that is,

$$|T_{yd}(j\omega, \theta_j)| \leq U(\omega) = 40\text{dB},\ \forall\ \omega \in \mathbb{R},\ \forall \theta_j \in [0.4, 0.8] \tag{5.10}$$

where $T_{yd}(s)$ is the closed-loop transfer function from the disturbance $d(s)$ to the output $y(s)$, as shown in Figure 5.5.

5.3.2.1 LPV H_∞ control design

Based on the typical feedback control structure of Figure 5.1, the augmented LPV plant $P_{au}(s, \theta)$ can be well constructed by using a set of necessary and suitable weighting functions $W_i(s, \theta)$, as shown in Figure 5.5, where the measurement noise $n(s) = W_a(s, \theta)w_1(s)$, the disturbance $d(s) = W_b(s, \theta)w_2(s)$, the regulated signals $z_1(s) = W_1(s, \theta)v(s)$ and $z_2(s) = W_2(s, \theta)u(s)$. By partitioning $P_{au}(s, \theta)$ according to the sizes of $z(s) = [z_1(s), z_2(s)]^T$ and $w(s) = [w_1(s), w_2(s)]^T$, $P_{au}(s, \theta)$ can be described as

$$\begin{bmatrix} z_1(s) \\ z_2(s) \\ y(s) \end{bmatrix} = P_{au}(s, \theta) \begin{bmatrix} w_1(s) \\ w_2(s) \\ u(s) \end{bmatrix}$$

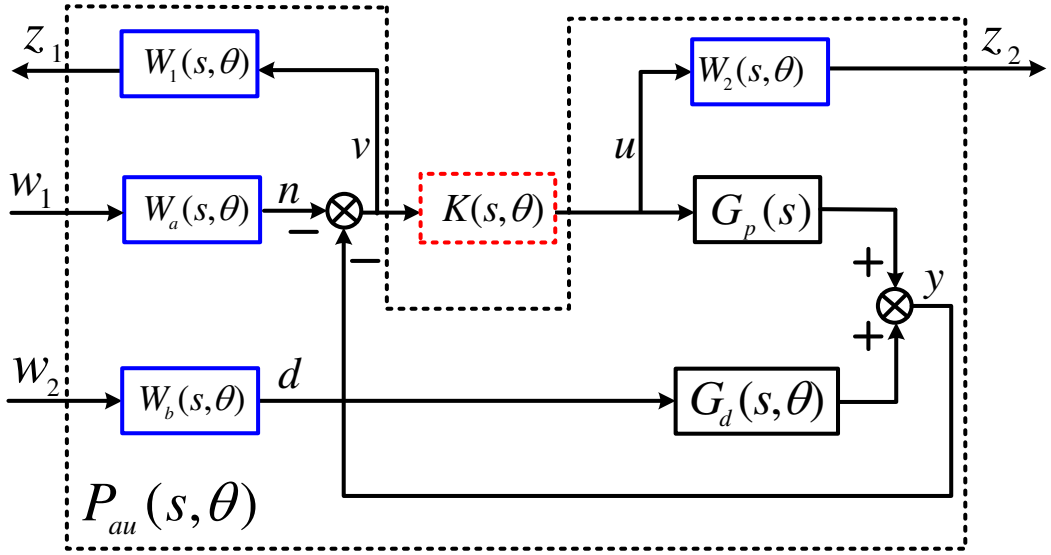

Figure 5.5: LPV H_∞ control structure with parameter-dependent weighting functions

To have the smallest order of $P_{au}(s,\theta)$, we have

$$P_{au}(s,\theta) = W_{\text{out}}(s,\theta)\left\{\begin{bmatrix}1 & 0 & 0\\ 0 & 0 & 1\\ -1 & 0 & 0\end{bmatrix} + \begin{bmatrix}-1\\ 0\\ -1\end{bmatrix}\left[G_d(s,\theta),\ G_p(s)\right]\begin{bmatrix}0 & 1 & 0\\ 0 & 0 & 1\end{bmatrix}\right\} W_{\text{in}}(s,\theta) \tag{5.11}$$

with

$$W_{\text{out}}(s,\theta) = \begin{bmatrix}W_1(s,\theta) & 0 & 0\\ 0 & W_2(s,\theta) & 0\\ 0 & 0 & 1\end{bmatrix} \text{ and } W_{\text{in}}(s,\theta) = \begin{bmatrix}W_a(s,\theta) & 0 & 0\\ 0 & W_b(s,\theta) & 0\\ 0 & 0 & 1\end{bmatrix}$$

Substituting $[G_d(s,\theta),\ G_p(s)]$ of Equation (5.9) into Equation (5.11), we have the simplest LFR of $P_{au}(s,\theta)$, where either $[G_d(s,\theta),\ G_p(s)]$ or $W_i(s,\theta)$ occurs just one time. It is then used for the controller synthesis and the robustness analysis.

With the LPV H_∞ control design of Figure 5.5, $W_2(s,\theta)$ can be used to enforce constraints on the magnitudes of $|K(j\omega)S(j\omega)|$ and $|G_d(j\omega,\theta)K(j\omega)S(j\omega)|$, which are closely related to the control energy. Therefore, to adapt the control energy to θ, $W_2(s,\theta)$ has to depend on θ, and other constant weighting functions

are used to determine the fixed specification of vibration reduction and the requirement on the modulus margin M_m, which is closely related to the stability robustness and defined as:

$$M_m = \inf_{\omega} |1 + L(j\omega)| = \frac{1}{\sup_{\omega} \frac{1}{|1+L(j\omega)|}} = \frac{1}{\sup_{\omega} |S(j\omega)|}, \forall \omega \in \mathbb{R} \tag{5.12}$$

where $S(j\omega) = (1 + L(j\omega))^{-1}$ is the sensitivity function of the closed-loop system. Based on the Nyquist stability criterion, the larger M_m, the better stability robustness (Skogestad and Postlethwaite, 2005).

Based on the principle of phase and gain control policies, a second order $W_2(s, \theta)$ is used:

$$W_2(s, \theta) = k_{W_2}(\theta) \times \frac{(s + M\omega_b)(s + fM\omega_b)}{(s + \epsilon)(s + fM^2\omega_b)} \tag{5.13}$$

where M, ω_b, ϵ, f are constants and the gain $k_{W_2}(\theta)$ determines the dependance of $W_2(s, \theta)$ on θ. With LFR, $W_2(s, \theta)$ can be represented as

$$W_2(s, \theta) = \left(\frac{1}{s}\right) I_2 \star \left[\begin{array}{cc|c} 0 & 1 & 0 \\ -\epsilon f M^2\omega_b & -(\epsilon + fM^2\omega_b) & 1 \\ \hline (M\omega_b)^2 f - \epsilon f M^2\omega_b & M\omega_b(1 + f) - (\epsilon + fM^2\omega_b) & 1 \end{array}\right] \times \cdots$$

$$\left[\begin{array}{cc|c} 1 & 0 & 0 \\ 0 & 1 & 0 \\ \hline 0 & 0 & k_{W_2}(\theta) \end{array}\right] \tag{5.14}$$

and $k_{W_2}(\theta)$ can be represented as

$$k_{W_2}(\theta) = \theta \star \left[\begin{array}{c|c} A_{k_{W_2}} & B_{k_{W_2}} \\ \hline C_{k_{W_2}} & D_{k_{W_2}} \end{array}\right] \tag{5.15}$$

where the constant matrices $A_{k_{W_2}} \in \mathbb{R}^{l \times l}$, $B_{k_d} \in \mathbb{R}^{l \times 1}$, $C_{k_d} \in \mathbb{R}^{1 \times l}$ and $D_{k_d} \in \mathbb{R}^{1 \times 1}$ have to be determined, and l is the necessary fractional order for $k_{W_2}(\theta)$. As the determination of $k_d(\theta)$, for some values of $\theta_j \in [0.4, 0.8]$, we select the corresponding value of $k_{W_2}(\theta_j)$ to satisfy the complete set of control objec-

tives, as shown in Table 5.2. Then, these data can be used for the interpolation of $k_{W_2}(\theta), \forall\theta \in [0.4, 0.8]$ with the least mean square method, that is, $A_{k_{W_2}} = 4.044,\ B_{k_{W_2}} = 4.00,\ C_{k_{W_2}} = -3.637,\ D_{k_{W_2}} = -3.709$ with the fractional order $l = 1$. The other parameters of $W_2(s,\theta)$ are $M = 100.0,\ f = 35.0,\ \omega_b =$

θ_j	0.4	0.5	0.6	0.7	0.8
$k_{W_2}(\theta_j)$	5.4	3.7	2.4	1.8	1.5

Table 5.2: The chosen θ_j and $k_{W_2}(\theta_j)$ for the interpolation of $k_{W_2}(\theta)$

4.5, $\epsilon = 1 \times 10^{-3}$. With these parameters, we have the LFR of $W_2(s,\theta)$ of Equation (5.14) and the dependence of $|W_2(j\omega,\theta)|$ on $\theta \in [0.4, 0.8]$ is illustrated in Figure 5.6. In this case, to consider the fixed specification of vibration reduction of Equation (5.10) and ensure $M_m(\theta) \geq 0.866,\ \forall\ \omega \in \mathbb{R}$, the other constant weighting functions are $W_a(s) = 1.0,\ W_1(s) = 0.866,\ W_b(s) = 0.0115$.

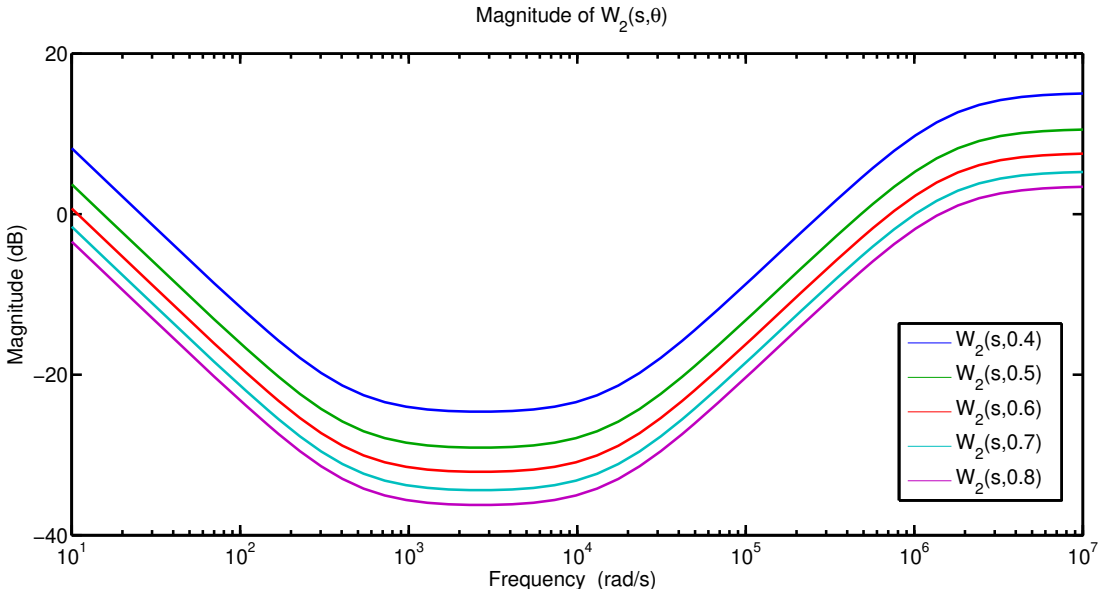

Figure 5.6: The dependence of $|W_2(j\omega,\theta)|$ on $\theta \in [0.4, 0.8]$

By incorporating these weighting functions into Equation (5.11), the simplest LFR of $P_{au}(s,\theta)$ is obtained, which is then used for the $K_{LPV}(s,\theta)$ synthesis with the LPV control technique listed in B.1. The LFR realization of the designed $K_{LPV}(s,\theta)$ is presented in B.2. With the designed $K_{LPV}(s,\theta)$,

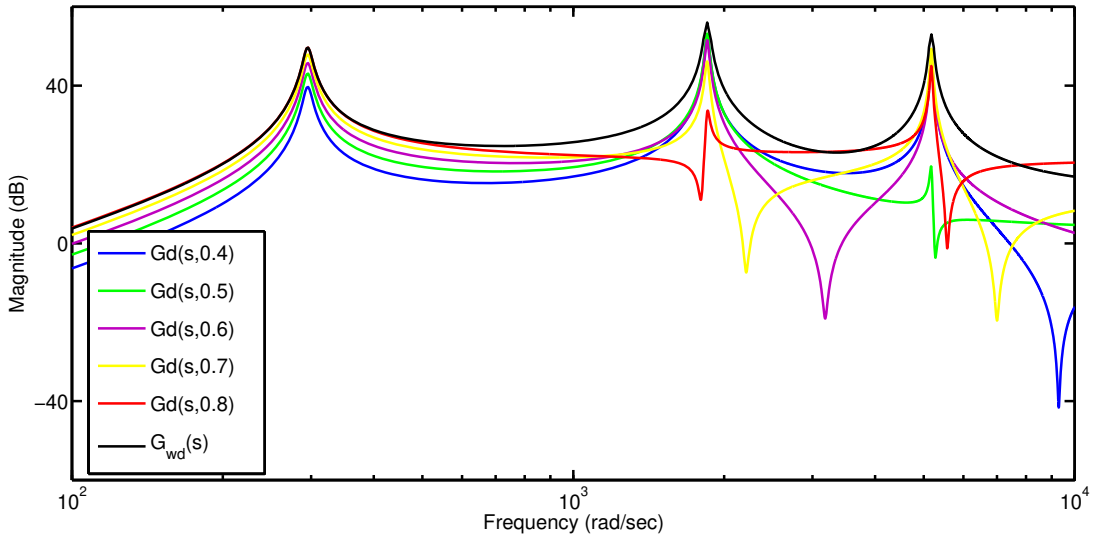

Figure 5.7: The worst-case $G_d(s,\theta)$ for $\theta \in [0.4, 0.8]$

the $\mathcal{L}_2$ gain of $\mathcal{F}_l(P_{au}(s,\theta), K_{LPV}(s,\theta))$ is smaller than one, necessarily we have $\|\mathcal{F}_l(P_{au}(s,\theta_j), K_{LPV}(s,\theta_j))\|_\infty < 1$, that is, for any $\theta_j \in [0.4, 0.8]$, we have

$$\begin{aligned} ||T_{yd}(s,\theta_j)||_\infty &< \frac{1}{\|W_1(s)W_b(s)\|_\infty} = 40\text{dB} \\ M_m(\theta_j) &= \frac{1}{\|S(s,\theta_j)\|_\infty} \geq \|W_1(s)W_a(s)\|_\infty = 0.866 \end{aligned}$$

This implies that a priori considered control objectives are simultaneously satisfied with the designed $K_{LPV}(s,\theta)$.

5.3.2.2 Worst-case H_∞ control design

In addition to $K_{LPV}(s,\theta)$, a worst-case H_∞ controller $K_w(s)$ is also designed. First, over the frequency of interest the worst-case disturbance dynamical model $G_{wd}(s)$ is obtained by fine gridding θ of $G_d(s,\theta)$, as shown in Figure 5.7. Obviously, $G_{wd}(s)$ includes all possible $G_d(s,\theta)$ for any $\theta \in [0.4, 0.8]$ with very little conservatism. Then, to satisfy the same control objectives as $K_{LPV}(s,\theta)$ does, *e.g.* the specification of vibration reduction and the requirement on M_m, the constant $W_2(s)$ is used with the parameters $M = 100.0$, $f = 35.0$, $\omega_b = 4.5$, $\epsilon = 1 \times 10^{-3}$, $k_{W_2} = 2.2$. The other weighting functions are the same as used for the

$K_{LPV}(s,\theta)$ synthesis. With these weighting functions, the $K_w(s)$ is obtained:

$$K_w(s) = \frac{0.1(s+1.6\times10^6)(s-255.8)(s-1.8\times10^{-3})}{(s+1.4\times10^4)(s+7189.0)(s+2050.0)}\times$$
$$\frac{(s^2-2801.0s+8.6\times10^6)(s^2+9150s+6.8\times10^7)}{(s^2+347.9s+4.3\times10^4)(s^2+6599.0s+4.9\times10^7)}$$

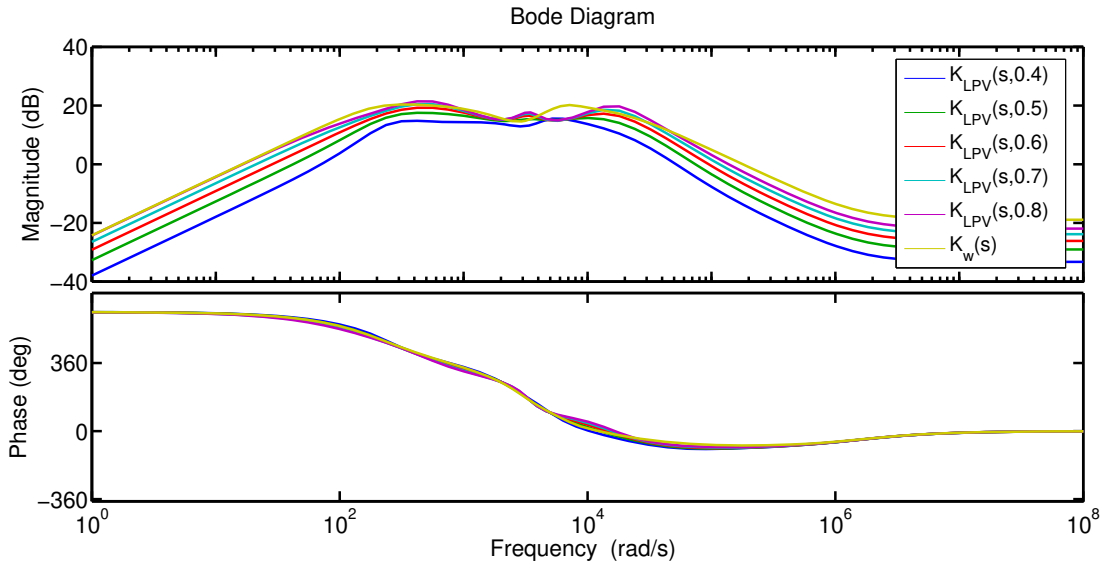

Figure 5.8: Comparisons between $K_{LPV}(s,\theta)$ and $K_w(s)$ for $\theta \in [0.4, 0.8]$

The comparisons between $K_{LPV}(s,\theta)$ and $K_w(s)$ in the frequency domain are illustrated in Figure 5.8. As expected, both $K_{LPV}(s,\theta)$ and $K_w(s)$ roll off at high frequencies to avoid the spillover problem and the $|K_{LPV}(j\omega,\theta)|$ depends on θ, which is smaller than $|K_w(j\omega)|$ at almost any frequency for $\theta \in [0.4, 0.8]$. The phases of $K_{LPV}(j\omega,\theta)$ and $K_w(j\omega)$ are nearly the same. These comparisons are consistent with the principle of phase and gain control policies. For this parameter-dependent system, the schedule variable θ only exists in $G_d(s,\theta)$ and $G_p(s)$ is independent on θ. From the phase control policy, to satisfy the fixed specification of vibration reduction while saving the control energy, $|L(j\omega,\theta) = K(s,\theta)G_p(s)|$ has to change with θ. On the other hand, for the stability robustness to parametric uncertainties, since the phase of $G_p(s)$ does

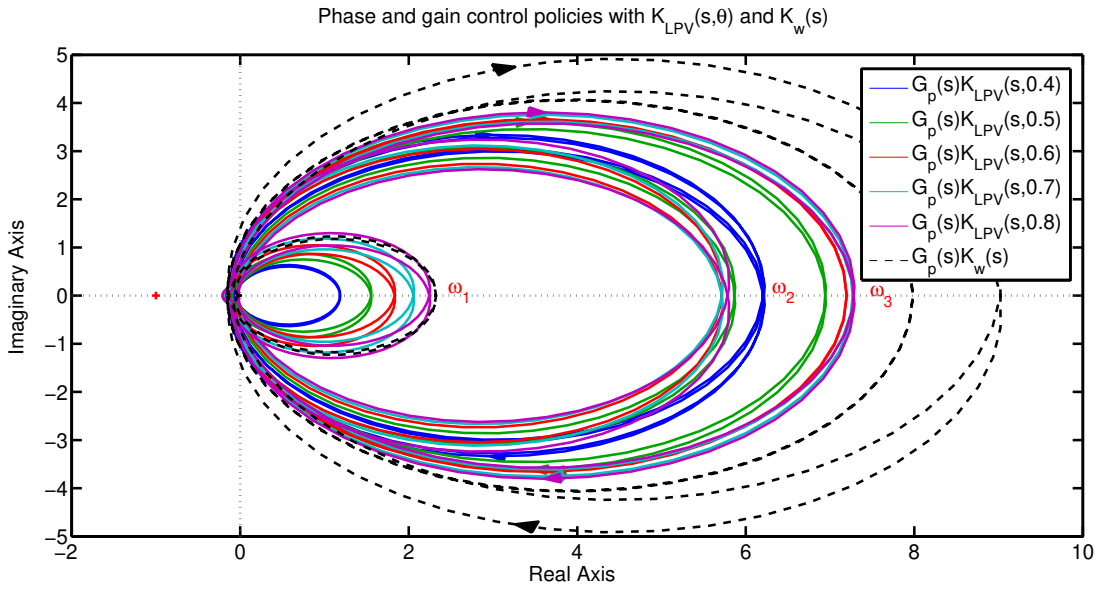

Figure 5.9: Phase and gain control policies with $K_{LPV}(s,\theta)$ and $K_w(s)$: ω_i represents the i^{th} controlled resonant frequency

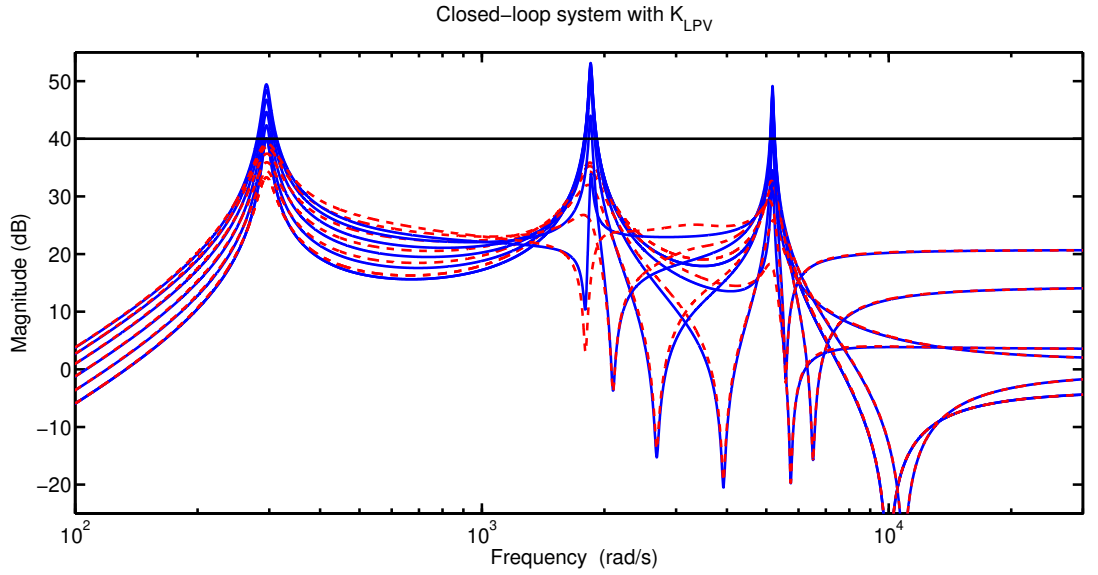

Figure 5.10: Closed-loop system with $K_{LPV}(s,\theta)$ for $\theta \in [0.4, 0.8]$: the blue solid curves represent the open-loop systems and the red dashed curves represent the closed-loop systems by gridded θ

not depend on θ, the phase of $K(s,\theta)$ can also be constant for any θ. As illustrated in Figure 5.9, the Nyquist plot of $L(s,\theta_j)$ verifies that, around the controlled resonant frequencies, $|L(j\omega,\theta_j)|$ is large enough for effective vibration reduction and $L(s,\theta_j)$ stays in right half plane to have qualitative stability robustness to parametric uncertainties. The vibration reduction of the closed-loop system using $K_{LPV}(s,\theta)$ is shown in Figure 5.10. As expected, for any allowable $\theta \in [0.4, 0.8]$, the specification of vibration reduction of Equation (5.10) is satisfied with $K_{LPV}(s,\theta)$. Since around the controlled resonant frequencies, $|K_{LPV}(j\omega,\theta)| < |K_w(j\omega)|, \forall\theta$, from the principle of phase control policy, $K_w(s)$ can necessarily satisfy the specification of vibration reduction.

5.3.3 Quantitative robustness analysis of the closed-loop system

Although, in the designs of $K_{LPV}(s,\theta)$ and $K_w(s)$, qualitative robustness properties of the closed-loop system are considered, both deterministic and probabilistic robustness analyses are necessary to quantitatively verify the robustness properties to parametric and dynamic uncertainties. For this numerical case, the natural frequencies and damping ratios are assumed to have 20% variations, that is,

$$\begin{aligned} \omega_i &= \omega_{i0} + \omega_{i1}\delta_{\omega_i};\ |\delta_{\omega_i}| \le 1, \omega_{i1} = 0.2\omega_{i0}, i = 1,2,3 \\ \zeta_i &= \zeta_{i0} + \zeta_{i1}\delta_{\zeta_i};\ \ |\delta_{\zeta_i}| \le 1, \zeta_{i1} = 0.2\zeta_{i0},\ i = 1,2,3 \end{aligned}$$

where $\omega_{i0},\ \zeta_{i0}$ are the nominal values of these modal parameters. In addition, the scheduled variable $\theta \in [0.4, 0.8]$ is normalized such that

$$\theta = \theta_0 + \theta_1\delta_\theta;\ |\delta_\theta| \le 1$$

with $\theta_0 = 0.6$ and $\theta_1 = 0.2$. Thus, the gain $k_{di}(\theta)$ can be represented as

$$k_{di}(\theta) = k_{di0} + k_{di1}\delta_\theta;\ |\delta_\theta| \le 1, i = 1,2,3$$

where k_{di0} is obtained with $\delta_\theta = 0$. Note that, θ is assumed to be a bounded time-invariant uncertain parameter in the robustness analysis. As shown in Figure 5.11, the additive dynamic uncertainty $\Delta_{\text{Dyn}}(s)$ is used with a suitable dynamic normalization function $W_{\text{Dyn}}(s)$ to represent the neglected high-frequency dynamics of $G_p(s)$, that is,

$$G_p(s) = G_{p0}(s) + W_{\text{Dyn}}(s)\Delta_{\text{Dyn}}(s), \ \ \|\Delta_{\text{Dyn}}(s)\|_\infty \leq 1$$

where $G_{p0}(s)$ is the reduced nominal plant dynamical model including the first three resonant modes. To consider the robust performance, a fictitious unit normalized performance uncertainty $\Delta_{\text{Perf}}(s)$ is also used with the corresponding performance normalization function $W_{\text{Perf}}(s)$ (Skogestad and Postlethwaite, 2005).

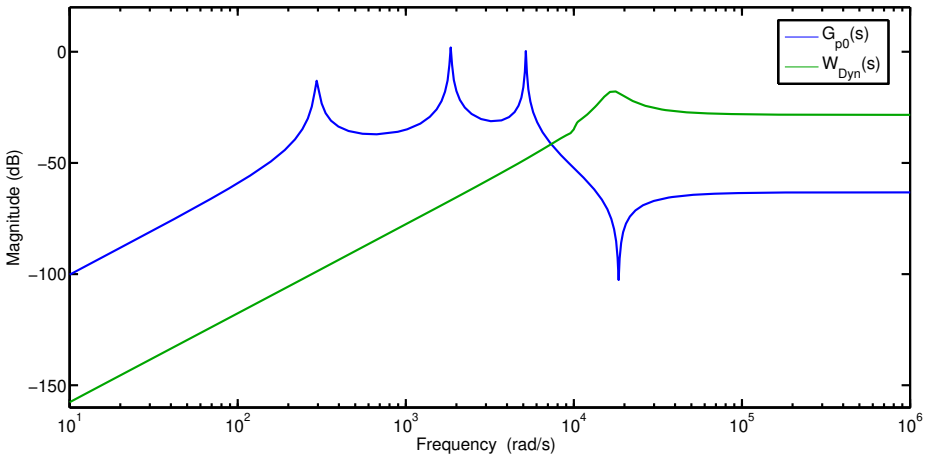

Figure 5.11: The additive dynamic uncertainty normalized by $W_{\text{Dyn}}(s)$

With above uncertainty modeling, the unit normalized diagonal augmented uncertainty $\Delta' = \mathbf{diag}(\Delta'_1, \ \Delta'_2) \in \boldsymbol{B}_{\hat{\Delta}}$ can be used, where $\boldsymbol{B}_{\hat{\Delta}}$ is the norm bounded diagonal uncertainty block as defined in Zhang et al. (2013b). The $\Delta'_1 = \mathbf{diag}(\Delta_{\text{Para}}, \Delta_{\text{Dyn}})$ represents the parametric uncertainty and the dynamic one, and $\Delta'_2 = \Delta_{\text{Perf}}$ is the norm bounded fictitious performance uncertainty.

Particularly, for the designed $K_{LPV}(s,\theta)$, we have

$$\Delta_{\text{Para}} = \textbf{diag}\ (\delta_{\omega_1} I_2, \delta_{\omega_2} I_2, \delta_{\omega_3} I_2, \delta_{\zeta_1}, \delta_{\zeta_2}, \delta_{\zeta_3}, \delta_\theta I_5)$$

where $\delta_\theta I_5$ is due to the fact that δ_θ occurs three times in $K_{LPV}(s,\theta)$ and two times in $G_d(s,\theta)$.

As performed in Zhang et al. (2013b), reliable μ analysis is used to obtain the deterministic robustness margin k_{DRM} of the closed-loop system, as shown in Table 5.3. Since the upper and lower bounds of k_{DRM} coincide well, the estimated k_{DRM} is reliable, in other words, the closed-loop system remains stable for any $\Delta \in 1.02\Delta_1'$ with $K_w(s)$ and for any $\Delta \in 1.35\Delta_1'$ with $K_{LPV}(s,\theta)$. By ν analysis (Skogestad and Postlethwaite, 2005), we have the deterministic worst-case performance, as illustrated in Figure 5.12. It shows that the specification of vibration reduction is fulfilled for any $\Delta \in 1.0\Delta_1'$ with $K_w(s)$ and $K_{LPV}(s,\theta)$. Above μ and ν analyses quantitatively ensure that the closed-loop stability and the specification of vibration reduction are satisfied in the presence of 20% variation on the modal parameters and the assumed dynamic uncertainty.

Bounds on k_{DRM}	$K_w(s)$	$K_{LPV}(s,\theta)$
Lower bound on k_{DRM}	1.355	1.020
Upper bound on k_{DRM}	1.360	1.026

Table 5.3: Deterministic robustness margin k_{DRM} with $K_w(s)$ and $K_{LPV}(s,\theta)$

Besides, the probabilistic robustness analysis using random algorithm is performed to consider probabilistic information of parametric uncertainties and provide complements and comparisons to the deterministic robustness analysis. For this numerical case, both uniformly and Gaussian distributed ω_i are considered and ζ_k is assumed to have uniform distribution. As performed in Zhang et al. (2013b), using Monte Carlo Simulation, the results from probabilistic stability analysis are illustrated in Table 5.4 with $\epsilon = 0.01, \delta = 0.01$. They show that, with probability $1-\delta = 99\%$, for either uniformly or Gaussian distributed ω_i, the closed-loop system remains stable for all sampled $\Delta \in 1.02\Delta_1'$ using $K_w(s)$ and for all sampled $\Delta \in 1.35\Delta_1'$ using $K_{LPV}(s,\theta)$. Additionally, a few destabilizing perturbations $\Delta_{\text{des}} \in 1.15\Delta_1'$ are found using $K_{LPV}(s,\theta)$, which means that there

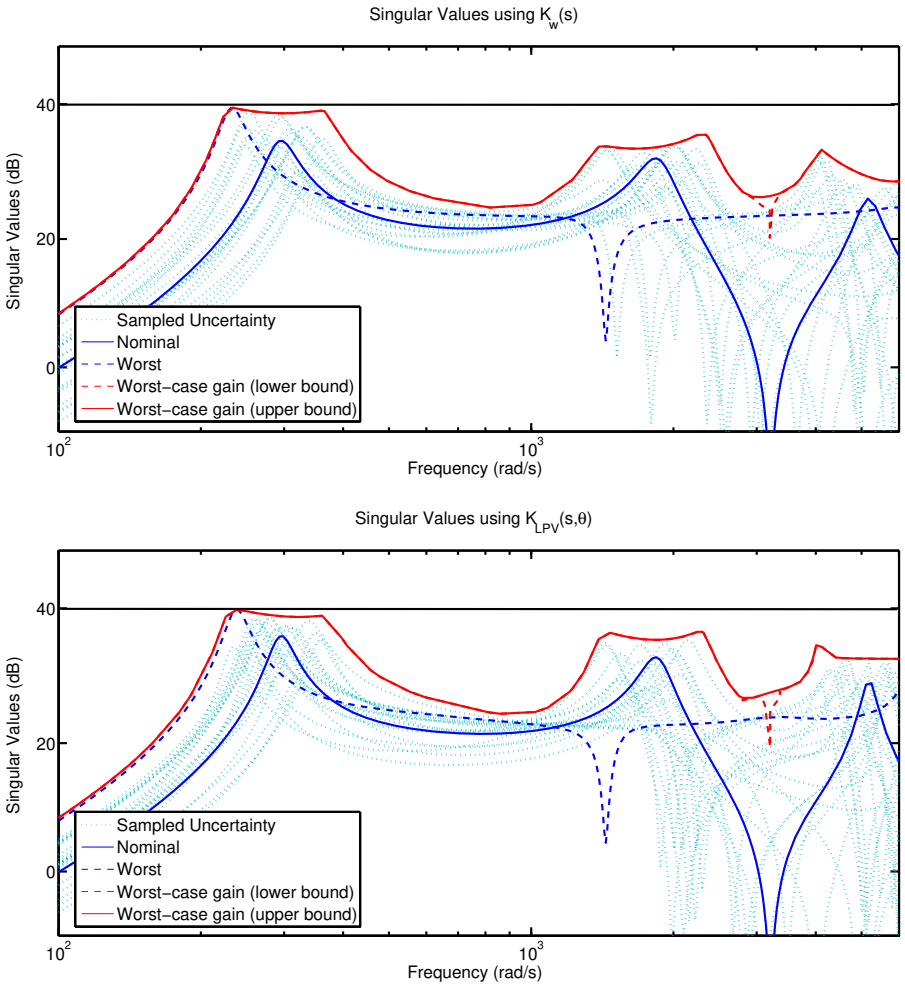

Figure 5.12: Deterministic worst-case performance analysis with $\Delta \in \Delta_1$

exist litter conservatism in the probabilistic stability analysis. These results also demonstrate that the k_{DRM} estimated from μ analysis is reliable. On the other hand, it shows that for Gaussian distributed ω_i, if a 10.0% loss of probabilistic robust stability is tolerated, the corresponding $k_{\mathrm{PRM}} = 1.75$ is increased by 71.6% with respect to its deterministic counterpart $k_{\mathrm{DRM}} = 1.02$ and increased by 9.37% with respect to the result for uniformly distributed ω_i. Probabilistic worst-case performance analysis is also performed, as summarized in Table 5.5. It shows that, with probability 99.0%, the specification of vibration reduction is fulfilled for all sampled $\Delta_1' \in 1.00\boldsymbol{B}_{\Delta_1'}$ with $K_w(s)$ and $K_{LPV}(s,\theta)$, and when

$\Delta_1' \in 1.20\boldsymbol{B}_{\Delta_1'}$, a few perturbations can be found to violate the specification of vibration reduction. This is consistent with the result from ν analysis.

Controller	Uniformly distributed ω_i	Gaussian distributed ω_i
$K_w(s)$	$\hat{p}_n(1.35) = 100\%$	$\hat{p}_n(1.35) = 100\%$
$K_w(s)$	$\hat{p}_n(1.60) = 90\%$	$\hat{p}_n(1.65) = 90.0\%$
$K_{LPV}(s,\theta)$	$\hat{p}_n(1.02) = 100\%$	$\hat{p}_n(1.02) = 100\%$
$K_{LPV}(s,\theta)$	$\hat{p}_n(1.60) = 90\%$	$\hat{p}_n(1.75) = 90\%$

Table 5.4: Probabilistic stability analysis: $\epsilon = 0.01, \delta = 0.01$

Controller	Uniformly distributed ω_i	Gaussian distributed ω_i
$K_w(s)$	$\bar{\lambda}_m(1.00) = 39.75\text{dB} < 40.00\text{dB}$ $\bar{\lambda}_m(1.20) = 40.60\text{dB} > 40.00\text{dB}$	$\bar{\lambda}_m(1.00) = 39.60\text{dB} < 40.00\text{dB}$ $\bar{\lambda}_m(1.20) = 39.99\text{dB} < 40.00\text{dB}$
$K_{LPV}(s,\theta)$	$\bar{\lambda}_m(1.00) = 39.96\text{dB} < 40.00\text{dB}$ $\bar{\lambda}_m(1.20) = 45.50\text{dB} > 40.00\text{dB}$	$\bar{\lambda}_m(1.00) = 39.85\text{dB} < 40.00\text{dB}$ $\bar{\lambda}_m(1.20) = 43.94\text{dB} > 40.00\text{dB}$

Table 5.5: Probabilistic worst-case performance analysis: $\epsilon = 0.001, \delta = 0.01$

Above robustness analyses demonstrate that, in the presence of assumed parametric and dynamic uncertainties including the time-varying force position $\theta \in [0.4, 0.8]$, both $K_w(s)$ and $K_{LPV}(s,\theta)$ can satisfy the specification of vibration reduction and provide attractive robustness properties of the closed-loop system.

5.4 Performance comparisons in the time domain

As above mentioned, the main motivation for the application of the proposed LPV control design is not only to design satisfying robust controllers for effective vibration reduction in the presence of parametric and dynamic uncertainties, but also to save the necessarily required control energy and reduce the control input. In fact, the specification of vibration reduction can be achieved with relatively simpler acceleration feedback control (AFC), for example, based on the worst-case disturbance dynamical model $G_{wd}(s)$, $K_{AFC}(s)$ can be designed for comparison

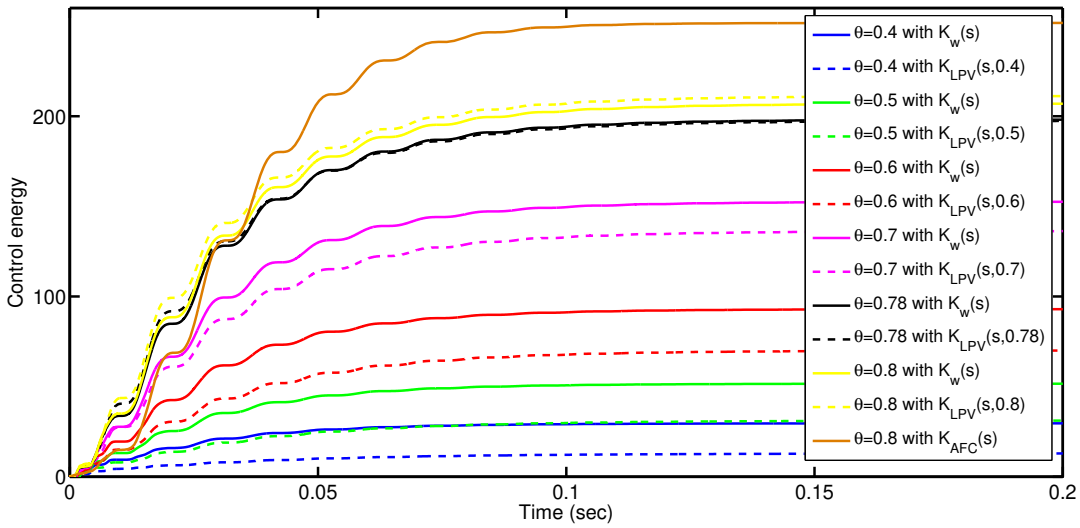

Figure 5.13: Comparisons of the control energy consumption using $K_w(s)$, $K_{AFC}(s)$ and $K_{LPV}(s,\theta)$

purpose with the cross-over point method (Bayon de Noyer and Hanagud, 1998a):

$$K_{AFC}(s) = \frac{-8.0\times10^7(s^2+2025.0s+1.1\times10^6)}{(s^2+165.3s+8.7\times10^4)(s^2+1080s+3.4\times10^6)}\times \frac{(s^2-926.1s+6.4\times10^5)}{(s^2+2020.0s+2.7\times10^7)}$$

As numerically verified, $K_{AFC}(s)$ can also satisfy the specification of vibration reduction as $K_w(s)$ and $K_{LPV}(s)$ do.

To emphasize the advantages of $K_{LPV}(s)$ in terms of the control energy and the control input, within MATLAB/Simulink R2012 environment, a unit step signal is used as the external force and several numerical simulations are evaluated in the time domain. As shown in Figure 5.13, compared to $K_{AFC}(s)$, less control energy is required by $K_w(s)$. As explained in Zhang et al. (2013a), this is mainly due to the fixed structure of AFC that makes $|K_{AFC}(j\omega)|$ too large at very low frequencies, where no control energy is actually required. Furthermore, as $G_d(s,\theta)$ depend on $\theta \in [0.4, 0.8]$, the required control energy to satisfy the fixed specification of vibration reduction greatly varies, and $K_{LPV}(s,\theta)$ has the ability to adapt its bandwidth to θ such that $K_{LPV}(s,\theta)$ consumes less con-

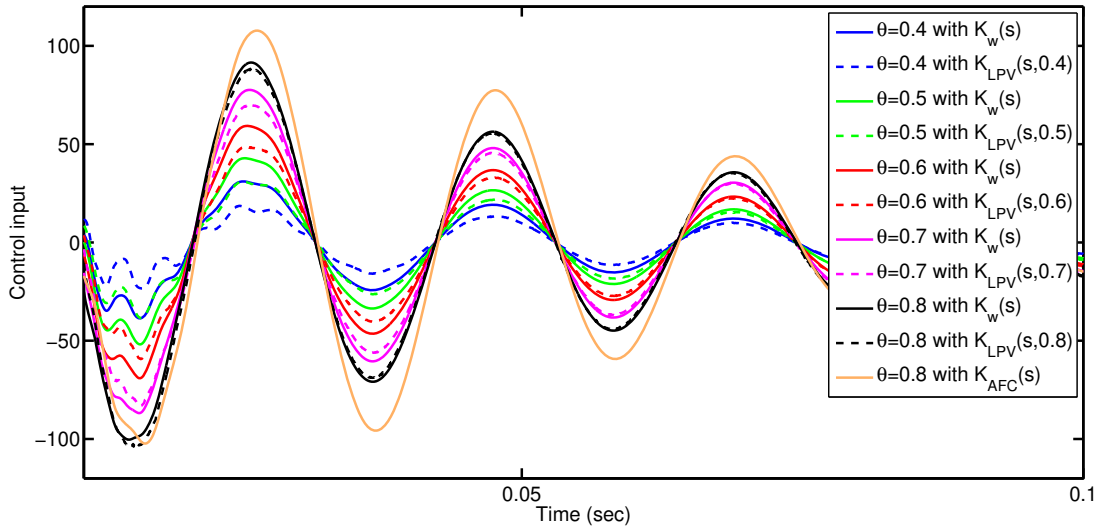

Figure 5.14: Comparisons of the control input using $K_w(s)$, $K_{AFC}(s)$ and $K_{LPV}(s,\theta)$

trol energy than $K_w(s)$ does for any $\theta \in [0.4, 0.78]$ and $K_{AFC}(s)$ does for any $\theta \in [0.4, 0.8]$. The fact that $K_{LPV}(s,\theta)$ can save the control energy is beneficial in avoiding the insufficient phenomenon of the control energy and desirable for practical implementation. On the other hand, as shown in Figure 5.14, for any $\theta \in [0.4, 0.8]$, the required control input using $K_{LPV}(s,\theta)$ is smaller than that using $K_w(s)$ or $K_{AFC}(s)$. This is useful to avoid exceeding the control saturation and the actuator operated voltage. It is also notable that $K_{LPV}(s,\theta)$, $K_w(s)$ and $K_{AFC}(s)$ can achieve not only the same specification of vibration reduction in the frequency domain but also the system output in the time domain, as illustrated in Figure 5.15 where the cases with $\theta = 0.4, 0.8$ are used for the sake of simplicity.

5.5 Summary

This chapter builds off of our previous researches on the quantitative robust control method for LTI systems using classical H_∞ control designs and reliable robustness analyses, and focuses on reducing the required control energy and the control input using efficient LPV control technique. With this proposed control

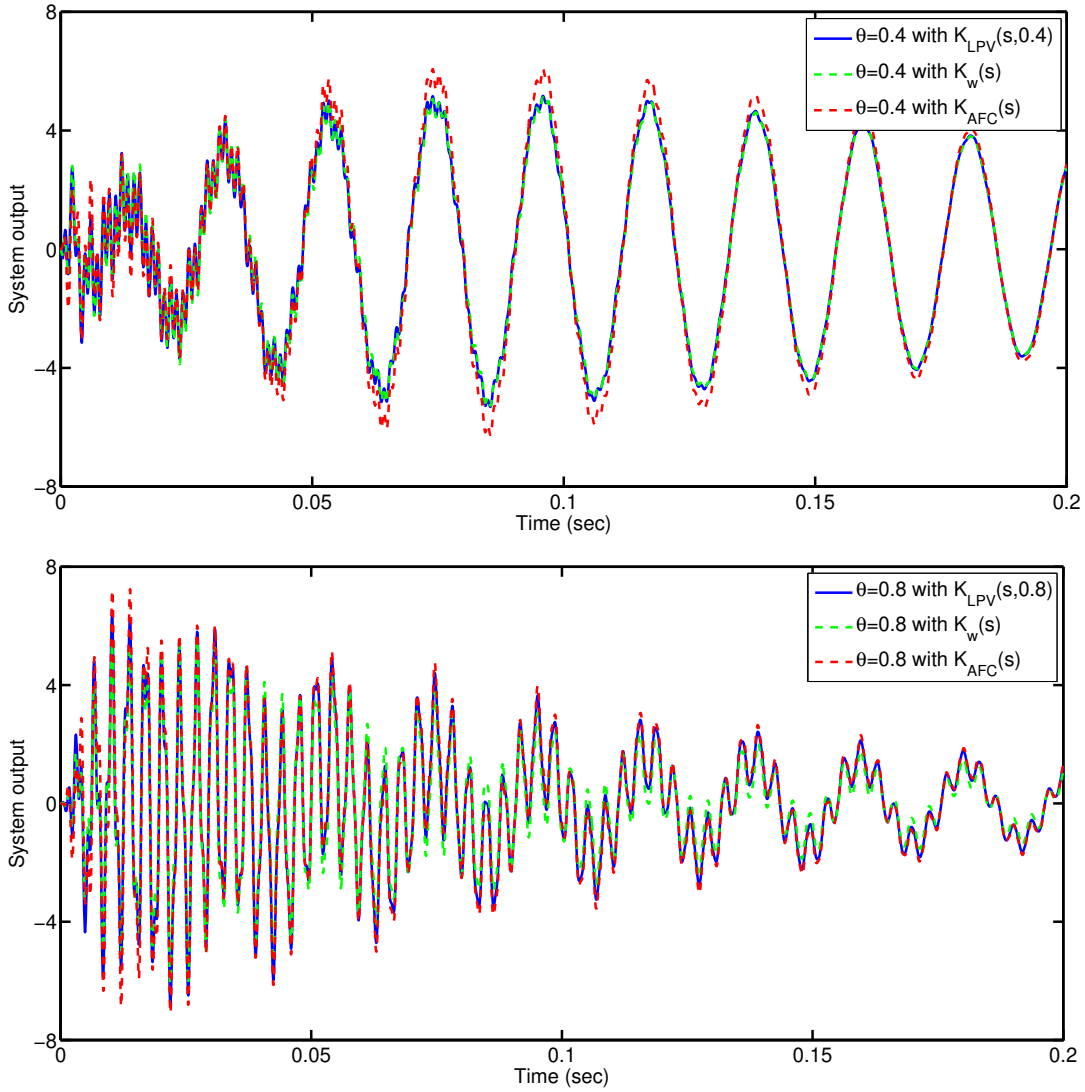

Figure 5.15: Comparisons of the system output using $K_w(s)$, $K_{AFC}(s)$ and $K_{LPV}(s,\theta)$ with $\theta = 0.4, 0.8$

method, the varying parameters of the LPV system represented by θ can be fully investigated and the trade-off among various control objectives, *e.g.* the specification of vibration reduction and the required control energy, can be achieved by systematical adjustments of the weighting functions which could also depend on θ. Compared to AFC and the classical H_∞ control, the proposed control method can explicitly reduce the required control energy and, in some extend, the con-

trol input, while maintaining almost the same control performances both in the frequency and time domains.

In this chapter, some parameter independent Lyapunov functions are used for the synthesis of $K_{LPV}(s,\theta)$. It provides a satisfactory LPV controller for the investigated case. If, in the applications under consideration, the employed parameter independent approach appears to be very conservative, parameter dependent LMI formulations can be used for the synthesis of $K_{LPV}(s,\theta)$, which is expected to be less conservative. The details of the approach can be found in Dinh et al. (2005); Dinh (2005). However, this requires much more computational effort and thus large scale industrial problems cannot be considered. Besides, the complexity of the correspondingly designed LPV controller has considerable complexity on θ and this is not available for its real-time implementation (Dinh, 2005; Scorletti and Fromion, 2008b).

Chapter 6

Conclusions and future research

By way of conclusion, the main contributions of this thesis are summarized and suggestions for possible future research are outlined.

6.1 Conclusions of the research

In this research, considering the inevitable parametric and dynamic uncertainties involved in the system modeling, a quantitative robust control methodology for active vibration control of flexible structures is proposed to consider the complete set of control objectives, *i.e.* the quantitative specification of vibration reduction, the moderate control energy and the robustness properties of the closed-loop system. To achieve this goal, firstly a positive frequency-dependent function is used to define the specification of vibration reduction and phase and gain control policies are proposed to impose frequency-dependent requirements on the phase and the magnitude of the controller. These control policies can then be employed in the dynamic output feedback H_∞ control designs to develop a qualitative robust control methodology for both LTI and LPV systems. This control methodology is general and can be used for both SISO and MIMO systems with collocated or non-collocated sensors and actuators. With this control methodology, the trade-off among various control objectives can be systematically achieved and the specification of vibration is quantitatively ensured for the nominal dynamical models, however, the robustness properties are not quantitatively a priori ensured.

Therefore, deterministic and probabilistic robustness analysis is performed in this research to provide reliable and comprehensive quantitative robustness properties, and extends the qualitative robust control methodology to the quantitative one. Specifically, to obtain the probabilistic information of parametric uncertainties and to directly consider the uncertainties on structural properties in the robustness analysis, the generalized polynomial chaos (gPC) framework is used for the uncertainty quantification using the finite element analysis. It is also proved that for some LPV systems, compared to classical H_∞ controller, the LPV H_∞ controller depending on the varying parameter can reduce the required control energy and, in some extend, the magnitude of the control signal, while maintaining almost the same control performances both in the frequency domain and the time domain. It is clear that, the proposed quantitatively robust control methodology is developed by building a bridge among several techniques from mechanical engineering and automatical control to make full advantages of these techniques and reduce the gap between them.

It must be emphasized that the proposed control methodology does not expect to replace either probabilistic control approaches or other robust control techniques which have been proposed in literature, but offers an additional straightforward and effective method to engineers in the field of robust vibration control of flexible structures.

6.2 Future research

In the future research, in addition to considering the neglected high frequency dynamics with a dynamic uncertainty, the normally neglected dynamics of sensors and actuators can also be considered in robustness analyses. The gPC framework can be used to consider more sources of structural uncertainties not only on the flexible structures but also on the actuators or sensors, for example, to investigate the effects of the placement and sizing of the piezoelectric actuators and sensors on the plant and disturbance dynamical models. This could be useful in the optimization of the placement and sizing of the piezoelectric actuators and sensors using the closed-loop robustness properties as criterion.

Although the motivation of this research is strongly influenced by application

to quantitative robust active vibration control of flexible structures, it is important to appreciate that most of the design processes and employed techniques are general and can be applied to any structural control problems. In the following research, with few modifications, this control methodology will be available in active control of more complicated flexible structures (Jemai et al., 1999), active suspensions to adapt road conditions (Fialho and Balas, 2002), active noise control (Jemai et al., 2002) and so on, where several actuators and sensors can be used.

In fact, many practical control problems involve the systems whose dynamics depend on some measurable exogenous parameters. For example, many vibration control systems are required to function across a variety of different temperatures, however, the variation of ambient temperature can change the structural natural frequencies and piezoelectric stress and permittivity coefficients, thus the applied control effort has to consider such temperature dependence (Hegewald and Inman, 2001; Gupta et al., 2012; Chettah et al., 2009). This kind of control problem is readily to be handled with the proposed quantitative robust LPV control method which considers the varying temperature as the scheduled variable. On the other hand, since the LPV control is firstly proposed for nonlinear systems (Rugh and Shamma, 2000; Carter, 1998), the proposed control method can also be used for active vibration control of nonlinear systems to consider the nonlinear friction effects and so on, *e.g.* Olsso (1996); Hirschorn and Miller (1999); Zhou et al. (2006); Ho et al. (2013).

For more convenient application of the proposed control methodology, a friendly graphical user interface (GUI) is desirable to incorporate related techniques in a systematical and uniform way, *e.g.* the system modeling, the uncertainty quantification, the determination of control objectives, the selection of weighting functions, and various robustness analysis. This GUI could be useful for the engineers who do not have enough both mechanical and automatic knowledge to use the general control methodology for their different purposes.

Motivated by the work of Dong et al. (2013), the performance evaluation of the designed H_∞ controllers could also been conducted in a closed-loop finite element (FE) environment such as COMSOL for general piezoelectric smart structures. For this purpose, the H_∞ controllers which are designed based on the

reduced-order models are incorporated into the FE models which can be regarded as a realistic full model of the smart structures. This allows us to explicitly consider the uncertainties on structural properties, the varying external load or the temperature dependence in the FE environment, thus directly illustrating the robustness properties of the closed-loop system in the FE environment.

Appendix A

H_∞ controller synthesis

To solve the suboptimal H_∞ control problem, the augmented plant $P(s)$ is represented in the state-space form,

$$\begin{aligned} \dot{x}(t) &= Ax(t) + B_w w(t) + B_u u(t) \\ z(t) &= C_z x(t) + D_{zw} w(t) + D_{zu} u(t) \\ v(t) &= C_v x(t) + D_{vw} w(t) + D_{vu} u(t) \end{aligned} \tag{A.1}$$

Correspondingly, $P(s)$ can be defined as

$$P(s) = C(s\mathrm{I} - A)^{-1}B + D \tag{A.2}$$

where $B = [B_1 \ B_2]$, $C = \begin{bmatrix} C_z \\ C_v \end{bmatrix}$, $D = \begin{bmatrix} D_{zw} & D_{zu} \\ D_{vw} & D_{vu} \end{bmatrix}$. The set of matrices $(A,\ B,\ C,\ D)$ is referred to as a state-space realization of $N(s)$ and $x(t)$ is the augmented plant state vector corresponding to this realization. With the state-space realization, we have the customary notation of $P(s)$ as

$$P(s) = \left[\begin{array}{c|cc} A & B_w & B_u \\ \hline C_z & D_{zw} & D_{zu} \\ C_v & D_{vw} & D_{vu} \end{array}\right] \tag{A.3}$$

As $u(s) = K(s)v(s)$, in the time domain $K(s)$ takes the typical state-space form of linear time invariant (LTI) systems,

$$\begin{aligned} \dot{x}_K(t) &= A_K x_K(t) + B_K v(t) \\ u(t) &= C_K x_K(t) + D_K v(t) \end{aligned} \tag{A.4}$$

where the set of matrices $(A_K,\ B_K,\ C_K,\ D_K)$ is referred to as a state-space realization of $K(s)$ and $x_K(t)$ is the controller state vector corresponding to this realization. The controller can be denoted as

$$K(s) = \left[\begin{array}{c|c} A_K & B_K \\ \hline C_K & D_K \end{array}\right] \tag{A.5}$$

It is notable that the set of matrices $(A_K,\ B_K,\ C_K,\ D_K)$ satisfying the input-output properties of $K(s)$ is not unique. Therefore, solving the suboptimal controller synthesis problem translates to find one set of matrices $A_K,\ B_K,\ C_K,\ D_K$.

The following solution to the H_∞ controller $K(s)$ is mainly adapted from Zhou et al. (1996). There exist four assumptions for the augmented plant $P(s)$, that is,

1. $(A,\ B_u)$ is stabilizing and $(C_v,\ A)$ is detectable: this guarantees the existence of the stabilizing controllers, that is, $T_{zw}(s) \in \mathcal{RH}_\infty$.

2. D_{zu} and D_{vw} are full rank: this ensures the inclusion of nonsingular weighting functions and that w contains d and n with nonsingular weighting functions.

3. $\begin{bmatrix} A - j\omega \mathrm{I} & B_u \\ C_z & D_{zu} \end{bmatrix}$ has full column rank for all ω: this guarantees $P_{zu}(s)$ has no zero at imaginary axis.

4. $\begin{bmatrix} A - j\omega \mathrm{I} & B_w \\ C_v & D_{vw} \end{bmatrix}$ has full row rank for all ω: this guarantees $P_{vw}(s)$ has no zero at imaginary axis.

As interpreted in Smith (2006), the assumptions 2. and 3. ensure there is no frequency at which any of the output signals is not influenced by $K(s)$, while the

assumptions 2. and 4. ensure that the effects of the disturbance can be measured by $K(s)$ at any frequency. These four assumptions are imperative. For the sake of simplicity, some supplementary assumptions are used, that is,

$$D_{zw} = 0,\ D_{vu} = 0,\ D_{zu}^T \left[\begin{array}{cc} C_z & D_{zu} \end{array}\right] = \left[\begin{array}{cc} 0 & \mathrm{I} \end{array}\right],\ \left[\begin{array}{c} B_w \\ D_{vw} \end{array}\right] D_{vw}^T = \left[\begin{array}{c} 0 \\ \mathrm{I} \end{array}\right]$$

Based on these assumptions, we have the following necessary and sufficient conditions for the existence of an admissible controller $K(s)$ such that $||T_{zw}(s)||_\infty < \gamma$ for a given γ:

1. The Hamiltonian matrices $\left[\begin{array}{cc} A & \gamma^{-2}B_wB_w^T - B_uB_u^T \\ -C_z^TC_z & -A^T \end{array}\right]$ has no eigenvalue on the imaginary axis and there exists a symmetric matrix $X_\infty > 0$ such that

$$X_\infty A + A^T X_\infty + X_\infty(\gamma^{-2}B_wB_w^T - B_uB_u^T)X_\infty + C_z^TC_z = 0$$

2. The Hamiltonian matrices $\left[\begin{array}{cc} A^T & \gamma^{-2}C_z^TC_z^T - C_v^TC_v \\ -B_wB_w^T & -A \end{array}\right]$ has no eigenvalue on the imaginary axis and there exists a symmetric matrix $Y_\infty > 0$ such that

$$Y_\infty A^T + AY_\infty + Y_\infty(\gamma^{-2}C_z^TC_z^T - C_v^TC_v)Y_\infty + B_wB_w^T = 0$$

3. $\rho(X_\infty Y_\infty) < \gamma^2$ where $\rho(\cdot)$ represents the spectral radius.

Moreover, when these conditions hold, the set of $K(s)$ for the suboptimal H_∞ control problem is $K(s) = \mathcal{F}_l(K_a(s), \Phi(s))$, where $\Phi(s)$ is a stable transfer function with $||\Phi(s)||_\infty < \gamma$ and

$$K_a(s) = \left[\begin{array}{c|cc} \hat{A}_\infty & -Z_\infty L_\infty & Z_\infty B_u \\ \hline F_\infty & 0 & \mathrm{I} \\ -C_v & \mathrm{I} & 0 \end{array}\right]$$

where

$$\begin{aligned}
\hat{A}_\infty &= A + \gamma^{-2} B_w B_w^T X_\infty + B_u F_\infty + Z_\infty L_\infty C_v \\
F_\infty &= -B_u^T X_\infty \\
L_\infty &= -Y_\infty C_v^T \\
Z_\infty &= (\mathrm{I} - \gamma^{-2} X_\infty Y_\infty)^{-1}
\end{aligned}$$

With $\Phi(s) = 0$, we have a specifical central $K(s)$, that is,

$$K_0(s) = \left[\begin{array}{c|c} \hat{A}_\infty & -Z_\infty L_\infty \\ \hline F_\infty & 0 \end{array}\right]$$

With Matlab Robust toolbox R2012, a suboptimal H_∞ controller $K(s)$ can be solved with the function 'hinfsyn' such that $\gamma_{opt} < ||T_{zw}(s)||_\infty < \gamma$. The value of γ_{opt} can thus be calculated by dichotomy.

Based on above discussion, we can summarize the steps that should be taken when designing the H_∞ controller design:

Step 1: Perform a system modeling to obtain the general plant $N(s)$ as discussed in Section 2.2.1. Since the flexible structures have an infinite number of resonant modes, a truncated model is practically used to retain the resonant modes of interest.

Step 2: According to the set of control objectives, define the regulated variables and incorporate necessary and suitable weighting functions in $N(s)$ to construct the augmented plant $P(s)$ as discussed in Section 2.2.2.

Step 3: Synthesize the H_∞ controller

1. verify that the assumptions are satisfied;
2. choose a value of γ and solve corresponding X_∞ and Y_∞;
3. check that $\rho(X_\infty Y_\infty) < \gamma^2$;
4. calculate $K_a(s)$ and $\Phi(s)$ and have $K(s) = \mathcal{F}_l(K_a(s), \Phi(s))$;
5. decrease γ and return to 2 until the desired value of γ is obtained.

Step 4: With the designed $K(s)$, the robustness analysis is required to verify the robustness properties of the closed-loop system.

The first step can be accomplished by a variety of structural modeling methods such as the analytical formulation, FEM and the system identification, which are all used in our research. The second step is critical in the controller design. The set of control objectives have to consider not only the vibration reduction for the controlled resonant modes but also other control objectives, *e.g.* moderate control energy, the stability robustness to parametric and dynamic uncertainties. The determination of the weighting functions is discussed in detail in Chapter 3. With the weighting functions, building the augmented plant is relatively simple with Matlab Toolbox or using linear fraction representation (LFR) such as the enhanced LFR-toolbox (Hecker et al., 2005). The processes for the controller synthesis are grouped in the fourth step. Actually, the whole process can be automatically implemented with the efficient algorithms. Once the controller is available, in the presence of parametric and dynamic uncertainties the robustness analysis is required to verify if the closed-loop system is robustly stable and if it satisfies the control objectives in the worst case or from a practically point of view. The robustness analysis is briefly discussed in the following section. The failure in one of these tests requires a return to Step 2 and to repeat the design procedure. It is notable that in the controller design, a trade-off among various control objectives must be investigated. Besides, the property of the plant may also place the limitations on the achievable control objectives, that is, the input-output controllability of the plant as defined on page 163 of Skogestad and Postlethwaite (2005), which can only be affected by changing the plant itself, *e.g.* relocating the sensors and actuators, use more powerful actuator, change the control objectives and so on. This is beyond the scope of our research but has to be considered in practical controller design. Note that the H_∞ control problem can also be solved with the LMI techniques in Step 3 (Gahinet and Apkarian, 1994).

Appendix B

LPV control design using parameter independent Lyapunov functions

B.1 Employed LPV control technique

In this article, we use the LPV control method proposed in Scorletti and L. EI Ghaoui (1998), which models the augmented LPV plant $P_{au}(s,\theta)$ with LFR and uses parameter independent Lyapunov functions. By the scalings selection, this method allows us to make a trade-off between conservatism and computational complexity. With LFR, the $P_{au}(s,\theta)$ of Equation (5.4) can also be modeled as

$$\begin{bmatrix} \dot{x} \\ q \\ z \\ y \end{bmatrix} = \begin{bmatrix} M & M_u \\ M_y & 0 \end{bmatrix} \begin{bmatrix} x \\ p \\ w \\ u \end{bmatrix} \quad \text{and} \quad \begin{bmatrix} x \\ p \end{bmatrix} = \Delta \begin{bmatrix} \dot{x} \\ q \end{bmatrix}$$

where $\Delta = \mathbf{diag}\left(\int I_n,\ \mathbf{diag}(\theta_i(t)I_{n_i})\right)$. Furthermore, we can assume that $\theta_{\min i} \leq \theta_i \leq \theta_{\max i}$ and thus the set Θ can be defined as

$$\Theta = \{\theta, |\theta_i \in [\theta_{\min i}, \theta_{\max i}]\} \tag{B.1}$$

This approach for obtaining a design method is the transformation of the control problem in a finite dimensional (BMI) optimization problem. To this end, let us introduce the following matrices

$$\mathcal{P}_M = \begin{bmatrix} I_n & 0 & 0 & 0 \\ 0 & 0 & I_n & 0 \\ 0 & I_{n_z} & 0 & 0 \\ 0 & 0 & 0 & I_{n_w} \end{bmatrix},\ \mathcal{P}_N = \begin{bmatrix} I_n & 0 & 0 & 0 \\ 0 & 0 & I_n & 0 \\ 0 & I_{n_w} & 0 & 0 \\ 0 & 0 & 0 & I_{n_z} \end{bmatrix}$$

$$\begin{aligned} X &= \mathbf{diag}(0_n, \mathbf{diag}(-2I_n)) \\ Y &= \mathbf{diag}(I_n, \mathbf{diag}((\theta_{\min i} + \theta_{\max i})I_{n_i})) \\ Z &= \mathbf{diag}(0_n, \mathbf{diag}(-2\theta_{\min i}\theta_{\max i}I_{n_i})) \end{aligned}$$

$$\begin{bmatrix} X & Y \\ Y^T & Z \end{bmatrix} \begin{bmatrix} -\tilde{Z} & \tilde{Y}^T \\ \tilde{Y} & -\tilde{X} \end{bmatrix} = I \text{ and } \begin{bmatrix} X_{perf} & Y_{perf} \\ Y_{perf}^T & Z_{perf} \end{bmatrix} \begin{bmatrix} -\tilde{Z}_{perf} & \tilde{Y}_{perf}^T \\ \tilde{Y}_{perf} & -\tilde{X}_{perf} \end{bmatrix} = I$$

with $X_{perf} = -I,\ Y_{perf} = 0$ and $Z_{perf} = \gamma^2 I$.

Theorem B.1.1. *If there exist matrices S, T, G and H such that*

$$M_y^{\perp^T} \begin{bmatrix} M \\ I_{(n+n_w)} \end{bmatrix}^T \mathcal{M} \begin{bmatrix} M \\ I_{(n+n_w)} \end{bmatrix} M_y^{\perp} < 0 \tag{B.2}$$

$$M_u^{T^{\perp^T}} \begin{bmatrix} M^T \\ I_{(n+n_z)} \end{bmatrix}^T \mathcal{N} \begin{bmatrix} M^T \\ I_{(n+n_z)} \end{bmatrix} M_u^{T^{\perp}} < 0 \tag{B.3}$$

where the matrices $\mathcal{M}$ *and* $\mathcal{N}$ *are defined as follows:*

$$\begin{aligned}\mathcal{M} &= \mathcal{P}_M^T \mathbf{diag}\left(\begin{bmatrix} ZS & Y^TS+G \\ YS+G^T & XS \end{bmatrix}, -\begin{bmatrix} X_{perf} & Y_{perf} \\ Y_{perf}^T & Z_{perf} \end{bmatrix}\right)\mathcal{P}_M \\ \mathcal{N} &= \mathcal{P}_N^T \mathbf{diag}\left(\begin{bmatrix} \tilde{Z}T & \tilde{Y}^TT+H \\ \tilde{Y}T+H^T & \tilde{X}T \end{bmatrix}, -\begin{bmatrix} \tilde{X}_{perf} & \tilde{Y}_{perf} \\ \tilde{Y}_{perf}^T & \tilde{Z}_{perf} \end{bmatrix}\right)\mathcal{P}_N\end{aligned}$$

where

$$\begin{aligned}S &= \mathbf{diag}(P, \mathbf{diag}(S_i)), \quad T = \mathbf{diag}(Q, \mathbf{diag}(T_i)) \\ G &= \mathbf{diag}(0_n, \mathbf{diag}(G_i)), \quad S = \mathbf{diag}(0_n, \mathbf{diag}(H_i))\end{aligned}$$

with the $n \times n$ *matrices* P *and* Q*, with the* $n_i \times n_i$ *matrices* $S_i = S_i^T$*,* $T_i = T_i^T$*,* $G_i = -G_i^T$*,* $H_i = -H_i^T$ *are such that*

$$\begin{bmatrix} S_i & I \\ I & T_i \end{bmatrix} > 0$$

and

$$\begin{bmatrix} P & I \\ I & Q \end{bmatrix} > 0$$

then there exist an LPV controller such that the closed-loop system is internally stable with an $\mathcal{L}_2$ *gain less than* γ*.*

This theorem actually presents a set of LMI constraints: first, a given γ is used to test the conditions of the previous theorem; then, the smallest γ is searched to satisfy the conditions of the theorem. If theses conditions can be satisfied, the matrices of the LFR representation of $K_{LPV}(s, \theta)$ can be using a feasibility optimization problem. Explicit formulations of this optimization problem can be found in Scorletti and L. EI Ghaoui (1998).

B.2 LFR realization of the designed $K_{LPV}(s,\theta)$

As illustrated with the Figure B.1, the input-output realization of the designed $K_{LPV}(s,\theta)$ is $y = \mathcal{F}_u(M,\Delta)u$ with $\Delta = \text{diag}(I_8/s, I_3\theta)$, where $\mathcal{F}_u$ is the upper LFT, the matrix M is defined on the page 19 of J-F. Magni (2006) and can be appropriately partitioned according to the order of the controller and the size of θ, *e.g.* 8 is equal to the order of $P_{au}(s,\theta)$ and 3 is the sum of $m = 2$ and $l = 1$.

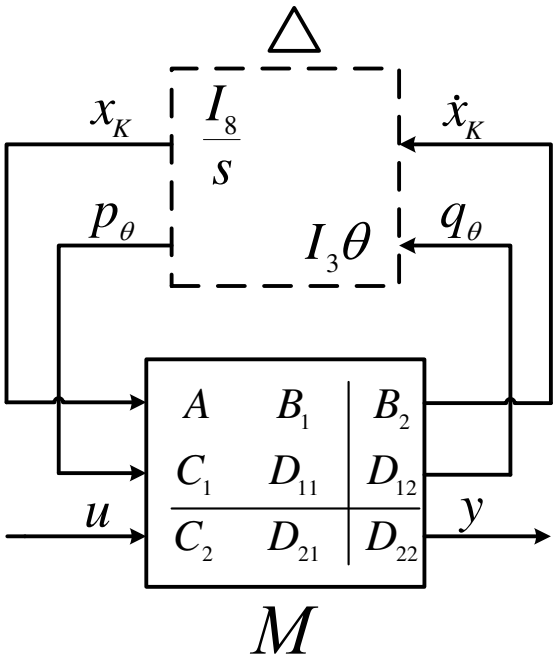

Figure B.1: LFR realization of $K_{LPV}(s,\theta)$

By directly closing the θ loop of Figure B.1, the matrices defined in Equation (5.5) are obtained, that is,

$$\begin{aligned}
A_K(\theta(t)) &= A + B_1 I_3\theta(t)(I - D_{11}I_3\theta(t))^{-1}C_1 \\
B_K(\theta(t)) &= B_2 + B_1 I_3\theta(t)(I - D_{11}I_3\theta(t))^{-1}D_{12} \\
C_K(\theta(t)) &= C_2 + D_{21} I_3\theta(t)(I - D_{11}I_3\theta(t))^{-1}C_1 \\
D_K(\theta(t)) &= D_{22} + D_{21} I_3\theta(t)(I - D_{11}I_3\theta(t))^{-1}D_{12}
\end{aligned}$$

Note that from the lemma 3.2.1 in J-F. Magni (2006), it is known that the input-

output LFR realization of $K_{LPV}(s,\theta)$, that is,

$$y = \mathcal{F}_u\left(\begin{bmatrix} A & B_1 & B_2 \\ C_1 & D_{11} & D_{12} \\ C_2 & D_{21} & D_{22} \end{bmatrix}, \begin{bmatrix} \frac{I_8}{s} & 0 \\ 0 & I_3\theta \end{bmatrix}\right) u$$

can also be realized by the equivalent state-space LFR

$$\begin{bmatrix} \dot{x}_K \\ y \end{bmatrix} = \mathcal{F}_u\left(\begin{bmatrix} D_{11} & C_1 & D_{12} \\ B_1 & A & B_2 \\ D_{21} & C_2 & D_{22} \end{bmatrix}, I_3\theta\right) \begin{bmatrix} x_K \\ u \end{bmatrix}$$

This transformation reduces the complexity of θ in $K_{LPV}(s,\theta)$, since θ is not repeated in $A_K(\theta(t)), B(\theta(t)), C(\theta(t))$ and $D(\theta(t))$ but occurs only once. With this realization, the related matrices are listed as below:

$$A = \begin{bmatrix} -4.5301 & -2612.1 & -131.06 & 193.44 & 98.995 & 47.589 & -41.269 & -8.4422 \\ 2640.2 & -37395 & 77398 & -116221 & -59215 & -27983 & 23891 & 5416.7 \\ -80.853 & 468.79 & -4075.4 & -9911.2 & -1816.2 & 2061.2 & -1600.5 & 1170.1 \\ -129.76 & 1293.5 & 5756.9 & -11144 & -4433.0 & 511.88 & -1975.4 & 2172.6 \\ 249.50 & -1779.2 & -1149.4 & 16932 & 6095.2 & 1643.2 & 3384.2 & -3267.4 \\ -328.35 & 2874.3 & 5640.6 & -28393 & -13090 & -829.59 & -4561.9 & 5234.0 \\ -1097.0 & 8725.4 & 7915.2 & -91020 & -36269 & 1798.3 & -16248 & 17843 \\ 278.66 & -2243.3 & -2280.2 & 25220.3 & 10344 & -619.34 & 4012.3 & -4840.8 \end{bmatrix}$$

$$B_1 = \begin{bmatrix} -0.09651 & 8.9632 & -10.206 \\ 55.657 & -4844.1 & 5680.0 \\ -1.5235 & 414.87 & 11.311 \\ -5.9535 & 2440.4 & -2100.0 \\ 8.8184 & -3867.4 & 3229.1 \\ -15.140 & 5572.3 & -4309.4 \\ -45.7728 & 17186 & -12987 \\ 12.308 & -4306.7 & 3159.4 \end{bmatrix}, \quad B_2 = \begin{bmatrix} -0.2321 \\ 148.51 \\ 41.497 \\ 58.073 \\ -85.43 \\ 132.77 \\ 467.92 \\ -130.58 \end{bmatrix}$$

B.2 LFR realization of the designed $K_{LPV}(s,\theta)$

$$
C_1 = \begin{bmatrix} -0.4918 & -286.57 & -14.425 & 21.660 & 11.036 & 5.2154 & -4.4528 & -1.0095 \\ 0.0076 & -0.0904 & 2.5651 & -2.8923 & -1.9579 & -0.9170 & 0.3092 & 0.6601 \\ 0.0070 & -0.1192 & 2.3009 & -2.6212 & -1.6963 & -0.7777 & 0.2801 & 0.5827 \end{bmatrix}
$$

$$
D_{11} = \begin{bmatrix} 1.5864 \times 10^{-2} & 9.0284 \times 10^{-1} & -1.0586 \\ -1.7395 \times 10^{-3} & 2.4222 \times 10^{-1} & -4.7265 \times 10^{-1} \\ -1.4990 \times 10^{-3} & 5.7731 \times 10^{-1} & -7.4509 \times 10^{-1} \end{bmatrix}, \; D_{12} = \begin{bmatrix} -0.0276 \\ 0.0079 \\ 0.0069 \end{bmatrix}
$$

$$
C_2 = \begin{bmatrix} 0.8770 & 511.01 & 25.722 & -38.625 & -19.679 & -9.3001 & 7.9401 & 1.8002 \end{bmatrix}
$$

$$
D_{21} = \begin{bmatrix} -1.0393 & -1.6099 & 1.8877 \end{bmatrix}, \; D_{22} = 0.04935
$$

Appendix C

Publications during the thesis

C.1 Journal papers

- Zhang, K., Scorletti, G., Ichchou, M., Mieyeville, F. Phase and gain control policies for robust active vibration control of flexible structures using smart materials. *Smart Materials and Structures* 22 (2013) 075025 (15 pages) doi:10.1088/0964-1726/22/7/075025.

- Zhang, K., Scorletti, G., Ichchou, M., Mieyeville, F. Robust active vibration control of piezoelectric flexible structures using deterministic and probabilistic analysis. *Journal of Intelligent Material Systems and Structures*(2013). doi:10.1177/1045389X13500574.

- Zhang, K., Scorletti, G., Ichchou, M., Mieyeville, F. Quantitative robust LPV H_∞ vibration control of flexible structures for saving the control energy. Under review *Journal of Intelligent Material Systems and Structures*.

C.2 Refereed conference papers

- Zhang, K., Ichchou, M., Scorletti, G., Mieyeville, F. H_∞ control of flexible structures using a non-collocated piezoelectric actuator and accelerometer.

In *1st International Conference on Composites Structures Dynamics (DYNACOMP)*, Arcachon, France, May 22-24, 2012.

- Zhang, K., Ichchou, M., Scorletti, G., Mieyeville, F. Robust vibration control of flexible structures using smart materials with uncertainties. In *6th European Congress on Computational Methods in Applied Sciences and Engineering (ECCOMAS 2012)*, Vienna, Austria, September 10-14, 2012, Pages:75-92.

- Zhang, K., Ichchou, M., Scorletti, G., Mieyeville, F. Probabilistic robust active vibration control of piezoelectric flexible structures. In *1st Euro-Mediterranean Conference on Structural Dynamics and Vibroacoustics (MEDYNA)*, Marrakech, Morocco, April 23-25, 2013.

List of Figures

List of Figures

List of Tables

Bibliography

M.J. Balas. Feedback control of flexible systems. *IEEE Transactions on Automatic Control*, 23(4):673–679, 1978a. 2

M.J. Balas. Active control of flexible systems. *Journal of Optimization Theory and Applications*, 25(3):415–436, 1978b. 2

S.K. Choi, R.V. Grandhi, R.A. Canfield, and C.L. Pettit. Polynomial chaos expansion with latin hypercube sampling for estimating response variability. *AIAA Journal*, 42(6):1191–1198, 2004a. 2, 19, 95

W. Symens, H. Van Brussel, and J. Swevers. Gain-scheduling control of machine tools with varying structural flexibility. *CIRP Annals-Manufacturing Technology*, 53(1):321–324, 2004. 2

B. Paijmans, W. Symens, H. Van Brussel, and J. Swevers. A gain-scheduling-control technique for mechatronic systems with position-dependent dynamics. In *2006 American Control Conference*, 2006. 2, 122

B. Paijmans. *Interpolating Gain-Scheduling Control for Mechatronic Systems with Parameter-Dependent Dynamics*. PhD thesis, University of Leuven, 2007. 2, 115

T. Hegewald and D.J. Inman. Vibration suppression via smart structures across a temperature range. *Journal of Intelligent Material Systems and Structures*, 12(3):191–203, 2001. 3, 13, 71, 151

P. Shimon and Y. Hurmuzlu. A theoretical and experimental study of advanced control methods to suppress vibrations in a small square plate subject to tem-

perature variations. *Journal of Sound and Vibration*, 302(3):409–424, 2007. 3

V. Gupta, M. Sharma, and N. Thakur. Active structural vibration control: Robust to temperature variations. *Mechanical Systems and Signal Processing*, 33: 167–180, 2012. 3, 151

F. Li, Z. Xu, X.Y. Wei, and X. Yao. Determination of temperature dependence of piezoelectric coefficients matrix of lead zirconate titanate ceramics by quasi-static and resonance method. *Journal of Physics D: Applied Physics*, 42(9): 095417, 2009. 3

S. Hecker. *Generation of Low Order LFT Representations for Robust Control Applications*. PhD thesis, Technical University Munich, 2006. 3, 20, 32, 121

K. Umesh and R. Ganguli. Material uncertainty effect on vibration control of smart composite plate using polynomial chaos expansion. *Mechanics of Advanced Materials and Structures*, 20(7):580–591, 2013. doi: 10.1080/15376494.2011.643279. 3, 19

J.S. Liu. *Monte Carlo strategies in scientific computing*. Springer Verlag, London, 2008. 3, 91

R. Ghanem and P.D. Spanos. *Stochastic Finite Elements: A Spectral Approach*. Springer Verlag, London, New York, 1991. 3, 19

B.T. Polyak and R. Tempo. Probabilistic robust design with linear quadratic regulators. *Systems and Control Letters*, 43(5):343–353, 2001. 3

D. Xiu and G.E. Karniadakis. The wiener-askey polynomial chaos for stochastic differential equations. *SIAM Journal on Scientific Computing*, 24(2):619–644, 2002. 3, 19, 91, 94, 95, 170

S.K. Choi, R.V. Grandhi, and R.A. Canfield. Structural reliability under non-gaussian stochastic behavior. *Computers and structures*, 82(13):1113–1121, 2004b. 3

Bibliography

T.Y. Hou, W. Luo, B. Rozovskii, and H.M. Zhou. Wiener chaos expansions and numerical solutions of randomly forced equations of fluid mechanics. *Journal of Computational Physics*, 216(2):687–706, 2006. 3, 19

B.A. Templeton, M. Ahmadian, and S.C. Southward. Probabilistic control using H_2 control design and polynomial chaos: Experimental design, analysis, and results. *Probabilistic Engineering Mechanics*, 30:9–19, 2012. 3, 91

M. Athans. The role and use of the stochastic linear-quadratic-Gaussian problem in control system design. *IEEE Transactions on Automatic Control*, 16(6): 529–552, 1971. 4

G. Zames. Feedback and optimal sensitivity: model reference transformations, multiplicative seminorms, and approximate inverses. *IEEE Transactions on Automatic Control*, 26(2):301–320, 1981. 4, 13

K. Zhou, J. Doyle, and K. Glover. *Robust and Optimal Control*. Prentice, Hall Upper Saddle River, NJ, 1996. 4, 5, 20, 22, 23, 55, 59, 63, 92, 97, 98, 124, 126, 131, 154

K. Glover and J.C. Doyle. State-space formulae for all stabilizing controllers that satisfy an H_∞-norm bound and relations to risk sensitivity. *Systems and Control Letters*, 11(167–172), 1988. 4

A. Packard and J.C. Doyle. The complex structured singular value. *Automatica*, 29(1):71–109, 1993. 4, 28, 30, 31

S. Skogestad and I. Postlethwaite. *Multivariable Feedback Control-Analysis and Design*. John Wiley and Sons, 2005. 4, 7, 17, 27, 28, 55, 65, 92, 116, 118, 135, 141, 142, 157

V.L. Kharitonov. Asymptotic stability of an equilibrium position of a family of systems of linear differential equations. *Differentsial'nye Uravneniya*, 14: 2086–2088, 1978. 5

S.P. Bhattacharyya, H. Chapellat, and L.H. Keel. *Robust Control: The Parametric Approach*. Prentice, Hall Upper Saddle River, NJ, 1995. 5

Bibliography

G. Zames. On the input-output stability of time-varying nonlinear feedback systems part one: Conditions derived using concepts of loop gain, conicity, and positivity. *IEEE Transactions on Automatic Control*, 11(2):228–238, 1966. 5, 27

R. Tempo, G. Calafiore, and F. Dabbene. *Randomized Algorithms for Analysis and Control of Uncertain Systems*. Springer Verlag, London, 2005. 5, 34, 35

G.J. Balas and J.C. Doyle. Robustness and performance trade-offs in control design for flexible structures. *IEEE Transactions on Control Systems Technology*, 2(4):352–361, 1994. 5, 24, 106

H.K. Khalil. *Nonlinear Systems*. Prentice-Hall New Jersey, 2nd edition, 1996. 6, 59, 60

A. Lanzon and I.R. Petersen. Stability robustness of a feedback interconnection of systems with negative imaginary frequency response. *IEEE Transactions on Automatic Control*, 53(4):1042–1046, 2008. 6, 59, 60

C.J. Goh and W.Y. Yan. Approximate pole placement for acceleration feedback control of flexible structures. *Journal of Guidance, Control, and Dynamics*, 19 (1):256–259, 1996. 6, 13, 69

M.B. Bayon de Noyer and S.V. Hanagud. Single actuator and multi-mode acceleration feedback control. *Journal of Intelligent Material Systems and Structures*, 9(7):522–533, 1998a. 7, 62, 68, 70, 79, 119, 145

J.C. Doyle, K. Glover, P.P. Khargonekar, and B.A. Francis. State-space solutions to standard H_2 and H_∞ control problems. *IEEE Transactions on Automatic Control*, 34(8):831–847, 1989. 7, 14, 73

P. Gahinet and P. Apkarian. A linear matrix inequality approach to H_∞ control. *International Journal of Robust and Nonlinear Control*, 4:421–448, 1994. 7, 14, 157

W.P. Mason. Piezoelectricity, its history and applications. *Journal of the Acoustical Society of America*, 70(6):1561–1566, 1981. 11

Bibliography

A. Ballato. Piezoelectricity: history and new thrusts. In *IEEE Ultrasonics Symposium*, volume 1, pages 575–583, 1996. 11

S.O.R. Moheimani and A.J. Fleming. *Piezoelectric Transducers for Vibration Control and Damping*. Springer Verlag, London, 2006. 12, 75, 78, 101, 128, 129

Y. Wang and D.J. Inman. Comparison of control laws for vibration suppression based on energy consumption. *Journal of Intelligent Material Systems and Structures*, 22(8):795–809, 2011. 12, 117

R. H. Cannon and E. Schmitz. Initial experiments on the end-point control of a flexible robot. *International Journal of Robotics Research*, 3(3):62–75, 1984. 12

E. Garcia, J. Dosch, and D.J. Inman. The application of smart structures to the vibration suppression problem. *Journal of Intelligent Material Systems and Structures*, 3(4):659–667, 1992. 12

D.C. Dd, J.L. Junkins, and R.W. Longman. Active control technology for large space structures. *Journal of Guidance, Control, and Dynamics*, 16(5):801–821, 1993. 12

S.S. Han, S.B. Choi, and J.H. Kim. Position control of a flexible gantry robot arm using smart material actuators. *Journal of Robotic Systems*, 16(10):581–595, 1999a. 12

S. Wu, T.L. Turner, and S.A. Rizzi. Piezoelectric shunt vibration damping of an F-15 panel under high-acoustic excitation. In *SPIE on Smart Structures and Materials: Damping and Isolation*, pages 276–287, 2000. 12

M.O. Tokhi, Z. Mohamed, and M.H. Shaheed. Dynamic characterisation of a flexible manipulator system. *Robotica*, 19(5):571–580, 2001. 12

L. Vaillon and C. Philippe. Passive and active microvibration control for very high pointing accuracy space systems. *Smart materials and structures*, 8(6): 719–728, 1999. 12

Bibliography

S. Salapaka, A. Sebastian, J.P. Cleveland, and M.V. Salapaka. Design, identification and control of a fast nanopositioning device. In *2002 American Control Conference*, pages 1966–1971, 2002. 12

M. Benosman and G. Vey. Control of flexible manipulators: A survey. *Robotica*, 22(5):533–545, 2004. 12

J.H. Han, K.H. Rew, and I. Lee. An experimental study of active vibration control of composite structures with a piezo-ceramic actuator and a piezo-film sensor. *Smart Materials and Structures*, 6(5):549, 1999b. 12, 13

Z. Qiu, J. Han, X. Zhang, Y. Wang, and Z. Wu. Active vibration control of a flexible beam using a non-collocated acceleration sensor and piezoelectric patch actuator. *Journal of Sound and Vibration*, 326(3):438–455, 2009. 12, 13, 101, 104

E.F. Crawley and J. de Luis. Use of piezoelectric actuators as elements of intelligent structures. *AIAA Journal*, 25:1373–1385, 1987. 12

N.W. Hagood, W. Chung, and A. von Flotow. Modeling of piezoelectric dynamics for active structural control. *Journal of Intelligent Material Systems and Structures*, 1:327–354, 1990. 12

H.S. Tzou and C.I. Tseng. Distributed piezoelectric sensor/actuator design for dynamic measurement/control of distributed parameter systems: a piezoelectric finite element approach. *Journal of Sound and Vibration*, 138(1):17–34, 1990. 12

C.K. Lee. Theory of laminated piezoelectric plates for the design of distributed sensors/actuators. part i: Governing equations and reciprocal relationships. *The Journal of the Acoustical Society of America*, 87:1144–1158, 1990. 12

G.J. Balas and J.C. Doyle. Identification of flexible structures for robust control. *IEEE Control Systems Magazine*, 10(4):51–58, 1990. 12

A. Benjeddou. Advances in piezoelectric finite element modeling of adaptive structural elements: a survey. *Computers and Structures*, 76(1):347–363, 2000. 12

Bibliography

W. Chang, S.V Gopinathan, V.V. Varadan, and V.K. Varadan. Design of robust vibration controller for a smart panel using finite element model. *Journal of Vibration and Acoustics*, 124:265–276, 2002. 12, 14, 16

X.J. Dong, G. Meng, and J.C. Peng. Vibration control of piezoelectric smart structures based on system identification technique: Numerical simulation and experimental study. *Journal of Sound and Vibration*, 297:680–693, 2006. 12, 94

M.J. Balas. Trends in large space structure control theory: fondest hopes, wildest dreams. *IEEE Transactions on Automatic Control*, 27(3):522–535, 1982. 12

F. Juntao. Active vibration control of flexible steel cantilever beam using piezoelectric actuators. In *37th Southeastern Symposium on System Theory*, pages 35–39, 2005. 13

S.M. Khot, N.P. Yelve, R. Tomar, S. Desai, and S. Vittal. Active vibration control of cantilever beam by using PID based output feedback controller. *Journal of Vibration and Control*, 18(3):366–372, 2012. 13

M.J. Balas. Direct velocity feedback control of large space structures. *Journal of Guidance, Control, and Dynamics*, 2(3):252–253, 1979. 13, 59, 61, 62

S.Y. Wang, S.T. Quek, and K.K. Ang. Vibration control of smart piezoelectric composite plates. *Smart materials and Structures*, 10(4):637–644, 2001a. 13

Y. Aoki, P. Gardonio, and S.J. Elliott. Modelling of a piezoceramic patch actuator for velocity feedback control. *Smart Materials and Structures*, 17:015052, 2008. 13

J.L. Fanson and T.K. Caughey. Positive position feedback control for large space structures. *AIAA Journal*, 28(4):717–724, 1990. 13, 70

M.I. Friswell and D.J. Inman. The relationship between positive position feedback and output feedback controllers. *Smart Materials and Structures*, 8:285, 1999. 13

Bibliography

Z.C. Qiu, X.M. Zhang, H.X. Wu, and H.M. Zhang. Optimal placement and active vibration control for piezoelectric smart flexible cantilever plate. *Journal of Sound and Vibration*, 301(3):521–543, 2007. 13

T. Zhang and H.G. Li. Adaptive pole placement control for vibration control of a smart cantilevered beam in thermal environment. *Journal of Vibration and Control*, 19(10):1460–1470, 2013. doi: 10.1177/1077546312445596. 13

S.X. Xu and T.S. Koko. Finite element analysis and design of actively controlled piezoelectric smart structures. *Finite Elements in Analysis and Design*, 40(3): 241–262, 2004. 13

M.A. Trindade, A. Benjeddou, and R. Ohayon. Piezoelectric active vibration control of damped sandwich beams. *Journal of Sound and Vibration*, 246(4): 653–677, 2001. 13

P. Bhattacharya, H. Suhail, and P.K. Sinha. Finite element analysis and distributed control of laminated composite shells using LQR/IMSC approach. *Aerospace Science and Technology*, 6(4):273–281, 2002. 13

X.J. Dong, Z.K. Peng, L. Ye, H.X. Hua, and G. Meng. Performance evaluation of vibration controller for piezoelectric smart structures in finite element environment. *Journal of Vibration and Control*, 2013. 13, 151

T. Takawa, T. Fukuda, and K. Nakashima. Fuzzy control of vibration of a smart cfrp laminated beam. *Smart Materials and Structures*, 9(2), 2000. 13

Q.W. Zhong, S. Jincai, and Q. Yang. Active control of vibration using a fuzzy control method. *Journal of Sound and Vibration*, 275(3):917–930, 2004. 13

N.D. Zorić, M.S. Aleksandar, S.M. Zoran, and N.S. Slobodan. Optimal vibration control of smart composite beams with optimal size and location of piezoelectric sensing and actuation. *Journal of Intelligent Material Systems and Structures*, 24(4):499–526, 2013. 13

M.C. Pai and A. Sinha. Sliding mode output feedback control of vibration in a flexible structure. *Journal of Dynamic systems, Measurement and Control*, 129 (6):851–855, 2007. 13

Bibliography

B. Bandyopadhyay, T.C. Manjunath, and M. Umapathy. *Modeling, Control and Implementation of Smart Structures: A FEM-State Space Approach*. Springer Verlag, London, 2007. 13

L.G Wu and W.X. Zheng. Passivity-based sliding mode control of uncertain singular time-delay systems. *Automatica*, 45(9):2120 – 2127, 2009. 13

A.G. Wills, D. Bates, A.J. Fleming, B. Ninness, and S.O.R. Moheimani. Model predictive control applied to constraint handling in active noise and vibration control. *IEEE Transactions on Control Systems Technology*, 16(1):3–12, 2008. 13

G. Takács and B. Rohal-Ilkiv. *Model Predictive Vibration Control: Efficient Constrained MPC Vibration Control for Lightly Damped Mechanical Structures*. Springer Verlag, London, 2012. 13

M.T. Valoor, K. Chandrashekhara, and S. Agarwal. Self-adaptive vibration control of smart composite beams using recurrent neural architecture. *International journal of solids and structures*, 38(44):7857–7874, 2001. 13

K. Ma and M.N. Ghasemi-Nejhad. Adaptive simultaneous precision positioning and vibration control of intelligent composite structures. *Journal of Intelligent Material Systems and Structures*, 16(2):163–174, 2005. 13

R. Jha and J. Rower. Experimental investigation of active vibration control using neural networks and piezoelectric actuators. *Smart Materials and Structures*, 11(1), 2002. 13

R. Jha and C. He. Neural-network-based adaptive predictive control for vibration suppression of smart structures. *Smart Materials and Structures*, 11(6), 2002. 13

A. Baz, S. Poh, and J. Fedor. Independent modal space control with positive position feedback. *Journal of Dynamic Systems, Measurement, and Control*, 114:96–103, 1992. 13

H.R. Pota, S.O.R. Moheimani, and M. Smith. Resonant controllers for smart structures. *Smart Materials and Structures*, 11:1–8, 2002. 13, 61, 62

Bibliography

S.O.R. Moheimani and B.J.G. Vautier. Resonant control of structural vibration using charge-driven piezoelectric actuators. *IEEE Transactions on Control Systems Technology*, 13(6):1021–1035, 2005. 13, 61

S.S. Aphale, A.J. Fleming, and S.O.R. Moheimani. Integral resonant control of collocated smart structures. *Smart Materials and Structures*, 16(2):439, 2007. 13, 62

B. Boulet, B.A. Francis, P.C. Hughes, and T. Hong. μ synthesis for a large flexible space structure experimental testbed. *Journal of Guidance, Control, and Dynamics*, 24:967–977, 2001. 13

P. Li, L. Cheng, Y.Y Li, and N. Chen. Robust control of a vibrating plate using μ-synthesis approach. *Thin-walled structures*, 41(11):973–986, 2003. 13, 18

T. Li and Y. Ma. Robust vibration control of flexible tensegrity structure via μ synthesis. *Structural Control and Health Monitoring*, 20(2):53–66, 2013. 13

R.S. Smith, C.C. Chu, and J.L. Fanson. The design of H_∞ controllers for an experimental non-collocated flexible structure problem. *IEEE Transactions on Control Systems Technology*, 2(2):101–109, 1994. 13

K. Seto and I.N. Kar. A comparative study on H_∞ based vibration controller of a flexible structure system. In *2000 American Control Conference*, pages 513–518, 2000. 13, 14, 15

G. Barrault, D. Halim, and C. Hansen. High frequency spatial vibration control using H_∞ method. *Mechanical Systems and Signal processing*, 21(4):1541–1560, 2007. 13, 64, 66

L. Iorga, H. Baruh, and I. Ursu. A review of H_∞ robust control of piezoelectric smart structures. *Applied Mechanics Reviews*, 61(4):040802, 2008. 13

J.D. Caigny, J.F. Camino, R.C.L.F. Oliveira, P.L.D. Peres, and J. Swevers. A vibroacoustic application of modeling and control of linear parameter-varying systems. *Journal of the Brazilian Society of Mechanical Sciences and Engineering*, 32(4):409–419, 2010. 13, 115

Bibliography

C. Onat, M. Sahin, Y. Yaman, S. E. Prasad, and S. Nemana. Design of an LPV based fractional controller for the vibration. In *International Workshop Smart Materials, Structures & NDT in Aerospace Conference*, Canada, 2011. 13

J.L. Crassidis, A. Baz, and N. Wereley. H_∞ control of active constrained layer damping. *Journal of Vibration and Control*, 6(1):113, 2000. 14, 15, 16

X. Zhang, C. Shao, S. Li, D. Xu, and A.G. Erdman. Robust H_∞ vibration control for flexible linkage mechanism systems with piezoelectric sensors and actuators. *Journal of Sound and Vibration*, 243(1):145–155, 2001. 14, 15, 16, 118

J.J. Zhang, L.L. He, E.C. Wang, and R.Z. Gao. Active vibration control of flexible structures using piezoelectric materials. In *2009 International Conference on Advanced Computer Control (ICACC 2009)*, pages 540–545, 2009a. 14

F. Jabbari, W.E. Schmitendorf, and J.N. Yang. H_∞ control for seismic-excited buildings with acceleration feedback. *Journal of Engineering Mechanics*, 121 (9):994–1002, 1995. 14

J. Dosch, D. Leoand, and D.J. Inman. Modeling and control for vibration suppression of a flexible active structure. *Journal of Guidance, Control, and Dynamics*, 18(2):340–346, 1995. 14, 16

A.M. Sadri, R.J. Wynne, and J.R. Wright. Robust strategies for active vibration control of plate-like structures: theory and experiment. *Proceedings of the Institution of Mechanical Engineers, Part I: Journal of Systems and Control Engineering*, 213(6):489–504, 1999. 14, 16

I.N. Kar, T. Miyakura, and K. Seto. Bending and torsional vibration control of a flexible plate structure using H_∞-based robust control law. *IEEE Transactions on Control Systems Technology*, 8(3):545–553, 2000a. 14

T.X. Liu, H.X. Hua, and Z. Zhang. Robust control of plate vibration via active constrained layer damping. *Thin-Walled Structures*, 42(3):427–448, 2004. 14, 15

S.L. Xie, X.N. Zhang, J.H. Zhang, and L. Yu. H_∞ robust vibration control of a thin plate covered with a controllable constrained damping layer. *Journal of Vibration and Control*, 10(1):115–133, 2004. 14, 15, 16

J.J. Zhang, L.L. He, E.C. Wang, and R.Z. Gao. Robust active vibration control of flexible structures based on H_∞ control theorem. In *2009 International Workshop on Intelligent Systems and Applications (ISA 2009)*, pages 1–6, 2009b. 14

A. Kilicarslan. *Robust Gain Scheduling Control with Applications in Smart materials and Biomedical Robotics*. PhD thesis, University of Houston, 2010. 14

L.R. Douat, I. Queinnec, G. Garcia, M. Michelin, and F. Pierrot. H_∞ control applied to the vibration minimization of the parallel robot par2. In *IEEE International Conference on Control Applications*, pages 947–952, 2011. 14

L.R. Douat. *Identification et Commande pour l'atténuation des Vibrations du Robot Parallèle Par2*. PhD thesis, Institut National des Sciences Appliquées de Toulouse (INSA Toulouse), 2011. 14

R. Kumar. Enhanced active constrained layer damping (ACLD) treatment using stand-off-layer: robust controllers design, experimental implementation and comparison. *Journal of Vibration and Control*, 19(3):439–460, 2012. 14, 118, 122

J. Sefton and K. Glover. Pole/zero cancellations in the general H_∞ problem with reference to a two block design. *Systems and Control Letters*, 14(4):295–306, 1990. 14

G. Scorletti and V. Fromion. *Automatique fréquentielle avancée*. Ecole Centrale de Lyon, Master EEAP GSA, Université de Lyon 1, INSA de Lyon,http://cel.archives-ouvertes.fr/cel-0042384, 2008a. 14, 37, 39, 48, 80, 87, 131, 167

A. Forrai, S. Hashimoto, A. Isojima, H. Funato, and K. Kamiyama. Gray box identification of flexible structures: application to robust active vibration sup-

pression control. *Earthquake Engineering & Structural Dynamics*, 30(8):1203–1220, 2001a. 14, 15, 16

A.K. Rao, K. Natesan, M.S. Bhat, and R. Ganguli. Experimental demonstration of H_∞ control based active vibration suppression in composite fin-tip of aircraft using optimally placed piezoelectric patch actuators. *Journal of Intelligent Material Systems and Structures*, 19(6):651–669, 2007. 14, 15

I.N. Kar, K. Seto, and F. Doi. Multimode vibration control of a flexible structure using H_∞-based robust control. *IEEE/ASME Transactions on Mechatronics*, 5(1):23–31, 2000b. 15, 16

L. Huo, G. Song, H. Li, and K. Grigoriadis. H_∞ robust control design of active structural vibration suppression using an active mass damper. *Smart Materials and Structures*, 17:015021, 2008. 15, 118

P. Shimon, E. Richer, and Y. Hurmuzlu. Theoretical and experimental study of efficient control of vibrations in a clamped square plate. *Journal of Sound and Vibration*, 282(1–2):453–473, 2005. 15

S. Font, G. Duc, and F. Carrere. H_∞ control of a magnetic bearing. In *3rd IEEE Conference on Control Applications*, volume 1, pages 581–585, 1994. 16, 49, 79

F. Carrere, G. Duc, and S. Font. Commande fréquentielle robuste-application aux paliers magnétiques. *Techniques de l'ingénieur. Informatique industrielle*, 2(R7432):R7432–1, 1997. 16

F.J.O. Moreira, J.R.F. Arruda, and D.J. Inman. Design of a reduced-order H_∞ controller for smart structure satellite applications. *Philosophical Transactions: Mathematical, Physical and Engineering Sciences*, 359:2251–2269, 2001. 16, 116

Y. Yaman, T. Çalışkan, V. Nalbantoğlu, E. Prasad, and D. Waechter. Active vibration control of a smart beam. In *Canada-US CanSmart Workshop on Smart Materials and Structures*, pages 137–147, 2001. 16

Y. Yaman, T. Çalışkan, V. Nalbantoğlu, E. Prasad, and D. Waechter. Active vibration control of a smart plate. *ICAS 2002, International Council of the Aeronautical Sciences,Toronto, Canada*, 2002. 16

Bibliography

R. Caracciolo, D. Richiedei, A. Trevisani, and V. Zanotto. Robust mixed-norm position and vibration control of flexible link mechanisms. *Mechatronics*, 15 (7):767–791, 2005. 16

G. Filardi, O. Sename, A. Besançon-Voda, and H.J. Schröder. Robust H_∞ control of a DVD drive under parametric uncertainties. In *17th European Control Conference*, pages 1–7, 2003. 16, 17

C.A. Desoer and M. Vidyasagar. *Feedback Systems: Input-Output Properties*. Academic Press, New York, 1975. 16, 28, 66

J.C. Morris, P. Apkarian, and J.C. Doyle. Synthesizing robust mode shapes with μ and implicit model following. In *1st IEEE Conference on Control Applications*, volume 2, pages 1018–1023, 1992. 16

S. Hong, C.H. Park, and H.C. Park. Vibration control of beams using multiobjective state-feedback control. *Smart Materials and Structures*, 15:157, 2006. 16

S.G. Wang, H.Y. Yeh, and P.N. Roschke. Robust control for structural systems with parametric and unstructured uncertainties. *Journal of Vibration and Control*, 7(5):753–772, 2001b. 16

S.G. Wang. Robust active control for uncertain structural systems with acceleration sensors. *Journal of Structural Control*, 10(1):59–76, 2003. 16

H.L Stalford. Robust control of uncertain systems in the absence of matching conditions: Scalar input. In *26th IEEE Conference on Decision and Control*, volume 26, pages 1298 –1307, 1987. 16

J.C. Doyle. Guaranteed margins for LQG regulators. *IEEE Transactions on Automatic Control*, 23(4):756–757, 1978. 16

L. Iorga, H. Baruh, and I. Ursu. H_∞ control with μ-analysis of a piezoelectric actuated plate. *Journal of Vibration and Control*, 15(8):1143–1171, 2009. 16, 99

Bibliography

Y. Bai and K.M. Grigoriadis. H_∞ collocated control of structural systems: An analytical bound approach. *Journal of Guidance, Control, and Dynamics*, 28: 850–855, 2005. 16

A.M. Demetriou, K.M. Grigoriadis, and R.J. Sweeney. Collocated H_∞ control of a cantilevered beam using an analytical upper-bound approach. *Journal of Intelligent Material Systems and Structures*, 20(7):865–873, 2009. 16

Y. Chen, W. Zhang, and H. Gao. Finite frequency H_∞ control for building under earthquake excitation. *Mechatronics*, 20(1):128–142, 2010. 17

D. Halim and S.O.R. Moheimani. Experimental implementation of spatial H_∞ control on a piezoelectric laminate beam. *IEEE/ASME Transactions on Mechatronics*, 7(3):346–356, 2002. 17

J.C. Doyle. Analysis of feedback systems with structured uncertainties. In *IEE Proceedings D on Control Theory and Applications*, pages 242–250, 1982. 17

J.C. Doyle. Structured uncertainty in control system design. In *24th IEEE Conference on Decision and Control*, pages 260–265, 1985. 17

M.K.H. Fan, A.L. Tits, and J.C. Doyle. Robustness in the presence of mixed parametric uncertainty and unmodeled dynamics. *IEEE Transactions on Automatic Control*, 36(1):25–38, 1991. 17

J.C. Doyle, A. Packard, and K. Zhou. Review of LFTs, LMI's, and μ. In *30th IEEE Conference on Decision and Control*, pages 1227–1260, 1991. 17

P.R. Braatz, P.M. Young, J.C. Doyle, and M. Morari. Computational complexity of μ calculation. *IEEE Transactions on Automatic Control*, 39(5):1000–1002, 1994. 17, 33, 99

D.V. Blondel and J.N. Tsitsiklis. A survey of computational complexity results in systems and control. *Automatica*, 36(9):1249–1274, 2000. 17, 33

P.M. Young and J.C. Dolye. Computation of μ with real and complex uncertainties. In *29th IEEE Conference on Decirion and Control*, pages 1230–1235, 1990. 17, 33, 99

Bibliography

P.M. Young, M. Newlin, and J.C. Doyle. Practical computation of the mixed μ problem. In *1992 American Control Conference*, pages 2190–2194, 1992. 17, 33, 99

J. Freudenberg and B. Morton. Robust control of a booster vehicle using H_∞ and SSV techniques. In *31st IEEE Conference on Decision and Control*, pages 2448–2453, 1992. 17, 33, 99

J. Qiu and J. Tani. Vibration control of a cylindrical shell using distributed piezoelectric sensors and actuators. *Journal of Intelligent Material Systems and Structures*, 6(4):474–481, 1995. 18

J. Tani, J. Qiu, and H. Miura. Vibration control of a cylindrical shell using piezoelectric actuators. *Journal of Intelligent Material Systems and Structures*, 6(3):380–388, 1995. 18

M. Karkoub, G.J. Balas, K. Tamma, and M. Donath. Robust control of flexible manipulators via μ-synthesis. *Control Engineering Practice*, 8(7):725–734, 2000. 18

P. Gáspár, I. I. Szászi, and J. Bokor. Robust control design for mechanical systems using mixed μ synthesis. *Periodica Polytechnica Ser. Transport Engineering*, 30(1-2):37–52, 2002. 18

P. Gáspár, I. Szászi, and J. Bokor. Design of robust controllers for active vehicle suspension using the mixed μ synthesis. *Vehicle System Dynamics*, 40(4):193–228, 2003. 18

L.G. Crespo and S.P. Kenny. Reliability-based control design for uncertain systems. *Journal of Guidance, Control, and Dynamics*, 28(4):649–658, 2005. 18

A.H.S. Ang and W.K. Tang. *Probability Concepts in Engineering Planning and Design*, volume 1–2. John Wiley and Sons, 1984. 18

K.L. Wood, K.N. Otto, and E.K. Antonsson. Engineering design calculations with fuzzy parameters. *Fuzzy Sets and Systems*, 52:1–20, 1992. 18

Bibliography

G. Shafer. *A Mathematical Theory of Evidence*. Princeton University Press, New York, 1976. 19

P. Soundappan, E. Nikolaidis, R.T. Haftka, R.V. Grandhi, and R. Canfield. Comparison of evidence theory and Bayesian theory for uncertainty modelling. *Reliability Engineering and System Safety*, 85:295–311, 2004. 19

Y. Ben-Haim. *Info-gap decision theory: decisions under severe uncertainty*. Academic Press, 2001. 19

A. Manan and J.E. Cooper. Prediction of uncertain frequency response function bounds using polynomial chaos expansion. *Journal of Sound and Vibration*, 329:3348–3358, March 2010. 19, 91

N. Wiener. The homogeneous chaos. *American Journal of Mathematics*, 60(4): 897–936, 1938. 19

P.D. Spanos and R. Ghanem. Stochastic finite element expansion for random media. *Journal of Engineering Mechanics*, 115(5):1035–1053, 1989. 19

R. Ghanem. Scales of fluctuation and the propagation of uncertainty in random porous media. *Water Resources Research*, 34(9):2123–2136, 1998. 19

R. Ghanem. Ingredients for a general purpose stochastic finite elements implementation. *Computer Methods in Applied Mechanics and Engineering*, 168(1): 19–34, 1999. 19

B. Sudret. Global sensitivity analysis using polynomial chaos expansions. *Reliability Engineering & System Safety*, 93(7):964–979, 2008. 19

D.K Kishor, R. Ganguli, and S. Gopalakrishnan. Uncertainty analysis of vibrational frequencies of an incompressible liquid in a rectangular tank with and without a baffle using polynomial chaos expansion. *Acta Mechanica*, 220(1–4): 257–273, 2011. 19, 91

L. Nechak, S. Berger, and E. Aubry. A polynomial chaos approach to the robust analysis of the dynamic behaviour of friction systems. *European Journal of Mechanics-A/Solids*, 30(4):594–607, 2011. 19

Bibliography

I. Babuška, R. Tempone, and G.E. Zouraris. Galerkin finite element approximations of stochastic elliptic partial differential equations. *SIAM Journal on Numerical Analysis*, 42(2):800–825, 2004. 19

D. Xiu and J.S. Hesthaven. High-order collocation methods for differential equations with random inputs. *SIAM Journal on Scientific Computing*, 27(3):1118–1139, 2005. 19

M.D. Mckay, R.J. Beckman, and W.J. Conover. A comparison of three methods for selecting values of input variables in the analysis of output from a computer code. *Technometrics*, 21(2):239–245, 1979. 19

D. Xiu. *Numerical methods for stochastic computations: a spectral method approach*. Princeton University Press, 2010. 19

A. Korniienko. *Réseau de PLLs Distribuées pour Synthèse Automatique d'horloge de MPSOCs Synchrones*. PhD thesis, Ecole Centrale de Lyon, 2011. 23, 166

K. Zhang, G. Scorletti, M. Ichchou, and F. Mieyeville. Phase and gain control policies for robust active vibration control of flexible structures. *Smart Materials and Structures*, 22(7):075025 (15 pages), 2013a. 23, 37, 118, 120, 125, 133, 145

K. Glover and J.C. Doyle. A state space approach to H_∞ optimal control. In *Three Decades of Mathematical System Theory*, volume 135. Springer-Verlag, 1989. 23

S. Boyd and C. Barratt. *Linear Controller Design: Limits of Performance*. Prentice Hall Englewood Cliffs, NJ, 1992. 25, 122, 166

S. Poljak and J. Rohn. Checking robust nonsingularity is NP-hard. *Mathematics of Control, Signals and Systems*, 6(1):1–9, 1993. 33

A. Nemirovskii. Several NP-hard problems arising in robust stability analysis. *Mathematics of Control, Signals and Systems*, 6(2):99–105, 1993. 33

Bibliography

G.E. Coxson and C.L. DeMarco. The computational complexity of approximating the minimal perturbation scaling to achieve instability in an interval matrix. *Mathematics of Control, Signals and Systems*, 7(4):279–291, 1994. 33

G. Ferreres, J.M. Biannic, and J.F. Magni. Robustness analysis of flexible structures: practical algorithms. *International Journal of Robust and Nonlinear Control*, 13(8):715–733, 2003. 33, 99

G.C. Calafiore, F. Dabbene, and R. Tempo. Randomized algorithms for probabilistic robustness with real and complex structured uncertainty. *IEEE Transactions on Automatic Control*, 45:2218–2235, 2000. 33, 92, 126

S.P. Boyd, L. EI Ghaoui, E. Feron, and V. Balakrishnan. *Linear Matrix Inequalities in Systems and Control Theory*. Philadelphia, PA: SIAM, 1994. 33

G. Calafiore and F. Dabbene. A probabilistic framework for problems with real structured uncertainty in systems and control. *Automatica*, 38(8):1265–1276, 2002. 34

G.C. Calafiore and F. Dabbene. *Probabilistic and Randomized Methods for Design under Uncertainty*. Springer-Verlag, London, 2006. 34

G. Calafiore, F. Dabbene, and R. Tempo. Research on probabilistic methods for control system design. *Automatica*, 47(7):1279–1293, 2011. 34, 35

R. Tempo, E.W. Bai, and F. Dabbene. Probabilistic robustness analysis: Explicit bounds for the minimum number of samples. *Systems and Control Letters*, 30 (5):237–242, 1997. 35, 100, 101

L. Meirovitch. *Elements of Vibration Analysis*. Sydney McGraw Hill, 2nd edition, 1986. 36, 75, 128

D.J. Ewins. *Modal Testing: Theory, Practice and Application*. Research Studies Press, 2nd edition, 2000. 37

L. Ljung. *System Identification: Theory for the User*. Prentice Hall, 2nd edition, 1999. 37

Bibliography

D.W. Gu, P.H. Petkov, and M.M. Konstantinov. *Robust Control Design with MATLAB*. Springer Verlag, London, 2005. 42, 43, 44, 81

S. Hecker, A. Varga, and J-F. Magni. Enhanced LFR-toolbox for Matlab. *Aerospace Science and Technology*, 9(2):173–180, 2005. 49, 121, 157

G. Scorletti and V. Fromion. A new LMI approach to performance control of linear parameter-varying systems. In *1998 American Control Conference*, volume 1, pages 542–546, 1998. 50

M. Dinh, G. Scorletti, V. Fromion, and E. Magarotto. Parameter dependent H_∞ control by finite dimensional LMI optimization: application to trade-off dependent control. *International Journal of Robust and Nonlinear Control*, 15 (9):383–406, 2005. 50, 121, 122, 148

H.R. Pota, S.O.R. Moheimani, and M. Smith. Resonant controllers for flexible structures. In *38th IEEE Conference on Decision and Control*, volume 1, pages 631–636, 1999. 53

H. Bourlès and G.K. Kwan. *Linear Systems*. John Wiley and Sons, 2010. 54

M. Šebek and Z. Hurák. An often missed detail: Formula relating peek sensitivity with gain margin less than one. In *17th International Conference on Process Control*, 2009. 55

D. Garcia, A. Karimi, and R. Longchamp. Robust PID controller tuning with specification on modulus margin. In *2004 American Control Conference*, volume 4, pages 3297–3302, 2004. 55

R.W. Jones and M.T. Tham. Maximum sensitivity based PID controller tuning: A survey and comparison. In *SICE-ICASE International Joint Conference*, pages 3258–3263. IEEE Computer Society, 2006. 55

Z.C. Zhao, Z.Y. Liu, and J.G. Zhang. IMC-PID tuning method based on sensitivity specification for process with time-delay. *Journal of Central South University of Technology*, 18(4):1153, 2011. 55

Bibliography

A. Lanzon and I.R. Petersen. A modified positive-real type stability condition. In *2007 European Control Conference*, pages 3912–3918, 2007. 59

C.J. Goh and T.K. Caughey. On the stability problem caused by finite actuator dynamics in the collocated control of large space structures. *International Journal of Control*, 41(3):787–802, 1985. 61, 62, 70

E. Sim and S.W. Lee. Active vibration control of flexible structures with acceleration feedback. *Journal of Guidance, Control, and Dynamics*, 16(2):413–415, 1993. 61, 62

C.E. Rohrs, L. Valavani, M. Athans, and G. Stein. Robustness of continuous-time adaptive control algorithms in the presence of unmodeled dynamics. *IEEE Transactions on Automatic Control*, 30(9):881–889, 1985. 62

W.M. Griggs, B.D.O. Anderson, and A. Lanzon. A "mixed" small gain and passivity theorem in the frequency domain. *Systems and Control Letters*, 56: 596–602, 2007. 62

S.M. Kim and J.E. Oh. A modal filter approach to non-collocated vibration control of structures. *Journal of Sound and Vibration*, 332(9):2207–2221, 2013. 62, 119

R.H. Cannon Jr and D.E. Rosenthal. Experiments on control of flexible structure with noncollocated sensors and actuators. *Journal of Guidance, Control, and Dynamics*, 7(5):546–553, 1984. 62

G. Gatti, M.J. Brennan, and P. Gardonio. Active damping of a beam using a physically collocated accelerometer and piezoelectric patch actuator. *Journal of Sound and Vibration*, 303(3):798–813, 2007. 62

I.R. Petersen and A. Lanzon. Feedback control of negative-imaginary systems: flexible structures with colocated actuators and sensors. *IEEE Control Systems Magazine*, 30(5):54–72, 2010. 62

Z.Y. Song, A. Lanzon, S. Patra, and I.R. Petersen. Towards controller synthesis for systems with negative imaginary frequency response. *IEEE Transactions on Automatic Control*, 55(6):1506C1511, 2010. 62

Bibliography

S. Engelken, S. Patra, A. Lanzon, and I.R. Petersen. Stability analysis of negative imaginary systems with real parametric uncertainty–the siso case. *IET Control Theory and Applications*, 4(11):2631–2638, 2010. 62

B. Bhikkaji, S.O.R. Moheimani, and I.R. Petersen. A negative imaginary approach to modeling and control of a collocated structure. *IEEE/ASME Transactions on Mechatronics*, 17(4):717–727, 2012. 62

Z.Y. Song, A. Lanzon, S. Patra, and I.R. Petersen. Robust performance analysis for uncertain negative-imaginary systems. *International Journal of Robust and Nonlinear Control*, 22(3):262–281, 2012. 62

T. Iwasaki, S. Hara, and H. Yamauchi. Dynamical system design from a control perspective: Finite frequency positive-realness approach. *IEEE Transactions on Automatic Control*, 48(8):1337–1354, 2003. 63

J.L. Xiong, I.R. Petersen, and A. Lanzon. Finite frequency negative imaginary systems. *IEEE Transactions on Automatic Control*, 57(11), 2012. 63

G. Barrault, D. Halim, C. Hansen, and A. Lenzi. High frequency spatial vibration control for complex structures. *Applied Acoustics*, 69(11):933–944, 2008. 64, 66

M.B. Bayon de Noyer and S.V. Hanagud. A comparison of H_2 optimized design and cross-over point design for acceleration feedback control. In *39th AIAA/ASME/ASCE/AHS, Structures, Structural Dynamics and Materials Conference*, pages 3250–3258, 1998b. 70

T.K. Caughey and C.J. Goh. Analysis and control of quasi distributed parameter systems. Technical report, Dynamics Laboratory DYNL-82-3, California Institute of Technology, Pasadena, 1982. 70

A. Preumont. *Vibration Control of Active Structures: An introduction*. Springer Verlag, Berlin, 3rd edition, 2011. 70, 71

C.J. Goh and T.H. Lee. Adaptive modal parameters identification for collocated position feedback vibration control. *International Journal of Control*, 53(3): 597–617, 1991. 70

Bibliography

J. Dosch, D.J. Inman, and E. Garcia. A self-sensing piezoelectric actuator for collocated control. *Journal of Intelligent Material Systems and Structures*, 3 (1):166–185, 1992. 70, 71

B.P. Baillargeon and S.S. Vel. Active vibration suppression of sandwich beams using piezoelectric shear actuators: experiments and numerical simulations. *Journal of Intelligent Material Systems and Structures*, 16(6):517–530, 2005. 70

G.T Fagan. An experimental investigation into active damage control systems using positive position feedback for AVC. Master's thesis, Blacksburg (VA): Virginia Polytechnic Institute and State University, 1993. 70

V. Sethi, G.B. Song, and P.Z. Qiao. System identification and active vibration control of a composite i-beam using smart materials. *Structural Control and Health Monitoring*, 13:868–884, 2006. 71

J.L. Fanson and J.C. Chen. Structural control by the use of piezoelectric active members. *NASA-Conference-Pubication*, 1986. 71

E. Pereiraa and S.S. Aphaleb. Stability of positive-position feedback controllers with low-frequency restrictions. *Journal of Sound and Vibration*, 332(12):2900 – 2909, 2013. 71

S. Font, G. Duc, and F. Carrere. Commande fréquentielle robuste application aux paliers magnétiques. *Techniques de l'ingénieur. Informatique industrielle*, 2(R7432):R7432–1, 1997. 73

J.S. Bendat and A.G. Piersol. *Engineering Applications of Correlation and Spectral Analysis*. John Wiley and Sons, 1980. 76

J. Schoukens and R. Pintelon. *Identification of Linear Systems, A Pratical Guide to Accurate Modeling*. Pergamon Press, New York, 1991. 77, 94

V. Piefort. *Finite Element Modelling of Piezoelectric Active Structures*. PhD thesis, Universite Libre de Bruxelles, 2001. 78, 93

X. Zhong, M. Ichchou, F. Gillot, and A. Saidi. A dynamic-reliable multiple model adaptive controller for active vehicle suspension under uncertainties. *Smart Materials and Structures*, 19(045007), 2010. 86

G. Scorletti. Some results about the stabilization and the L2-gain control of LFT systems. In *IEEE IMACS Multiconference on Computational Engineering in Systems Applications*, pages 1240–1245, 1996. 86, 126

B.A. Templeton. *A Polynomial Chaos Approach to Control Design*. PhD thesis, Blacksburg (VA): Virginia Polytechnic Institute and State University, 2009. 91

R. Tempo, G. Calafiore, and F. Dabbene. *Randomized Algorithms for Analysis and Control of Uncertain Systems*. Communications and Control Engineering Series. Springer Verlag, London, London, 2004. 91, 100

F.S. Hover and M.S. Triantafyllou. Application of polynomial chaos in stability and control. *Automatica*, 42(5):789–795, 2006. 91

J. Fisher and R. Bhattacharya. Linear quadratic regulation of systems with stochastic parameter uncertainties. *Automatica*, 45(12):2831–2841, 2009. 91

P.L.T. Duong and M. Lee. Multi-model PID controller design: Polynomial chaos approach. In *International Conference on Control Automation and Systems*, pages 690–695, Gyeonggi-do, 27–30 Oct 2010. 91, 93

A. Smith, A. Monti, and F. Ponci. Robust controller using polynomial chaos theory. In *Conference Record of the 2006 IEEE, Industry Applications Conference, 41st IAS Annual Meeting.*, volume 5, pages 2511–2517, 2006. 93

T. Nestorović, N. Durrani, and M. Trajkov. Experimental model identification and vibration control of a smart cantilever beam using piezoelectric actuators and sensors. *Journal of Electroceramics*, 29(1):42–55, 2012. 94

G. Ferreres and V. Fromion. A new upper bound for the skewed structured singular value. *International Journal of Robust and Nonlinear Control*, 9(1): 33–49, 1999. 98

Bibliography

G. Ferreres, J.M. Biannic, and J.F. Magni. A skew mu toolbox (SMT) for robustness analysis. In *IEEE International Symposium on Computer Aided Control Systems Design*, pages 309–314, 2004. 99

K.D. Dhuri and P. Seshu. Piezo actuator placement and sizing for good control effectiveness and minimal change in original system dynamics. *Smart Materials and Structures*, 15:1661–1672, 2007a. 101

K.D. Dhuri and P. Seshu. Favorable locations for piezo actuators in plates with good control effectiveness and minimal change in system dynamics. *Smart Materials and Structures*, 16(6):2526–2542, 2007b. 101

K.D. Dhuri and P. Seshu. Multi-objective optimization of piezo actuator placement and sizing using genetic algorithm. *Journal of Sound and Vibration*, 323: 495–514, 2009. 101

W.J. Rugh and J.S. Shamma. Research on gain scheduling. *Automatica*, 36(10): 1401–1425, 2000. 115, 151

S. Boyd and L. Vandenberghe. *Convex Optimization*. Cambridge University Press, 2004. 115

G.J. Balas, I. Fialho, A. Packard, J. Renfrow, and C. Mullaney. On the design of LPV controllers for the F-14 aircraft lateral-directional axis during powered approach. In *1997 American Control Conference*, volume 1, pages 123–127, 1997. 115

W. Tan, A. Packard, and G.J. Balas. Quasi-LPV modeling and LPV control of a generic missile. In *2000 American Control Conference*, volume 5, pages 3692–3696, 2000. 115

A. Jadbabaie and J. Hauser. Control of a thrust-vectored flying wing: a receding horizon-LPV approach. *International Journal of Robust and Nonlinear Control*, 12:869–896, 2002. 115

J. Witte, H. Balini, and C. Scherer. Robust and lpv control of an AMB system. In *2010 American Control Conference*, pages 2194–2199. IEEE, 2010. 115

Bibliography

G.J. Balas. Linear, parameter-varying control and its application to a turbofan engine. *International Journal of Robust and Nonlinear Control*, 12(9):763–796, 2002. 115

P. Ballesteros and C. Bonn. A frequency-tunable LPV controller for narrowband active noise and vibration control. In *2011 American Control Conference*, pages 1340–1345, 2011. 115

W. Symens, B. Paijmans, H. Van Brussel, and J. Swevers. Performance comparison of LPV control and interpolating control for a pick-and-place machine with position-dependent dynamics. In *9th International Conference on Motion and Vibration Control*, 2008. 115

I. Fialho and G.J. Balas. Road adaptive active suspension design using linear parameter-varying gain-scheduling. *IEEE Transactions on Control Systems Technology*, 10(1):43–54, 2002. 115, 151

M.N. Ichchou, T. Loukil, O. Bareille, G. Chamberland, and J. Qiu. A reduced energy supply strategy in active vibration control. *Smart Materials and Structures*, 20:125008, 2011. 116

Y. Wang and D.J. Inman. Experimental validation for a multifunctional wing spar with sensing, harvesting, and gust alleviation capabilities. *IEEE/ASME Transactions on Mechatronics*, 18(4):1289–1299, 2013a. 116, 118

Y. Wang and D.J. Inman. Simultaneous energy harvesting and gust alleviation for a multifunctional composite wing spar using reduced energy control via piezoceramics. *Journal of Composite Materials*, 47(1):125–146, 2013b. 116, 118

C.D. Yang and Y.P. Sun. Mixed H_2/H_∞ state-feedback design for microsatellite attitude control. *Control Engineering Practice*, 10(9):951–970, 2002. 116

A. Saberi, A.A. Stoorvogel, and P. Sannuti. *Control of Linear Systems with Regulation and Input Constraints. Communications and Control Engineering.* Springer Verlag, London, 2000. 116, 119

Bibliography

A.L. Materazzi and F. Ubertini. Robust structural control with system constraints. *Structural Control and Health Monitoring*, 19(3):472–490, 2012. 116, 118

F. Assadian. A comparative study of optimal linear controllers for vibration suppression. *Journal of the Franklin Institute*, 339(3):347–360, 2002. 116, 117

S. Kondoh, C. Yatomi, and K. Inoue. The positioning of sensors and actuators in the vibration control of flexible systems. *JSME International Journal. Ser. 3, Vibration, Control Engineering, Engineering for Industry*, 33(2):789–802, 1990. 116

O. Bardou, P. Gardonio, S.J. Elliott, and R.J. Pinnington. Active power minimization and power absorption in a plate with force and moment excitation. *Journal of Sound and Vibration*, 208(1):111–151, 1997. 116

H.K Lee, S.T. Chen, and A.C. Lee. Optimal control of vibration suppression in flexible systems via dislocated sensor/actuator positioning. *Journal of the Franklin Institute*, 333(5):789–802, 1996. 116

A. Baz and S. Poh. Performance of an active control system with piezoelectric actuators. *Journal of Sound and Vibration*, 126(2):327–343, 1988. 116

K.R. Kumar and S. Narayanan. Active vibration control of beams with optimal placement of piezoelectric sensor/actuator pairs. *Smart Materials and Structures*, 17(5):055008, 2008. 117

N.D. Zorić, A.M. Simonović, Z.S. Mitrović, and N.S. Stupar. Optimal vibration control of smart composite beams with optimal size and location of piezoelectric sensing and actuation. *Journal of Intelligent Material Systems and Structures*, 24(4):499–526, 2013. 117

V. Gupta, M. Sharma, and N. Thakur. Optimization criteria for optimal placement of piezoelectric sensors and actuators on a smart structure: a technical review. *Journal of Intelligent Material Systems and Structures*, 21(12):1227–1243, 2010. 117

Bibliography

P. Van Phuoc, G. Nam Seo, and P. Hoon Cheol. Vibration suppression of a flexible robot manipulator with a lightweight piezo-composite actuator. *International Journal of Control, Automation and Systems*, 7(2):243–251, 2009. 117

K.Y. Chen, M.S. Huang, and R.F. Fung. The comparisons of minimum-energy control of the mass-spring-damper system. In *9th World Congress on Intelligent Control and Automation (WCICA)*, pages 666–671, 2011. 117

R. Kumar, S.P. Singh, and H.N. Chandrawat. Adaptive vibration control of smart structures: a comparative study. *Smart Materials and Structures*, 15(5):1358, 2006. 118

Z.C. Qiu. Experiments on vibration suppression for a piezoelectric flexible cantilever plate using nonlinear controllers. *Journal of Vibration and Control*, 2013. doi: 10.1177/1077546313487762. 118

S. Sivrioglu, K. Nonami, and M. Saigo. Low power consumption nonlinear control with H_∞ compensator for a zero-bias flywheel AMB system. *Journal of Vibration and Control*, 10(8):1151–1166, 2004. 118

K. Zhang, G. Scorletti, M. Ichchou, and F. Mieyeville. Robust active vibration control of piezoelectric flexible structures using deterministic and probabilistic analysis. *Journal of Intelligent Material Systems and Structures*, page doi:10.1177/1045389X13500574, 2013b. 118, 122, 141, 142

W. Reinelt. H_∞ loop shaping for systems with hard bounds. In *Proc. of the Int Symp on Quantitative Feedback Theory and Robust Frequency Domain Methods*, pages 89–103, 1999. 118

W. Reinelt. Robust control of a Two-Mass-Spring system subject to its input constraints. In *2000 American Control Conference*, pages 1817–1821, 2000. 118, 119

W. Reinelt. Loop shaping of multivariable systems with hard constraints on the control signal. *Electrical Engineering*, 83(4):169–177, 2001. 118

Bibliography

A. Forrai, T. Tanoi, S. Hashimoto, H. Funato, and K. Kamiyama. Robust controller design with hard constraints on the control signal. *Electrical Engineering*, 83(4):179–186, 2001b. 118, 120

A. Forrai, S. Hashimoto, H. Funato, and K. Kamiyama. Robust active vibration suppression control with constraint on the control signal: application to flexible structures. *Earthquake engineering & structural dynamics*, 32(11):1655–1676, 2003. 118, 120

N. Darivandi, K. Morris, and A. Khajepour. An algorithm for LQ optimal actuator location. *Smart Materials and Structures*, 22(3):035001, 2013. 119

M. Dinh. *Synthèse Dépendant De Paramètres par Optimisation LMI de Dimension Finie: Application à la Synthèse de Correcteurs Reréglables*. PhD thesis, Université de Caen/Basse-Normandie, 2005. 121, 148

G. Scorletti and L. EI Ghaoui. Improved LMI conditions for gain scheduling and related control problems. *International Journal of Robust and Nonlinear Control*, 8(10):845–877, 1998. 122, 123, 126, 158, 160

D.G. Wood. *Control of Parameter-Dependent Mechanical Systems*. PhD thesis, Cambridge, 1995. 122

G. Scorletti and V. Fromion. Synthesis tools for complex space systems, theory & concepts. Technical note, CNRS/INRA, 2008b. 122, 123, 124, 126, 148

C.W. Scherer. LPV control and full block multipliers. *Automatica*, 37(3):361–375, 2001. 123

P.A. Bliman. Stabilization of LPV systems. In *42nd IEEE Conference on Decision and Control*, volume 6, pages 6103–6108, 2003. 124

G. Becker. Parameter-dependent control of an under-actuated mechanical system. In *34th IEEE Conference on Decision and Control*, volume 1, pages 543–548, 1995. 124

F. Wu, X.H. Yang, A. Packard, and G. Becker. Induced L2-norm control for LPV systems with bounded parameter variation rates. *International Journal of Robust and Nonlinear Control*, 6:983–998, 1996. 124

S. Lim. *Analysis and Control of Linear Parameter-varying Systems*. PhD thesis, Standford University, 1999. 124

C.W. Scherer. Robust performance analysis for parameter dependent systems using tensor product splines. In *37th IEEE Conference on Decision and Control*, volume 2, pages 2216–2221. IEEE, 1998. 124

B. Jemai, M.N. Ichchou, L. Jézéquel, and M. Noe. An assembled plate active control damping set-up: optimization and control. *Journal of Sound and Vibration*, 225(2):327–343, 1999. 151

B. Jemai, M.N. Ichchou, and L. Jézéquel. Double panel partition (AVNC) by means of optimized piezoceramic structural boundary control. *Journal of Vibration and Control*, 8(5):595–617, 2002. 151

A. Chettah, M.N. Ichchou, O. Bareille, S. Chedly, and J.P. Onteniente. Dynamic mechanical properties and weight optimization of vibrated ground recycled rubber. *Journal of Vibration and Control*, 15(10):1513–1539, 2009. 151

L.H. Carter. *Linear Parameter Varying Representations for Nonlinear Control Design*. PhD thesis, The University of Texas at Austin, Texas, United States, 1998. 151

H. Olsso. *Control Systems with Friction*. PhD thesis, Department of Automatic Control, Lund Institute of Technology, 1996. 151

R.M. Hirschorn and G. Miller. Control of nonlinear systems with friction. *IEEE Transactions on Control Systems Technology*, 7(5):588–595, 1999. 151

H.M. Zhou, X.J. Zheng, and Y.H. Zhou. Active vibration control of nonlinear giant magnetostrictive actuators. *Smart Materials and Structures*, 15(3):792–798, 2006. 151

Bibliography

C. Ho, Z.Q. Lang, B. Sapiński, and S.A. Billings. Vibration isolation using nonlinear damping implemented by a feedback-controlled MR damper. *Smart Materials and Structures*, 22(10):105010 (11 pages), 2013. 151

R.S. Smith. *Robust Control: Theory and Application*. Lecture Notes, University of California, Santa Barbara, 2006. 154

J-F. Magni. User manual of the linear fractional representation toolbox. Technical report, ONERA, Systems, Control and Flight Dynamics Department, 2006. 161

Index